

AD-A058 017

PRINCETON UNIV N J JAMES FORRESTAL RESEARCH CENTER
APPLICATION OF WELL-STIRRED REACTOR THEORY TO THE PREDICTION OF--ETC(U)
MAY 58 A H BONNELL
SQUID-MIT-18-T

F/G 21/2

N60RI-105(03)

NL

UNCLASSIFIED

1 OF 3
AD
A058017



ADA058017

AD No. _____
DDC FILE COPY

PROJECT SQUID
Technical Report
MIT-18-T

MASTER

MIT-18-T

6 APPLICATION OF WELL-STIRRED REACTOR THEORY
TO THE PREDICTION OF COMBUSTOR PERFORMANCE

6.5/3

by

LEVEL

10 Allan Hardy/Bonnell

B. S. E. University of Michigan
(1953)

12 252 p.

15 NG OYI-105 (03)

Submitted in Partial Fulfillment of the
Requirements for the Degree of
Doctor of Science in Chemical Engineering
at the

DDC
RECEIVED
AUG 15 1978
A

Massachusetts Institute of Technology
(1958)

14 SQUID-MIT-18-T

DISTRIBUTION STATEMENT A
Approved for public release
Distribution Unlimited

Signature of Author:

Department of Chemical Engineering
111 May 1958

Signatures of Professors
in Charge of Research:

9 Doctoral thesis

Hoyt C. Hottel

Glenn C. Williams

Signature of Chairman,
Departmental Committee
on Graduate Students:

Glenn C. Williams

190 500

ACKNOWLEDGEMENTS

The author is indebted to Professor H. C. Hottel and Professor G. C. Williams for suggesting this problem and for their guidance throughout the course of the work. The author would also like to thank Mr. W. P. Jensen and the staff of the Fuels Research Laboratory for their many helpful suggestions in the design and construction of the apparatus.

Special thanks are due Mr. R. E. Rosensweig who was of invaluable aid during much of the experimental work and to Mr. A. C. Tobey for his suggestion and encouragement in many phases of this problem.

This work was sponsored by Project SQUID, which is jointly supported by the Office of Naval Research, the Office of Scientific Research (Air Force), and the Office of Ordnance Research (Army), under Contract No. N6-ori-105, Task Order, III.

TABLE OF CONTENTS

	<u>Page</u>
Chapter I.	
<u>SUMMARY</u>	2
Chapter II.	
<u>INTRODUCTION</u>	9
Scope of Thesis.....	9
Combustion Chamber Fluid Dynamics	11
Combustion Reaction Kinetics; Well-Stirred Reactor Behavior....	14
Behavior of Plug-Flow and Staged Stirred Reactors.....	26
Staged Reactors with Intermediate Reactions.....	33
Experimental Stirred Reactor Per- formance.....	37
Combustion Chamber Models in the Literature.....	42
Summary.....	49
Chapter III.	
<u>MODELS OF COMBUSTION CHAMBERS</u>	51
Two-Stability Limit Model.....	51
Model Showing Effect of Recircu- lation.....	73
Model Showing Effect of Non- Uniform Fuel-Air Ratio.....	81
Models of More Complex Situations	82
Summary.....	83

Chapter IV.		<u>Page</u>
	<u>EXPERIMENTAL EQUIPMENT AND PROCEDURES.</u>	85
	Combustion Chamber.....	85
	Sampling Equipment.....	94
	Experimental Procedures.....	98
	Blowout Measurement at Constant Pressure.....	98
	Combustion Efficiency Measurements One-Jet Chamber.....	101
	Effect of Pressure on Blowout.....	104
	Combustion Efficiency Measurement. Three-Jet Chamber.....	105
Chapter V.		
	<u>EXPERIMENTAL RESULTS.....</u>	106
	Three-Jet Chamber Operation.....	106
	Single-Jet Chamber Operation.....	112
Chapter VI.		
	<u>DISCUSSION OF RESULTS.....</u>	124
	Experimental Errors.....	124
	Air Leakage.....	125
	Departure from Ideal Reactor Conditions.....	128
	Errors in Measurement.....	139
	Analysis of Three-Jet Chamber Performance.....	141
	Analysis of One-Jet Chamber Performance.....	149
	Summary.....	163

	<u>Page</u>
Chapter VII.	
<u>CONCLUSIONS AND RECOMMENDATIONS.....</u>	165
Appendix A.	
<u>DERIVATION OF THE WELL-STIRRED REACTOR EQUATION.....</u>	169
Appendix B.	
<u>MULTI-STEP KINETIC SCHEMES.....</u>	177
Appendix C.	
<u>ESTIMATED HEAT LOSS FROM THREE-JET CHAMBER.....</u>	188
Appendix D.	
<u>DETAILS OF EQUIPMENT AND APPARATUS.....</u>	195
Appendix E.	
<u>SAMPLE CALCULATIONS</u>	
A. Blowout or Loading Rates.....	208
B. Combustion Efficiency.....	212
C. Pressure Exponent.....	213
Appendix F.	
<u>SUMMARY OF CALCULATED VALUES.....</u>	220
F-1. Blowout Measurements, Three-Jet Chamber.....	220
F-2. Flame Volume, Three-Jet Chamber	224
F-3. Combustion Efficiency, Three-Jet Chamber.....	225
F-4. Blowout Measurement, One-Jet Chamber.....	226

	<u>Page</u>
F-5. Combustion Efficiency, One-Jet Chamber.....	227
F-6. Pressure Exponent, One-Jet Chamber.....	228
Appendix G.	
<u>SCHLIEREN PHOTOGRAPHY, THREE-JET CHAMBER</u>	230
Appendix H.	
<u>LITERATURE CITATIONS</u>	234
Appendix I.	
<u>TABLE OF NOMENCLATURE</u>	236
Appendix J.	
<u>AUTOBIOGRAPHICAL NOTE</u>	238

LIST OF FIGURES

<u>Number</u>	<u>Title</u>	<u>Page</u>
II-1	Typical Can-Type Combustor.....	11
II-2	Well-Stirred Reactor Performance.....	19
II-3	Integration of Well-Stirred Reactor Curve to Find Plug-Flow Reactor Performance.....	28
II-4	Plug-Flow Reactor Curve.....	28
II-5	Staged Well-Stirred Reactor Operation.....	32
II-6	Relative Reaction Rates in a Two-Step Reactor.....	36
II-7	Volume Requirement in a Two-Step Reactor....	36
II-8	Stirred Reactor Stability Limit Data.....	39
II-9	Recalculated Performance of Spaulding's Model.....	47
III-1	Physical Picture of Recirculation.....	54
III-2	Model Diagram (Two-Stability Limit Model)...	54
III-3	Well-Stirred Reactor Curve For Two-Stability Limit Model.....	54
III-4	Performance of a Two-Stability Limit Model..	59
III-5	One-Sided Blowout Condition in Two-Stability Limit Model.....	68
III-6	Final Blowout Limit For Two-Stability Limit Model.....	68
III-7	Effect of Feed Rate on Two-Stability Limit Model.....	70
III-8	Effect of Recirculation in a Combustor Model.....	74
III-9	β_0 , β_1 , and β_2 for Recirculation Model....	79
III-10	Effect of Split Fuel Feed on Recirculation Model.....	79

<u>Number</u>	<u>Title</u>	<u>Page</u>
IV-1	Combustion Chamber for Recirculation Studies.....	89
IV-2	Photograph of Chamber With Three Feed Jets and Flues.....	90
IV-3	Photograph of Assembled Chamber.....	90
IV-4	Photograph of Vacuum Tank Ready for Experiment.....	90
IV-5	Flow Diagram of Apparatus.....	92
IV-6	Photograph of Control Panel (Manometers)...	93
IV-7	Photograph of Control Panel (Sampling Board).....	93
IV-8	Photograph of One-Jet Chamber.....	93
IV-9	Reverse Flow Cooling Water Sampling Probe.	95
IV-10	Straight-Through Cooling Water Sampling Probe.....	95
IV-11	Photograph of Probes Used.....	95
IV-12	Flow Diagram of Sampling Train.....	97
V-1	Flame Pattern in Three-Jet Chamber, Four Zones Active.....	108
V-2	Flame Pattern in Three-Jet Chamber, Two Zones Active.....	108
V-3	Flame Pattern in Three-Jet Chamber, One Zone Active.....	108
V-4	Blowout Data, Three-Jet Chamber.....	109
V-5	Combustion Zone Volume, Three-Jet Chamber.	111
V-6	Combustion Efficiency - Three-Jet Chamber.	111
V-7	Flame Pattern, One-Jet Chamber, Low Flow Rate.....	113

<u>Number</u>	<u>Title</u>	<u>Page</u>
V-8	Flame Pattern, One-Jet Chamber, High Flow Rate.....	113
V-9	Stability Data, One-Jet Chamber.....	113
V-10	Overall Combustion Efficiency, One-Jet Chamber.....	114
V-11	Combustion Efficiency Traverse, One-Jet Chamber.....	118
V-12	Burnedness in One-Jet Chamber at Various Positions.....	119
V-13	Photographs Showing Traverse Stations.....	120
V-14	Effect of Pressure on Blowout Feed Rate One-Jet Chamber.....	121
V-15	Effect of Fuel-Air Ratio on Pressure Exponent.....	122
VI-1	Heat Loss Rate in Three-Jet Chamber.....	132
VI-2	Effect of Heat Loss on Stirred Reactor Operation.....	136
VI-3	Effect of Pressure Exponent on Stirred Reactor Operation.....	138
VI-4	Two-Stability Limit Model Blowout Conditions	142
VI-5	Comparison of Stirred Reactor Blowout Data and Three-Jet Chamber Data.....	145
VI-6	Comparison of Stirred Reactor Blowout Data and One-Jet Chamber Data.....	151
VI-7	Extended Recirculation Model.....	156
VI-8	Effect of Number of Zones in Extended Recirculation Model, Blowout Loading Rate Constant	156
VI-9	Extended Recirculation Model, Recirculation Ratio Constant.....	158

APPLICATION OF WELL-STIRRED REACTOR THEORY
TO THE PREDICTION OF COMBUSTOR PERFORMANCE

by

Allan Hardy Bonnell

B. S. E. University of Michigan
(1953)

Submitted in Partial Fulfillment of the
Requirements for the Degree of
Doctor of Science in Chemical Engineering
at the

Massachusetts Institute of Technology
(1958)

Signature of Author:

Department of Chemical Engineering
May 1958

Signatures of Professors
in Charge of Research:

Hoyt C. Hottel

Glenn C. Williams

Signature of Chairman,
Departmental Committee
on Graduate Students:

Glenn C. Williams

ABSTRACT

APPLICATION OF WELL-STIRRED REACTOR THEORY TO THE PREDICTION OF COMBUSTOR PERFORMANCE

By

Allan Hardy Bonnell


Submitted to the Department of Chemical Engineering on
May 19, 1958 in partial fulfillment of the requirements
for the degree of Doctor of Science.

Analysis and prediction of the performance characteristics of complex processes has often been successfully accomplished by use of single conceptual models. In the models such processes are visualized in terms of important basic mechanisms of the process which can interact in an idealized manner.

Exemplary in the field of combustion has been the use of wrinkled flame front models to analyze the behavior of low-intensity turbulent flames. In high-output combustion systems, however, substantial portions of the combustion chamber may be devoted to homogeneous combustion, and in such situations wrinkled flame front models break down.

In the work reported here conceptual models of high-output systems are considered in which the combustion chamber is visualized as consisting only of a small number of interacting elements composed of homogeneous reaction volumes. Pressure interaction and recirculation are considered. Performance curves developed for four typical models show qualitatively flow interactions and residual flame phenomena typically observed in real combustion chambers.

Predicted performance characteristics based on the above models were compared with experimental data obtained in a small combustion chamber burning premixed propane-air mixtures. Stability limits, combustion efficiency-loading rate data, and visual observation of flame and flow were typical measurements made on chamber performance.



The performance characteristics of combustion chambers predicted by these models, - including the existence of primary and secondary blowout, the effects of air-fuel ratio on blowout, the effects of recirculation and of non-uniform fuel-air ratio on combustion efficiency, the existence of conditions which can lead to pulsing combustion, the magnitude of the combustion rate, - all these are in encouraging agreement with measured performance of actual chambers.

Additional experimental work is required to establish more quantitatively the ability of simple conceptual models to predict actual combustor performance, but the experimental work discussed here provides reasonable assurance that such models have practical utility. It is recommended that reasons for the deviations between the model predictions and the experimental performance be investigated further.

Thesis Supervisor:

Hoyt C. Hottel

Title:

Professor of Fuel Engineering

Thesis Supervisor:

Glenn C. Williams

Title:

Professor of Chemical Eng'g

ACCESSION NO.	
NTIS	NTIS Section
DOC	DOC Section
A	

Department of Chemical Engineering
Massachusetts Institute of Technology
Cambridge 39, Massachusetts

May 19, 1958

Professor L. F. Hamilton
Secretary of the Faculty
Massachusetts Institute of Technology
Cambridge 39, Massachusetts

Dear Professor Hamilton:

In partial fulfillment of the requirements for the degree of Doctor of Science in Chemical Engineering, I hereby submit the thesis entitled "Application of Well-Stirred Reactor Theory to the Prediction of Combustor Performance".

Respectfully submitted,

Allan H. Bonnell

<u>Number</u>	<u>Title</u>	<u>Page</u>
VI-10	Extended Recirculation Model, Number of Zones Constant.....	161
VI-11	Comparison of Model Theory and Experimental Combustor Performance.....	162
A-1	Normalized Stirred Reactor Performance.....	176
B-1	Performance of a Two-Step Reaction; Step 1.	184
B-2	Performance of a Two-Step Reaction; Step 2.	185
B-3	Performance of a Two-Step Reaction; Combined Results in a Well-Stirred Reactor.....	186
B-4	Performance of a Two-Step Reaction; Lines of Constant $d\beta/d\gamma$ on Composition Diagram...	187
C-1	Emissivity or Absorptivity of Vycor.....	193
C-2	Heat Loss of Three-Jet Chamber.....	194
D-1	Enlarged Detail of Nozzle.....	197
D-2	Combustion Chamber Assembly.....	198
D-3	Orifice Locations.....	199
D-4	Orifice Calibrations, Orifice O-1 Low Range	200
D-5	Orifice Calibrations, Orifice O-1 Med Range	201
D-6	Orifice Calibrations, Orifice O-1 High Range	202
D-7	Orifice Calibrations, Orifice O-2 Low Range	203
D-8	Orifice Calibrations, Orifice O-2 High Range	204
D-9	Orifice Calibrations, Orifices O-4 to O-6	205
D-10	Compressibility of Propane.....	206
D-11	Capillary Flow Meter Calibration.....	207

<u>Number</u>	<u>Title</u>	<u>Page</u>
E-1	Pressure vs $P^{1.8}$	210
E-2	Temperature Correction Factors.....	211
E-3	Background Gas Correction Factor.....	215
E-4	Mols Dry Combustion Products Per Mol of Wet Products.....	216
E-5	Mols of Oxygen Consumed and Remaining at Complete Combustion.....	217
E-6	Adiabatic Flame Temperature.....	218
E-7	Required Sampling Rate.....	219
G-1	Typical Schlieren Photographs.....	233

CHAPTER I

SUMMARY

The importance of mixing as a rate-limiting step in combustion processes has long been recognized. Prior to the development of high-output combustors for jet propulsion, however, mixing rates were sufficiently slow in most practical combustors to make chemical reaction rates appear infinitely fast by comparison.

The use of a simple conceptual model to aid in visualization of the processes involved in typical high-output combustion chambers could simplify the experimental development of new chamber designs. Since in the chambers under consideration both chemical reaction rates and mixing rates have important roles, it would be necessary to incorporate both phenomena into such a model. The model should predict behavior characteristics of combustion chambers (such as combustion efficiency, stability and tendency to resonate) resulting not only from limitations set by chemical reaction rate or mixing rates, but also from interactions of two or more phenomena. Although a sufficiently complex model could completely describe a chamber behavior pattern, the results of application of the model concepts to prediction of performance would be impressive only if the model were simple.

In the models discussed here, the combustion chamber is considered to be divided into a small number of zones each of which is assumed to be uniform in composition. Flow between these zones is postulated as representing the fluid-flow and mixing pattern. Within each zone, since the composition is uniform, it is postulated that the chemical reaction rate is determined uniquely by the composition and temperature of that zone. In the present discussion heat transfer is neglected; however, adiabaticity is not a necessary assumption. The relation between burning rate and composition is taken from stirred reactor data on hydrocarbon combustion and is limited to a burning rate-composition relation involving only one composition variable. More complex reaction schemes could be used, but the lengthy computations required for models involving these severely limit the number of composition variables which may be considered. Models similar in some respects to those discussed here have appeared in the recent literature (2, 6, 18, 24); however, little has been done to relate their predicted performance quantitatively to the performance of practical combustion chambers.

The purposes of this investigation were: (1) to consider some possible conceptual models of combustion chambers which allow for interaction between flow phenomena and reaction rate phenomena, (2) to study the operation of a simple experimental combustion chamber and (3) to examine the question

of whether the performance predicted by simple conceptual models can be quantitatively fitted to the measured performance of the experimental combustion chamber.

Data with which the predicted performance characteristics could be compared were obtained from a small experimental combustion chamber. The chamber design was chosen to be simple and yet to give characteristics typical of practical chambers. In the chamber used a small, rectangular two-dimensional combustion zone was fired with either one or three feed jets. Opposing the feed jets were corresponding exit flues. The combustion zone was formed by kaolin firebricks whose arrangement could be readily altered depending on the number of feed jets used. The front and back sides of the combustion zone were closed with Vycor windows which permitted direct observation of the flame. The feed jets were each 0.030" wide by 2" deep in the 2-dimensional direction, and mounted in the floor of the chamber with their axes accurately aligned. The opposing exit flues in the chamber roof were 1/2" wide. When three jets were used the chamber was 3" wide with 1" spacing between jet centerlines. With one feed jet a 2" chamber width was used. A pre-mixed propane-air mixture was prepared and metered individually to each jet to insure uniform operation.

Operating characteristics of these chambers demonstrated two general phenomena. In using the three-jet chamber it was

found that the three jets coalesced a short distance above the nozzles, and at low firing rates combustion proceeded on either side of the central core thus created. As the firing rate was increased one of these two zones became unstable. Consequent to this partial blowout there was a readjustment of the flow pattern in which the remaining active zone expanded in size. At a higher firing rate it was possible to blow out the remaining active zone.

In the one-jet chamber no symmetrical combustion pattern was observed. The jet from the centrally located feed bent over against one of the chamber walls, and combustion proceeded in a circulatory fashion in the large zone thus created. At low firing rates combustion appeared principally around the edges of the circulatory zone with the "eye" of the zone containing only completely burned gases. As the flow rate was increased the burned center shrank as the zone of most intense combustion moved inward, until at blowout only a small residual flame in the center of the vortex remained.

Four models were considered in this work. In the first of these, an interaction between the pressure effect of combustion and the chemical reaction rate was considered. The model, purporting to simulate a chamber with feed and discharge along lines located centrally on opposite walls, consisted of two well-stirred reactors of constant total volume separated from each other by an elastic barrier

capable of moving in response to pressure differences so that the deflection was directly proportional to the pressure difference between the reactors. The two reactors were assumed to be fed equally with a pre-mixed fuel-air mixture and when the pressure difference between the reactors was zero, the two reactors had equal volumes.

When the firing rate to this model was changed, two stability limits were predicted, the first corresponding to an initial blowout of one of the two reactors followed by a shift in the barrier position toward the colder side and the second to blowout of the remaining active reactor at a higher feed rate. These two blowout limits corresponded to loading rates in the zones equivalent to stirred reactor blowout rates. This was qualitatively the behavior observed experimentally in the three-jet chamber studied. Although a quantitative fitting of the predicted performance to all of the data on the experimental chamber was not possible, the relative firing rates between the two blowout limits was predicted with some success.

The second combustor model considered allowed for recirculation of partially burned combustion products in a pattern such as that typically produced by a jet firing fuel-air mixture into a combustion zone. This model is similar to one suggested by Spaulding (24) after the major portion of this work had been completed; however, the

performance predicted by the model suggested here was drastically different from that predicted by Spaulding. In the recirculation model two zones are postulated, representing the central jet core and recirculation zone found in actual combustors. Each of these zones is postulated to be a well-stirred reactor. Fresh fuel-air mixture is mixed instantaneously with partially burned recirculated gases from the recirculation zone and the resulting mixture is then fed into the initial stirred reactor representing the jet core. Gases leaving the central core volume are divided into two portions, one being recirculated through the recirculation zone and the other leaving the model as burned products. This model showed two interesting characteristics at low recirculation ratios, residual flame phenomena and potential flickering flame operation. At higher recirculation ratios these phenomena disappeared. In a third model, similar to the second, allowance was made for non-uniform distribution of fuel. This was achieved by introducing only a part of the fuel but all of the air into the central core zone and the remainder of the fuel into the recirculation zone along with the recirculated gases. The third model, with the split-fuel-feed, showed essentially the same behavior as that of the second model.

Study of the performance of the experimental one-jet combustor indicated that a simple recirculation model was

inadequate to describe its performance. To fit the data a fourth model was considered in which successive recirculation zones were added. In this model a typical zone received recirculated gases from its immediate successor and supplied recirculated gases to its immediate predecessor. This model predicted a performance similar to that of the simple recirculation model, but the relative blowout limits for the main flame and the residual flame were in better agreement with experimental data on the one-jet chamber.

The performance characteristics of combustion chambers predicted by these models, - including the existence of primary and secondary blowout, the effects of air-fuel ratio on blowout, the effects of recirculation and of non-uniform fuel-air ratio on combustion efficiency, the existence of conditions which can lead to pulsing combustion, the magnitude of the combustion rate, -- all these are in encouraging agreement with measured performance of actual chambers.

Additional experimental work is required to establish more quantitatively the ability of simple conceptual models to predict actual combustor performance, but the experimental work discussed here provides reasonable assurance that such models have practical utility. It is recommended that reasons for the deviations between the model predictions and the experimental performance be investigated further.

CHAPTER II

INTRODUCTION

Scope of Thesis

Mixing has long been recognized as a dominant factor in many industrial combustion processes. However, there has been a growing realization that chemical reaction rates place important limitations on the performance of high-output combustors, especially those found in aviation propulsion systems. This has led in recent years to the study of the well-stirred reactor as a device which may be used to relate burning rate to chemical kinetics as affected by composition, temperature and pressure rather than to mixing processes alone.

Practical combustors for high-output combustion systems lie intermediate with respect to volumetric heat release rates between purely mixing-controlled industrial furnaces and the chemically rate-limited well-stirred reactor. This suggests that mixing may be reduced in importance as a rate limiting process in many practical combustors. Furthermore, much experimental data obtained on high-output combustors can only be explained by postulating some chemical rate limitations. In principle, therefore, to predict the behavior of high-output combustors from fundamental data, one would have to account for the simultaneous effects of both chemical reaction rates and

mixing rates in the combustion chamber. Both of these phenomena are highly complex, and their interactions may lead to unexpected results. Typical of these results are the marked effects of different firing rates on combustion efficiencies, and discontinuous shifts in flow patterns and efficiency in certain firing rate ranges.

One might hope to divide the various phenomena occurring in a combustion chamber, particularly of efficiency and stability, into regions of operation where either mixing rate or chemical reaction rate is the dominant phenomenon. These could then be treated as independent problems in terms of the present theories of mixing and of chemical kinetics. This method has the deficiency, however, of being unable to predict performance in the transition regions where many interesting problems occur.

To study these regions the approach proposed here is to use simplified models of both the mixing and combustion rate phenomena, and to combine them to allow for interaction in the transition regions. The simplified conceptual models of combustion chambers cannot be expected to include all of the variables or effects; however, in principle a sufficiently complex model should be able to completely describe the performance of any combustion chamber.

In setting up the models to be presented here knowledge of simple combustion chamber fluid dynamics and of well-

stirred reactor theory is required. The introductory material is thus divided into three sections. The first section deals with the fluid dynamics of combustion chambers, the second discusses well-stirred reactor theory, and the third reviews the literature on combustion chamber models.

Combustion Chamber Fluid Dynamics

The fluid-flow pattern of a modern can-type combustor, typical of the combustors used in nearly all current gas-turbines, is highly complex, and, as yet, has not received adequate attention. A sectional view of a typical combustor is shown in Figure II-1. Liquid fuel is sprayed into the front end of the chamber, and combustion air enters through a pattern of holes around the surface of the can.

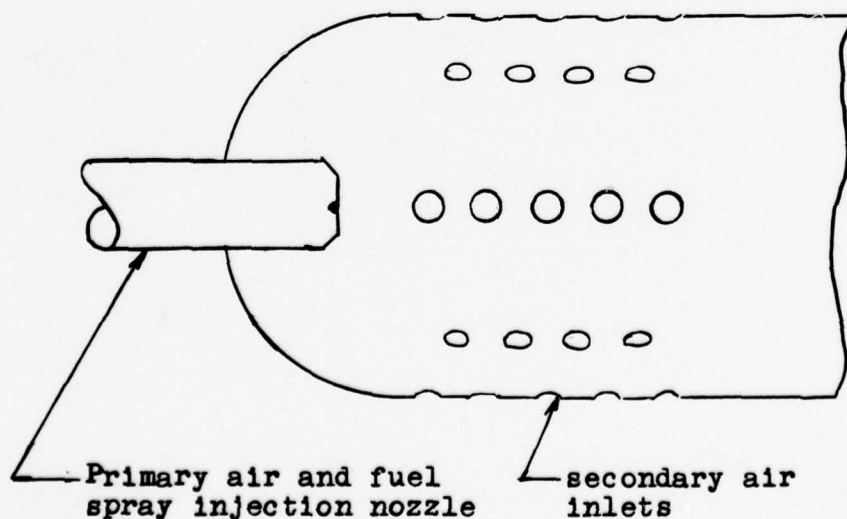


Figure II-1: Typical can-type combustor

In a device such as this moderate mixing is achieved by the "jet" effect of the air and fuel inlets. This mixing must serve three purposes: (1) to contact the fuel and oxidant so that combustion can occur, (2) to provide sufficient recirculation of hot combustion products to the fuel inlet so that the flame will stabilize, and (3) to create sufficient turbulence to burn the fuel at the desired volumetric heat release rate.

Little work has been done on the analysis of jet mixing in chambers where there is mixing of recirculating fluid with the jet. On the other hand, considerable work has been done on jet mixing in pipes where the recirculation phenomenon has been eliminated by the introduction of a secondary fluid (11, 12, 29). The general conclusion is that so long as the jet boundary does not reach the wall, the behavior of the enclosed jet is identical to that of a free jet. It is reasonable to expect that the same results would be found in an enclosed system with recirculation.

In a practical chamber the problem is considerably complicated by the interaction of two or more jets as well as by deviations of the jet from idealized theory as the confining walls are reached. In a multi-jet system, individual jets tend to lose their identity and, instead, make their contribution to the overall turbulence level in the chamber. The arrangement of the jets may be such as to give flow patterns ranging from no identifiable pattern to a well-

defined pattern.

In the combustion chambers considered here, the flow pattern is imagined to be of this latter type. The jets are arranged to give a well-developed circulatory pattern, and flame is stabilized by the recirculation of hot burned gases to the fresh feed inlets. Typically, fresh feed and burned products counter-diffuse (turbulently) along a portion of the circulatory pattern. This process provides ignition for fresh gases in the mainstream of the flow pattern as well as maintaining active combustion in the sheltered recirculation zones.

The approach to well-stirredness in systems of this type is influenced by two factors: (1) the portion of the chamber devoted to recirculation and (2) the level of turbulence in the chamber. If only a small portion of the chamber is devoted to gross recirculation, the chamber will approach well-stirredness only through extremely intense turbulence in the chamber. Likewise, if the gross recirculation pattern is of a large diameter, high turbulence is required to couple the central portion of the pattern with the outer regions. Spaulding (24) suggests that gross circulation is a more efficient means of achieving mixedness than is high turbulence. (Efficiency is in terms of pressure drop required to achieve a given level of mixedness.)

Because of high reaction rates of combustion, incomplete mixing within a chamber leads to zones of high and low combustion rates. Consequently, completeness of mixing has been associated with high volumetric heat release rates. It has been postulated that it is possible to obtain even higher volumetric combustion rates by proper arrangement of combustor elements (6); however, these have not yet been achieved in practice. In visualizing models of combustion chambers such as these, the effects of recirculation which can be important in some regions must be recognized in the model.

Combustion Reaction Kinetics; Well-Stirred Reactor Behavior

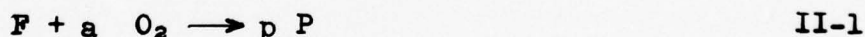
The subject of combustion reaction kinetics has been treated by a large number of authors. General reviews of high temperature kinetics have been given by Shuler (21), Ubbelholde (27), and vonElbe (28). This subject will not be treated in detail here; only those aspects of the problem directly applicable to the present work will be discussed.

By far the largest proportion of chemical kinetics studies have been made in the region of low or moderate temperatures compared to the temperatures of normal combustion reaction (for example, extensive work on cool flames). These studies describe the combustion reactions in highly complex terms, and because of the relatively low temperatures involved, there is considerable doubt that these data can be extrapolated

to normal combustion temperatures. Furthermore, because of the primary interest here in the interaction of combustion and fluid flow, it is desirable to employ a much simpler picture of the chemical kinetics.

Such a simple picture of combustion kinetics is one in which it is hoped that a simple n th order reaction between fuel and oxygen will adequately describe the combustion kinetics. This assumption has been used by Longwell (13) and Avery (2) in the analysis of a well-stirred reactor. It is assumed that the reaction order is of α order in fuel and $n-\alpha$ order in oxygen and that Arrhenius form of activation energy represents the effect of temperature on the reaction rate.

Let the overall reaction between fuel and oxygen be:



and let ϕ times the stoichiometrically required fuel be used.

If the identifiable components of the mixture at any stage of completion of combustion are products of complete combustion, fuel, and oxygen, specification of a single quantity, for example β , the burned fraction of the fuel fed, together with the stoichiometry, is sufficient to identify the mixture. For each additional intermediate or competing reaction involving a new specie (or species), one more quantity, γ , δ , etc, must be specified to fix the composition; and the choice of how best to define the new term will depend

on the postulated chemistry of the process. The mole fraction, f_X , of any component "X" is thus representable as f_X ($\phi, \beta, \gamma, \delta, \dots$), or for a fixed value of ϕ , \bar{f}_X ($\beta, \gamma, \delta, \dots$), and the single argument β is sufficient for the simplest possible picture of the combustion process.

The well-stirred reactor is by definition a chamber in which the composition, measured at the inlet by $\beta_0, \gamma_0, \delta_0$, changes instantly to that measured by β, γ, δ ; and the composition is everywhere that of the outlet. In this system the temperature, T , is fixed by the exit composition and the inlet temperature T_0 (i.e. an adiabatic reaction), and for a fixed ϕ can be represented as \bar{f}_T ($\beta, \gamma, \delta, \dots, T_0$). For the simplest case in which the product composition and, consequently, T is assumed to be fixed by the single variable β , it is obvious that either β or T may be used as a measure of combustion progress or burnedness. Assumption of linearity between T and β , leading to the relation

$$\beta = \frac{T - T_0}{T_{af} - T_0}$$

(where T_{af} is the adiabatic flame temperature) simplifies numerical calculation, but is not necessary.

As many chemical rate equations are required as there are arguments $\beta, \gamma, \delta, \dots$ necessary to fix the composition. Additional rate equations will be required if alternative routes between reactants and products exist. The present

treatment is restricted to the simplest description of the combustion process, requiring only one rate equation. This is most conveniently the rate of consumption of fuel, given by;

$$-\frac{dN_F}{Vdt} = \sqrt{T} k' e^{-E/RT} C_{O_2}^{(n-\alpha)} C_F^\alpha \quad \text{II-2}$$

on the assumption that the reaction is of overall n th order and of α order in fuel. Substituting $\bar{f}_F(\beta)(P/RT)$ for C_F and $\bar{f}_{O_2}(\beta)(P/RT)$ for C_{O_2} , one has;

$$-\frac{dN_F}{Vdt} = P^n \frac{k' e^{-E/RT}}{R^{nT}(n-1/2)} \bar{f}_F^\alpha(\beta) \bar{f}_{O_2}^{(-\alpha)}(\beta) \quad \text{II-3}$$

Since T and β are uniquely related, Equation II-3 may be written:

$$-\frac{dN_F}{P^n V dt} = \psi_1(\beta) \quad \text{II-3a}$$

In a well-stirred reactor fed at the molal fuel feed rate G with the burnedness changing from an inlet value β_0 to an outlet value β , the fuel consumption rate is $G(\beta - \beta_0)$; this replaces $-dN_F/dt$. Therefore, Equation II-3a becomes;

$$\frac{G}{VP^n} = \frac{\psi_1(\beta)}{\beta - \beta_0} \quad \text{II-4}$$

and for a reactor being fed an unburned fuel-air mixture, this may be written:

$$\frac{G}{VP^n} = \frac{\psi_1(\beta)}{\beta} = \psi_2(\beta) \quad \text{II-5}$$

A typical curve representing Equation II-5 appears as Fig. II-2. The numerical magnitude of G/VP^n shown in Fig. II-2 is a consequence of the normalization proceeding and is not indicative of the actual values experimentally observed. The normalization of this curve is discussed in Appendix A.

It will be noted that there are three solutions to Equation II-5 for a given value of G/VP^n at low values of this quantity. Of these, only two may be experimentally found. The uppermost (solid line) solution represents the hot, stably-burning system, and the lowermost ($\beta=0$ axis) the cold, "non-reacting" system. Solutions along the dotted middle branch of Figure II-2 are thermally unstable, since if a reactor were operating on this section of the curve, a small perturbation in burnedness or flow rate would cause the reactor efflux either to move up to the top-most branch of the curve or to drop down to the lowest branch of the curve. As the feed rate is increased, the burnedness decreases, until a feed rate is reached where $d\beta/dG$ is infinite. This point represents the blowout feed rate, since beyond this feed rate the only solution to Equation II-5 corresponds to the "non-reacting" system. This blowout point is a unique function of the fuel/air ratio, and has been a basic measurement in the work which has been reported in the literature on the well-stirred reactor.

In applying the well-stirred reactor theory to experimental data, Longwell and Weiss (14) and Baker (3) have used

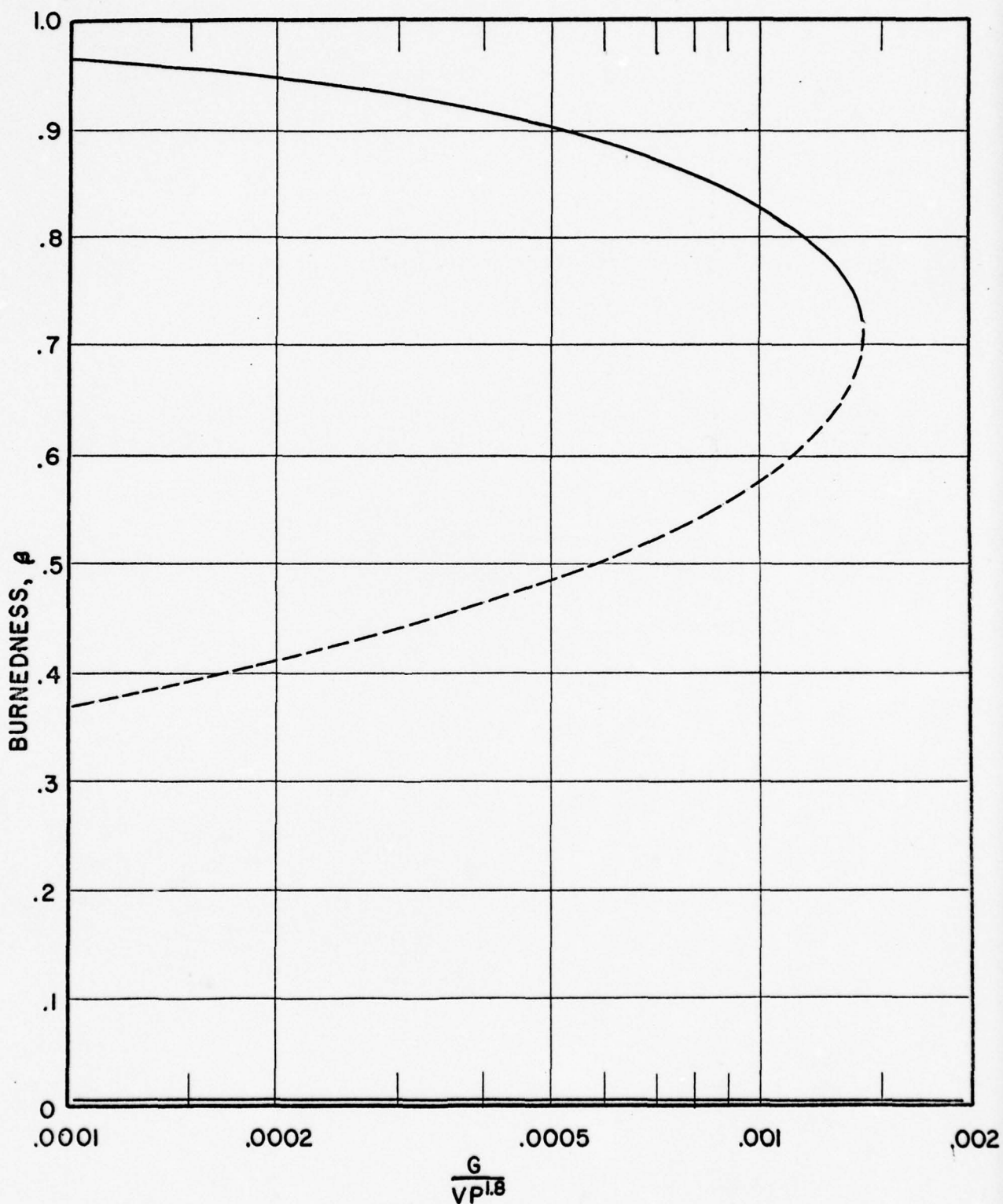
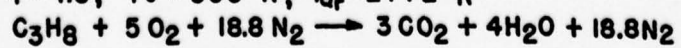


FIGURE II-2: WELL-STIRRED REACTOR PERFORMANCE

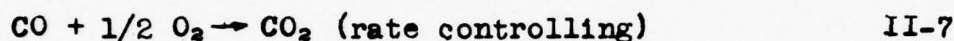
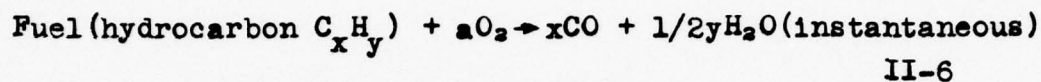
$\phi = 1.0$; $T_o = 500^\circ R$; $T_{af} = 2772^\circ R$



the simple (one rate equation) theory. In this approach no allowance is made for the existence of intermediate combustion products. Hence, any products of partial combustion are replaced by stoichiometrically equivalent quantities of unburned fuel and completely burned products such that the oxygen consumption efficiency remains unchanged. The burnedness, β , is defined in terms of this latter quantity in these experiments.

Since it is admittedly unrealistic to assume that there are no intermediate combustion products in the well-stirred combustor, both Longwell and Weiss and Baker have spent considerable effort in postulating stoichiometric and reaction schemes which will give a more realistic picture of the combustion products actually found. In the experimental work reported by Longwell and Weiss (14) gas analyses of samples drawn from the interior of the reactor were reported. These data show that very little unburned fuel appears in the reactor, and that only when the combustor is fed a rich fuel-air mixture do any appreciable quantities of hydrocarbons appear. In these samples the major unburned component reported is carbon monoxide, and hydrogen is the only other combustible reported in significant quantities for lean mixtures. Baker (3) in sampling data taken in another well-stirred reactor experiment confirms these observations.

Longwell suggested the following reaction equations to explain the data:

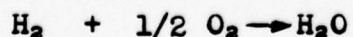
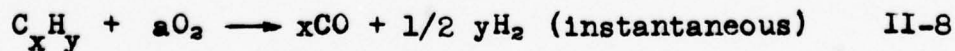


This scheme allowed Longwell to fit his fuel-lean data; however, it is not adaptable to fuel-rich data since there is insufficient oxygen to allow completion of the first step beyond a certain fuel-air ratio (depending on the carbon/hydrogen ratio of the fuel).

In fitting this reaction scheme to the simple well-stirred reactor equations (Equation II-5), one must be careful not to confuse the fractional oxygen consumption with the fractional carbon monoxide consumption. Since the rate-controlling reaction is equation II-7, the substitutions into II-5 must be appropriate to this stoichiometric equation. The fractional fuel consumption, β , is now defined as the fraction of CO available from the fuel which has been converted to CO_2 . Temperatures, accounting for the heat liberated by Equation II-6, and concentrations are calculated as a function of this redefined β . It should be noted that this definition of burnedness is different from oxygen consumption efficiency, since at zero CO consumption the oxygen consumption efficiency is that

required to react all of the fuel to CO and H₂O. Baker points out that proper substitution into Equation II-5 leads to the conclusion that for near-stoichiometric mixtures on the lean side, enough heat is liberated by reaction II-6 to prevent blowout of the reactor, no matter how fast it is fed. Longwell's correlation of his lean blowout data, unfortunately, confuses this distinction. Although his theoretical blowout curve extends to stoichiometric fuel-air ratio, close examination of this derivation reveals that an improper substitution was made for β in the denominator of Equation II-5.

Baker suggested two additional reaction schemes, one for the rich side and one for the lean side. Because of the anomolous behavior of the reaction scheme of Equations II-6 and II-7 (i.e. no blowout found near stoichiometric), Baker suggested an alternative scheme in which there was less heat liberated in the first stage of the reaction. This scheme is as follows:



and the restriction is placed on II-9 that:

$$\frac{(CO)(H_2O)}{(CO_2)(H_2)} = k_{wg} \quad \text{II-10}$$

where k_{wg} is the water-gas equilibrium constant at the temperature of the reactor.

On the rich side it is postulated that fuel and oxygen are consumed in the same ratio as the prevailing fuel/air ratio to form the equilibrium mixture of carbon monoxide, carbon dioxide, hydrogen and water. This scheme is the same as that proposed by Longwell and Weiss for rich mixtures.

In Baker's lean-side reaction scheme, II-8 to II-10, there is a much lower temperature rise in the first step than in the scheme proposed by Longwell and Weiss, and Baker was able to calculate blowout rates from this mechanism for all lean fuel/air mixtures. However, it was pointed out that the ratios of CO , CO_2 , H_2 and H_2O experimentally found in the gas samples did not correspond to water-gas equilibrium.

Edgerton, Saunders, and Spaulding (8) have discussed the well-stirred reactor theory in general, and they have pointed out some of the implications of the simplified theory dealt with thus far. The composition of a partially burned mixture has been defined by a single quantity. This definition was originally restricted to that case where the rate-limiting step in the combustion of fuel was the initial reaction between fuel and oxygen. However, in any reaction scheme in which a single reaction is the rate-limiting

step, the composition of the mixture may be uniquely defined by a single argument such as β . Thus, a partially burned mixture whose composition is measured by β may be obtained either by partial combustion to this composition or by mixing unburned fuel/air mixture with completely burned gases. In this latter case, all instantaneous reactions must be allowed to occur (e.g. the conversion of hydrocarbon to CO and H₂O, Equation II-6) without any conversion of the reactants involved in the rate-limiting step. This postulation that the composition of a partially burned mixture is uniquely defined by a single parameter is of fundamental importance in calculating the behavior of combustion chamber models.

DeZubay (6) has called attention to an ambiguity in the meaning of "burnedness" which arises from Baker's and Longwell's assumption of stoichiometry for rich fuel-air mixtures (e.g. fuel and oxygen disappear in the same proportion as the prevailing fuel/air ratio). For this stoichiometry a burnedness of unity for a rich fuel-air mixture corresponds to a mixture in which there are no unreacted hydrocarbons, in conformity with the experimental facts. It is evident, however, that the result of mixing a completely burned rich and lean mixtures would be a mixture in which further combustion could occur. DeZubay has suggested that this ambiguity in the meaning of burnedness

can be clarified by the use of a "fuel availability factor" in addition to "burnedness" to specify the composition of the mixture. This composition variable permits one to account for the additional combustion which could occur if air or a lean fuel-air mixture is mixed with a burned or partially burned rich mixture.

The introduction of multi-step reactions with more than one rate constant and composition variable considerably complicates the stirred reactor problem. This possibility has not yet received adequate attention in the literature. Edgerton, Saunders and Spaulding (8) in their paper discuss this problem qualitatively. They point out that so long as one of the reaction rates is substantially slower than the others the simple formulation of the stirred-reactor problem is still valid. They further suggest that near the completion of the combustion process, a single reaction predominates, thus making valid the assumption that composition is independent of the path by which the burnedness is reached. In the intermediate ranges of burnedness, however, it is postulated that the assumption of only one significant rate constant is unjustified. If more than one rate constant is required to describe the combustion reaction, then, in the general case, the composition and temperature are not uniquely defined by a single variable, but they depend on the path by which a given burnedness level is

reached. To allow for variation in the burning rate at a given temperature, Edgerton, Saunders and Spaulding suggest a "band of uncertainty", which includes all possible burning rates corresponding to a given temperature level.

Behavior of Plug-flow and Staged Stirred Reactors

Because the performance of two-stage stirred reactors, multi-stage stirred reactors, and plug-flow reactors are all derivable from the same basic rate equation, (Equation II-5), they are all derivable from one another. Consider first the plug-flow reactor. Such a reactor may be pictured as an infinite series of infinitesimal well-stirred reactors. Since the flow rate through each of these is the same, they are best considered as stirred reactors in which volume is the independent variable. Equation II-5, restricted to the case where only the single argument β is required and for constant pressure operation, is inverted to give:

$$\frac{VP^n}{G} = \frac{\beta - \beta_0}{\psi_1(\beta)} \quad \text{II-11}$$

A typical slab of a plug-flow reactor, having a volume of dV , being fed with reactants of composition β , and discharging products of composition $\beta + d\beta$, is represented by Equation II-11 with V replaced by dV and the accomplished

burnedness, $\beta - \beta_0$, by $d\beta$;

$$\frac{P^n}{G} dV = \frac{d\beta}{\psi_1(\beta)} \quad \text{II-12}$$

If the reaction rate function, ψ_1 , is available, as for example from a postulated chemical mechanism of combustion, Equation II-12 may be integrated directly to give the performance of a plug-flow reactor. If, on the other hand, data are available from a stirred reactor experiment in the form of $\psi_2(\beta)$ ($\psi_2 = \psi_1/\beta$), then the stirred reactor relationship may be used to integrate II-12:

Equation II-12 may be written:

$$\frac{P^n}{G} dV = \frac{\beta}{\psi_1(\beta)} \frac{d\beta}{\beta} = \frac{1}{\psi_2(\beta)} d \ln \beta \quad \text{II-13}$$

or, integrating between the limits $\beta=\beta_0$, $V=V_0$ and $\beta=\beta$, $V=V$:

$$\frac{P^n}{G}(V-V_0) = \int_{\ln \beta_0}^{\ln \beta} \frac{d \ln \beta}{\psi_2(\beta)} \quad \text{II-14}$$

If, one plots the stirred reactor performance curve in the form $1/\psi_2(\beta)$ vs β on a logarithmic scale, the area under the curve from β_0 to β (see Fig. II-3 with x and y coordinates reversed to correspond to previous plots) represents the generalized volume $(V-V_0)P^n/G$ necessary to carry out that much reaction in plug-flow; and that area

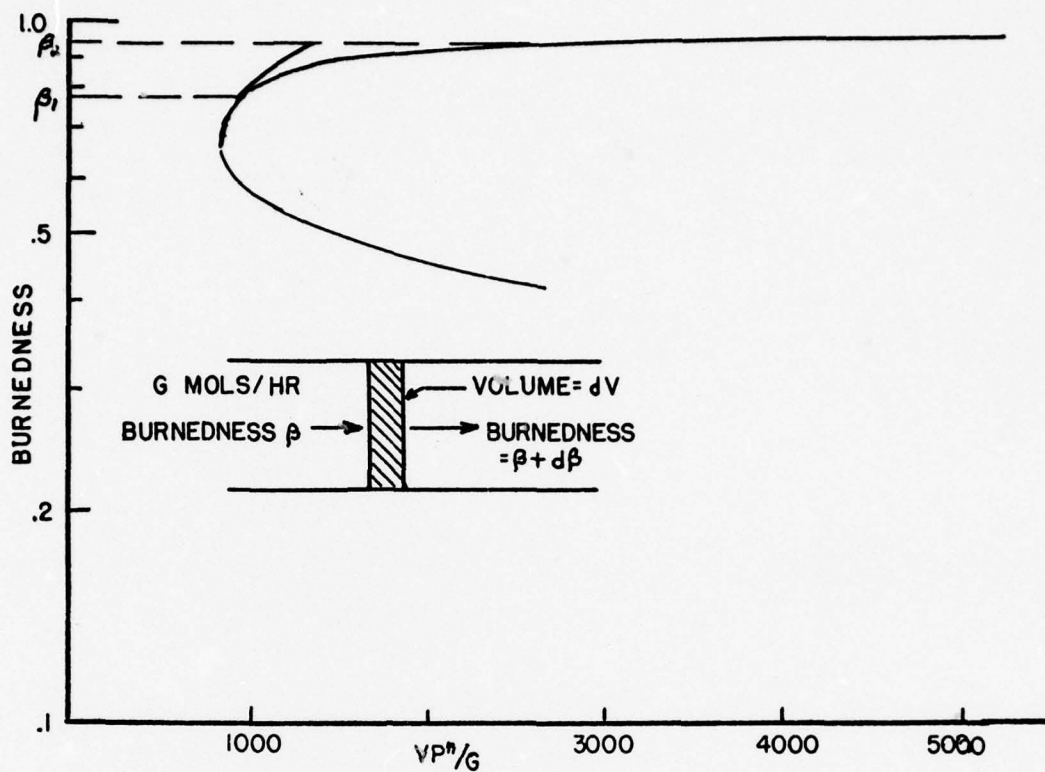


FIGURE II-3: INTEGRATION OF WELL-STIRRED REACTOR CURVE TO FIND PLUG-FLOW REACTOR PERFORMANCE

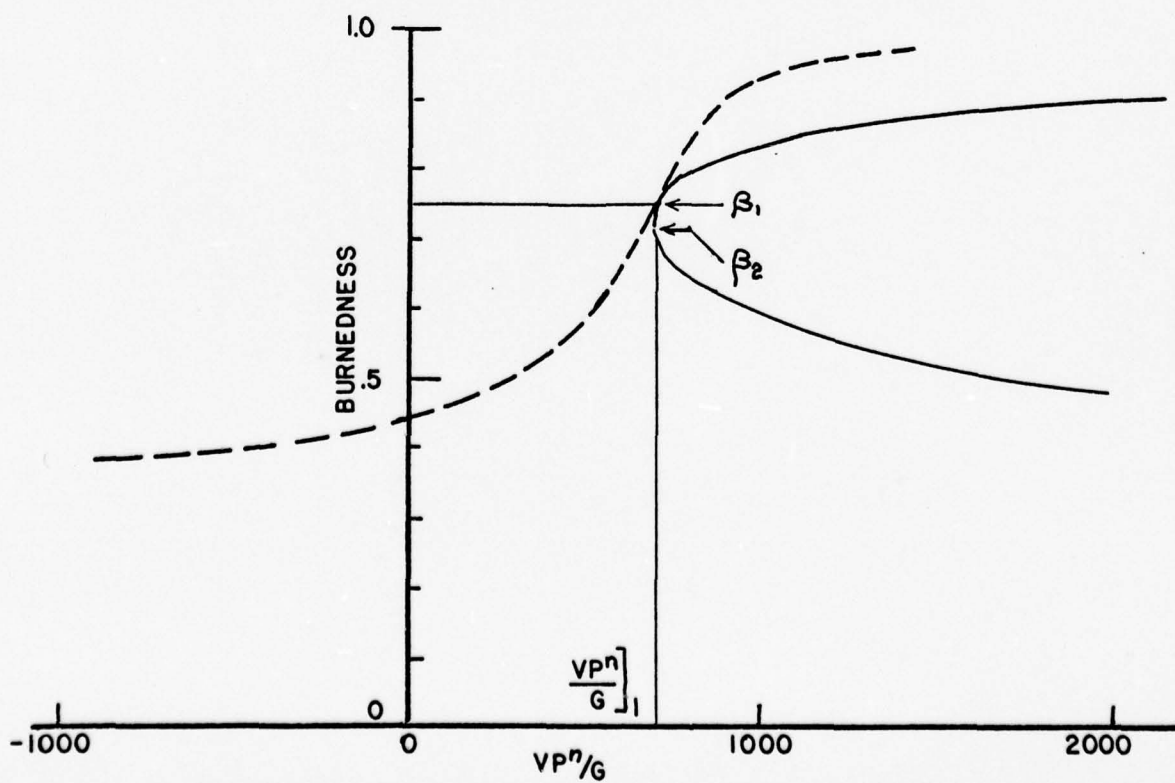


FIGURE II-4: PLUG-FLOW REACTOR CURVE (DOTTED)

can be plotted on the same plot (dotted line). In Figure II-4 the results of integration over the full range of β is shown on arithmetic coordinates (dotted line) together with the basic stirred reactor curve. The plug-flow curve has been displaced laterally to be tangent to the stirred-reactor curve at a generalized volume of VP^n/G_1 , the significance of which requires comment: On a plot of β vs VP^n/G on arithmetic coordinates, the point of tangency to a line from the origin represents a stirred reactor operating at the maximum possible rate per unit volume, and the condition for this point is:

$$\frac{\beta}{1/\psi_2(\beta)} = \frac{d\beta}{d[1/\psi_2(\beta)]} \quad \text{II-15}$$

Differentiating Equation II-5 and II-14 with respect to volume (these are the curves represented on Figure II-4), one obtains:

$$\frac{P^n}{G} \frac{dV}{d\beta} \Big|_{\text{WSR}} = \frac{d[1/\psi_2(\beta)]}{d\beta} \frac{P^n}{G} \frac{dV}{d\beta} \Big|_{\text{PFR}} = \frac{1}{\psi_2(\beta)} \frac{d \ln \beta}{d\beta}$$

Noting that the point where these two slopes are equal is given by:

$$d(1/\psi_2(\beta)) = d \ln \beta / \psi_2(\beta) \quad \text{II-16}$$

one sees that tangency occurs at the β , V combination corresponding to the maximum burning rate in a stirred

reactor. Note that for any value of β above β_1 , the incremental volume in a plug-flow reactor is less than in a well-stirred reactor, but to increase the burnedness from any point lying between β_2 , the stability limit of the stirred reactor, and β_1 to the value β_1 , a greater volume is required in a plug flow reactor than in a well-stirred reactor. For points below β_2 the well-stirred reactor is unstable. The minimum total volume required to accomplish any burnedness lying above β_1 is, therefore, the sum of the volume of a well-stirred reactor operating to give products at β_1 followed by a plug-flow reactor to reach the burnedness β .

It is noticed that the plug-flow curve of Fig. II-4 looks very much like the profile of a laminar flame front in which burnedness has been plotted against L/S_L , the measure of time. However, in the calculation for Figure II-3 there is no allowance for diffusion of heat or mass such as gives rise to a laminar flame propagation rate, and although the abscissa has dimensions proportional to a length/flame speed ratio, there is no definite distance associated with the abscissa; consequently, there is no clear analogue to flame propagation.

The performance of a well-stirred reactor being fed a partly burned feed is readily obtained from the primary stirred reactor curve such as Figure II-5, in which β is

plotted against $1/\psi_2$ (equal to VP^n/G). The slope of a line from the origin to a point on the curve represents the burning rate per unit volume in any system in which the burnedness is β . Since when the feed is partially burned, the burnedness to be accomplished is $\beta - \beta_0$ rather than β , the generalized volume necessary is $(VP^n/G) (\beta - \beta_0)/(\beta)$. This appears in Figure II-5 as $\Delta(VP^n/G)$. Figure II-5 can also be considered an example of operating two reactors in series. The first reactor, fed with the unburned fuel ($\beta_0 = 0$), requires the volume $V_1 P^n/G$ to deliver products of composition β_1 , and the second reactor, fed with products of burnedness β_1 and delivering products of burnedness β_2 , requires the additional volume $\Delta(VP^n/G)$. Application of this principle leads directly to the following conclusions for a pair of stirred reactors: (Note the inset in Figure II-5. Two lines to the origin have been drawn, one tangent to the nose of the curve, and the other passing through the blowout point of the curve.) For cases where the burnedness leaving the second reactor lies above point "C", and all combinations of reactor pairs will require less volume than a single stirred reactor giving the same final burnedness. If the burnedness leaving the second reactor lies between points "B" and "C" it is always possible to have a pair of reactors operating more favorably than a single reactor, although not all reactor

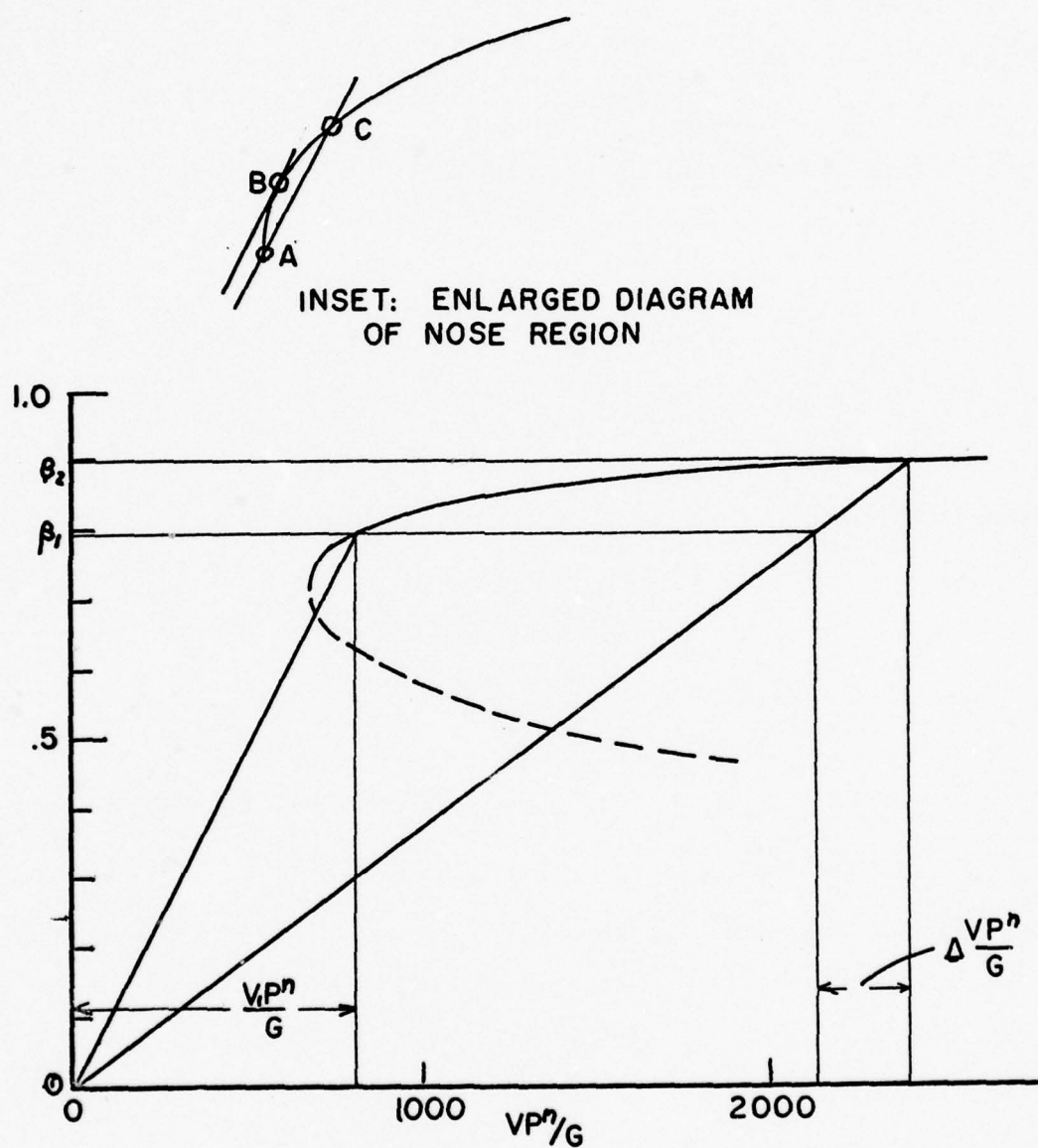


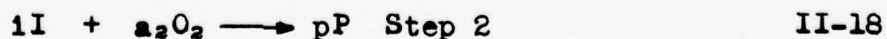
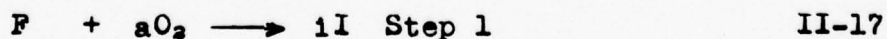
FIGURE II-5: STAGED WELL-STIRRED REACTOR OPERATION

pairs in this range are better. If the final burnedness leaving the second reactor lies between "A" and "B" there is no possible combination of reactor pairs which requires less total volume than a single reactor.

Staged Reactors with Intermediate Reactions

The discussion of reactor combination has been limited, thus far to the case where only one composition variable is required to describe the mixture. If two or more variables are required, the treatment of staged reactors is considerably complicated. The problems involved are best illustrated by consideration of a simple case.

Consider a combustion process in which fuel is partially oxidized in the first step to form "i" moles of an intermediate "i" and "I" then reacts with additional oxygen to form complete combustion products. For this reaction two rate equations are required.



$$-\frac{dN_F}{Vdt} = \sqrt{T} k_1' e^{-E_1/RT} C_F^{a_1} C_{O_2}^{n_1-a_1} \quad \text{II-19}$$

$$-\frac{dN_I}{dt} = 1 \left[\sqrt{T} k_2' e^{-E_2/RT} C_F^{a_2} C_{O_2}^{n_2-a_2} - T k_1' e^{-E_1/RT} C_F^{a_1} C_{O_2}^{n_1-a_1} \right] \quad \text{II-20}$$

In a manner similar to the previously discussed equation for the simple stirred reactor kinetics, these equations may be reduced to functions of two variables β and γ , representing the progress of reaction of steps 1 and 2 respectively:

$$\frac{G}{VP^n} (\beta - \beta_0) = f_1(\beta, \gamma) \quad \text{II-21}$$

$$\frac{G}{VP^n} (\gamma - \gamma_0) = f_2(\beta, \gamma) \quad \text{II-22}$$

Simultaneous solution of these equations is required to find the performance of a one-stage stirred reactor at any given feed rate. If it is desired to operate a two-stage reactor, the gas composition of the final stage, in general, will not be the same as the composition of a one-stage reactor whose exit temperature (or fractional oxygen consumption) is the same; and a second simultaneous solution is required for the β_0, γ_0 combination corresponding to the partially burned gases leaving the first stage.

To simplify calculations of these equations it is desirable to represent graphically the simultaneous solutions obtained from any given β_0, γ_0 starting combination (obtained in an unspecified manner). The composition of the exit gases from any reactor may be represented on a diagram of β vs γ for this two reaction postulated mechanism. On this same diagram lines of $\beta \gamma$ combinations

having a constant ratio of the relative disappearance rates of fuel and intermediate may also be mapped ($d\beta/d\gamma = C$) (Figure II-6). Thus, in a stirred reactor whose outlet composition is represented by β γ , the $d\beta/d\gamma$ in this reactor may be read directly from this diagram, and this ratio must be equal to the ratio of $(\beta - \beta_0)/(\gamma - \gamma_0)$ in that reactor. Therefore, for any combination representing either outlet or inlet conditions of a stirred reactor, lines representing possible inlet or outlet β, γ combinations may be plotted. Having found the inlet and outlet conditions from a diagram such as Figure II-6, recourse to either Equation II-21 or II-22 will give the volume required in that reactor. These equations may be represented graphically to speed calculations (Figure II-7).

Using these two plots the performance of any desired combination of plug-flow and stirred reactors in which a two-step kinetic scheme is postulated may be calculated. It is evident, however, that the addition of a third variable would complicate the problem still further. Because of the unwieldy calculation required for rigorously treating the combination of stirred reactors with multi-step reactions, one must hope that a simple one-step reaction scheme will provide an accurate enough representation of the gross kinetics to permit calculation of model performances. This will be true, if, as suggested by Edgerton, Saunders

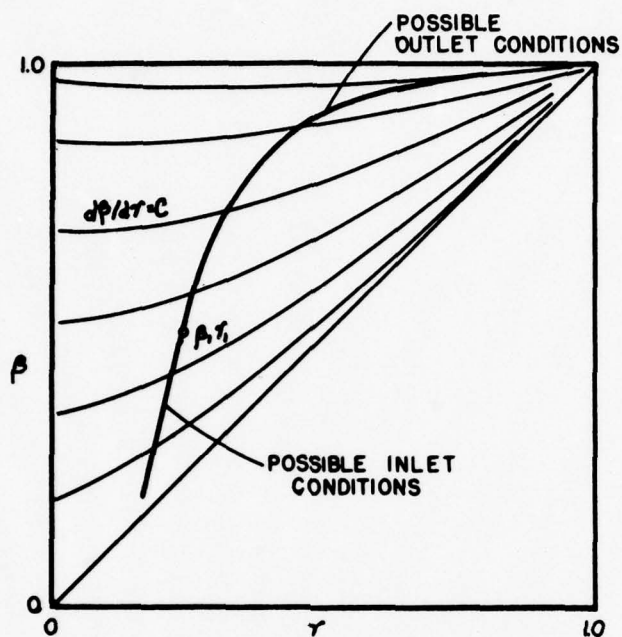


FIGURE II-6: LINES OF $d\beta/d\tau = C$. TYPICAL PATHS OF REACTOR COMPOSITION FOR A TERMINAL CONDITION (INLET OR OUTLET) OF β, τ SHOWN

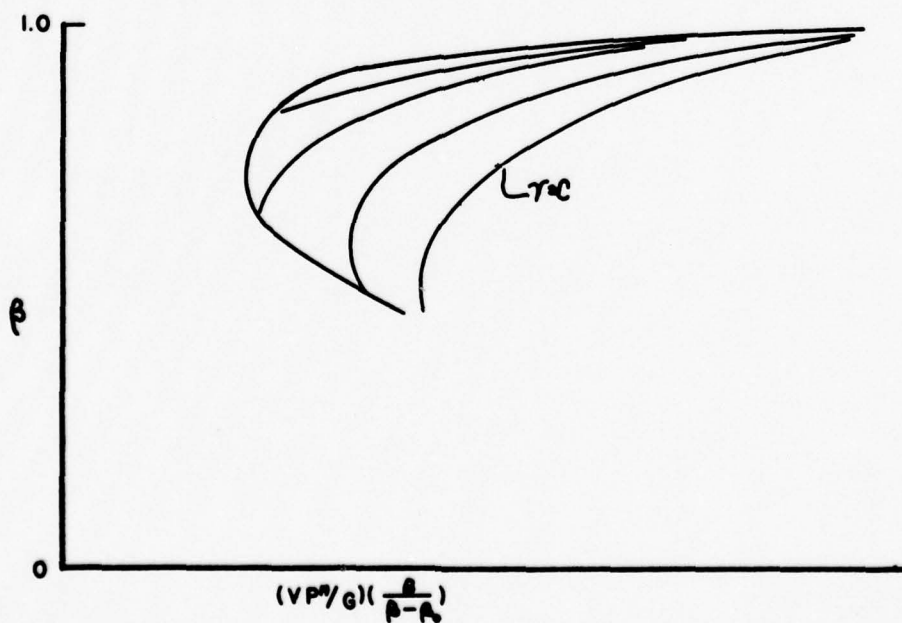


FIGURE II-7: VOLUME REQUIRED FOR GIVEN INLET & OUTLET CONDITIONS

and Spaulding, one reaction predominates over all others in the range of practical interest.

Experimental Stirred Reactor Performance

Experimentally, the study of the stirred reactor in combustion problems presents primarily the problem of mixing fresh feed gases with the gases in the reactor at an extremely high rate. This high mixing rate is required to mix the gases before a significant amount of reaction can occur. This obviously cannot be accomplished by simple mechanical stirring. After some developmental work, Longwell and Weiss (14) proposed the now familiar stirred reactor in which a combination of intense turbulence and gross recirculation, caused by a large number of small jets issuing from a small concentric sphere into the spherical reactor, mix the reacting gases moderately well.

The data which have been published on this device have been primarily blowout data. Three investigators (3, 5, 14) have studied blowout loading factors as a function of fuel-air ratio in reactors of this design. Longwell and Weiss (14) were the first to study this. They reported a pressure exponent of 1.8 as giving the best correlation

of their data, and they claimed that there was no significant effect of hole size. Baker, in a somewhat later investigation, reported a trend of pressure exponent with fuel-air ratio and recommended a pressure exponent of 1.3. He also found a consistent effect of hole size. Because of the differences in the results reported by Longwell and Weiss and by Baker, Blichner (5) conducted a further investigation on Baker's reactor. Blichner's results substantiated those of Baker. He found an exponent lower than that reported by Longwell and Weiss, and showed a significant effect of hole size. A comparison of the blowout data reported in these three investigations is shown in Figure 11-8. Throughout this thesis data of this type are reported on coordinates of air loading rate, $N_A/V P^{1.8}$, and generalized fuel fraction F . This latter quantity is given by $\phi/1 + \phi$, where ϕ is the fraction of stoichiometric fuel. F is 0.5 for a stoichiometric mixture, lean mixtures are less than $F = 0.5$, and rich mixtures greater. In this comparison all three sets of data are shown for a pressure exponent of 1.8, and no distinction between hole size is made. All three sets of data are corrected to an inlet temperature of 300°K using the temperature correction factors suggested by Longwell and Weiss.

Both Longwell and Weiss and Baker have reported sampling data. Sampling traverses were made along a

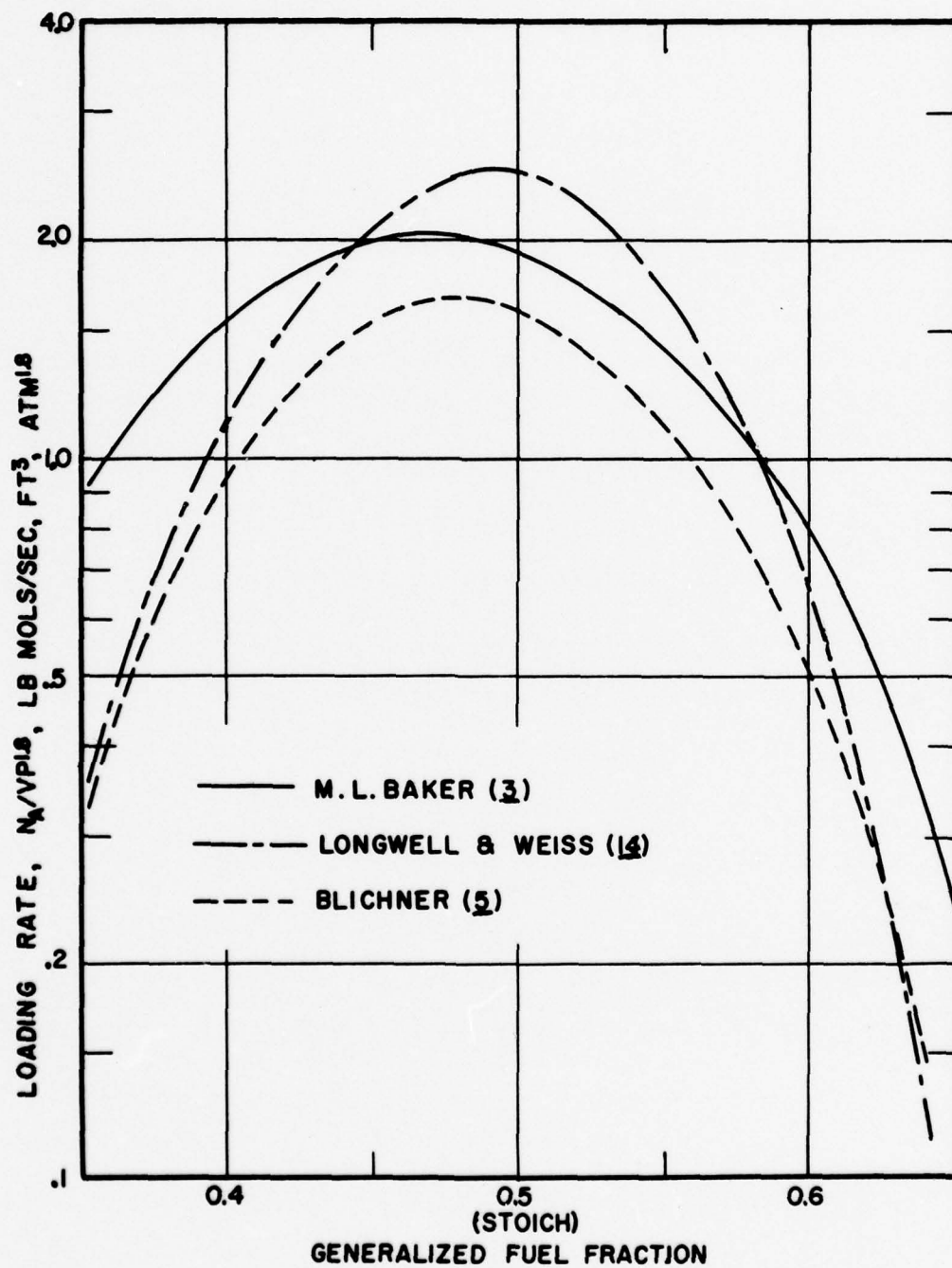


FIGURE II-8: STIRRED REACTOR STABILITY LIMIT DATA, CORRECTED TO AN INLET TEMPERATURE OF 300°K.

radius of the reactor to determine to what extent composition varied within a reactor. Longwell and Weiss reported that the composition was substantially constant over about 95% of the volume. Baker points out, however that for their sampling runs the burnedness level in the reactor was high (over 90%), and consequently even if there were a composition change it would not be great. Longwell and Weiss' data if plotted on percent unburned basis show a much greater relative change in composition within the reactor. Since measurement of the variation in burnedness at high burnedness levels is not a very sensitive measure of the mixedness of the reactor, Baker proposed to measure the variation of burnedness within the reactor at a loading factor near blowout. He found a greater variation of burnedness with position as might be expected with this more stringent test, but even so, the reactor still appears to be moderately well-mixed.

Despite the evidence of the effect of hole size and of sampling traverses that the reactor is not completely mixed, the stirred reactor still remains a useful device for studying the overall kinetic behavior of burning gases since the evidence indicates that the mixing is rapid enough so that chemical reaction rates are the predominant phenomena controlling the reactor performance. Thus, using the blow-out data of the stirred reactor, it is possible to

evaluate both a pseudo-collision constant and a pseudo-activation energy for the reaction. These quantities, though representing the gross reaction rather than the detail of the individual stages of the combustion process are useful in the evaluation of various fuels and in the prediction of practical combustor performance.

In addition, Longwell and Weiss have reported sampling runs in which combustion efficiency as a function of loading factor for a constant fuel-air ratio was measured. These data showed a poor agreement with the theoretical curve for a simple bi-molecular collision process with reaction rate constants predicted from blowout data. However, other than this one bit of data, no work appears to have been done on the operating characteristics of the stirred reactor within the stable combustion region. In the application of stirred reactor data to the prediction of practical combustor performance, it is necessary to have such information since combustion efficiency as well as combustor stability is important in chamber operation and design. Since the requisite data of feed rate vs efficiency are not available, a calculated curve will be used here. The curve is the one shown in Figure II-2. This curve was calculated using combustion stoichiometry in which propane is burned to CO_2 and H_2O in one step. A stoichiometric mixture was postulated with an inlet temperature of 500°K ,

a flame temperature at complete combustion of 2772°K , and an activation energy of $40,000 \text{ cal/mol}$. The magnitude obtained of the quantity G/VP^n is a consequence of the normalizing procedure used in calculating this curve, and these values must be multiplied by a constant factor to make the blowout value correspond to the observed blowout rate for a stirred reactor.

Combustion Chamber Models in the Literature

Based on the performance of the stirred reactor various simple combinations of reactors can be postulated and their behavior calculated. Some models of this type have already been presented and discussed in the literature. Postulation of such models may have as objectives: (1) In theoretical studies one may attempt to find the ideal or optimum performance which can be expected from combustion chambers, and (2) In the study of real combustor performance one may seek to find a simple combination of combustor elements which will describe the performance of the chamber under study with respect to changes in the various operating or design variables. Several examples of the former type have appeared in the recent literature.

Avery and Hart (2) considered a model of a can-type combustor in which a pre-mixed fuel-air mixture was fed into the can. The combustor was piloted in an unspecified manner by a partly burned stream of the same fuel-air ratio

as the fresh feed to the can and of the same burnedness as the gases leaving the can. The rate of feed of the fresh fuel-air mixture along the length of the combustor was so adjusted that the composition within the can remained constant.

Since under these restrictions the composition of the gases in the combustor is the same throughout, the burning rate within the chamber was calculated directly from well-stirred reactor principles. In addition the pattern of fuel-air mixture injection required to maintain this optimum condition was calculated. Although no experimental work has been reported on this model it is of interest since it is the first such proposed use of basic stirred reactor information.

In this original model of Avery and Hart no allowance was made in the energy balance for the effects of directed-velocity kinetic energy. In a later paper Rosen and Hart (19) proposed a modification of this model to account for kinetic energy effects. These authors considered a straight, tubular combustor piloted by a partially burned gas in the same manner as in the Avery and Hart model and fed with fresh fuel-air mixture through the combustor walls in such a manner as to maintain a constant static temperature within the chamber. These authors then wrote differential equations of continuity, and momentum and energy balances. From these it is possible to derive:

(1) the maximum throughput of unburned gases permitted by the assumption of constant static temperature (this is not blowout, but analogous to "choking" in compressible flow); (2) the relation required between kinetic energy, temperature and combustion efficiency, and (3) the minimum temperature (or maximum amount of enthalpy which may be put into kinetic energy) allowing stable combustion for a conventional n th order reaction.

The restriction of this model to a constant temperature case and the restriction of the Avery and Hart model to a constant efficiency case makes these models of relatively small value in analyzing the behavior of real combustors.

DeZubay (6) suggested a different approach to the modeling problem. He considered a combustor to which a rich fuel-air mixture was fed, and after combustion was partially completed, additional secondary air was added.

This problem was approached by considering the chamber to be divided into two portions, each a well-stirred reactor. The first portion was fed the rich fuel-air mixture, and the second received the partly burned products from the first chamber plus secondary air. In this model DeZubay demonstrated that it was possible for two stirred reactors to give a higher overall heat release rate than a single reactor fed the same overall fuel-air mixture and operating under the same conditions as the final reactor of the pair.

However, the force of this conclusion is somewhat clouded by the effects of the addition of secondary air.

The results which DeZubay presented also showed the quenching effect of adding air to the partly burned gases. It was shown that the addition of a large enough quantity of air would quench the reaction in the second reactor. Curves were given of heat release rate vs combustion efficiency leaving second reactor for various values of fuel-air ratio in the first of the two reactors. In all cases calculated by DeZubay the fuel-air ratio in the second stage and the relative volumes of the two stages were the same. For those cases where a large amount of secondary air was added more than one blowout point was found; i.e. as feed rate increased the second stage became unstable, and further increases in feed rate caused the first stage to blow out. It was also found, as might be expected, that the best operating conditions -- maximum heat release rates -- were found when the first stage had a fuel-air ratio of stoichiometric.

The models discussed thus far have treated the combustion chamber problem without cognizance of the effect of flow recirculation on combustion chamber performance. Since recirculation is generally postulated to have an important role, especially in combustor stability, any chamber model which is to be representative of combustor performance must

make allowance for the effect of recirculation. In a recent paper Spaulding (24) has presented an analysis of combustion chamber pressure drop requirements which does account for the effect of recirculation.

Spaulding considered a combustion chamber in which the gases flowed in a circulatory manner. Part of the chamber was devoted to a mixing section in which fresh, unburned gases mixed with recirculated gases; a portion of the mixture was recycled and a portion left the chamber as burned products. No combustion was postulated to occur in the mixing section. The remainder of the chamber was called the recirculation zone, and combustion occurred in this region as the gases recirculated in a plug-flow fashion.

Using an assumed stirred reactor performance curve, Spaulding could then calculate the performance of the model in response to changes in either firing rate or recirculation ratio. This model is very similar to the one proposed in this work for modeling combustion chamber performance. To facilitate comparison, Spaulding's model has been recalculated using the stirred reactor curve which was used through this work. The performance of Spaulding's model is shown in Figure II-9.

Although no experimental work was done directly on this model, Spaulding made some comparison of the model performance with the performance of some combustor

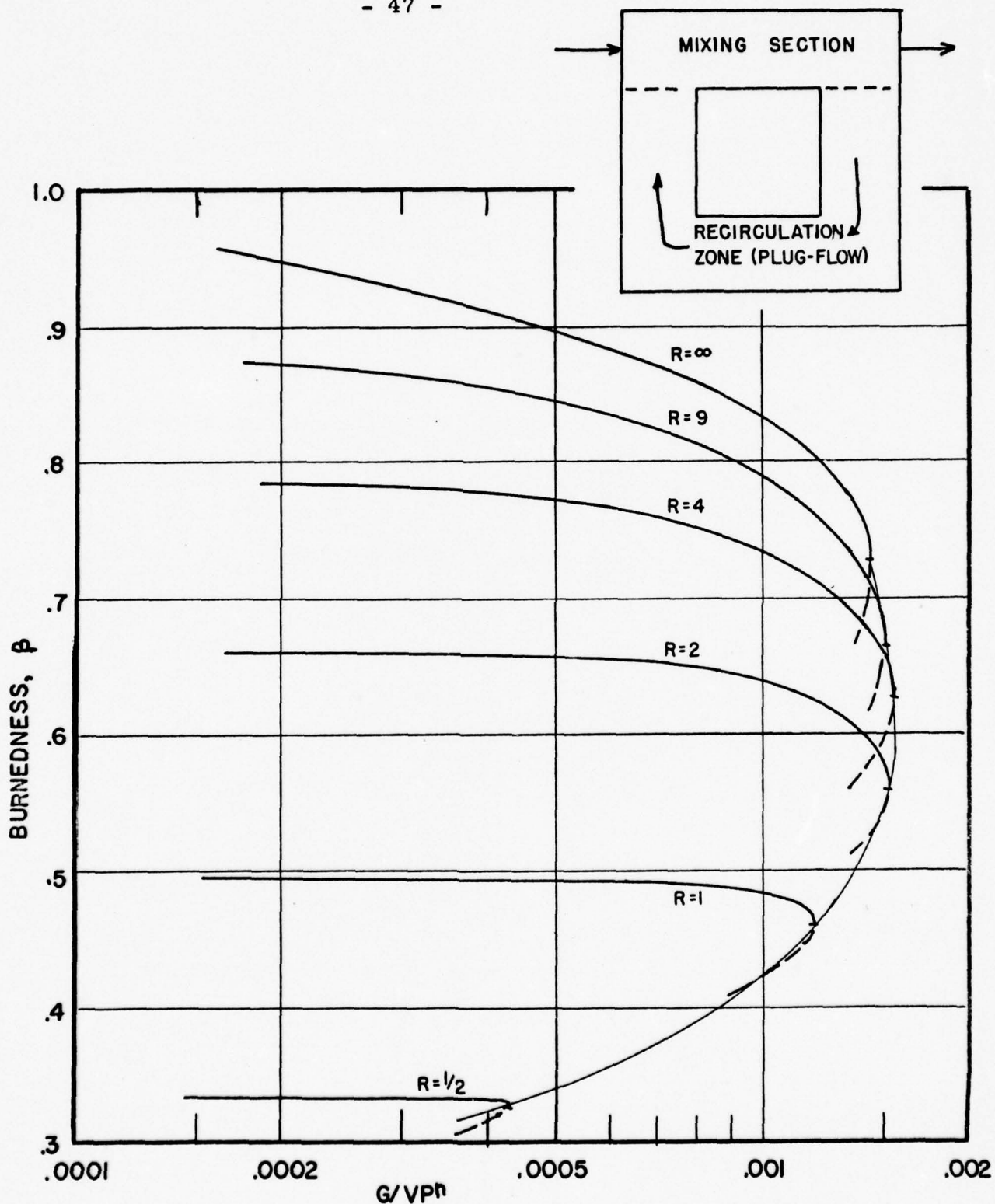


FIGURE II-9: RECALCULATED PERFORMANCE OF SPAULDING'S SIMPLE MODEL (24)

$$R = \frac{\text{MOLS GAS RECIRCULATED}}{\text{MOL FRESH GAS FED}}$$

configurations in his electric analogue to combustion (23). Because of differences between the model and combustor configurations, it was not expected that a good correlation would be obtained, however, the results of this comparison were encouraging.

Spaulding also considered an application of this model technique to the well-stirred reactor. From an assumed flow pattern of the jet, a model was established in which the outwardly-flowing cold gases received recirculated gases from the reverse-flowing recirculating gases in a continuous manner. The recirculation ratio was related in this model to the down-stream distance from the jet nozzle. Spaulding concluded from this analysis that the well-stirred reactor design suggested by Longwell and Weiss was, in fact, capable of producing moderately well-mixed zones, although there was some departure from the ideally well-mixed reactor performance.

One additional model of combustor performance has been proposed by Berl, Rice and Rosen (4). They analyzed the volume requirements for relatively low intensity combustion in terms of an extended laminar flame front theory. This model is not closely related to the models to be discussed here and will not be considered further.

Summary

In recent years it has become evident that the analysis of high-output combustor performance must take into account the rate-limiting effect of chemical reaction as well as the effect of mixing. However, it was not until the concept of grossly simplified kinetics was applied to combustion problems that the required analysis became practical. The development of an experimental stirred reactor has permitted the gross kinetic constants in such a simple analysis to be estimated. The availability of stirred reactor performance data has tempted some investigators to devise conceptual models of practical combustor performance in terms of stirred reactor combinations. With one exception, however, no allowance has been made for the effect of recirculation, nor has much experimental work been done to test the validity of these models. In this thesis some new models of combustor performance are proposed and compared with experimental combustor performance.

CHAPTER III

MODELS OF COMBUSTION CHAMBERS

The classical analysis of combustion chambers has been in terms of flame speeds. From the spreading angle of a stabilized flame in a duct and a knowledge of the stream velocity the velocity of the turbulent flame in its normal direction is calculated. The classical analyst then attempts to relate this turbulent flame speed to the laminar flame speed of the combustible mixture and to the turbulence level in the chamber which is assumed to cause extension of the area available for flame propagation.

In more complex chambers it is difficult to extend this analysis, since as the heat output rate of a chamber increases it becomes more difficult to define a meaningful boundary to represent a time-average flame front. As one approaches the chemically limiting rates in a device such as a well-stirred reactor it becomes difficult to justify the use of an extended flame-front model since substantial regions of the combustor are given over to homogeneous combustion.

The analysis of this latter class of chambers can be stated in terms of well-stirred reactor performance. Using stirred reactor data to give the burning rate, or fuel consumption rate per unit of volume, as a function of

temperature and a variety of composition variables, the continuity equation for a differential segment of chamber volume can be written. The time-rate of accumulation of each chemical specie plus the rate of creation or destruction of that specie by chemical reaction is equated to the diffusive and convective fluxes of the specie into the chosen control volume. An equation of this sort must be written for each of the species present and the resulting set must be solved either with an apriori knowledge of the fluid-flow pattern or with the momentum balance differential equations for the same control volume. Considerable simplifications of these equations must be made for a practical solution even in the simplest of chambers.

As an alternative analysis, one may imagine that relatively large regions of the combustor may be assigned average compositions which will give the burning rate in each region, and that these compositions may be related to the feed rate and composition of gases entering each zone. From a knowledge of the fluid-flow pattern the interchange of material between zones may be evaluated and the performance of the chamber synthesized.

A trivial model might consist in identifying the modest performance of a practical combustor with that of a well-stirred reactor operating at the same efficiency and firing rate but of much smaller volume, and in making the

assumption that the departure of the practical chamber from well-stirred reactor performance is due solely to incomplete use of the volume available. One would not expect so simple a model to fit over any extreme range of operating variables. If, however, one were to postulate a combustor composed not of just a single well-stirred volume and a single inactive volume but of a small number of volumes characterized as well-stirred or plug-flow elements, representing various regions of the real chamber connected in a combination of series, parallel, and recirculating flow patterns which is representative of the chamber flow pattern, one could expect such a conceptual model to predict the performance of a real chamber over a much wider range of operating variables. Simplicity in these models is paramount, for only if the model consisted of a small number of interacting elements would the results be impressive.

In any real combustor several types of zones are expected. With a jet of fuel-air mixture feeding a chamber, one expects the central core to be a relatively unburned zone. Around the sides of the jet the more nearly burned gases in the recirculation zones are in a well-mixed region because of the intense turbulence created by the central jet. In the corners of the chambers, regions of inactivity are expected since these regions are relatively stagnant. If the fuel and air are fed separately into a moderately

well-mixed chamber, similar zones are expected. In this case one would also expect to find variations in the fuel/air ratio in the various portions of the chamber.

In these models values must be assigned to the relative rates of interchange between the various zones and to their relative sizes. The magnitude of the variation in the fuel/air ratio, if any, must also be chosen. These values are associated with chamber design variables, and to the extent that reasonable values may be associated with the theoretical models, the models may be held to be successful.

Three conceptual models have been developed which predict some of the phenomena of practical combustors. One of these phenomena is the abrupt change in flow pattern observed in some combustors when the feed rate is increased. When a certain feed rate is reached the flame in one portion of the chamber disappears, and there is an accompanying increase in the volume of the remaining active zones at the expense of the zone which was extinguished. This behavior has been observed in a two-dimensional chamber fed by a multi-jet system of a premixed fuel/air mixture. A simplified conceptual model of such a jet-chamber combination will now be presented.

Figure III-1 shows such a chamber with the fuel/air mixture entering a single jet and products leaving at the

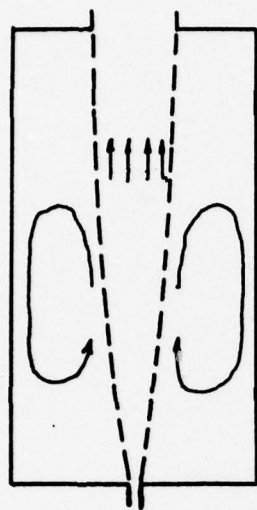


FIGURE III-1: PHYSICAL
PICTURE OF RECIRCULATION

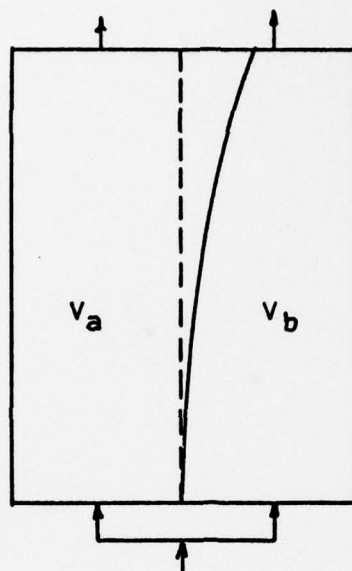


FIGURE III-2: MODEL
DIAGRAM

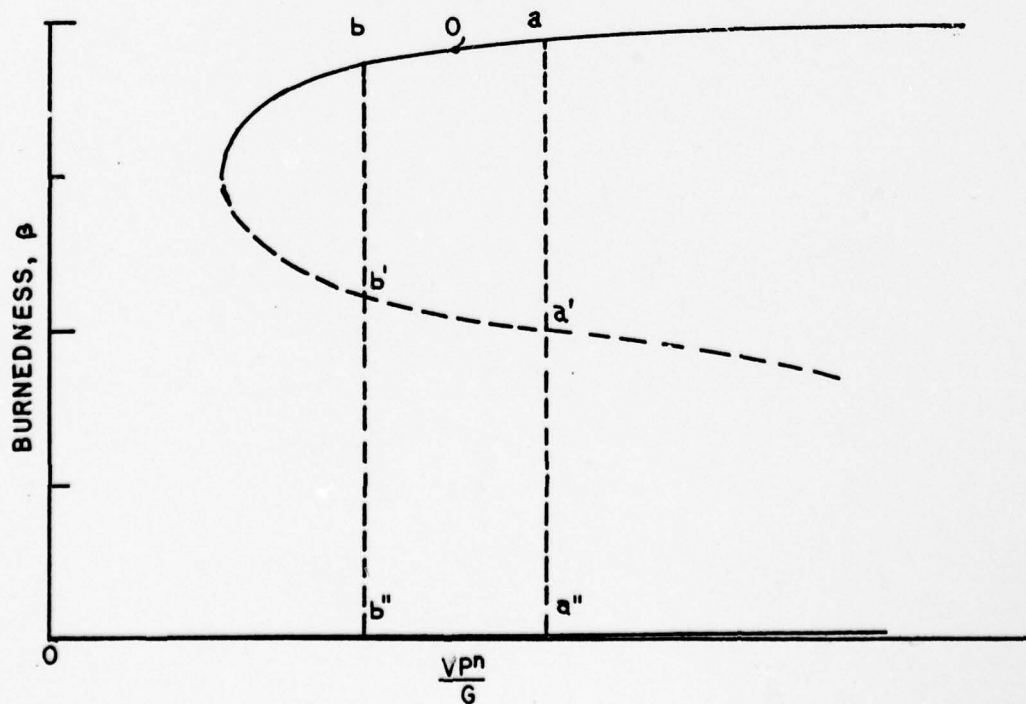


FIGURE III-3 WELL-STIRRED REACTOR CURVE FOR
TWO-STABILITY-LIMIT MODEL

top. Let the dotted lines bound the edges of those areas, taken normal to the axis of flow, through which the total upward gas flow is constant and equal to the feed rate. The volume thus bounded is called the "central core", and the region outside of this volume is called the "recirculation zone". It should be noted that the recirculation zone defined in this manner includes a complete vortex with gases flowing both upward and downward in contrast to a definition of the recirculation zone as that region where there is only downward gas flow. The dotted lines defining the boundary of the central core represent surfaces through any element of which there is no net mass flow, but there is equal and opposite turbulent diffusion through them. Because the feed to the zones external to the central core is on the average less burned than the gas which returns to the central core, the mean gas temperature in the outer zones is higher than that of the central core. Consequently the linear velocity of the outwardly moving gas is less than that of the inwardly moving, more completely burned gas; and the force producing this net inward momentum flux is a higher static pressure existing in the outer zones.

If both recirculation zones are equally active, the pressure effects on the two sides counter-balance. But if one zone is active and the other inactive, a pressure imbalance occurs, causing a deflection of the jet toward

the inactive side. This increases the volume of the active zone, thereby improving the opportunity for completion of combustion in it. The end effect is a bending of the jet, in response to the pressure exerted by the larger recirculation zone, to a position of equilibrium between the jet-momentum force and the pressure-area force of the hotter recirculation zone.

Since the system is two-dimensional the difference in the volumes of the recirculation zones may be assumed to be proportional to the pressure difference between them, and since the pressure effect is postulated to be the result of a transverse momentum flux, the pressure difference between the two zones should be roughly proportional to their temperature difference. To simplify this treatment, the central core will be assumed to be a high-speed, non-reacting jet stream in which the gases reside for a relatively short time, serving to supply feed gases to the recirculation zones, and the latter zones will be considered well-stirred reactors.

The block diagram representing this model, Figure 111-2, consists of two well-stirred reactors of constant total volume, separated from each other by an elastic barrier zone, the jet, which has the property of bending in response to pressure differences so that the change in volume of either of the reactors is directly proportional

to the pressure difference between the two. In the absence of a pressure difference the system is symmetrical. The fuel-air mixture will be assumed to be fed equally to the two reactors.

The deflection of the barrier is expressed in terms of the difference in the volumes of the two reactors;

$$\frac{V_a - V_b}{2} = k_1 (P_a - P_b) \quad \text{III-1}$$

and the pressure difference created by a difference in burnedness in the two reactors is:

$$P_a - P_b = k_2 (\beta_a - \beta_b) \quad \text{III-2}$$

Assume a well-stirred reactor performance curve is available (e.g. Figure III-3), giving the relation between burnedness and normalized volume.

In this model a series of stirred reactor pairs of various volume differences may be considered at each firing rate. For each volume difference considered the corresponding pressure difference between the two reactors may be found by combining Figure II-3 and Equation III-2. These pressure differences found may then be compared with the pressure difference required to maintain the postulated volume difference from Equation III-1. For each new firing rate considered a new series of volume differences and pressure differences may be found.

This calculation may be represented graphically. Let the total volume/feed ratio, equal to the initial ratio for each reactor, be represented by point "0" of Figure III-3, and let the barrier be deflected by an amount $(V_a - V_b)/2$, causing zones a and b to increase and decrease respectively by this amount. These volume changes are accompanied by corresponding changes in burnedness which may be found from Figure III-3 where a and b represent the new volume/feed ratios of sides a and b. Solutions for the burnedness in the new volumes exist on the branches at a, a", and b and b" (a' and b' are thermally unstable reactor conditions). These burnedness differences, 4 of them (plus 5 involving unstable reactor conditions), can be evaluated and from Equation III-2 the corresponding $(P_a - P_b)$'s can be found. These points for a typical case are plotted on Figure III-4. (The designations ab, ab' etc. represent reactor conditions of Figure III-3.) Repetition of this calculation for a series of volume differences leads to branches I and II of Figure III-4. Those portions of the curves which involve thermally unstable reactor conditions, i.e. the dotted portions of Figure III-3, are included for completeness but are dotted. Figure III-3 shows rather inadequately that Branch II is symmetrical around the origin; no symmetry around either axis intended.

The ab solution occurs when both reactors are hot,

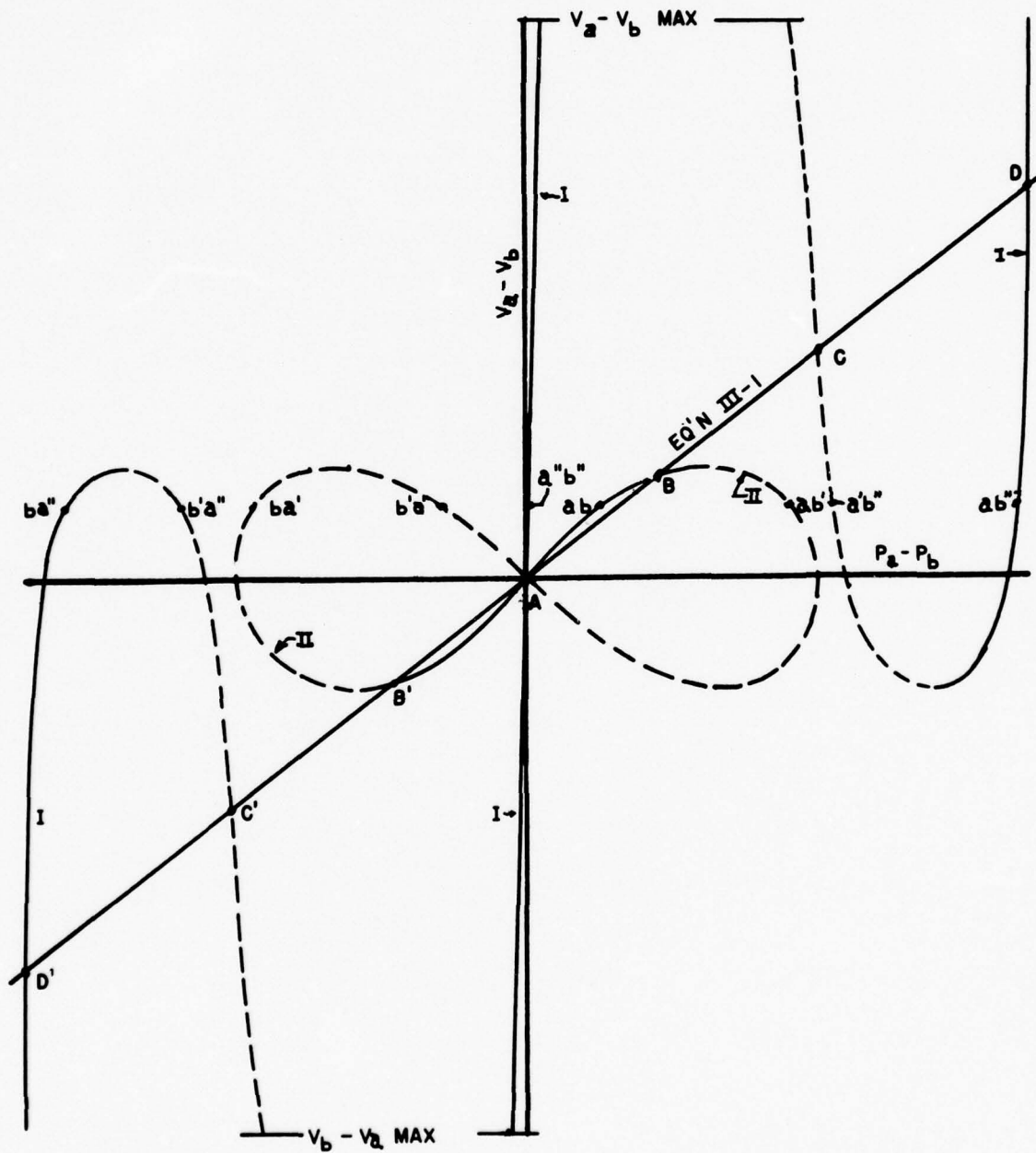


FIGURE III-4: PERFORMANCE OF A TWO-STABILITY-LIMIT COMBUSTION CHAMBER MODEL. GROSS VOLUME-FEED RATIO AND FEED COMPOSITION FIXED.

and a low $P_a - P_b$ is developed, lying on Branch II in the first quadrant. If side b is blown out, a high $P_a - P_b$ is developed at the point ab on Branch I, also in the first quadrant. Similar reasoning leads to the remainder of the points.

For each new value firing rate chosen a new pair of branches I and II will be found. It will be noted that at a sufficiently high firing rate the reactor pair will just be able to operate with both sides active. This occurs when point "O" of Figure III-3 is just at the blowout point of the well-stirred reactor curve. If the feed rate to the same reactor pair is increased further, it may still be possible for one side of the model to operate on the stable "hot" branch of the reactor curve if the volume difference is large enough; however, since the maximum volume difference possible occurs when V_a is twice its initial value, the maximum feed rate which permits a possible "hot" reactor is twice the feed rate corresponding to the above blowout point.

To find the stable operating points on Figure III-4, the line representing Equation III-1 is superimposed on branches I and II for the specific "O" chosen. (A non-linear relation between $V_a - V_b$ and $P_a - P_b$ could be used equally well). The equilibrium values of $V_a - V_b$ are found at the intersections of the line of Equation III-1 and either branch I or branch II. Branches I and II and the curve of

equation III-1 are symmetrical around the origin, i.e. it makes no difference which side becomes colder. Three stable solutions are found, the origin and the outermost intersections, A, D, and D'. The remaining four intersections are all unstable; C and C' because one side of the reactor pair is operating on the unstable branch of the well-stirred reactor relation, and B and B' because the barrier is in a metastable position. A stable barrier position is one in which a momentary change in $V_a - V_b$ causes a change in $P_a - P_b$ such that a net restoring force results. This means that at a stable intersection of the branches I or II with the line of Equation III-1 both curves must have a positive slope and the slope of the former must be greater than the slope of the latter.

The physical significance of the constants in Equations III-1 and III-2 is of importance in relating the theory to experimental and design problems. The interpretation of these constants may be seen by reducing Equations III-1 and III-2 to dimensionless relations.

In any chamber which has a pressure difference transverse to the flow direction of a jet a deflection of the jet will be found. This deflection would be expected to be a function of the ratio of pressure-area forces to the jet-momentum force, and assuming dimensional similitude, this function may be expressed:

$$\Delta y_r = \phi(\Delta P_r, x_r) \quad \text{III-3}$$

where $\Delta y_r = \Delta y/y_N$, $x_r = x/x_N$, and $\Delta P_r = \Delta P/\rho_N U_N^2$.

y_N = nozzle width, U_N = nozzle velocity,

ρ_N = nozzle density.

ΔP = the difference in pressure on the two sides of the jet averaged from the nozzle to the distance x from the nozzle.

Δy = the deflection of the jet centerline at the distance x from the nozzle.

The change in volume, $V - V_0$, for either side may be computed by integration of the deflection of the jet over the length L of the chamber:

$$\begin{aligned} V - V_0 &= w \int_0^L \Delta y \, dx = w y_N^2 \int_0^{L_r} \Delta y_r \, dx_r \\ &= w y_N^2 \int_0^{L_r} (\Delta P_r, x_r) \, dx_r \quad \text{III-4} \end{aligned}$$

This reduces to:

$$\frac{V_a - V_b}{2} = w y_N^2 \bar{\Phi}(\Delta P_r^*, L_r) \quad \text{III-5}$$

where ΔP_r is the reduced pressure difference averaged over the entire chamber length and w is the width of the two-

dimensional jet. This may be compared with Equation III-1 directly, and to be in conformity with it, i.e. to make the displacement proportional to ΔP_r^* , Equation III-5 must be of the form:

$$\frac{V_a - V_b}{2} = w y_N^2 (\Delta P_r^*) F(L_r) \quad \text{III-6}$$

This equation may be rewritten in dimensionless form:

$$\frac{V_a - V_b}{V_a + V_b} = \frac{w y_N^2}{V_a + V_b} \Delta P_r^* F(L_r) \quad \text{III-7}$$

The "jet" will now be defined more precisely as that part of the flow pattern of constant axial mass flow rate (i.e. the same portion of the flow referred to in Figure III-1); and that part of the system external to the boundary surfaces of this special jet will be called the "recirculation zone". (Since that part of the zone in contact with the jet core has a large positive axial velocity component, this is not the conventional jet referred to in the literature on jet structure.)

Because of the definition of the recirculation zones, these zones must be fed with fresh combustible gases by an eddy diffusional process, and burned gases must leave them similarly. These diffusion terms may be assigned average velocities U_0 outward and U_1 inward which are applicable

to the entire interface between the jet mainstream and the recirculation zone, and by the similarity principle:

$$U_o = a U_N \quad \text{III-8}$$

Using this outward velocity, the outward momentum flux \dot{m}_o associated with it can be evaluated:

$$\dot{m}_o = \rho_o U_o^2 = a^2 \rho_o U_N^2 \quad \text{III-9}$$

By applying a material balance, the gases leaving the recirculation zone, $\rho_1 U_1$, must be equal to the gases entering that zone:

$$\rho_o U_o = \rho_1 U_1 \quad \text{III-10}$$

The inward momentum flux, \dot{m}_1 , is then

$$\dot{m}_1 = \rho_1 U_1^2 = (\rho_o U_o^2) \rho_o / \rho_1 = a^2 \rho_o U_N^2 \rho_o / \rho_1 \quad \text{III-11}$$

Hence the net momentum flux at the boundary is:

$$\Delta \dot{m} = a^2 \rho_o U_N^2 \left(\frac{\rho_o}{\rho_1} - 1 \right) \quad \text{III-12}$$

and for two zones, the pressure difference between them may be calculated, assuming there is negligible temperature rise in the jet mainstream, by the equation;

$$P_a - P_b = a^2 \rho_N U_N^2 \left(\frac{T_a}{T_N} - \frac{T_b}{T_N} \right) \quad \text{III-13}$$

Now by an energy balance:

$$\frac{T}{T_N} = \beta \left(\frac{T_{af}}{T_N} - 1 \right) + 1 \quad \text{III-14}$$

Hence:

$$\Delta P_r^* = a^2 \left(\frac{T_{af}}{T_N} - 1 \right) (\beta_a - \beta_b) \quad \text{III-15}$$

This equation, when compared with Equation III-2 is of identical form, i.e. the pressure difference is directly proportional to the burnedness difference.

Figure III-4 may be replotted using coordinates of $(V_a - V_b)/(V_a + V_b)$ and $\beta_a - \beta_b$, yielding a generalized expression of the relative performance of the two sides of the model. In this diagram all possible combinations of $V_a - V_b$ and $\beta_a - \beta_b$ must lie within the square bounded by the limits of $(V_a - V_b)/(V_a + V_b) = \pm 1$ and $\beta_a - \beta_b = \pm 1$. On this same diagram the response of the jet to a burnedness difference may also be plotted, this relation being obtained by a combination of Equations III-7 and III-15:

$$\frac{V_a - V_b}{V_a + V_b} = \left[a^2 \left(\frac{T_{af}}{T_N} - 1 \right) \frac{2wy_N^2}{V_a + V_b} F(L_r) \right] (\beta_a - \beta_b) \quad \text{III-16}$$

This plot of the relations embodied in Equations III-1 and III-3 has the advantage that all of the geometrical design variables are lumped into one coefficient, namely the slope of the line representing III-16. Inspection will verify that for a given value of the overall loading factor, $G/(V_a + V_b)P^n$, the relative performance of the two reactors of the model (branches I and II of Figure III-4) when plotted on these coordinates will yield the same curve,

independent of the shape of the chamber. Different curves of branches I and II will be obtained for each value of the loading factor chosen. However, from Equation III-16, the response of the jet to the burnedness differences is independent of the velocity (or loading factor). Hence, in comparing the response of a given chamber, fed a given fuel/air ratio and fuel type, to changes in the feed rate a family of curves of branches I and II will be obtained which intersect the one line representing Equation III-16.

Design variables such as chamber and nozzle shape, on the other hand, are reflected only in the slope of the line representing Equation III-16. These variables, together with the volumetric expansion of the burned fuel/air mixture, $(T_{af}/T_N) - 1$, determine the fractional volume change produced by jet movement in response to a unit of burnedness difference in the two sides. In Equation III-16 the variables affected by chamber design are the constant a^2 which is related to the jet spreading angle and the quantity $[(2wy_N^2)/(V_a + V_b)]F(L_r)$ which is related to the chamber geometry. Changes in the feed composition and inlet temperature will affect both branches I and II (since this will change the basic stirred reactor relation shown in Figure III-3) and the jet sensitivity through $(T_{af}/T_N) - 1$.

Using a diagram such as Figure III-4 in the generalized form discussed above, both the response of the chamber to

changing feed rates and the stability characteristics of the chamber may be investigated. Consider the chamber to be burning initially in a stable, symmetrical pattern (operation corresponding to the origin of Figure III-4). If the total loading factor of the chamber is increased, point "O" of Figure III-3 will move toward the β axis. As it approaches the nose of the curve of Figure III-3, branch II of Figure III-4 becomes smaller and thinner (i.e. its slope at the origin becomes smaller and its $\beta_a - \beta_b$ intercept approaches the origin). This change in operating conditions will not affect the slope of the curve representing jet position. When the loading factor has increased sufficiently to make branch II become tangent to the jet position curve at the origin (Figure III-5), the origin becomes an unstable intersection of the jet position line and the reactor operating lines. Hence the only remaining stable solution is the intersection of the jet position line with branch I of Figure III-5, corresponding to one side burning stably and the other blown out. This calls for a sudden deflection in the jet to the new stable position of $V_a - V_b$. Further increase in the feed rate will cause the disappearance of branch II, and eventually branch I will become tangent to the line of Equation III-16 (Figure III-6). This represents the condition for total blowout of the chamber, since at this point

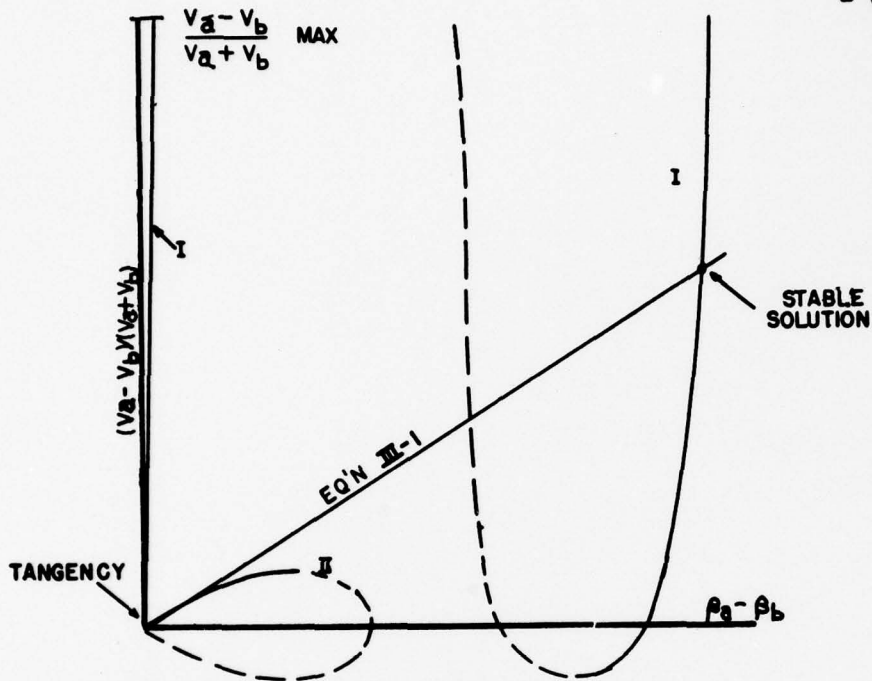


FIGURE III-5: ONE-SIDED BLOWOUT CONDITION IN THE TWO-STABILITY-LIMIT MODEL

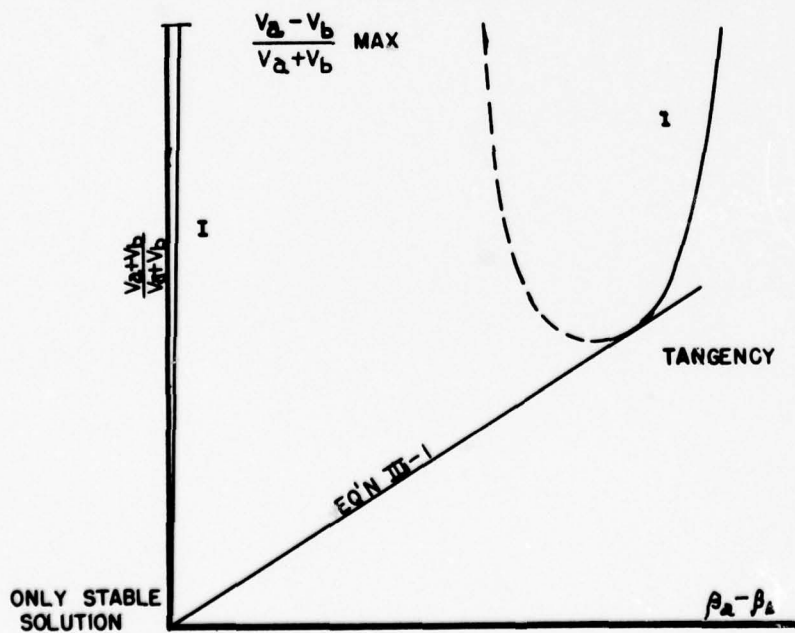


FIGURE III-6: FINAL STABILITY LIMIT FOR THE TWO-STABILITY-LIMIT MODEL

and higher feed rates there are no stable intersections of branch I of Figure III-6 with the line of Equation III-16.

This model also has interesting implications concerning behavior at other chamber feed rates. Figures III-7a to III-7f represent six feed rates with six corresponding pairs of branches I and II, along with a common curve showing the jet stiffness independent of feed rate. Here only the stable portions in the first quadrant of Figure III-4 are shown. On each of these diagrams a horizontal dotted line is drawn tangent to the nose of branch II. This represents the blowout point of branch II, i.e. the maximum volume difference allowable for a given volume/ feed ratio if both zones are to be simultaneously stable. If $V_a - V_b$ exceeds this level the smaller side will be blown out, and if $V_a - V_b$ is below this limit, either the smaller side will burn stably, or if it is blown out it may be relighted by a sufficiently strong source.

Consider a chamber operating at a volume/feed ratio represented by Figure III-7b with both sides active, i.e. with operation at the origin of Figure III-7b. If a disturbance, $V_a - V_b$, is imposed on the jet, the jet will tend to return to its central position unless the $V_a - V_b$ imposed is greater than the blowout limit represented by the dotted line. If this limit is exceeded then one side will become cold, and a high $P_a - P_b$ will be developed.

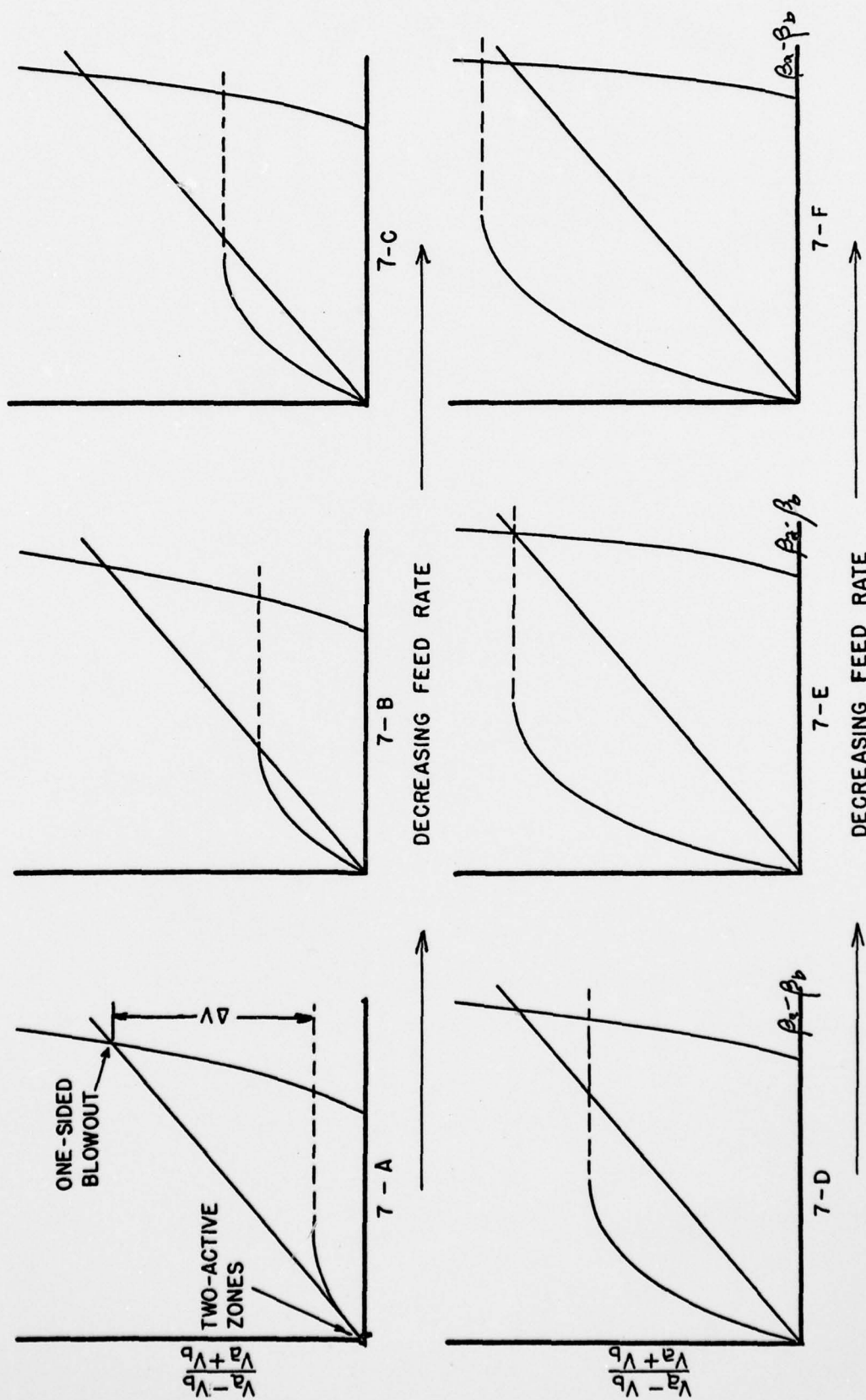


FIGURE III-7: EFFECT OF FEED RATE IN TWO-STABILITY-LIMIT MODEL.

The jet will consequently move to the one-sided blowout position (the branch I intersection) instead of returning to its central position. If the chamber is operating at the one-sided blowout position when the disturbance is imposed, then the reverse argument is applied; however, in this case the problem of re-light must be considered. Even if the disturbance is large enough to bring the small side to a re-lightable position, the small side will not relight if the ignition source is too weak; and the jet will return to the one-sided blowout position. Since in this case the disturbance required to reach the critical level is much larger than in the first case, it would be expected that the one-sided blowout position would be the more stable one.

At a lower feed rate than in Figure III-7b, such as represented by Figure III-7c, the blowout point of branch II is about centrally located with respect to the two stable jet positions. In a highly turbulent combustor in which there are high transfer rates from active zones to extinguished zones (conditions typical of many high-output combustors) it is easy to imagine that if the volume/feed ratio for any cold zone is above the minimum required for stability by the well-stirred reactor kinetics, ignition will occur. If simultaneously there is an equal likelihood that a disturbance in $V_a - V_b$ from either stable jet

position will cross the critical blowout level, conditions for a flickering flame exist.

At even lower feed rates, represented in Figure III-7d, the situation is reversed from that represented by Figure III-7b. In Figure III-7d the two-active-zone solution is the relatively more stable since a smaller disturbance is required to go from the one-sided blowout position to the maximum relight level than in the opposite direction.

In the sixth diagram, Figure III-7f, the feed rate is so low that the one-sided blowout solution is below the critical blowout level of branch II. Thus, assuming that relight will always occur if the opportunity exists, the only stable solution at this rate is the origin (two active zones).

This type of argument also leads to the conclusion that a hysteresis effect exists in this combustion chamber model. In reaching the transition from two-active zones to the one-sided blowout from low feed rates, chamber operation moves from a low feed rate condition represented by Figure III-7f to that high flow rate condition represented by Figure III-7a, where the origin becomes an unstable solution. Once the transition occurs, relight can be caused only by reducing the feed rate to a point where the one-sided blowout solution is below the blowout point of branch II. The feed rate where this critical

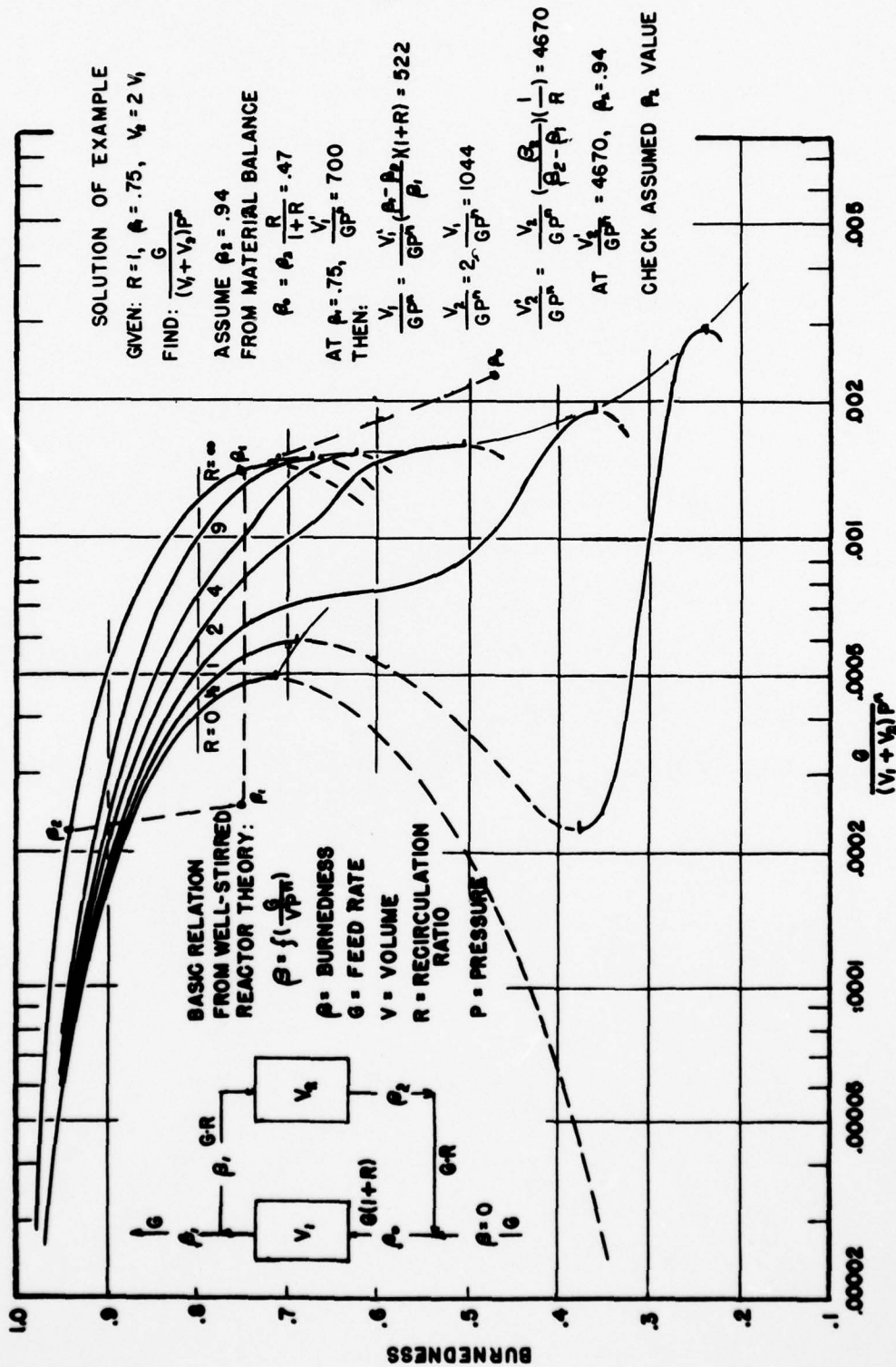
level is reached is represented in Figure III-7. Thus, it may be concluded that this simple model of a combustion chamber is useful not only for studying pressure interactions of two or more zones but also for suggesting mechanisms for other important chamber problems.

Model Showing Effect of Recirculation

Flow recirculation is another phenomenon of combustion chambers which is characteristic of many systems. This has been recognized by Spaulding (24) in a paper which appeared after the present model had been developed. Spaulding proposed a model of a recirculating system similar to the model developed here, although the treatment and conclusions are markedly different. In a chamber fed by a jet of fuel/air mixture the region of the jet near the base of the chamber aspirates burned gases from the surrounding region. These gases are replaced by reverse-flow from near the exit of the chamber.

In constructing a model of this behavior, Spaulding suggested that the gases flow around this loop in plug-flow. The central core serves only to mix the recirculated gases with the fresh feed. A portion of this mixture is discharged from the model as burned products, and the remainder recirculates in a plug-flow combustion zone. Spaulding has calculated two cases for this model; one

FIGURE III - 8
EFFECT OF RECYCLE IN A COMBUSTION CHAMBER MODEL



where there is no interchange between the jet mainstream and the recirculation zone (all recirculated material enters at the base of the jet) and a second case where allowance is made for continuous aspiration of burned gases from the recirculation zone along the length of the jet. The first of these cases is directly comparable to the results obtained here, and the behavior of this model is shown in Figure II-9.

No allowance has been made in Spaulding's model for combustion occurring in the central core of the jet. A model in which such an allowance is made is probably in better agreement with the actual situation. The consequences of allowing for combustion in the central core are illustrated by the model considered here. In this model both the central core and the recirculation zone have been treated as well-stirred reactors. Figure III-8 shows this model diagrammatically. Fresh feed enters and is mixed instantaneously with recycled burned gases. The mixed gases then enter zone V_1 , representing the central core of the jet. A portion of the partially burned products leaving V_1 is recycled through the recirculation zone V_2 , where further combustion occurs, and then is returned to V_1 again.

To find the feed rate to each of the zones, a recirculation ratio is defined as:

$$R = \frac{\text{Molal recirculation rate to zone } V_2}{\text{Molal fresh feed to model}}$$

This definition is the same as that used by Spaulding. From a performance curve showing the relation between feed rate and burnedness (i.e. Figure III-3), the response of this system to feed rate changes may now be calculated for a given ratio of V_2/V_1 and recirculation ratio R .

This calculation has been carried out for a fixed value of $V_2/V_1 = 2.0$ and for various recirculation ratios. Burnedness, as a function of feed/total volume is shown in Figure III-8.

Several performance characteristics of this system should be noted. If the chamber is operating at a recirculation ratio of zero, the volume V_2 allowed for recirculation represents "dead" space, and the central core V_1 has only fresh, unburned gases entering it. The central core, therefore, operates as a simple well-stirred reactor without any additional assistance from the recirculated gases. The curve representing the behavior of zero recirculation may be found by multiplying the curve for the simple well-stirred reactor by the fraction of the volume in the model which represents the active central core, (i.e. by $V_1/(V_1 + V_2)$; curve $R = 0$ of Figure III-8).

If, on the other hand, the recirculation ratio is infinite, the composition of both zones is identical, and the performance becomes that of the well-stirred reactor performance used to generate all of the other curves.

(Curve R = ∞ , Figure III-8).

For recirculation ratios neither zero nor infinite, significant interaction occurs between the central core and the recycle volume. This is illustrated by considering the relative contributions of each of the reactors to the total amount of combustion. Let the burnedness of the streams leaving reactors V_1 and V_2 be represented by β_1 and β_2 (the former also represents the burnedness of the gases entering V_2 and leaving the system); and let β_0 represent the burnedness of the gases fed to V_1 , obtained by mixing gas of composition β_2 with fresh feed. The contribution to burnedness of each reactor may be expressed quantitatively as the flow rate through the reactor times the increase in burnedness in that reactor:

$$G \cdot \beta_1 = G(1+R) \cdot (\beta_1 - \beta_0) + (G \cdot R) \cdot (\beta_2 - \beta_1)$$

$$\left[\begin{array}{c} \text{fresh} \\ \text{feed} \\ \text{rate to} \\ \text{model} \end{array} \right] \cdot \left[\begin{array}{c} \text{total} \\ \text{change} \\ \text{in burn-} \\ \text{edness} \\ \text{in model} \end{array} \right] = \left[\begin{array}{c} \text{feed} \\ \text{rate} \\ \text{to } V_1 \end{array} \right] \cdot \left[\begin{array}{c} \text{increase} \\ \text{in burn-} \\ \text{edness} \\ \text{in } V_1 \end{array} \right] + \left[\begin{array}{c} \text{feed} \\ \text{rate} \\ \text{to } V_2 \end{array} \right] \cdot \left[\begin{array}{c} \text{increase} \\ \text{in burn-} \\ \text{edness} \\ \text{in } V_2 \end{array} \right]$$

By dividing through by the total burning rate of the system, $G \cdot \beta_1$, two terms are obtained representing the fractional contributions, J , of each reactor:

$$J_1 = \frac{\beta_1 - \beta_0}{\beta_1} (1 + R)$$

$$J_2 = \frac{\beta_2 - \beta_1}{\beta_1} (R)$$

Choose an operating point corresponding to a moderately low feed rate, and consider the response of a fixed-volume reactor pair to an increase in feed rate.

Figure III-9 shows the behavior of various points in the model for a recirculation ratio of $1/2$ and a V_2/V_1 of 2. Curve β_1 is the burnedness in the reactor V_1 and also the burnedness leaving the system (this curve is also $R = 1/2$ of Figure III-8). Curve β_2 is the burnedness in the recirculation zone; and curve β_0 is the burnedness of the feed to V_1 obtained by mixing fresh, unburned feed with recirculated products. At a low feed rate (represented by dotted line "A") the feed material to V_2 , of composition β_1 , has a high burnedness and there is very little burning remaining to be accomplished in reactor V_2 . Under these conditions, the fractional utilization, J_2 , of the recirculation zone is low, i.e. most of the burning occurs in V_1 . At a higher feed rate, represented by line "C", the composition, when approached from low flow rates, corresponds to points 1, 3, and 5; and most of the burning still occurs in V_1 . However, since the burnedness in V_1 has decreased slightly, J_2 increases correspondingly. As the feed rate increases further past line "D", the central core becomes chilled, and blowout occurs, after which only the recycle volume is active (i.e. a residual flame). At feed rates beyond line "D" combustion occurs only along

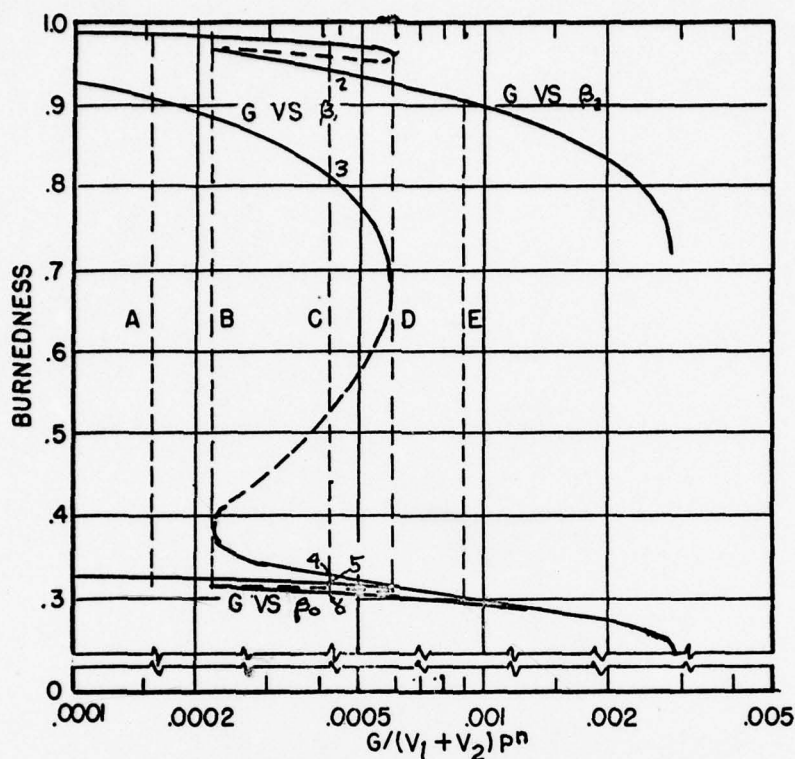


FIGURE III-9: β_0 , β_1 , & β_2 FOR RECIRCULATION MODEL
 $R = \frac{1}{2}$, $V_1/V_2 = 2$, $\phi = 1.0$

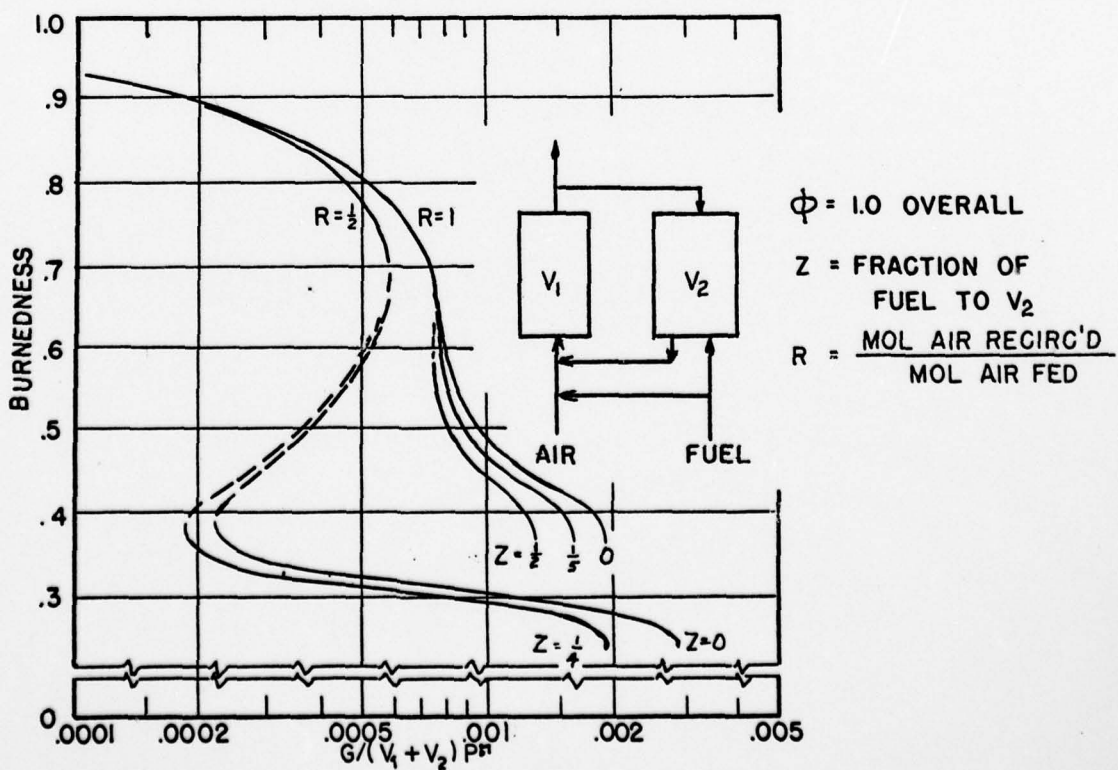


FIGURE III-10: EFFECT OF SPLIT FUEL FEED ON RECIRCULATION MODEL

the lowest branch of the curve (corresponding to dotted line "C"). At these feed conditions practically no combustion occurs in the central core, and J_2 is nearly unity.

If the flow rate is now decreased from this high level, the central core stays cold past line "D" and at line "C" the compositions 2, 4, and 6 are reached. When line "B" is reached there is a sudden relighting of the central core. This hysteresis loop is the most interesting part of these models, since it is a potential source of a flickering flame. In this region the central core may light or blowout in response to small disturbances in operating conditions with very little change in the burnedness of V_2 .

At higher recirculation ratios the behavior is similar but because of the "stirring" effect of higher recycle rates, the ratio of the fractional contributions of the two volumes, J_1/J_2 , approaches unity for a wider range of feed rates. As Figure III-8 shows, the undercut of the curve β_1 disappears at higher recirculation ratios, and as the recycle is continually increased, the inflection in the curves becomes less pronounced until it also disappears.

Model Showing Effect of Non-Uniform Fuel/Air Ratio

Another problem of interest is that of allowing for the effect of unequal fuel/air ratios in the various chamber zones. Such a condition would arise in a combustor where the fuel and air were injected separately into a moderately well-mixed system. A possible model of such a combustor is a variation of the above recirculation model, in which only a portion of the fuel, but all of the air, is fed into the central core and the remainder of the fuel is fed into the recirculation zone. This produces a richer mixture in the recycle volume than in the central core. The one additional variable required may be thought of as either the fraction of the original fuel introduced into the central core or the fuel/air ratio of the recirculation zone. The former has the advantage of showing the limitations on the variation of the fuel/air ratio of the recycle volume. The latter shows more directly the effect of the split fuel feed. Since the fuel/air ratio in the central volume is the same as the overall fuel/air ratio, it will not be affected by this split.

The results of calculations made on this recirculation model are shown in Figure III-10 for an overall fuel/air ratio which is stoichiometric for consistency with the previous models. Because of this condition,

other fuel/air ratios in the recirculation zone can only be a detriment to the overall heat release rate since the recycle zone must operate on less than the optimum efficiency curve. At low feed rates this effect is of little consequence since the gases in the recirculation zone are essentially completely burned in either case. However, if the feed rate is increased sufficiently the burning rate in the recirculation zone becomes significant, and the consequence of operating this volume at other than stoichiometric fuel/air ratio is apparent.

If the chamber were operating with a lean overall fuel/air ratio and the fuel/air ratio in the recirculation zone were stoichiometric the reverse situation would be expected. In this case the recirculation zone would be operating on a more favorable efficiency curve than the central core. In those feed rate ranges where the performance of the model for an overall lean fuel/air ratio would be higher than for the case of feeding all the fuel into the central core.

Models of More Complex Situations

Thus far, the models discussed have been restricted to specific phenomena. In modeling practical situations, however, one may wish to consider situations where two or more phenomena are simultaneously significant. If models

AD-A058 017

PRINCETON UNIV N J JAMES FORRESTAL RESEARCH CENTER

F/G 21/2

APPLICATION OF WELL-STIRRED REACTOR THEORY TO THE PREDICTION OF--ETC(U)

MAY 58 A H BONNELL

N60RI-105(03)

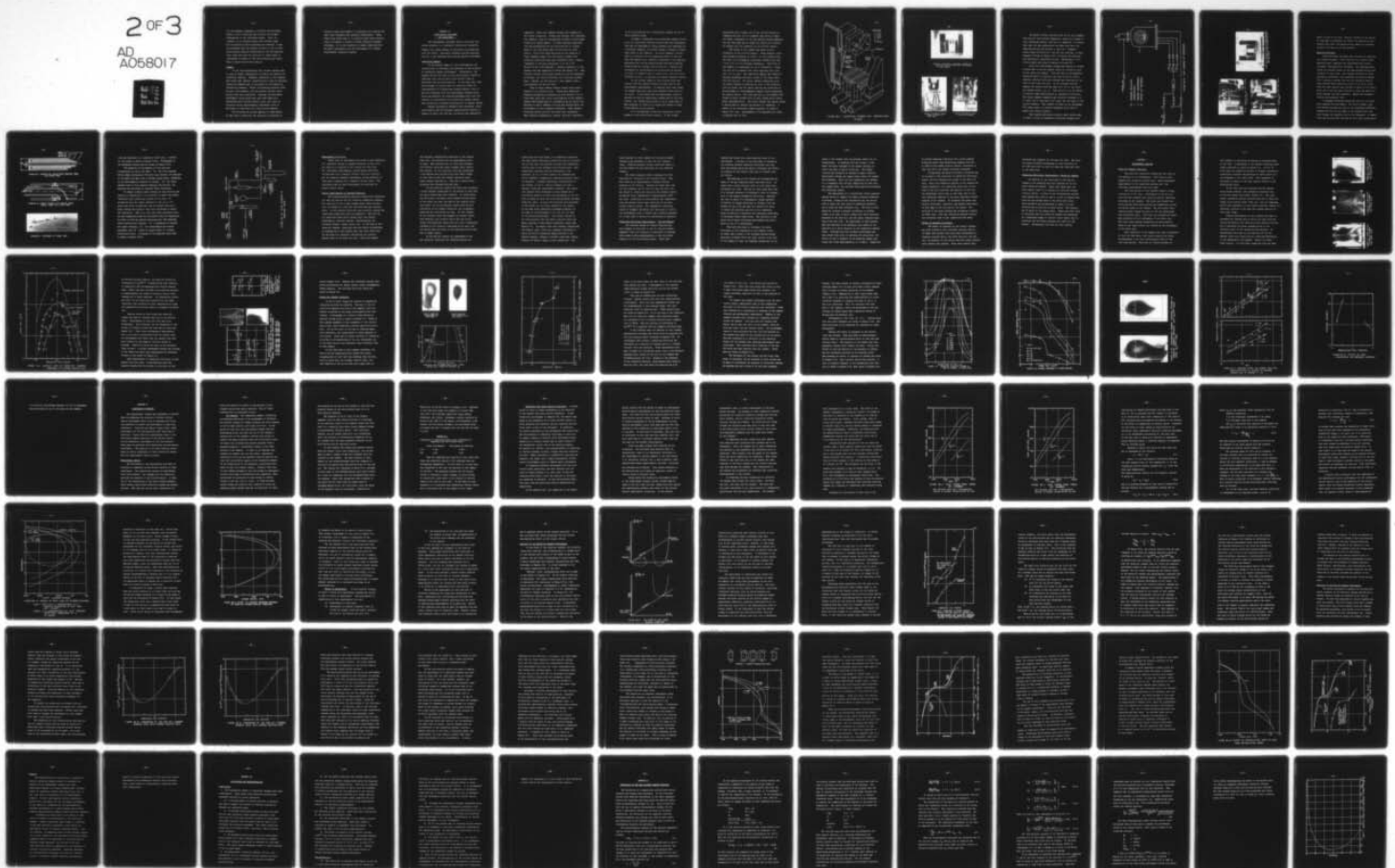
UNCLASSIFIED

SQUID-MIT-18-T

NL

2 OF 3

AD
A058017



for the separate phenomena of interest are available, models of such situations may be built from simple combinations of the individual models. Thus, for instance, in a situation where both residual flame and two-stability-limit phenomena are observed, it may be postulated that the chamber consists of two or more recirculation zones as represented by the two-stability limit model and that the structure of these zones is represented by models of the recirculation type rather than a simple well-stirred reactor.

Summary

It has been hypothesized that stirred reactors may be used in simple combinations to predict the behavior of combustion chambers. Examples considered in this chapter have shown that behavior characteristics found in practical combustion chambers may be duplicated by such models of interacting elements. Models illustrating pressure interactions, recirculation, and non-uniform fuel/air ratio effects have been considered. Although the calculated performance curves given here have been based on a theoretical well-stirred reactor curve, one could in principle use an experimentally determined curve of efficiency vs feed rate for a well-stirred reactor.

The criterion of success applied to these models is that only a relatively few variables be required to

specify a model performance in conformity with reality and that these variables have physical significance. These models have shown that it is possible under these restrictions to simulate a variety of known combustion chamber phenomena. It is now proposed to compare quantitatively the model performance with the performance of a simple experimental combustion chamber.

CHAPTER IV
EXPERIMENTAL EQUIPMENT
AND PROCEDURES

The experimental equipment used in this work consisted primarily of a specially constructed combustion chamber of a simple design to facilitate the comparison with the theory. Ancillary equipment included metering devices, a gas sampling train and gas analysis equipment.

Combustion Chamber

In the initial stages of this investigation the objective was to determine the influence of recirculation on combustion chamber performance. Consequently, the chamber desired was one in which recirculation played an important role, and in which some control could be exercised over the recirculation. At the same time, care was necessary to insure that the combustor chosen be representative of conventional chamber design, since it was felt desirable that the experimental program should avoid the necessity of studying phenomena which were the results of a peculiarity of a particular chamber rather than principles of general applicability to chamber design.

Several alternative chambers were considered. Since recirculation was the dominant characteristic desired, a chamber in which the flow was circulatory was immediately

suggested. Three such chamber designs have appeared in the recent literature. Schmidt and Schoppe (19) presented two chambers, both for non-premixed systems in which gases flowed in a spiral manner. In these chambers stabilization was accomplished by the recirculation of burning gases to the cold zones near the fuel and air inlet points. Very little data was given on the behavior of these chambers except that the authors claimed wide stability limits and high heat liberation rates, roughly comparable to can-type combustors (1 to 10×10^6 Btu/hr ft³ at 1 atm pressure). Another combustor of this general type was suggested by Hottel and Person (9). They studied a vortex type system similar to the one suggested by Schoppe, but with a different fuel injection arrangement; however, as did Schoppe's, this chamber used a non-premixed fuel and air feed.

None of these chamber designs seemed particularly adapted to the present study. Person gave moderately detailed information concerning the flow pattern, but he found that there was little recirculation in his chamber. Schmidt and Schoppe gave no information at all about flow patterns in their chambers nor were any details about the performance of their chambers presented. Other designs involving forced cyclonic flow were also considered. These various alternatives, however, were all considered

to be so non-typical of a conventional chamber as not to merit detailed study.

A simple, rectangular two-dimensional chamber fed by a jet of a pre-mixed fuel/air mixture was then considered. This had the advantage of being somewhat more analogous to a practical chamber, yet simple enough in design to permit easy study of its behavior. In such a chamber, recirculation is achieved by the aspirating effect of the jet. Near the chamber exit, material equivalent to the material aspirated must reverse direction and form recirculation zones around the central core of the jet. Control over the amount of recirculation can be achieved by varying the ratio of chamber width to nozzle width, and with quite different results, by varying the chamber dimension ratios.

In the initial stages of this problem there was concern over the possible effects of heat loss on the experimental measurements. To minimize wall heat losses the chamber was built with three parallel feed slots in its floor. It was hoped that the experiments could be carried out with no significant interaction of the jets; however, jet interactions proved to be so large that it was necessary to return to a single-jet design to study recirculation in this system.

It is interesting to note the similarity of this chamber to the well-stirred reactor. If the volume

associated with a single jet of the stirred reactor is compared with the jet of a chamber into which a single jet flows, similarity of the two systems becomes apparent. One may then hope that a single-jet system will provide an insight into the operation of the stirred reactor.

The design of the chamber was based on this similarity to the stirred reactor. Three parallel slots, each having an opening of 0.030" x 2" were placed along the floor of a rectangular combustion chamber which was 3 1/2" x 3" x 2" in internal dimensions. (The floor of the chamber is represented by the 3" dimension.) Along the roof of the chamber were three opposing exit flues 1/2" x 2" in size. The combustion chamber was formed by placing insulating firebrick inside of the frame which held the nozzles. The inside chamber dimensions would be readily altered by varying the size of the firebrick used as lining, and the nozzle spacing was controlled by an assortment of interchangeable spacer blocks separating the nozzle bodies. The front and back of the chamber were formed by Vycor windows held by steel frames and a sheet-metal retaining piece. The entire chamber was placed inside a vacuum tank to control the pressure of operation. A sketch of the combustion chamber assembly is shown in Figure IV-1, and photographs of the apparatus are shown in Figures IV-2 to IV-4.

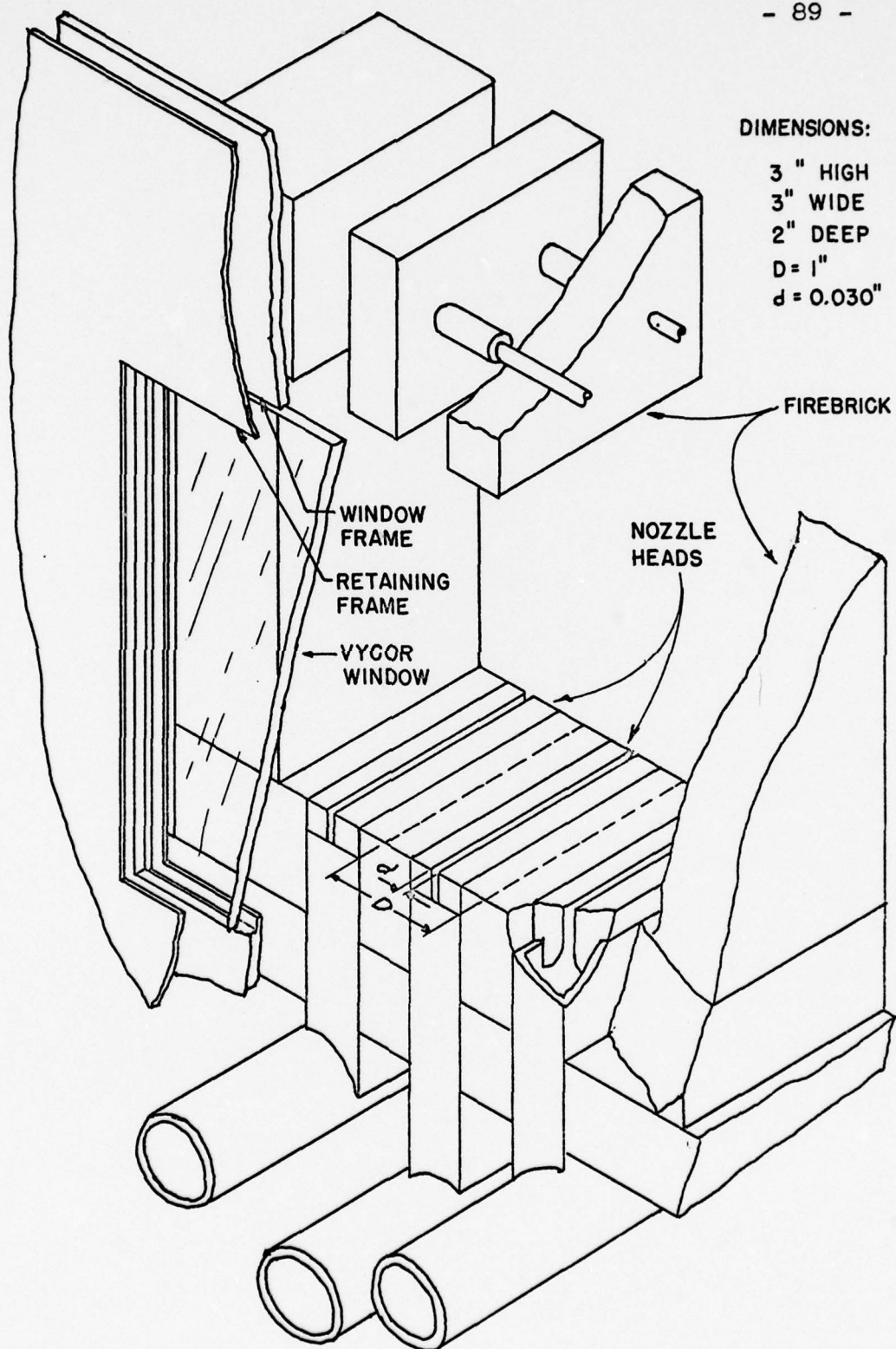


FIGURE IV-1: COMBUSTION CHAMBER FOR RECIRCULATION STUDIES

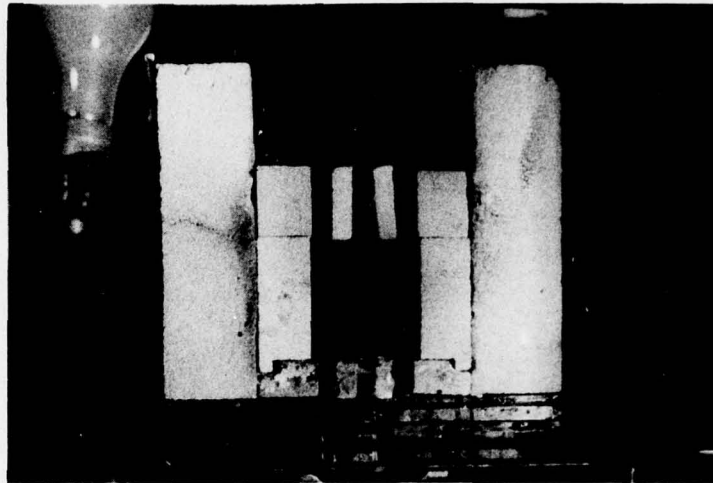


FIGURE IX-2: PHOTOGRAPH OF COMBUSTION CHAMBER WITH THREE FEED JETS AND THREE FLUES. SIDE WINDOWS OF VYCOR REMOVED.

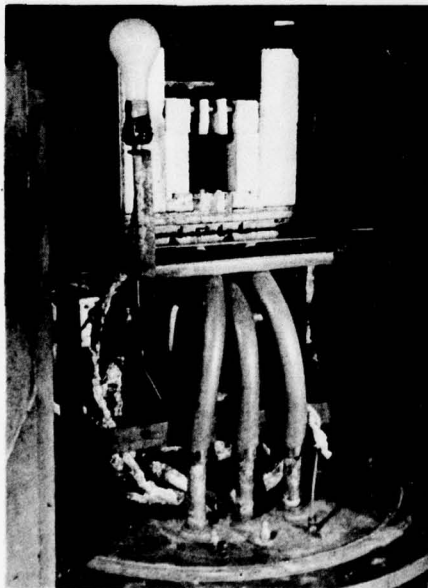


FIGURE IX-3: PHOTOGRAPH OF ASSEMBLED CHAMBER AND EQUIPMENT. SIDE WINDOWS REMOVED

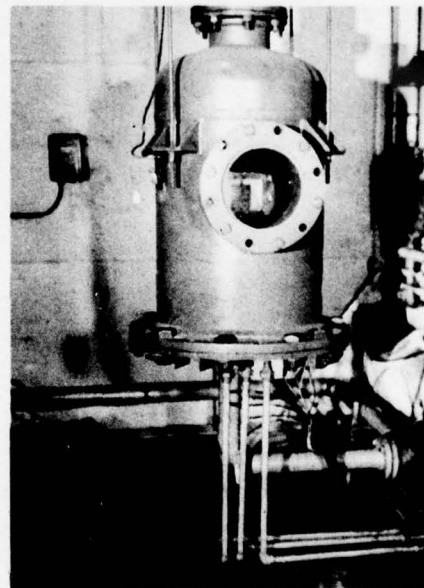


FIGURE IX-4: PHOTOGRAPH OF VACUUM TANK READY FOR EXPERIMENT.

Pre-mixed fuel/air mixtures were fed to this chamber. Fuel and air were metered separately, mixed in a length of pipe containing baffles, and fed to a manifold. To insure that each jet was operating at the same feed rate, the manifold mixture was metered to each jet. Standard square-edges orifices were used for all metering. A flow diagram is shown in Figure IV-5, including the metering and temperature measurement points. Photographs of the control panel are shown in Figures IV-6 and IV-7.

After the experimental program was started it became evident that a one-jet chamber should be studied as well as the three-jet chamber. This was done in the apparatus described above by replacing the side bricks so that a narrower interior width was obtained and shutting off the feed to the outer two jets. In the original one-jet chamber the inside width was made just $1/3$ of the three-jet chamber width, i.e. 1". This proved to be too narrow to achieve flame stabilization at reasonable feed rates. The inside chamber dimension was therefore enlarged to a 2" width (by 2" deep and 3 $1/2$ " high) for the study of the one-jet chamber. This chamber is shown in the photograph IV-8 (also shown is a mounted sampling probe used to sample the interior gases).

This chamber was placed inside a small vacuum tank so that it could be operated at pressures ranging from

FIGURE IV-5: FLOW DIAGRAM OF APPARATUS

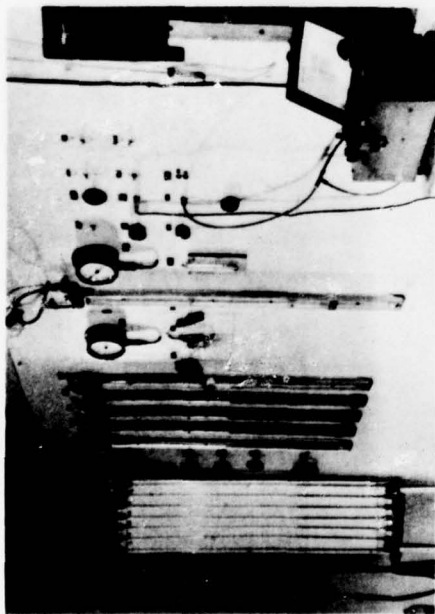


FIGURE IX-6: PHOTOGRAPH OF CONTROL PANEL SHOWING MANOMETERS AND MANOMETER BOARD.

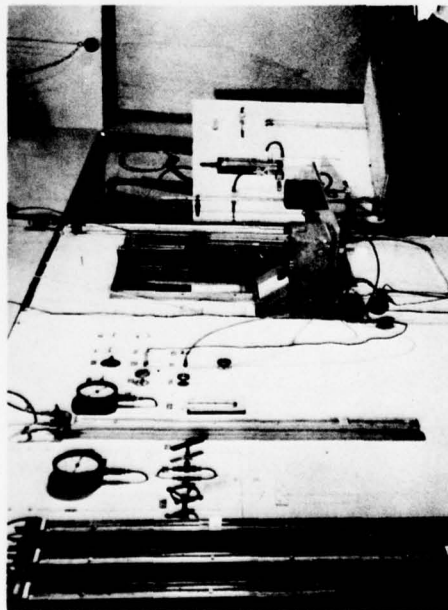


FIGURE IX-7: PHOTOGRAPH OF CONTROL PANEL SHOWING SAMPLING BOARD ASSEMBLY.

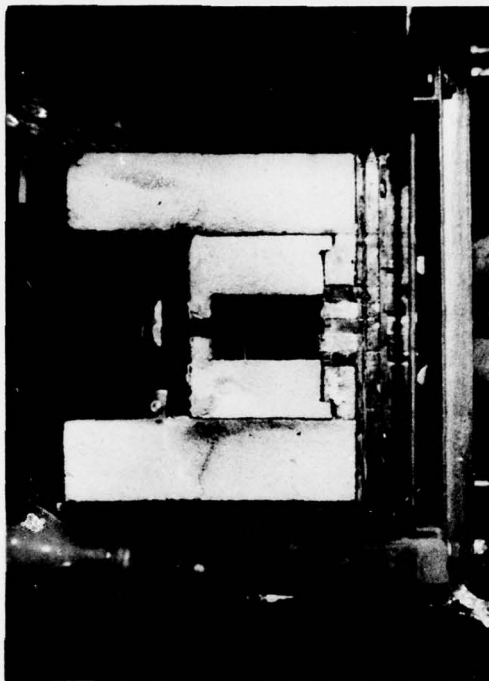


FIGURE IX-8: PHOTOGRAPH OF ONE-JET CHAMBER BRICKWORK. NOTE THE SAMPLING PROBE ENTERING FROM THE LEFT-HAND-SIDE.

about 0.1 atm to 0.5 atm. However, except for one series of runs made to determine the effect of pressure on the blowout feed rate, the data were all taken at a pressure of about 0.34 atm, or 10" Hg absolute.

Sampling Equipment

Some additional equipment was required for sampling the combustion gases. This consisted of a water-cooled sampling probe, sampling rate measurement and control equipment, and analytical equipment. For sampling gases inside the chamber probes of the same general design used by Baker (3) were used. This design consisted of three concentric hypodermic tubes assembled as shown in Figure IV-9, forming a central tube and two concentric annuli. High pressure water passed at a rate of 10 to 50 cc/min down the inner annulus and returned to drain in the outer. About 200 to 400 psi were required to send this amount of water through the probe assembly. Sample was withdrawn through the innermost tube.

A somewhat different design was used for the probe which sampled the exit gases. For this a single, long tube entered through one side of the supporting framework, crossed the flue in the plane of the chamber roof, and left through the opposite side of the framework. A sample inlet was drilled into the side of this long cooling water

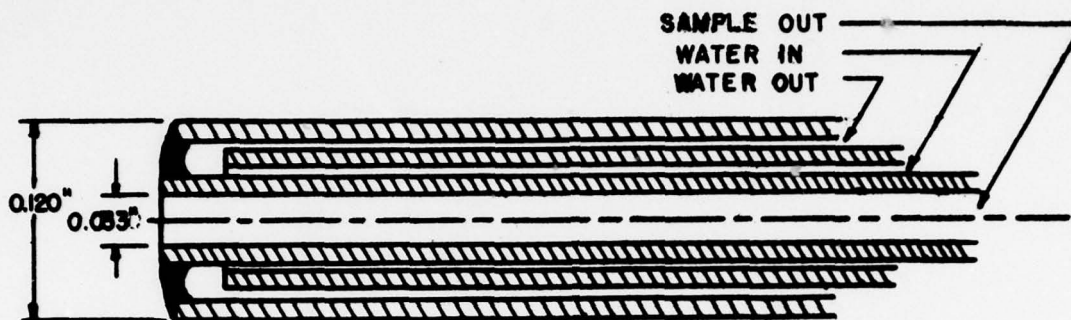


FIGURE IV-9: REVERSE-FLOW COOLING WATER SAMPLING PROBE
(10 X ACTUAL SIZE)

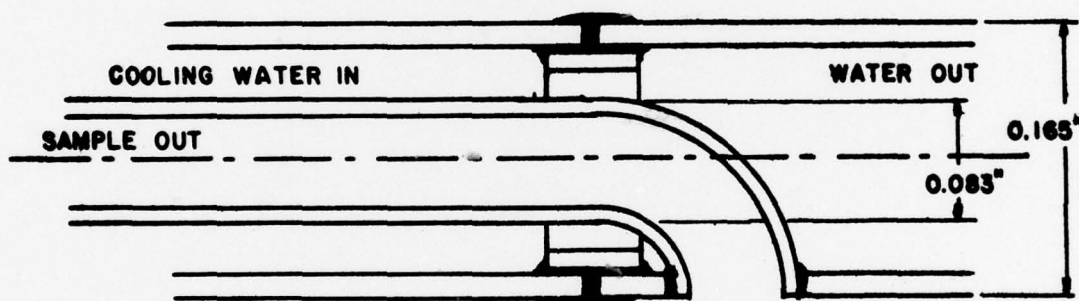


FIGURE IV-10: STRAIGHT-THROUGH FLOW COOLING WATER
SAMPLE PROBE (10 X ACTUAL SIZE)

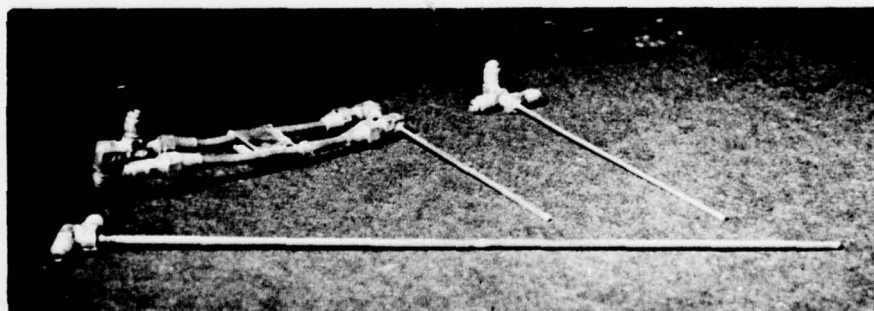


FIGURE IV-11: PHOTOGRAPH OF PROBES USED

tube and connected to a concentric inner tube. A sketch of this probe is shown in Figure IV-10. Photographs of the assembled probes used are shown in Figure IV-11.

The analysis of the samples in this work was accomplished in one of two ways: (1) For those samples where oxygen consumption efficiency was desired, the analysis of the gases was made with a Beckman Oxygen Meter, operating on the para-magnetic property of oxygen. (2) For those samples where a more complete analysis was desired, the analysis was performed by standard Orsat techniques.

To sample properly gases flowing at high velocity and varying in composition it is desirable to match the stream velocities just inside and outside of the tube. To accomplish this the impact pressure at the tip of the probe must first be measured, and the sample then withdrawn through the probe at that rate calculated to match the velocities. This is a trial and error procedure since the gas temperature must be calculated from the composition in order to find the desired sampling rate. The sampling train required must include: (1) a manometer to measure the impact pressure, (2) flow measurement and control equipment, and (3) either an oxygen meter or a sample collection bottle. A diagram of the sampling train used is shown in Figure IV-12.

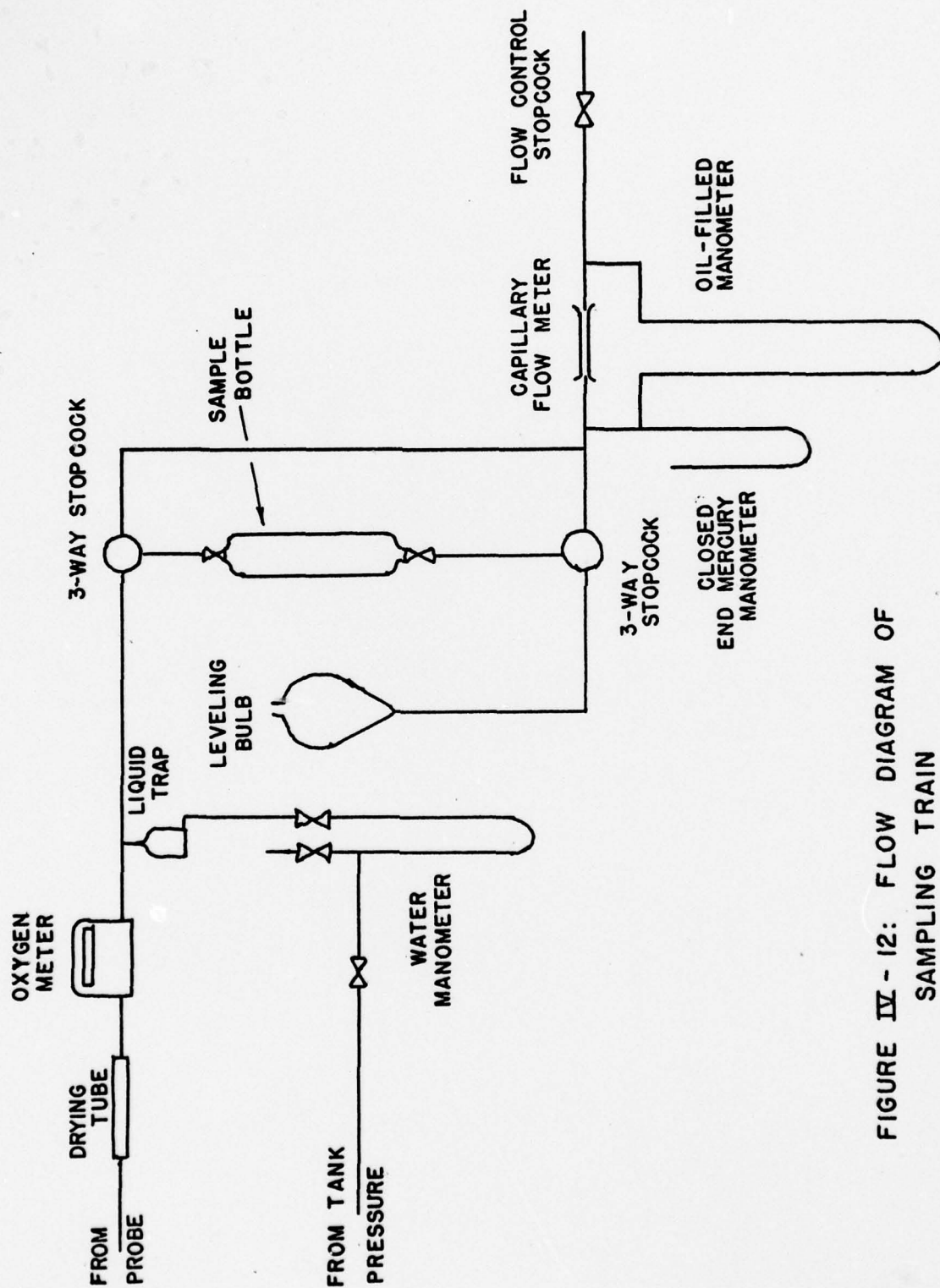


FIGURE IV - 12: FLOW DIAGRAM OF
SAMPLING TRAIN

Experimental Procedures

Three types of experiments were made on this apparatus:

- (1) stability limits at constant pressure, giving fuel-air ratio as a function of the blowout air feed rate;
- (2) efficiency measurements, giving oxygen efficiency vs feed rate for a constant fuel/air ratio and pressure;
- and (3) pressure exponent measurement, giving pressure vs feed rate at blowout for a constant fuel/air ratio. The procedures used in these experiments are described in greater detail below.

Blowout Measurements at Constant Pressure

The constant-pressure stability limits were determined for both the one-jet and the three-jet combustion chambers. The flame was lit by a high-voltage spark above the exit flue (or flues) at a very low feed rate and high fuel/air ratio. If the fuel/air ratio was then carefully reduced the flame would flash back into the combustor. The fuel and air rates were then slowly raised until the desired operating air rate was reached. Simultaneously the brickwork became a bright cherry red. In the case of the three-jet chamber, flash-back was more easily accomplished by feeding one of the outside jets, and then, after that jet had been lit, gradually introducing the fuel/air mixture feed to the other two jets. After the chamber

had reached a steady-state operation at the desired feed rate, the desired blow-out measurements could be made. With pressure and air feed rate constant, the fuel-air ratio was slowly changed until blowout was reached. As the stability limit was approached, a few minutes were allowed after each small change in fuel rate so that the chamber operation could reach thermal equilibrium. (The use of kaolin brick minimized the necessary waiting time.)

In the three-jet chamber the three jets coalesced a short distance downstream of the nozzles so that only two major flame areas were observed. At sufficiently low flow rates, two small zones trapped between pairs of the three jets near the base of the chamber would also light, but in the regions studied they did not contribute to the chamber stability, and in general, gases did not burn stably in them. In this chamber, as the fuel/air ratio was changed two blowout limits were observed, one in which one of the two active (large recirculation) zones blew out, with a consequent increase in the volume of remaining active zone, and the second when the flame in the remaining active zone was no longer stable.

In the one-jet chamber the phenomenon of the two stability limits was not observed because the

flame would not burn stably in a symmetrical position. The only stable combustion pattern was the one in which the jet was bent over against one wall with combustion visible only in the enlarged recirculation zone. This undoubtedly resulted from the narrowness of the chambers, as in a 3" wide chamber (as compared with the 2" chamber) a symmetrical combustion pattern could be obtained. A second interesting characteristic of the blowout in the 2", one-jet chamber was that a residual flame was consistently observed. The combustion pattern which developed in this chamber had a circulatory pattern in which the mainstream of the jet went up along one wall and recirculating gases returned along the other. A small recirculation zone developed in the center of the vortex created by this motion. At low feed rates combustion proceeded primarily at the edge of the mainstream of the jet and the edge of the recirculating gases. The central portion of the recirculation zone was nearly inactive since the gases reaching it were almost completely burned (see Figure V-7). As higher rates were reached, approaching the blowout limit, there was a gradual transition in which the active combustion region shifted to the central regions, forming a residual flame near blowout (Figure V-8 shows a stage in this transition). The

data reported for this chamber are the gross chamber loading rates necessary to blow out this residual flame. Constant-pressure blowout data were taken in the same manner as that described for the three-jet chamber.

For these chambers blowout loading rates were measured as a function of the fuel-air ratio. Data were taken at an approximately constant absolute pressure of 10" mercury. Several air rates were used for each chamber, and at each air rate the fuel rate was varied to obtain both lean and rich blowout limits. An ambient inlet temperature of approximately 540°R was used. Deviations in both pressure and temperature from the desired values were corrected for by well-stirred reactor theory. The temperature correction charts of Longwell and Weiss (14) were used to correct the experimental data to 540°R, and a pressure exponent of 1.8 was used to correct for deviations in pressure.

Combustion Efficiency Measurements - One-Jet-Chamber

The observed change in visible flame pattern with changes in feed rate to the 2", one-jet chamber suggested that its variation of efficiency vs loading rates might conform approximately to the calculated behavior of the recirculation model. Hence this

chamber was chosen for a more detailed study of its performance. A series of runs were made to determine the relation between combustion efficiency and feed rate and another group was made to determine the effect of pressure on the blowout feed rate at several fuel-air ratios.

The sampling of this chamber was accomplished by means of the gas sampling probes described above. In these runs a fixed fuel-air ratio of 1.35 times stoichiometric was used. Various air feed rates were used at a constant pressure to determine a curve of loading rate vs the oxygen consumption efficiency. Analysis was done by means of a paramagnetic oxygen analyzer. A traverse of oxygen efficiency vs distance into the chamber at one level was made for various air rates to locate the position and size of the combustion zones as well as to determine the combustion efficiency of the gases within these zones. The position of the probe tip in these traversing measurements was determined by use of a cathetometer.

Runs were also made to determine the gross efficiency of the combustion at the chamber outlet. In these runs a probe of the straight-through design described in Figure IV-10 was used, buried in the roof of the chamber so that the sampling opening was in the

plane of the chamber roof and pointed toward the oncoming gases. In sampling this gas stream, a case where the gases impinged on the sample opening, an effort was made to match velocities. The stream velocity was estimated by making an impact pressure measurement through the sample probe before the sample was withdrawn. Since the gas temperature was assumed to be dependent only the gas composition as read from the oxygen meter, the required trial-and-error procedure was relatively simple.

The measurement of a satisfactory static pressure against which to compare the impact pressure presented a problem. Purge air was introduced into the vacuum tank to sweep the tank clean of combustion products, and to keep the tank internals cool. The flow of this purge air created a pressure difference of several tenths of an inch of water between the static pressure measured at the tank wall and the impact pressure opening at the exit flue. An improvement in this measurement was achieved by an extension tube inside of the tank wall to a point adjacent to the combustion chamber frame. Although this poor pressure measurement may have caused some error in matching the velocities, the effect of such a mismatch on the measured oxygen efficiency was found experimentally to be small. Comparison

of several sampling velocities for a given chamber condition showed that mismatching ranging from 50% to 120% of the stream velocity caused a variation of less than 3% in the oxygen efficiency measured.

In measuring the gross efficiency, attention had to be given to the variation of combustion efficiency across the flue opening even though it was only 1/2" wide. Since the combustion pattern in the chamber was highly assymetric, the combustion efficiency on one side of the flue reflected the behavior of the cold jet mainstream, while that on the other side of the flue reflected behavior in the more completely burned regions of the chamber. To determine the gross combustion efficiency, therefore, gas samples were taken at each edge of the flue and at the center. The position of the probe opening was determined visually in these runs; this was considered adequate because the variation found in gas composition was small.

Effect of Pressure on Blowout

The effect of pressure on the blowout loading was also studied at four different fuel/air ratios. In these runs several feed rates were established at constant fuel/air ratio, and after each air rate was set, the pressure in the vacuum tank was slowly reduced until blowout was reached. After each blowout this

procedure was repeated for the next air rate. The fuel-air ratios studied corresponded to fuel fractions, F , of 0.600 and 0.575 on the rich side and 0.450 and 0.475 on the lean side.

Combustion Efficiency Measurements - Three-Jet Chamber

In addition to the above data on the one-jet chamber a few sampling data were obtained on the original three-jet chamber. These were taken near the rich blowout limit at a constant air rate and varying fuel-air ratios. A probe of the reversed-flow cooling water design was built so that it could be dropped down from the top through each of the three exit flues. Probe movement was accomplished by means of an air solenoid and an electric actuator motor. The analysis was by means of the oxygen meter. These data were taken to establish that the three-jet chamber was operating in a reasonable range of fuel/air ratio rather than to establish the efficiency-loading rate curve for the chamber. Consequently the data are very limited.

CHAPTER V

EXPERIMENTAL RESULTS

Three-Jet Chamber Operation

The three-jet combustion chamber was the first of the chambers to be investigated. Data taken on this chamber were primarily blowout data. Some photographic measurements of the combustion pattern and a few efficiency measurements were also made.

The flow pattern in this chamber showed a strong interaction of the jets. Convergence of the two outside jets was observed both with and without combustion occurring in the chamber. The three jets formed four recirculation zones whose pattern was symmetrical around the center plane of the chamber. The two inside recirculation zones trapped by pairs of the jet mainstreams were relatively small. The outer two occupied the space made available by the convergence of the three jets. The outer zones behaved essentially as recirculation zones to the large central jet created by the convergence of the three jets.

When combustion in the chamber was first established at very low flow rates, the flame occupied four zones, corresponding to the four recirculation zones of the cold flow pattern. There was no visible evidence in

this chamber of combustion occurring in the mainstreams of the jets. A photograph of the chamber operating under these conditions is shown in Figure V-1. It will be noted that the combustion pattern is slightly assymetric, indicating a possible mis-matching of nozzle sizes or a mis-alignment of the nozzle axes. This assymetry is discussed in detail in the next chapter (Errors in the Experimental Work).

As the feed rate was increased the two smaller zones became unstable, and combustion continued only in the two larger outer zones, Figure V-2. The final stable combustion pattern occurred when one of these two larger recirculation zones "blew out", and the remaining active zone expanded to a more stable position, Figure V-3. Continued increase in the feed rate caused blow-out of this final flame.

Blowout measurements on this chamber were made to determine the loading rate at which the shift from the two-active-zones to the one-active-zone pattern occurred, and to determine the gross loading factor at the stability limit of the one-active-zone pattern. No measurements were made on the stability of the two smaller zones since these did not contribute materially to the operation of the chamber. Figure V-4 shows these results. To facilitate comparison with the data

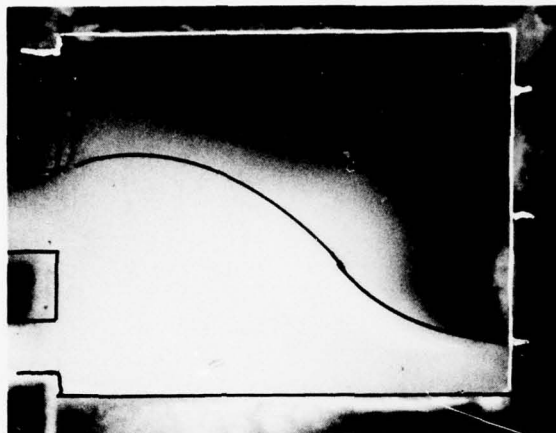


FIGURE I-3: FLAME PATTERN
IN THREE-JET CHAMBER.
ONE ZONE ACTIVE

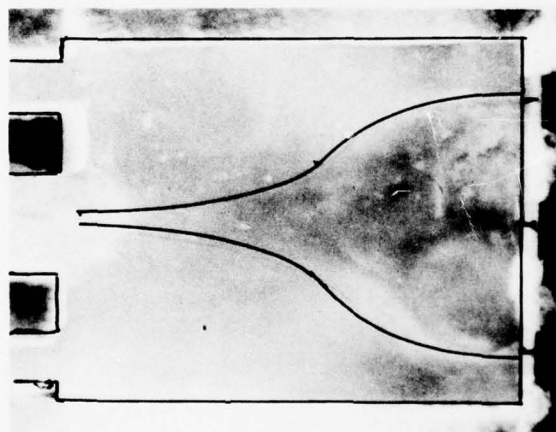


FIGURE I-2: FLAME PATTERN
IN THREE-JET CHAMBER.
TWO ZONES ACTIVE

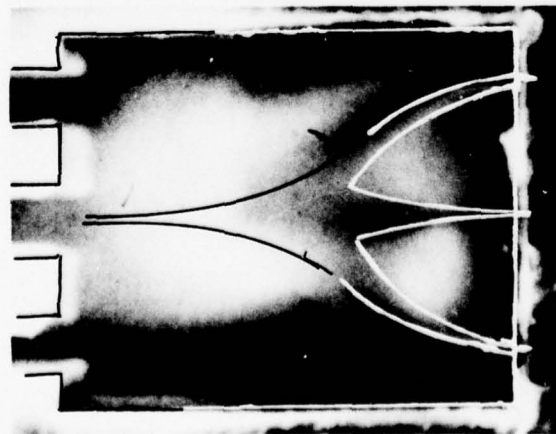


FIGURE I-1: FLAME PATTERN
IN THREE-JET CHAMBER.
FOUR ZONES ACTIVE

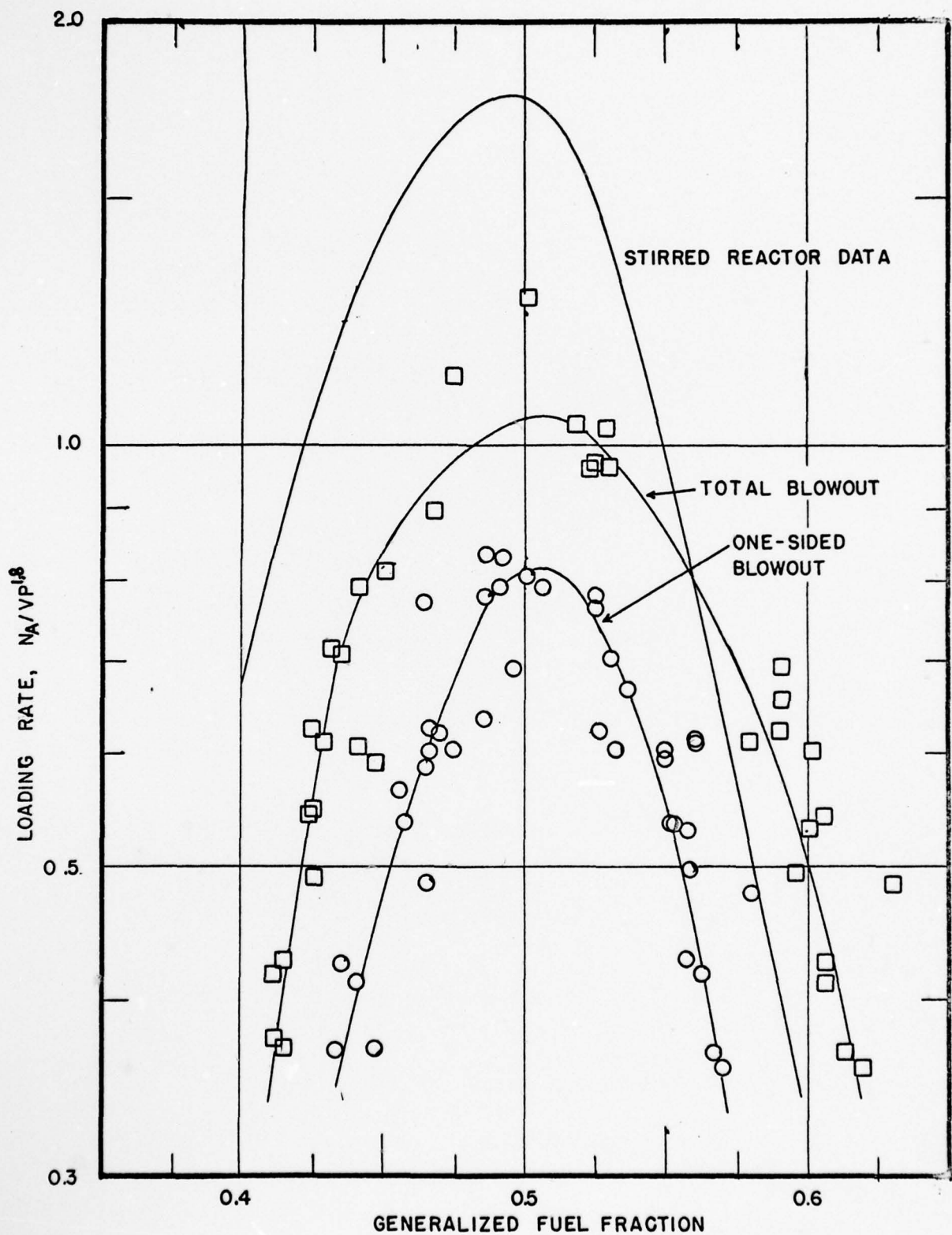


FIGURE V-4: BLOWOUT DATA OF THREE-JET CHAMBER COMPARED TO STIRRED REACTOR (14)

on the well-stirred reactor, the data are plotted on coordinates of $N_a/VP^{1.8}$ vs generalized fuel fraction, F , along with the corresponding well-stirred reactor data. These runs were all made at an absolute pressure of approximately ten inches of mercury, and an inlet temperature of 540°R (ambient). No temperature control was used, but the data were corrected for the small variations that occurred in inlet temperature by using the temperature-correction charts of Longwell and Weiss (14).

Another series of runs using this three-jet chamber was made to estimate the size of the various zones. Measurements of zone size were made from photographs. This technique for the estimation of the volume of combustion zones has been used by Simon and Wagner (22). Since these photographic measurements were to be used in conjunction with the blowout data, the photographs were taken with the chamber feed rate near blowout for the range of fuel/air ratios of interest. Figure V-5 gives the data on the estimated flame volumes. A typical photograph showing the outlines of the flame zone which were planimetered to determine volumes is also shown in Figure V-5.

Some measurements of combustion efficiency in this chamber were also made. A gas-sampling probe was inserted between the flue bricks to the level of the

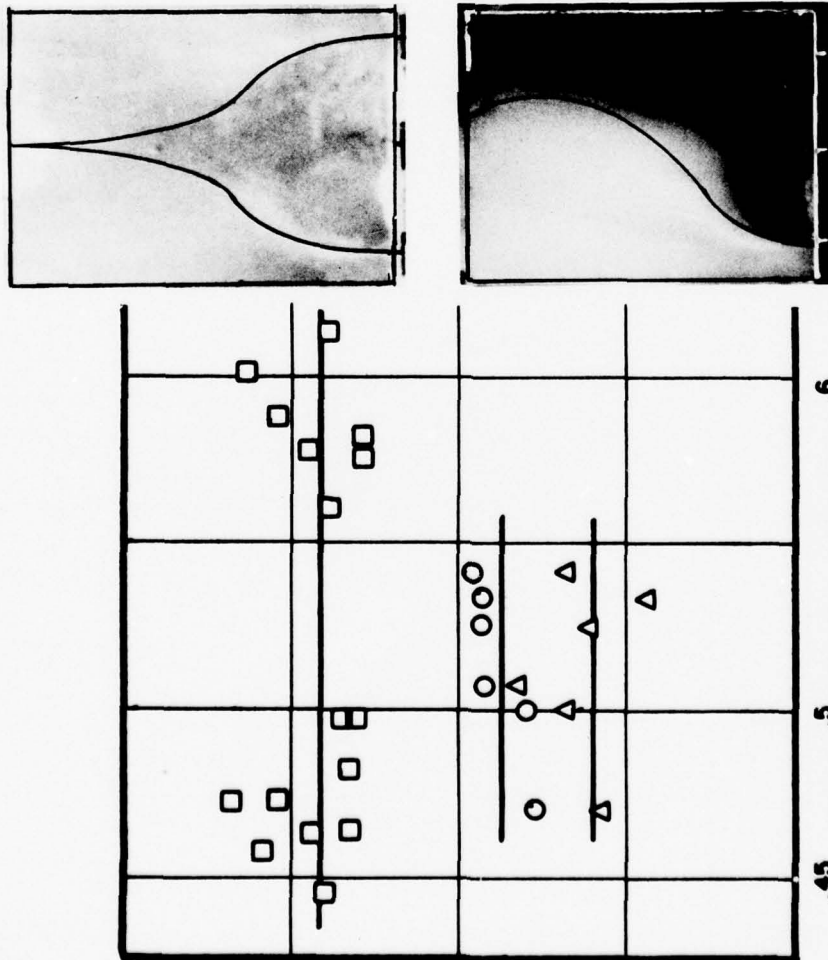


FIGURE 5: GENERALIZED FUEL FRACTION
COMBUSTION ZONE VOLUME DATA, THREE-JET
CHAMBER. (PHOTOGRAPHS SHOW AREAS MEASURED)

○ LEFT-HAND ZONE, TWO ZONES ACTIVE
Δ RIGHT-HAND ZONE, TWO ZONES ACTIVE
□ LEFT-HAND ZONE, ONE ZONE ACTIVE

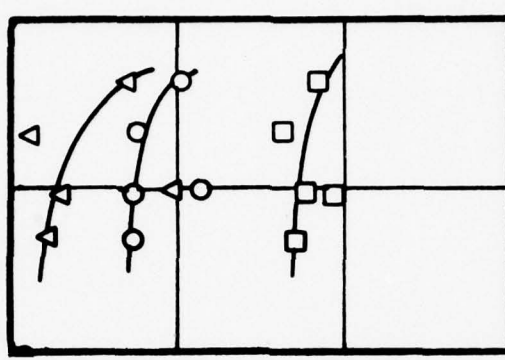


FIGURE 6: THREE-JET
OXYGEN EFFICIENCY VS
FUEL FRACTION AT
 $N_A/VP = 0.239$

○ LEFT-HAND FLUE
□ CENTER FLUE
Δ RIGHT-HAND FLUE

inside chamber roof. Samples were withdrawn through this probe and analyzed for oxygen content using a paramagnetic oxygen analyzer. The few data which were taken are shown in Figure V-6.

Single-Jet Chamber Operation

In the 2" wide, single-jet chamber no symmetrical combustion pattern was observed. The axis of the jet curved over against one side of the chamber, with combustion occurring in the large recirculation zone thus created. A photograph of a typical flame pattern at moderate firing rates is shown in Figure V-7. Flame in this chamber appeared in the boundaries of the recirculation zone, where relatively unburned gases were available. But in the "eye" of the zone no unburned gases could penetrate, and consequently no flame appeared in this volume. There was no visible evidence of combustion occurring in the mainstream of the jet, presumably due to the high velocity and consequent short residence time of this region.

As the feed rate to this chamber increased, the zone of active combustion moved toward the center, occupying more of the "eye" and receding from the wall, until at rates near the ultimate blowout limit, all that remained of the active zone was a small ball of



FIGURE X-7: FLAME PATTERN
ONE-JET CHAMBER. LOW
FLOW RATE, GASES IN EYE
NEARLY BURNED



FIGURE X-8: FLAME PATTERN
ONE-JET CHAMBER. HIGH
FLOW RATE, RESIDUAL FLAME
PARTLY FORMED

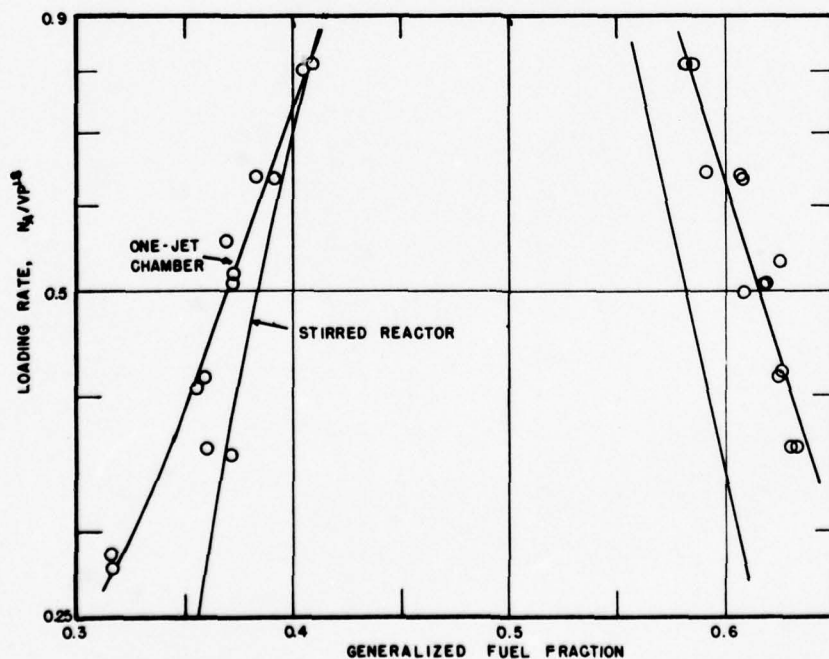


FIGURE X-9: ONE-JET CHAMBER STABILITY DATA. STIRRED
REACTOR DATA INCLUDED FOR COMPARISON (14).

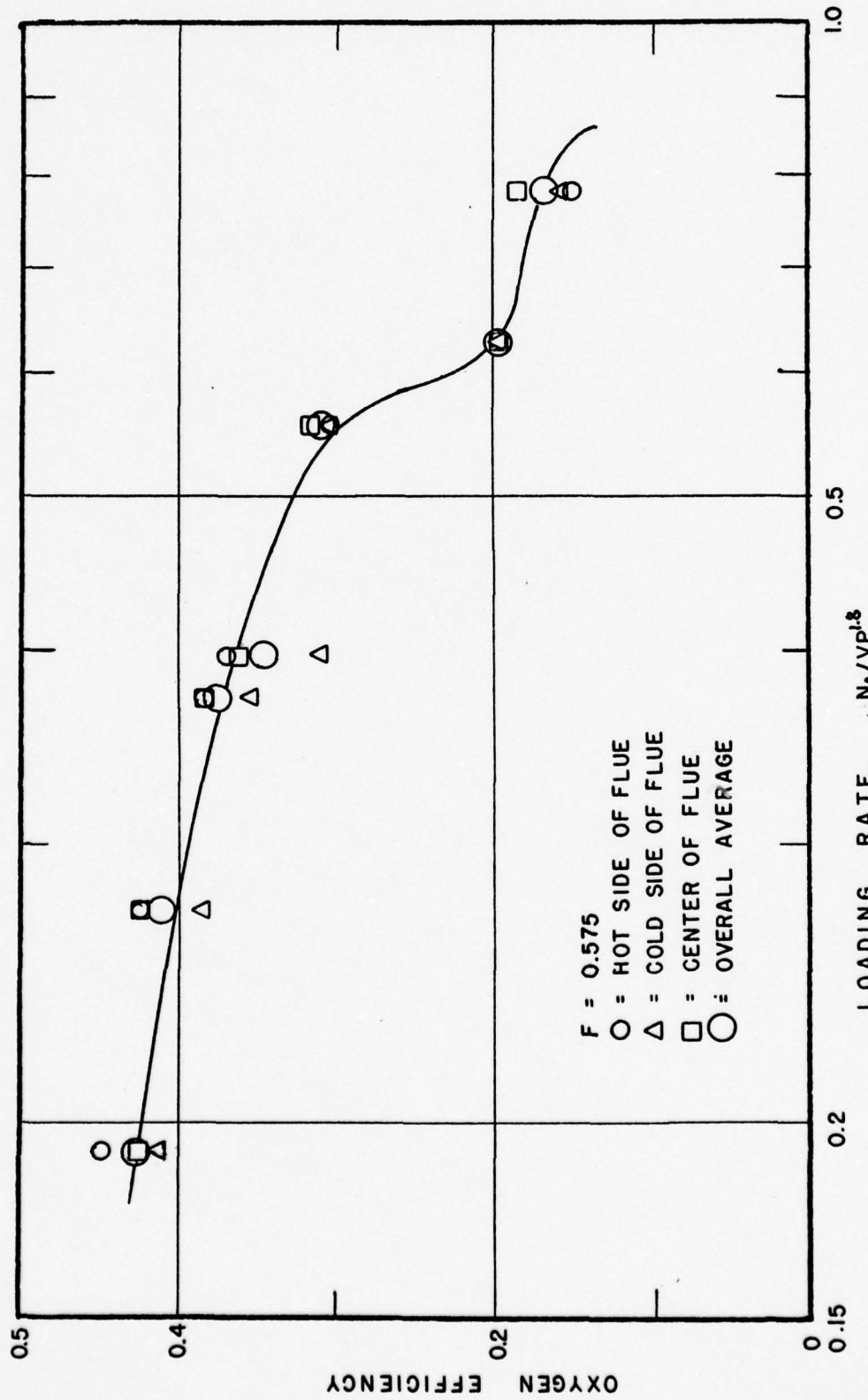


FIGURE V-10: OVERALL COMBUSTION EFFICIENCY OF ONE-JET CHAMBER

flame in the place where the dark "eye" of the low-flow-rate pattern had been. A photograph of the residual flame partially formed (but still not at the blowout limit) is shown in Figure V-8.

This one-jet chamber was the most extensively studied. Blowout limits were the first characteristic investigated. Since the only unambiguous blowout was the disappearance of the residual flame, only this stability limit is reported here. These blowout data are shown in Figure V-9. As in the case of the stability data for the three-jet chamber these data were taken at a pressure of 10" of mercury absolute and a temperature of 540°R. They are plotted on coordinates of $N_a/VP^{1.8}$ vs F together with the Longwell and Weiss data.

It was observed that the behavior of this chamber qualitatively followed that which would be expected from the recirculation model discussed in Chapter III. To investigate this further, combustion efficiency was determined as a function of loading rate at a constant fuel-air ratio and pressure. These measurements were made by means of a horizontal probe, with a side-entrance sampling port, buried in the roof of the chamber and extending across the flue. Because of the assymetry of the combustion pattern, three samples were taken at each air rate, one from each flue edge and one from

the center of the flue. The results are plotted in Figure V-10. Since this plot shows that there is only a small difference among these three samples, the simple arithmetic mean will be used in the analysis of the data.

To compare the chamber performance with the theoretical model, quantitative data on the composition and sizes of the various zones are also desirable. These were obtained by a combination of sampling in the chamber interior and photographic measurement. Samples of the chamber contents were obtained by a sampling traverse across the chamber. This was done for several feed rates, but at only one level in the chamber, about 2" from the floor, and one fuel/air ratio. One unfortunate result of this procedure was that the flow pattern in the chamber was upset by the introduction of the probe. This was indicated by a reduction in the stability limits for the chamber when sampling measurements were being made. This reduction was a function of how far the probe had been inserted into the chamber. These data are shown in Figure V-11.

The existence of the central eye and outer ring zones is indicated, and an estimate of zone volumes can be made by considering the midpoint in efficiency between the maximum and wall values to be the zone boundary.

However, the zone concept is better illustrated by cross-plotting Figure V-11 to give efficiency versus loading rate for each of several positions in the chamber (Figure V-12). Examination of that figure shows that the 2 and 3 cm. positions are characterized by a quite different response to loading from that of the 0, 1, and 4 cm. positions. The 5 cm. position (the cold wall of the chamber), where the mainstream of the non-burning jet passes shows some combustion because of mixing with the adjacent zone.

Photographs of the flame for two loading rates with the probe withdrawn are shown in Figure V-13. The probe positions in the sampling are indicated on these photographs.

Finally the effect of pressure on the blowout limit was studied. Runs were made by establishing a stable flame at a predetermined value of feed rate and fuel/air ratio. The pressure on the chamber was then gradually reduced until blowout occurred. During this series of runs the pattern of the approach to blowout was not noticeably affected by the pressure level. Data showing the effect of pressure on blowout are given in Figure V-14. Four fuel-air ratios were studied. A plot of pressure exponent vs the generalized fuel fraction is shown in Figure V-15. Also shown in Figure V-14

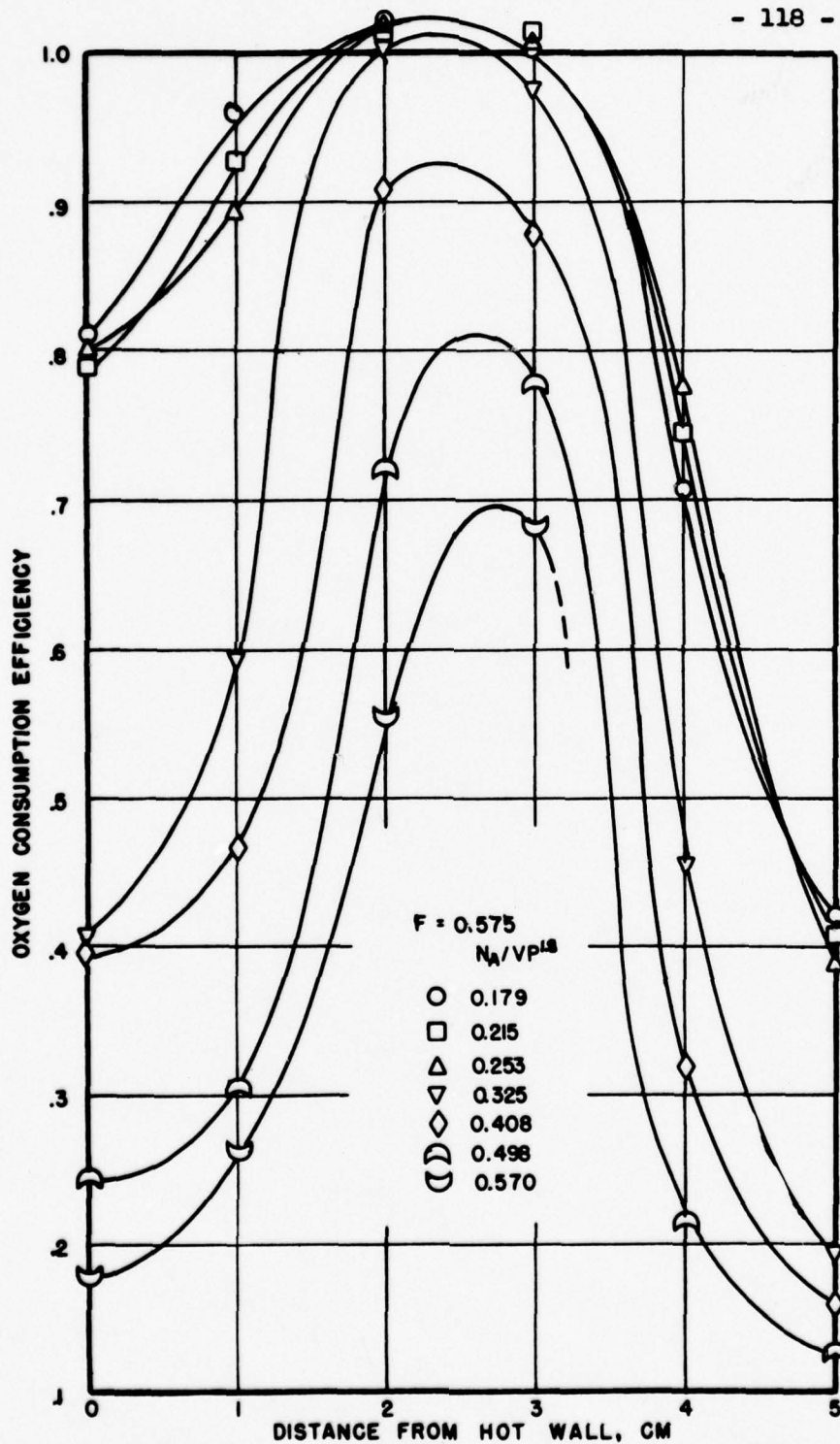


FIGURE V-II: COMBUSTION EFFICIENCY TRAVERSES IN ONE-JET CHAMBER (2" FROM FLOOR)

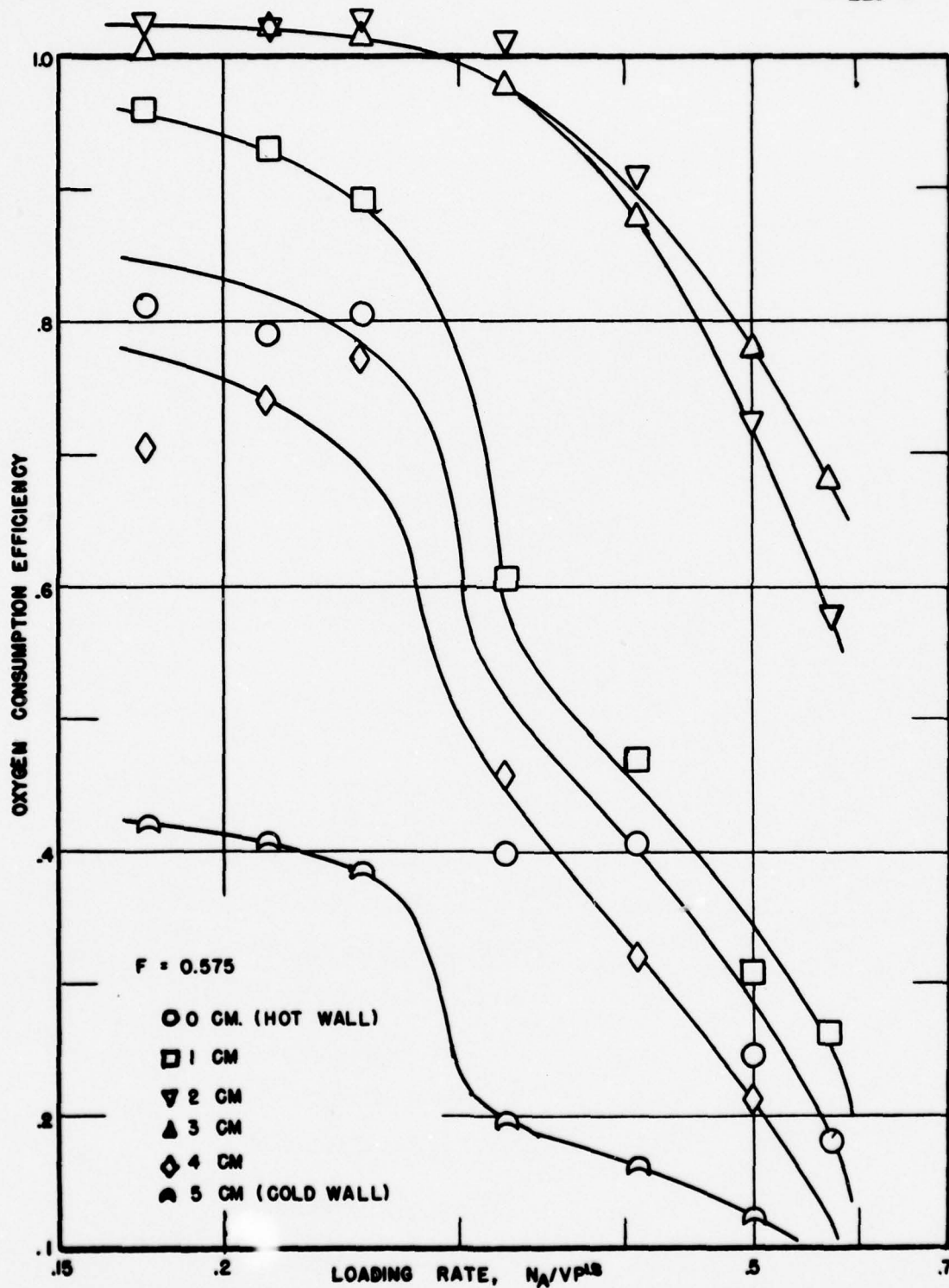


FIGURE X-12: CHAMBER BURNEDNESS AT VARIOUS POSITIONS

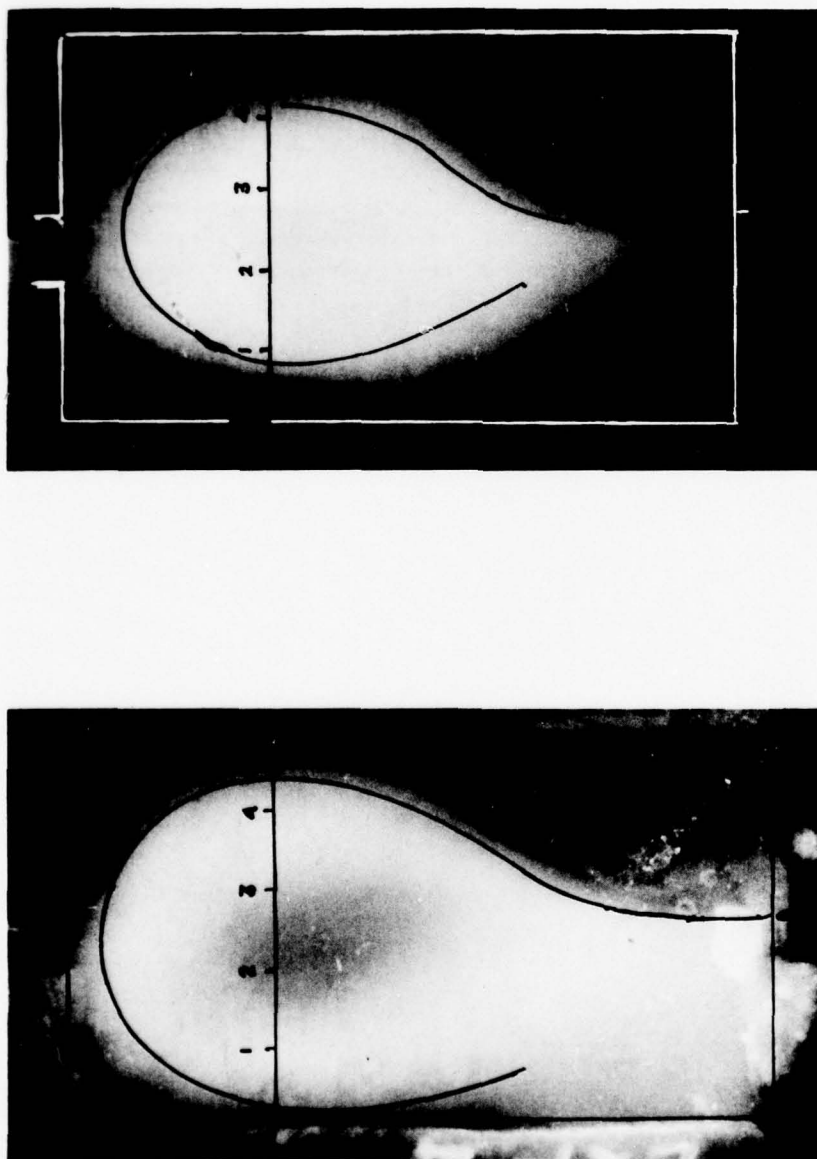


FIGURE Y-13: PHOTOGRAPHS SHOWING TRAVERSE STATIONS IN
SAMPLING CHAMBER CONTENTS. LEFT, $N_A/VP^{1/8} = 0.215$;
RIGHT, $N_A/VP^{1/8} = 0.498$.

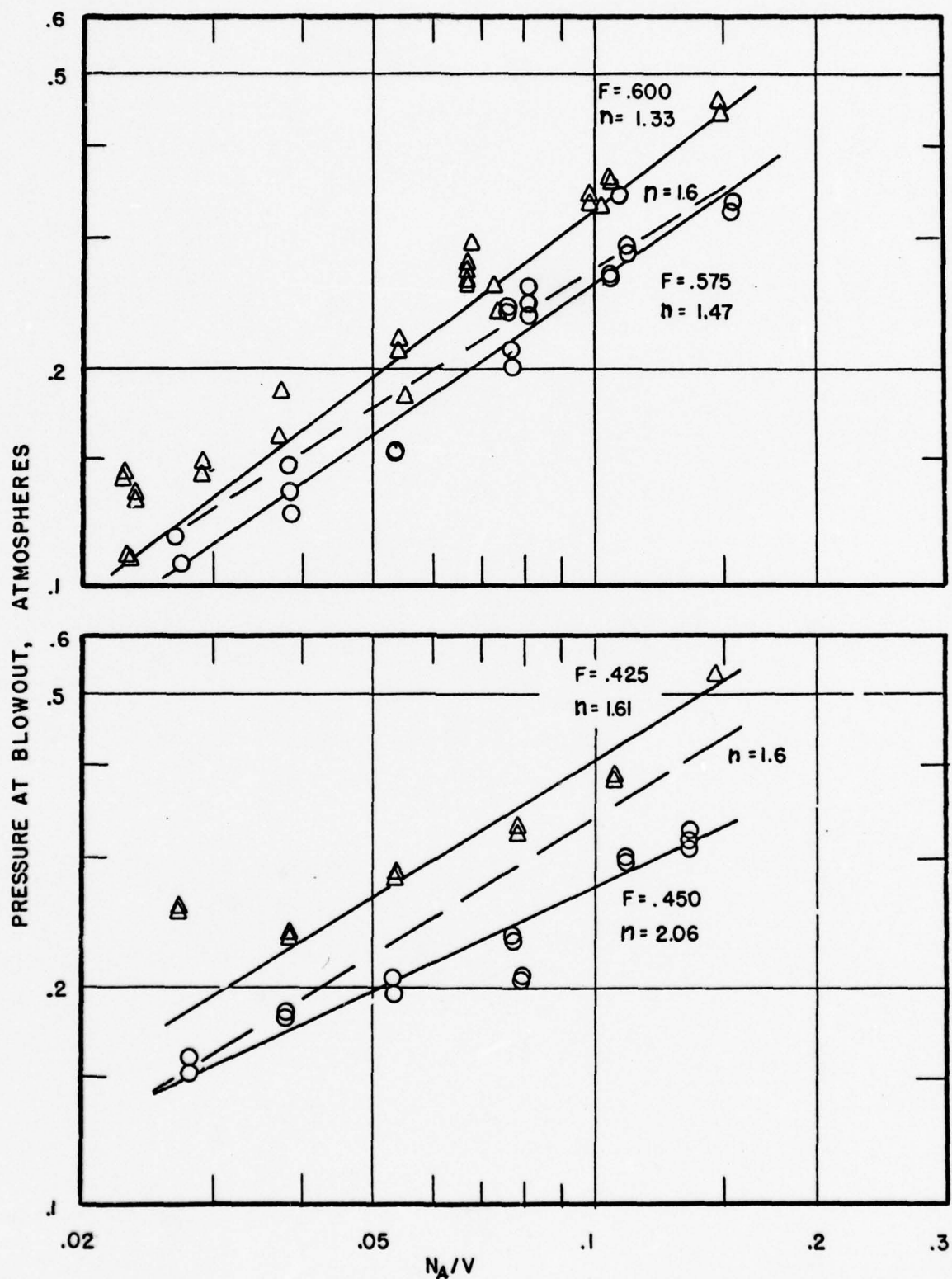


FIGURE V-14: PRESSURE EFFECT ON BLOWOUT FEED RATE.
FEED/VOLUME RATIO AT BLOWOUT VS PRESSURE
(DASHED LINE IS AVERAGE $n = 1.6$)

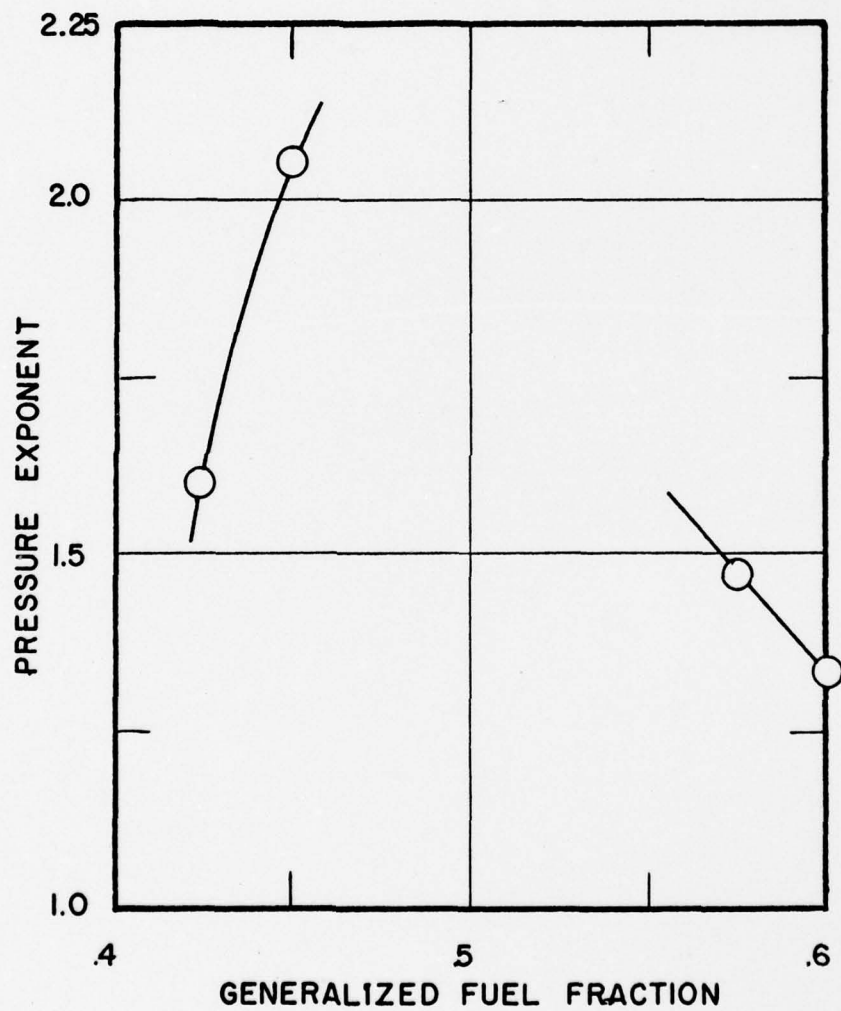


FIGURE V-15: EFFECT OF FEED COMPOSITION ON PRESSURE EXPONENT

- 123 -

is a line for the average exponent "n" of 1.6 representing the results of all of the data on this chamber.

CHAPTER VI

DISCUSSION OF RESULTS

The experimental program was undertaken to provide data for examining the question of whether stirred reactor performance data could be combined with fluid flow patterns to predict the performance of practical combustors. Using stirred reactor blowout data, model performance for the two-stability-limit model may be predicted. Since sufficient experimental data on the efficiency-loading relation for the stirred reactor are not available, performance of the recirculation model must be predicted from theoretical stirred-reactor performance. The analysis of the data consists principally of direct comparison of these theoretical models with the experimental reactor results.

Experimental Errors

The discussion of the experimental work must be prefaced by commentary on the errors involved in these experiments. Two significant sources of experimental error were present; air leakage into the combustion zone and non-ideality of the stirred reactor. A third lay in the construction of the nozzle header assembly which ideally should have perfectly aligned and matched nozzles. This last was not as much a problem as the

first two because the effect of mis-matched or mis-aligned nozzles was easily detected. Each of these problems will be discussed in turn.

Air Leakage. The combustion chamber, consisting as described previously of an arrangement of firebrick and nozzles between two frames carrying the Vycor windows, is fed by high velocity jets along its floor. In any system of this sort the jets aspirate gases from the surrounding fluid, and near the top of the chamber a reverse flow of the chamber a reverse flow occurs to replace the gases aspirated from the recirculation zone. To create this reverse-flow pattern requires (from a momentum balance) a low-pressure region in the lower portion of the chamber. If there is an improper seal between the chamber and its side walls, substantial quantities of air can be aspirated from the ambient air into this low pressure region of the combustion chamber. In the construction of the apparatus, precautions were taken to seal the chamber tightly. However, from time to time thermal warpage of the side frames or improperly fitted bricks made a satisfactory seal impossible. This problem may be alleviated to some extent by careful sizing of the exit flue or flues. If these are made narrow enough the pressure drop required to force the exhausted gases through them may be sufficient to raise

the pressure at the top of the chamber so that the low-pressure region in the recirculation zone is at or above ambient pressure.

The presence of an air leak in the chamber assembly could be most easily detected by a shifting of the stability limits of the chamber toward the rich side (i.e. stability data which lacked symmetry around a stoichiometric fuel/air ratio). This criterion, however, was not highly sensitive, as a substantial shift was required to differentiate asymmetry due to air leakage from the small asymmetry inherent in the well-stirred reactor stability curves.

To test whether the chamber was properly sealed when the blowout curves were symmetrical, one run was made in which a sample of gas was withdrawn from the interior of the chamber. An Orsat analysis of this sample for the carbon/nitrogen ratio was compared to the ratio calculated from the metered rates of fuel and air. The results are tabulated in Table VI-1. Included in this table is the hydrogen/carbon ratio which serves as a check by comparison with the hydrogen/carbon ratio for propane. Since only enough data were obtained to calculate the H/C ratio from the known ratio of nitrogen/oxygen in air (or visa-versa), only one check on the analysis could be calculated. Indicated in

Table VI-1 is the H/C ratio of propane, 2.67. Analyses of the fuel have shown the propane to be about 96% pure (10), the principal impurities being ethane, propylene, and butane. Assuming a typical analysis as given by Woo (30) of 0.8% ethane, 1.5% propylene, 1.5% butane, and the balance propane, the calculated atoms of carbon per mole of propane are 3.01 and the H/C ratio is 2.66.

TABLE VI-1

Comparison of Carbon/Nitrogen ratio Determined by
Sampling with the Metered Ratio

	Value from Sample	Calculated by Metering
C/N	0.150	0.156
H/C	2.68	2.66

When the sampling data reported in this table were taken the stability limits of the combustor were approximately symmetrical. In this table it is seen from the comparison of H/C that the analysis of the sample is reliable. The agreement between the C/N ratios, though it indicates a small leakage, is close enough to constitute a good check on the absence of serious leaks at the time of this test. On the basis of this analysis it is concluded that symmetrical blowout limits are a sufficient test of the absence of air leaks.

Departure from ideal reactor conditions A second source of error in these experiments is the departure of the chamber from ideal reactor operation. In the theoretical development of Chapter III, the models were based on the assumption of an ideal stirred reactor in which operation was adiabatic and the reaction rate was first order in each of the reactants. In principle, the models discussed are not necessarily thus restricted. Any relationship of combustion efficiency to feed rate or blowout loading to fuel/air ratio determined experimentally on a stirred reactor may be used in place of the theoretical curves used in the previous chapter. As pointed out, however, this generalization is restricted to reaction schemes in which a single reaction controls the rate. Where successive or competitive reactions are possible, one cannot use a single experimental stirred reactor performance curve to compute model performance.

In comparing combustor performance with the theoretical model prediction, one need consider only the first of these problems (i.e. heat loss) in the two-stability-limit model, since the reactors of the model are operating in parallel. In the recirculation model, both heat loss and multi-step reaction departures are significant.

In the present work, the comparison of the experi-

mental results with the theory is based on experimental stirred-reactor performance for the two-stability-limit model. For work with the recirculation model the idealized stirred reactor theory is used. Although it would be clearly preferable to use an experimental stirred reactor performance curve, such data have not yet been reported in the literature in sufficient detail to be of use here. To the author's knowledge, only one curve of efficiency vs feed rate has been reported (14), and this curve was at a different fuel/air ratio than the one used for the present investigation.

There are ample blowout data reported in the literature. The available data indicate that for hydrocarbons, there is no substantial difference in the performance of various members of the same family (i.e. saturates, olefins, etc.), and in general, most hydrocarbons behave approximately the same. Acetylene and hydrogen are different. This permits analysis of the blowout data to be based on empirical curves of blowout rates vs fuel/air ratio.

Using either the theoretical performance curves or the experimental blowout curves, account must be taken of the fact that the heat losses from this reactor are significantly greater than those for the stirred reactor experimental conditions. In the present

experimental work, no direct measurement of the heat losses was made. An estimate of their magnitude involved accounting for losses by radiation through and from the Vycor windows, and for conduction-convection losses directly through the windows. No correction for losses through the firebrick was made since it was felt that it was sufficiently thick to make losses in this direction negligible compared with the other heat losses in this chamber.

In computing the heat losses from this chamber both radiative and convective heat transfer had to be considered. Since the chamber was of small dimensions and operated at low pressures, gas radiation could be neglected. Heat transfer from the gases to the chamber walls and Vycor windows was by convection. Heat transferred to the walls and roof of the chamber was then radiated to the Vycor windows and the outside surroundings seen through the windows. Heat transferred to the windows was transferred by radiation and convection simultaneously to the outside.

In computing the heat transferred by radiation, the chamber was divided into three zones; the walls and roof, the floor and the windows. The walls and roof were considered to be a heat source at a temperature T_w (different from the gas temperature). The windows

were considered to be a heat sink. The floor of the chamber represented a refractory surface, returning as much heat by radiation to the chamber as it received from the walls and windows. Vycor windows, made of nearly pure quartz, transmit radiation whose wave length is shorter than 3.7μ , and are nearly opaque to radiation of longer wavelengths. Therefore, the absorptivities and emissivities of Vycor to radiation from various temperature sources (the walls and the floor) had to be accounted for in the calculations.

Calculations were carried out for the three-jet chamber using a heat transfer coefficient from the gases to the brick of $10 \text{ Btu/hr ft}^2 \text{ }^\circ\text{F}$ at the blowout velocity, and it was assumed that the heat transfer coefficient varied linearly with velocity. A convection coefficient from the Vycor windows to the ambient air was taken to be $2 \text{ Btu/hr ft}^2 \text{ }^\circ\text{F}$. The brickwork and the floor of the chamber were assumed to have an emissivity of 1.0. The Vycor was assumed to be black at wave lengths above 3.7μ , and transparent at wavelengths below this. The reflectivity of the Vycor was ignored in this calculation. Figure VI-1 shows the resultant heat loss rate from the chamber as a function of temperature and relative firing rate.

Allowance for the effect of heat loss in the

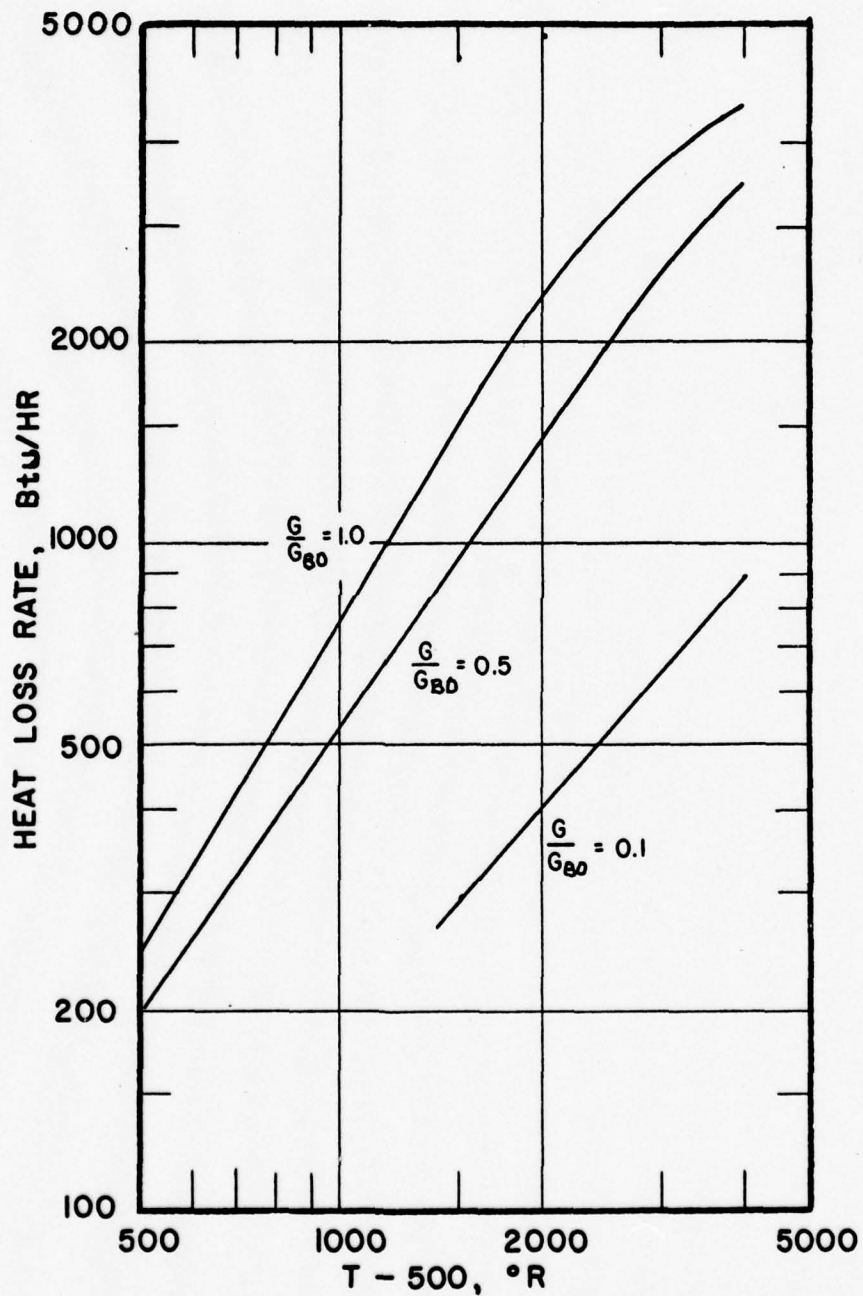


FIGURE VI-1: HEAT LOSSES FROM THREE-JET CHAMBER

HEAT RELEASE RATE FOR A STOICHIOMETRIC MIXTURE AT BLOWOUT = 120,000 Btu/HR ($\beta = 70\%$)

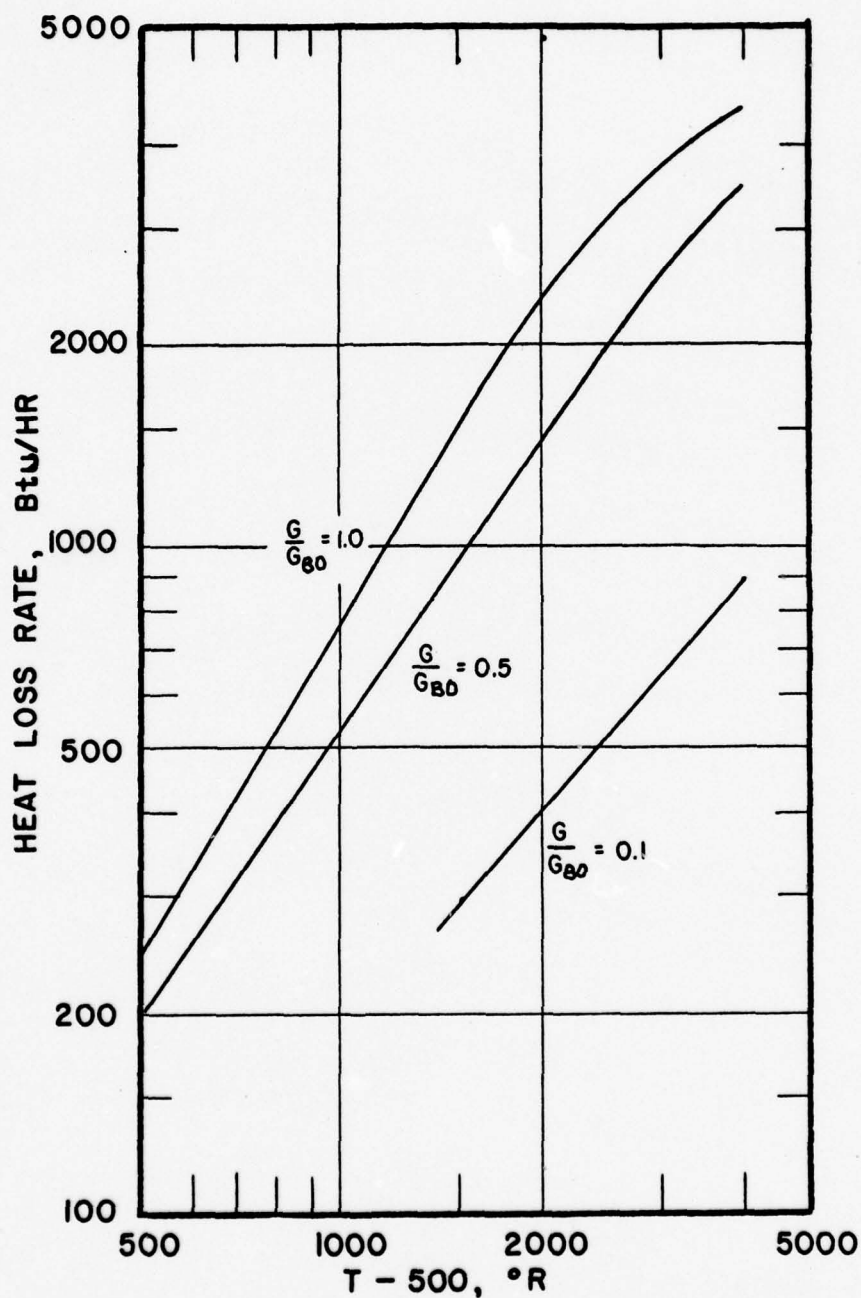


FIGURE VI-1: HEAT LOSSES FROM THREE-JET CHAMBER

HEAT RELEASE RATE FOR A STOICHIOMETRIC MIXTURE AT BLOWOUT = 120,000 Btu/hr ($\beta = 70\%$)

calculation of chamber performance has been made in the past (3, 14) by assuming the heat losses to correspond to an effectively lower inlet temperature to the reactor. This technique has been applied principally to the problem of the effect of temperature on blowout limits. Allowance for the effect of heat losses by substitution of an artificial inlet temperature requires a previous knowledge of, or an independent calculation of, the heat loss. If the heat loss is known as a function of temperature and/or Reynolds number, a modified approach is suggested. This is outlined below.

Consider a reactor for which the heat loss rate may be expressed by the relation:

$$q = UA(t - t_o) \quad \text{VI-1}$$

where U is the heat transfer coefficient based on the heat transfer area, A , the temperature, t , of the burning gas and the ambient temperature, t_o , (also the inlet gas temperature).

The simplified heat balance for the adiabatic reactor is given by:

$$t_a = t_o + \Delta_{af} \beta \quad \text{VI-2}$$

and by a process analogous to that used to obtain VI-2, the heat balance for a non-adiabatic reactor may be written:

$$G c_p (t - t_o) + UA (t - t_o) = \Delta_{af} \beta \quad \text{VI-3}$$

where Δ_{af} is the adiabatic flame temperature rise for complete combustion

β is the fractional burnedness of the gases

G is the molal feed rate to the chamber

and c_p is the molal heat capacity of the gases fed.

Rewriting VI-3 leads to an expression parallel to VI-2;

$$t = t_o + \frac{\Delta_{af}}{1 + \frac{UA}{G c_p}} \beta \quad \text{VI-4}$$

The heat balance represented by Equation VI-4 may now be combined in the usual manner with the equation describing the stirred reactor behavior.

Two limiting cases for VI-4 are of interest. If the heat transfer rate is controlled by forced convection or turbulent diffusion, then to a first approximation the heat transfer coefficient, U , may be assumed to be directly proportional to the mass feed rate, G . Then the denominator of the fraction in IV-4 becomes a constant, and the heat loss rate is a constant percentage of the total heat released, i.e. $t = t_o + \frac{\Delta_{af}}{1 + \alpha} \beta$. This is nearly equivalent to an adiabatic reactor operating on a fuel-air mixture diluted with additional inert gas such as nitrogen.

If, on the other hand, the heat transfer coefficient is independent of the Reynolds number, such as in

radiation or conduction, and if U may be treated as a constant over substantial ranges of temperature, then Equation VI-4 assumes the form:

$$t = t_o + \frac{\Delta_{af}}{1 + \frac{\gamma}{G}} \beta \quad \text{VI-5}$$

In radiant heat transfer the assumption of linear variation of heat loss with temperature over substantial temperature ranges is not good, but it is justified here by the simplicity thus introduced. Efficiency vs burnedness curves for a stirred reactor operating with heat losses corresponding to the two limiting heat loss cases above are shown in Figure VI-2. In this figure it is seen that the shape of the reactor performance curves near blowout is not greatly affected. At lower feed rates, however, the heat loss in the constant U case correspond to marked cooling of the gases and results in quenching the reaction. Thus significant departure from the adiabatic stirred reactor curve is predicted.

A second error introduced into the comparison of the experimental reactor performance with the theoretical stirred reactor lies in the departure of the stirred reactor from the simple bimolecular kinetic mechanism. There seems to be general agreement in the literature that the apparent overall order of high-temperature

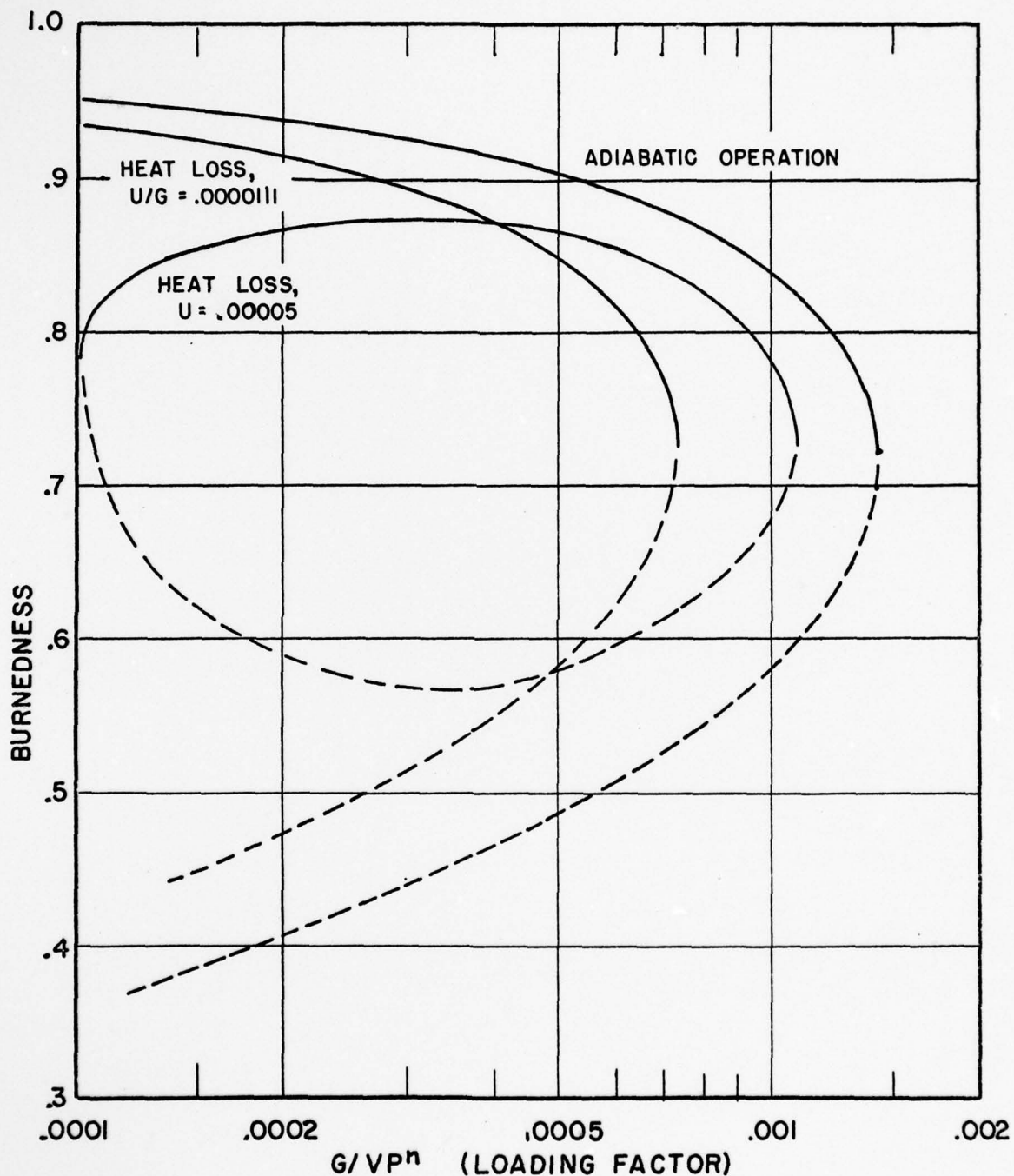


FIGURE VI - 2: EFFECT OF HEAT LOSS ON STIRRED REACTORS

CASE I: RATIO $U/G = C$, CORRESPONDING TO A
CONSTANT PERCENTAGE OF HEAT LOSS
($U/G = .0000111$)

CASE II: $U = C$, CORRESPONDING TO HEAT TRANSFER
COEFFICIENT INDEPENDENT OF G .
($U = .00005$)

reaction in combustion is less than two. Values from about 1.3 to 2.0 have been reported, with no general agreement on the exact value. Values between 1.6 and 1.8 are the most generally accepted. In the present work the pressure exponent of the reactor at blowout was determined for four different fuel/air ratios, and values of "n" ranging from 1.3 to 2.0 were found. It should be pointed out, however, that this variation may involve the simultaneous effect of the variation of reaction rate with composition and variation of mixing rate with Reynolds number, since the experiments were not run at a constant Reynolds number. Even when experiments are restricted to a single feed composition, the variation in results illustrated due to pressure may be to an unknown degree due as well to Reynolds number variation with its associated effect on mixing and to variation in heat loss with velocity change in feed rate.

A consequence of using a second order equation when the actual equation is of lower order but with the activation energy unchanged is a change in the shape of the curve as illustrated in Figure VI-3. In this figure the theoretical curve for a reaction rate first order in each of fuel and air is compared with the curve for a rate which is first order in air and 0.8 order in fuel. These latter values for exponents were recommended

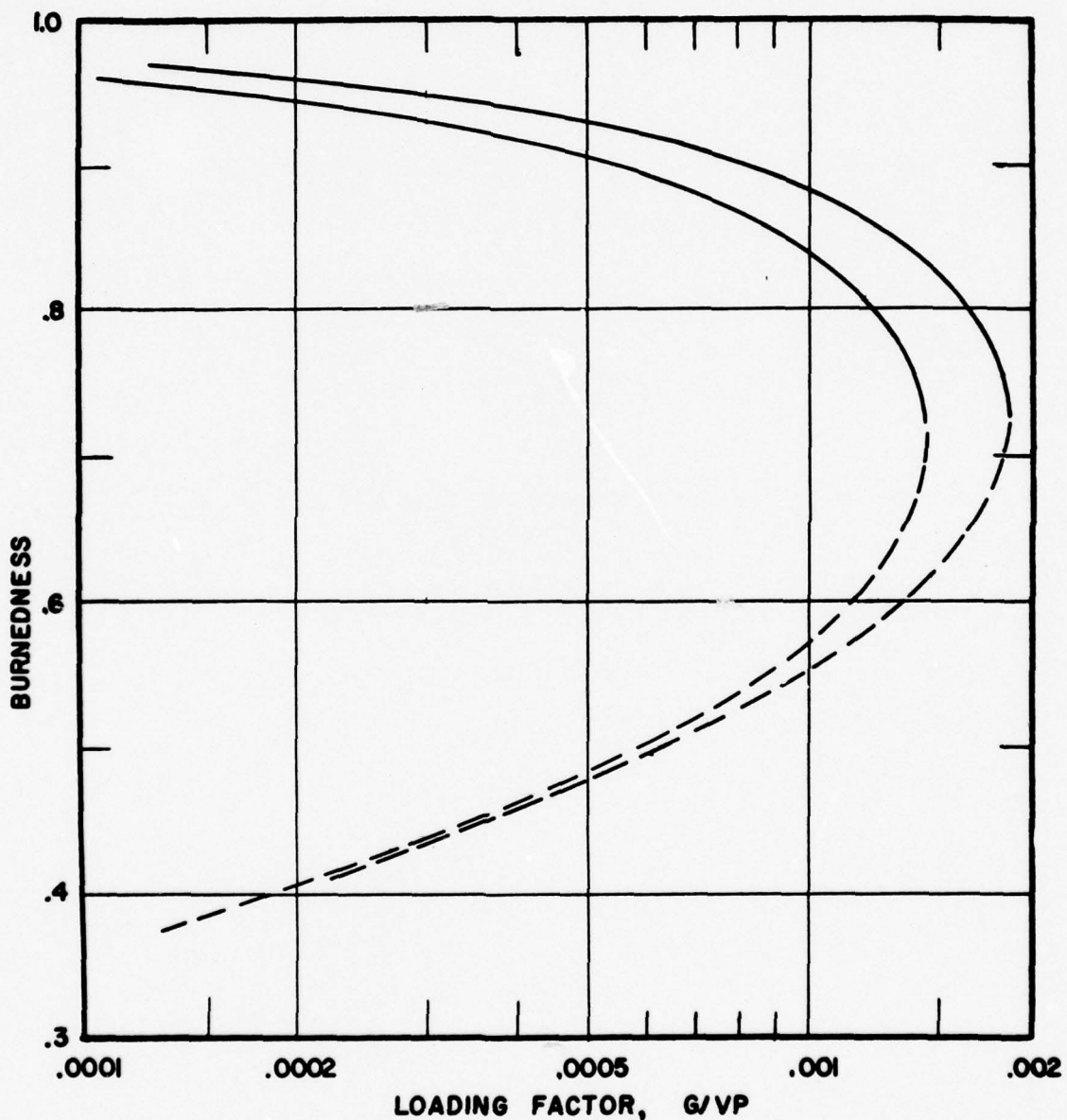


FIGURE VI-3: EFFECT OF CHANGING PRESSURE EXPONENT
ON PREDICTED STIRRED REACTOR OPERATION

by Longwell and Weiss on the basis of their studies. (The lateral displacement of the curve in Figure VI-3 is irrelevant, and is simply a consequence of not changing the numerical value of the "collision constant".)

For the present work it has been concluded that although accurate experimental data on the loading rate-efficiency behavior of the stirred reactor would be desirable, the use of theoretical curves for a comparison of the model behavior with the experimental behavior is necessary. Since in the firing rate range of interest the difference in shape between idealized stirred reactor curves of β vs G and reactor performance corrected for heat loss and order of reaction are not great, it does not appear justifiable to include these corrections. The corrections are not known sufficiently well to attach greater certainty to a corrected curve than to an uncorrected one.

Errors in Measurement A third general category of error to which this experimental program was subject is that of errors in measurement. The measurements of significance in this experimental work are:

- (1) measurement of flow rates
- (2) measurement of chamber dimension. This included the height, width and depth, location and size of the nozzles and exit flue

- (3) the parallelism of the jets when the three jet chamber is being used, and parallelism of the nozzle block assembly and the sidewalls of the chamber.

By far the most critical measurements were those on the size, spacing and alignment of the feed-jet assembly. Even slight errors here were sufficient to cause substantial reductions in the chamber stability. Every effort was made to obtain uniformity in the jet assembly. The slot openings were measured with a feeler gauge, and the jet alignment was checked by means of a scale with 1/100" graduations read with a magnifying glass. In the final analysis, however blowout measurements provided the best test of accurate assembly. Although it is believed that errors of this type do not significantly effect the blowout and efficiency studies, it is difficult to demonstrate this conclusively.

Errors in the measurement of flow rate and of brickwork dimensions are relatively unimportant in this work. Experience with calibrating and metering with standard square-edge orifices indicates that the error in metering was approximately 1% in mass flow. Errors of the dimension were kept as small as possible with the loose, friable type of refractory used. However, brickwork dimension errors which were known to be substantial

had no apparent effect on the chamber stability; so it was concluded that errors resulting from this source had negligible effect on the overall result.

Analysis of the Three-Jet Chamber Performance

In the study of the three-jet chamber, two stability limits were observed, one corresponding to a sudden shift in flow pattern with blowout of the flame in part of the chamber, and the other corresponding to total blowout. A theory explaining this behavior qualitatively has been discussed in Chapter III. It is now proposed to fit the theory quantitatively to the data.

Consider, first, approximations which can be made to the theory of Chapter III. As the blowout condition is approached, (the figure representing this condition is reproduced for conveniency in Figure VI-4), the stable intersections, corresponding to stable combustion, approaches the noses of Branches I or II, depending on the mode of chamber operation. In doing this, the corresponding operating point on the well-stirred reactor curve for the zone in question also approaches the blow-out point of the stirred reactor curve. A reasonable approximation which can be made to this situation is to say that the blowout of a stable zone will occur when that zone has reached the blowout loading rate calculated on the basis of the stirred reactor. Since it was

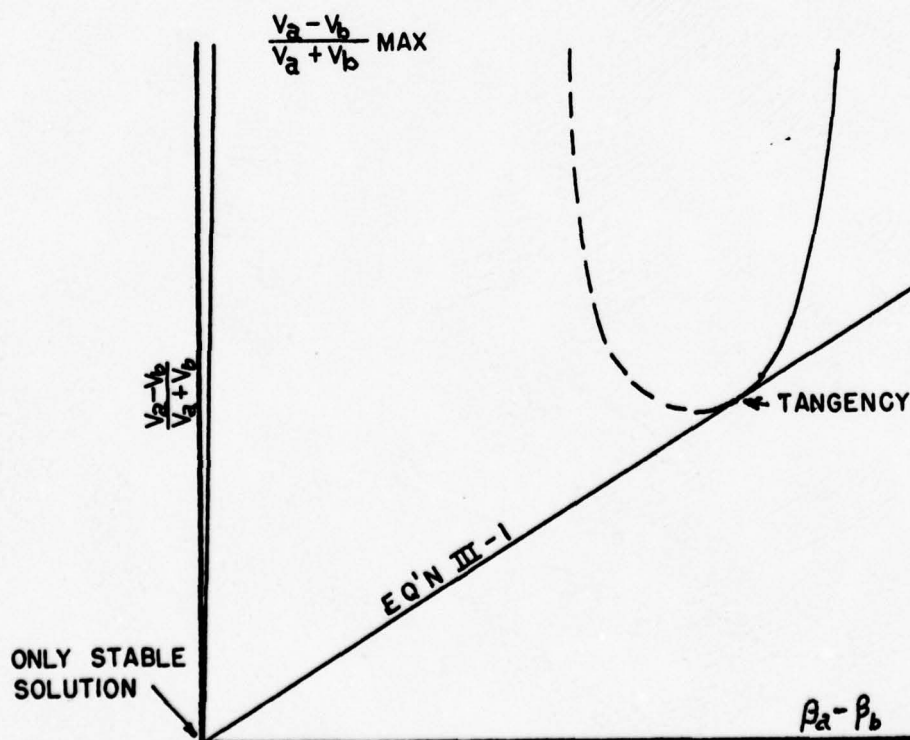
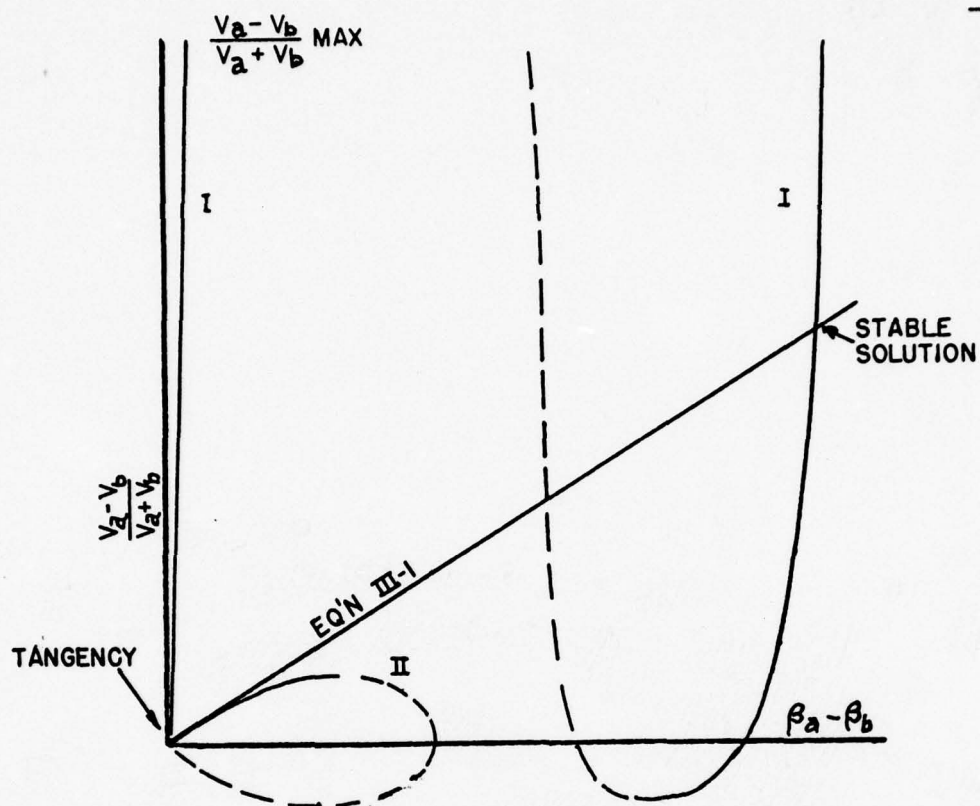


FIGURE VI-4: TWO-STABILITY-LIMIT MODEL
BLOWOUT CONDITIONS

theoretically predicted that blowout occurred in this model at a somewhat higher burnedness than that corresponding to stirred reactor blowout, this assumption is not rigorously valid. However, in this range of loading rates, burnedness changes very rapidly with loading, so that only a small error in blowout flow rate is introduced by this assumption. If knowledge of the volumes and feed rates of the two zones in this chamber is postulated, it is possible to predict whether the chamber will burn stably in the two-zone or one-zone configuration, or be completely blowout at a given feed rate.

The measurement of combustion zone volume in a turbulent bunsen cone has been accomplished by Simon and Wagner (22) using flame photographs of the blue luminosity of a pre-mixed fuel/air mixture. The theoretical validity of this method is uncertain, since some combustion reactions, such as carbon monoxide and hydrogen oxidation produce nearly non-luminous flames, whereas reactions involved in the initial stages of hydrocarbon combustion, generally involving C-H or C-C bond fracture, give rise to the characteristic color of normal flames. If the hypothesis is that the initial stages of combustion are rate-controlling, then the measurement of the luminous zone will give a reasonable

approximation to the volume of combustion. If carbon monoxide oxidation is postulated to be the rate-controlling step, then this measurement may be grossly misleading.

The feed rate to each half of the chamber is postulated to be a constant fraction of the total feed and in addition, a constant fraction of the fresh feed is assumed to grossly bypass the active volumes in the chamber. In the case of a symmetrical combustion pattern, this is a reasonable assumption. For asymmetrical combustion patterns it is assumed that this is still valid (i.e. when the combustion pattern changes due to a blowout of one side of the chamber, no change in the fraction of the fresh feed reaching the remaining active zone occurs).

Combining these assumptions with the data on the photographically measured flame volumes leads to the conclusion that both blowout curves for the three-jet chamber should be displaced from the well-stirred reactor curve by a constant multiplying factor, and that the two blowout curves for the three-jet chamber should be displaced from each other by a constant predicted from the difference in zone volumes only. Since Figure V-6 shows the zone volumes to be independent of fuel/air ratio, if the three-jet chamber were composed of stirred

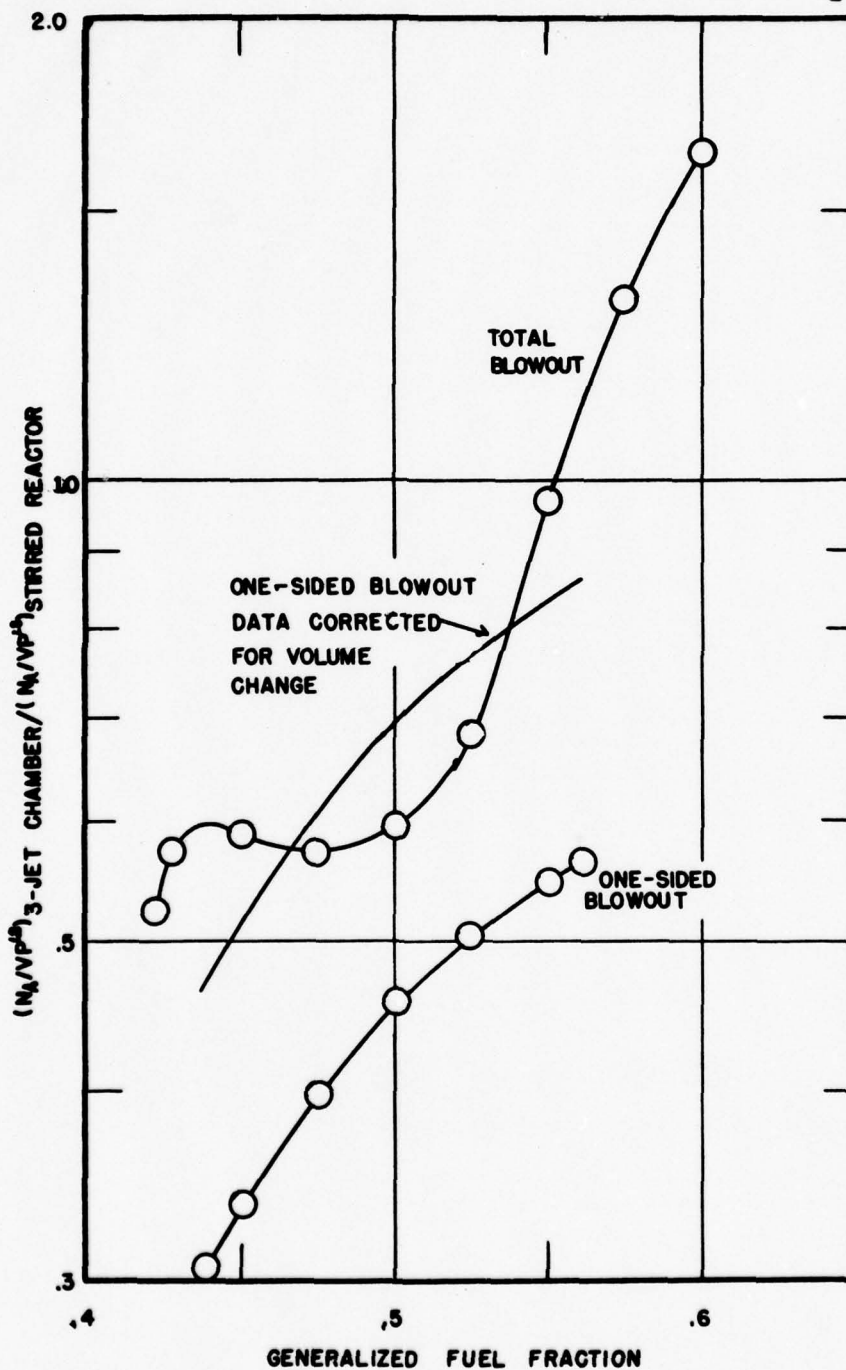


FIGURE VII-5: COMPARISON OF STIRRED REACTOR BLOWOUT DATA AND THREE-JET CHAMBER DATA. ONE-SIDED BLOWOUT DATA HAVE BEEN CORRECTED BY THE RATIO OF ZONE VOLUME AT ONE-SIDED BLOWOUT TO ZONE VOLUME AT TOTAL BLOWOUT.

reactor elements, one would expect that the performance curves of the well-stirred and the three-jet combustors should be displaced from each other by a constant which is independent of fuel/air ratio. This is not observed, as may be seen in Figure VI-5. This deviation from the expected behavior may result from the inadequacy of the assumptions above or it may reflect the inability of the stirred reactor to describe operation in the active zones.

The model also predicts that the two curve for the three-jet chamber should be separated from each other by a constant which may be derived from the zone-volume data. This may be argued formally:

- (1) If V_1 represents the volume of the smaller zone (of the two active zones),
- (2) V_2 represents the volume of the large zone when there is only one active zone, and
- (3) If Y represents the fraction of the feed reaching each zone which is the same for each active zone and independent of flow rate and zone volume,

then, $V_1/GY = L_1$, the loading factor for active zone 1 and $V_2/GY = L_2$, the loading factor for active zone 2.

When an active zone blows out, it is postulated that it is at the critical loading factor, L_{BO} , of the

stirred reactor at blowout. Hence $L_{BO_1} = L_{BO_2}$, or

$$\frac{Y_{G_{BO_1}}}{Y_{G_{BO_2}}} = \frac{V_1}{V_2} = \frac{G_{BO_1}}{G_{BO_2}}$$

In Figure VI-5, the stirred reactor curve has been compared to the three-jet chamber stability curves by plotting an ordinate of $(N_A/VP^{1.8})_{3jc} / (N_A/VP^{1.8})_{wsr}$ vs generalized fuel fraction. It is immediately apparent that the three-jet chamber does not follow the expected performance based on that of the well stirred reactor. However, the two curves representing the blowout limits of the three-jet chamber are approximately displaced from each other by the expected amount. The significance of the unexpected relative performance is not clear. It might be argued that this resulted from air leakage into the chamber. This argument is countered, however, with the evidence discussed at the outset of this chapter that the data are essentially free from air leakage errors. A second possible reason for this behavior is that the difference in the combustion characteristics of propane (used here) and octane (used by Longwell) is sufficient to cause this behavior. This argument is not supported by any evidence. Recent work done at M. I. T. (5) as yet unpublished) using pure propane as

the fuel in a well-stirred reactor gave the results indicated in Figure II-8, showing no difference in stirred reactor performance which could account for the observed difference in the three-jet chamber and the stirred reactor performance characteristics. Therefore, one is led to the conclusion that the observed difference represents a characteristic of the operation of the active zones not accounted for by the stirred reactor performance.

The efficiency measurements made on this chamber, though not extensive enough to fit to any model, are useful for showing that the chamber operates at a reasonable efficiency level. From these measurements it is also possible to estimate the quantity of gross bypassing of the combustion zones. If one takes a value of β of 90% for the burnedness of each of the zones (an average figure representative of the efficiency data reported by Longwell (14)), then for the gross efficiency to be about 70% leaving the three-jet chamber requires approximately 22% of the total feed to the chamber to bypass completely the combustion zones. The balance (78% of the total feed) enters the combustion zones and burns to a 90% efficiency. Were the ratio of gross loading factor for the three-jet chamber at blowout to the well-stirred reactor at

blowout known with certainty, it would be possible to calculate the fraction of volume in each recirculation zone which was active and that fraction which was inactive. However, because of the behavior of the ratio (Figure VI-5) no constant value for volume ratio is consistent with the rest of the theory.

In addition to the results reported here, an attempt was made to use Schlieren photography to gain an insight into the mechanism of chamber behavior. These efforts, unfortunately, were unsuccessful, due particularly to extraneous patterns caused by the hot glass and by the warm turbulent air ambient to the chamber in the vacuum vessel which were in the optical path.

Analysis of the One-Jet Chamber Performance

The theory developed to explain the two-stability limits observed in the three-jet chamber implied that a similar behavior should be observed in the one-jet chamber. To test this hypothesis a one-jet chamber was built and tested. The first design tried was a chamber of width $1/3$ rd that of the original three-jet chamber. As mentioned previously, this proved to be too narrow since its stability limit was unreasonably low. Stable operation was achieved by making the chamber 2" wide

rather than the original 1" width, still narrower, however, than the original 3" wide three-jet chamber. Stable combustion was easily established in the one-jet chamber, though the combustion pattern was not symmetrical (see Figure V-7 and 8). It is postulated that this asymmetrical combustion pattern is a consequence of a basic instability of the cold flow pattern in which there is no stable symmetrical flow pattern regardless of how slowly the chamber is fed. Because no symmetrical combustion pattern existed, there was no possibility of the dual stability limit found in the three-jet chamber. From the behavior of the combustion pattern as blowout was approached, a model analogous to the recirculation model discussed in Chapter III was suggested.

To compare the narrow one-jet chamber with the theoretical recirculation model of Chapter III, efficiency vs loading rate data were required. Blowout data were also taken to compare the performance of this chamber with that of the stirred reactor.

The comparison of the stirred reactor data and the one-jet chamber blowout data is shown in Figure VI-6. These data show a deviation from the stirred reactor which is not accounted for by the model. As in the case of the two-stability-limit model, the recirculation

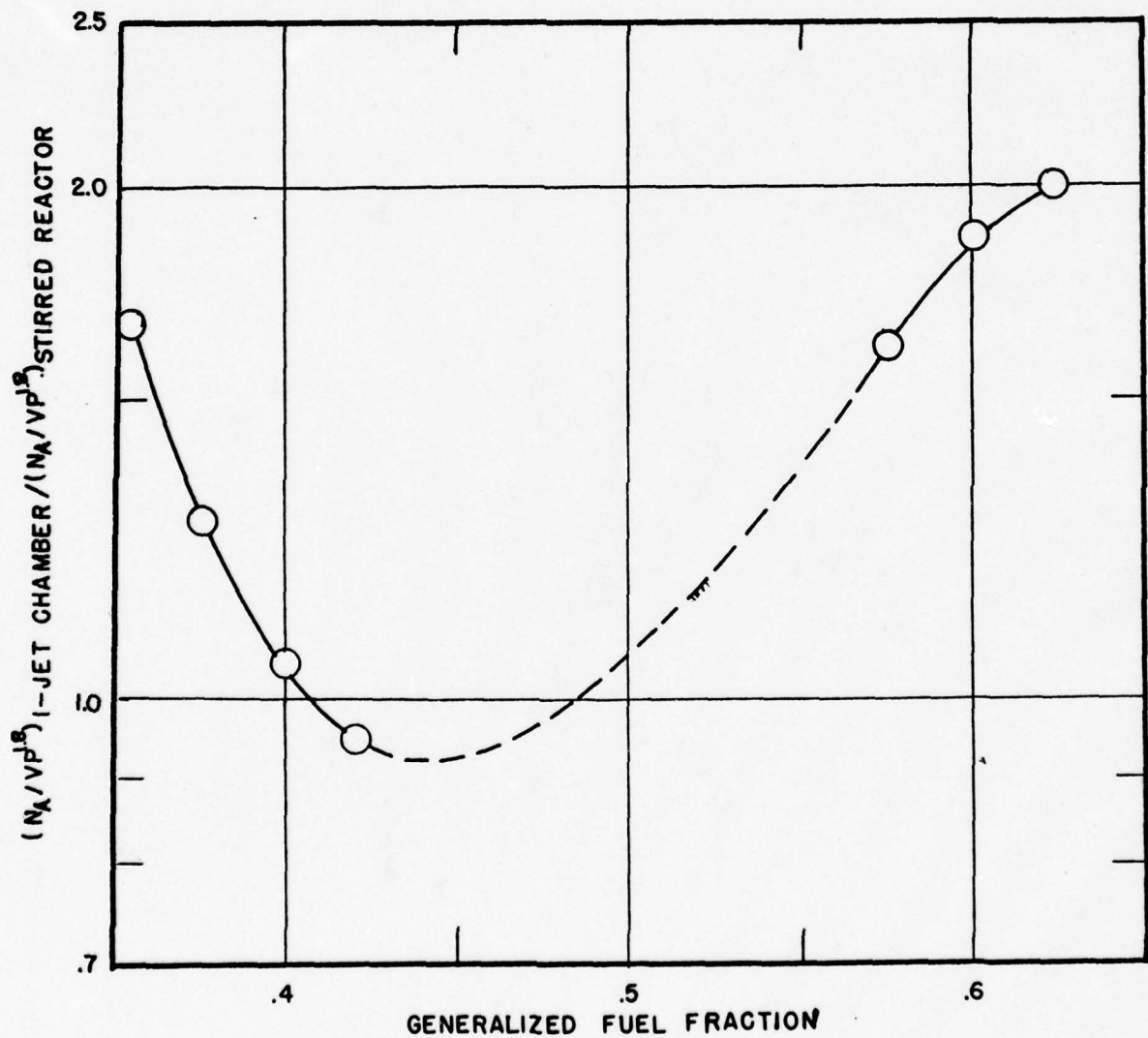


FIGURE VI-6: COMPARISON OF THE ONE-JET CHAMBER BLOWOUT DATA WITH STIRRED REACTOR DATA

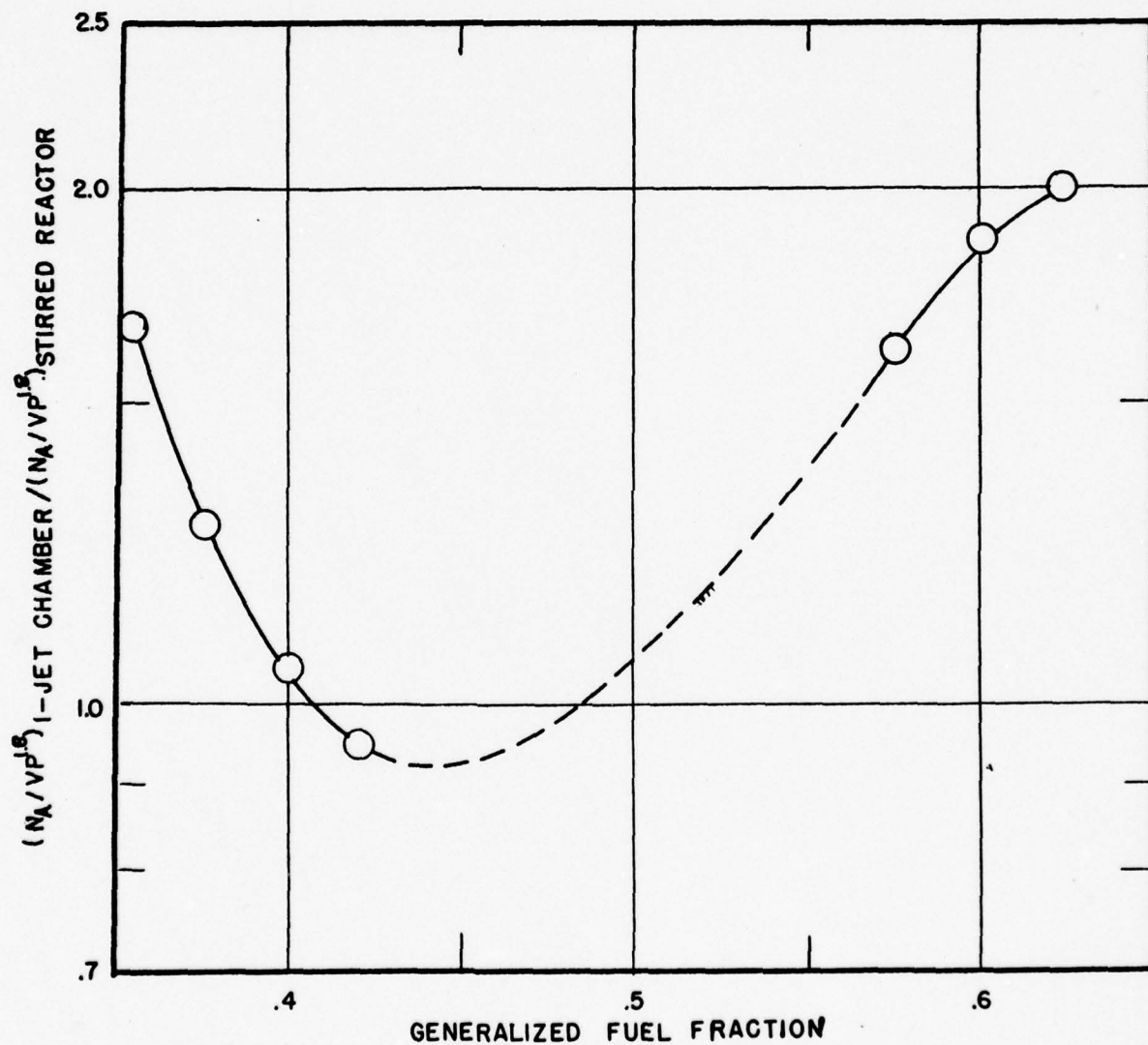


FIGURE VI-6: COMPARISON OF THE ONE-JET CHAMBER BLOWOUT DATA WITH STIRRED REACTOR DATA

model also predicts that there should be a constant difference between the stirred reactor blowout and the experimental chamber blowout. The trend observed here may reflect the departure of the stirred reactor from the assumed simple kinetic picture.

The recirculation models and the actual performance of a combustor are compared by the efficiency vs loading rate curve. Given this information about a combustor's performance, a value of R , the recirculation ratio, and V_2/V_1 may be chosen so that the theoretical behavior will match the model behavior. Both the position of the curve (blowout loading rate) and the chamber outlet efficiency are adjusted in these models by the use of gross bypassing and of inactive volumes. These two variables do not affect the basic shape of the efficiency loading rate curve. In addition, data on the size and composition of the individual zones will make correlation between theory and experiment more meaningful since fewer constants are then to be determined from the data. Such data were obtained by the use of sampling traversed across the chamber and by photographic measurements. The behavior of the combustor pattern as the flow approached the blowout limit suggests that the bright zone of Figure V-7 be taken as the central core (of volume V_1), and the dark eye of the pattern be taken as the

recirculation zone (of volume V_2). This results in such a small V_2/V_1 ratio, however, that a model calculated on this basis does not give a reasonable model performance.

In the recirculation models discussed in Chapter III, the performance of a combustion chamber was simulated by using only two zones whose relative volumes could be varied. In a real chamber, however, the postulation of only two zones and the consequent large and abrupt change in composition between them is inconsistent with reality. It is not surprising that a model incorporating this assumption might fail to provide a basis for correlating the data. As may be seen from the traverses of composition within the chamber, the change in burnedness in moving between the various zones in the chamber is gradual, and a model allowing for a more nearly continuous change would probably be in better agreement with the observed data.

If one considers a circulatory flow pattern in which gases may enter and leave at the circumference, the inner zone (or zones), further removed from the circumference of the combustion pattern, receive a smaller fraction of the fresh, combustible gases, and consequently, are less "heavily loaded" than those outer zones nearer to the circumference. In such a

combustor as the feed rate is increased, the outer zones will blow out first because of their heavier loading rate, and the inner zones will consequently receive a less well-burned feed since the outer, shielding zones now contain more unburned gases. In a conceptual model such as this, as the feed rate is increased the region of most intense burning rate will gradually recede from the circumference of the combustion pattern to the center until the inner-most zone of the model blows out, causing total extinction of the flame.

Although a two-zone approximation to this behavior has already been seen to be unsatisfactory, treatment of this model by integration of the performance of differential elements would be a formidable task. A satisfactory approximation considers recirculation models involving a small number of identical elements, each successive recirculation zone being fed by its immediate predecessor, and receiving recirculated gases from its immediate successor. Burned gases from a typical zone are split in two, one portion feeding the recirculation zone which is its immediate predecessor and the other feeding the zone which is its immediate successor. A diagram of such a model is shown in Figure VI-7. Since this extended recirculation model is an approximation to the circumferentially-fed

recirculation model described above, the recirculation ratios and relative zone volumes at each stage of the model are independent of previous model stations. The volumes (comparable to finite-difference intervals in a conventional finite-difference solution) are taken equal to each other (or in the case of cylindrical coordinates, for example, may be proportional to the distance from the origin) and the recirculation ratios representing the diffusional transport of matter in the chamber, are equal (or again may be proportional to the distance from the inner zone).

For prediction of combustor performance using this model only variable, the recirculation, is in principle required to find the behavior of the circumferentially-fed recirculation model. A characteristic recirculation ratio having been chosen, a model with a sufficient number of volumes is calculated to make its behavior practically the same as the infinite-number-of-zones case. In practice, the calculation of a model containing more than four or five zones is too laborious to consider by hand calculation techniques, and for models containing this small number of zones, the behavior of the model is strongly dependent on the number of zones in the model. This is shown in Figure VI-8, where three cases are calculated for three

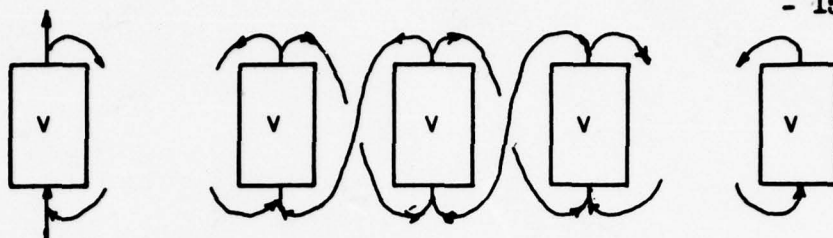
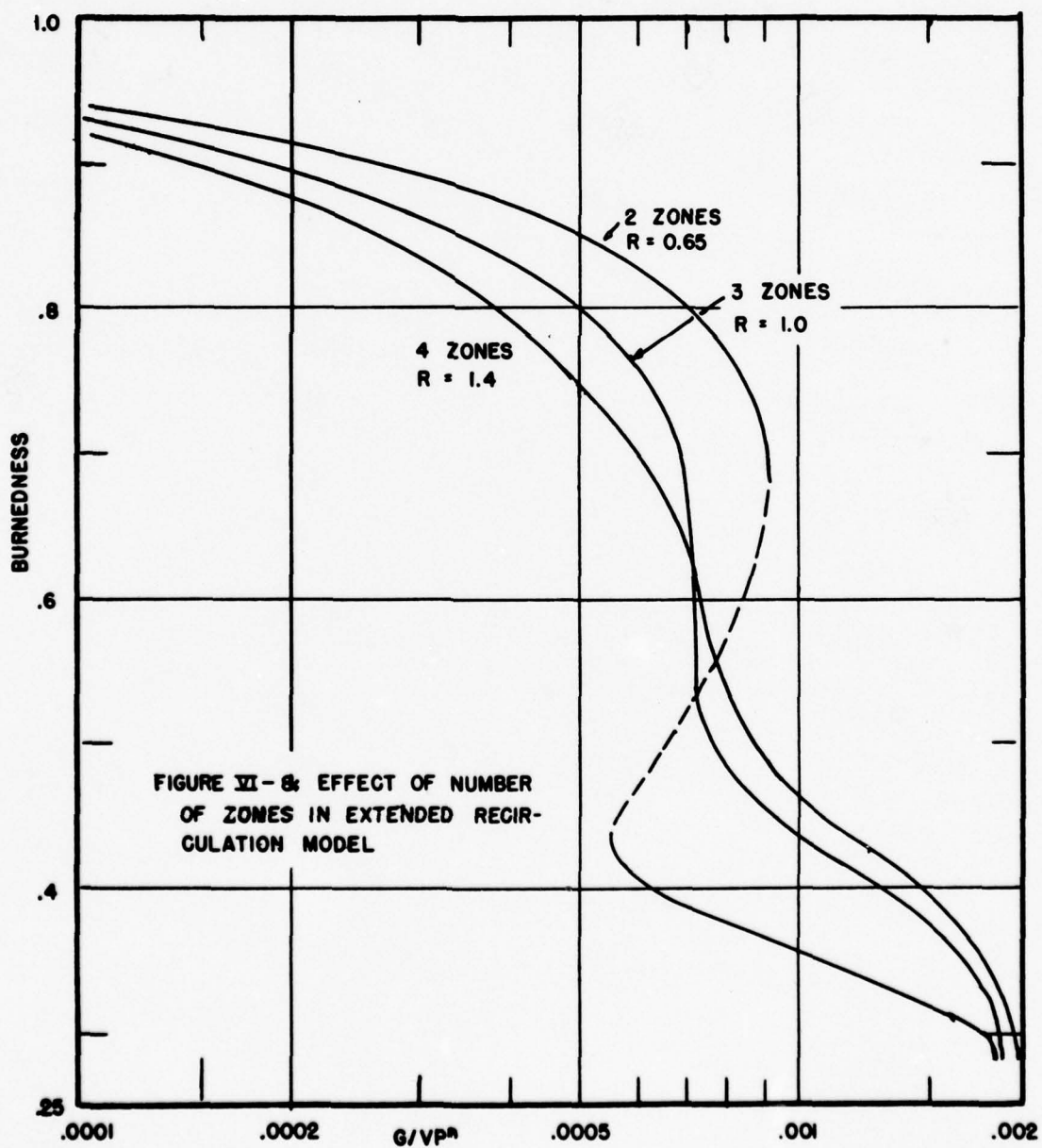


FIGURE VI-7: EXTENDED RECIRCULATION MODEL



different models. (for this calculation, R in each case was so chosen to bring the blowouts to about the same burnedness.) In these calculations both the volume sizes and the recirculation ratios have been taken to be independent of position in the model.

The effect of the number of volume units, p , in a model is better shown by comparison of the models on a basis of (total feed)/(first volume) ratio. Since at high burnedness the recirculation zones contribute little to the performance of a chamber, performance curves for models of different p 's will coincide when plotted on this basis. Using this basis the behavior of a model of constant recirculation ratio and initial volume but of varying number of zones is shown in Figure VI-9.

When the calculated performance curves are plotted in this manner, two interesting observations emerge: (1) additional zones do not cause corresponding additional humps in the performance curve (as did the first recirculation zone), and (2) increasing the number of zones of the model increases the stability of the residual flame, but does not affect the stability of the first zone significantly. This suggests that if a residual flame zone exists in a combustor, there will be a sudden change in combustion efficiency as the

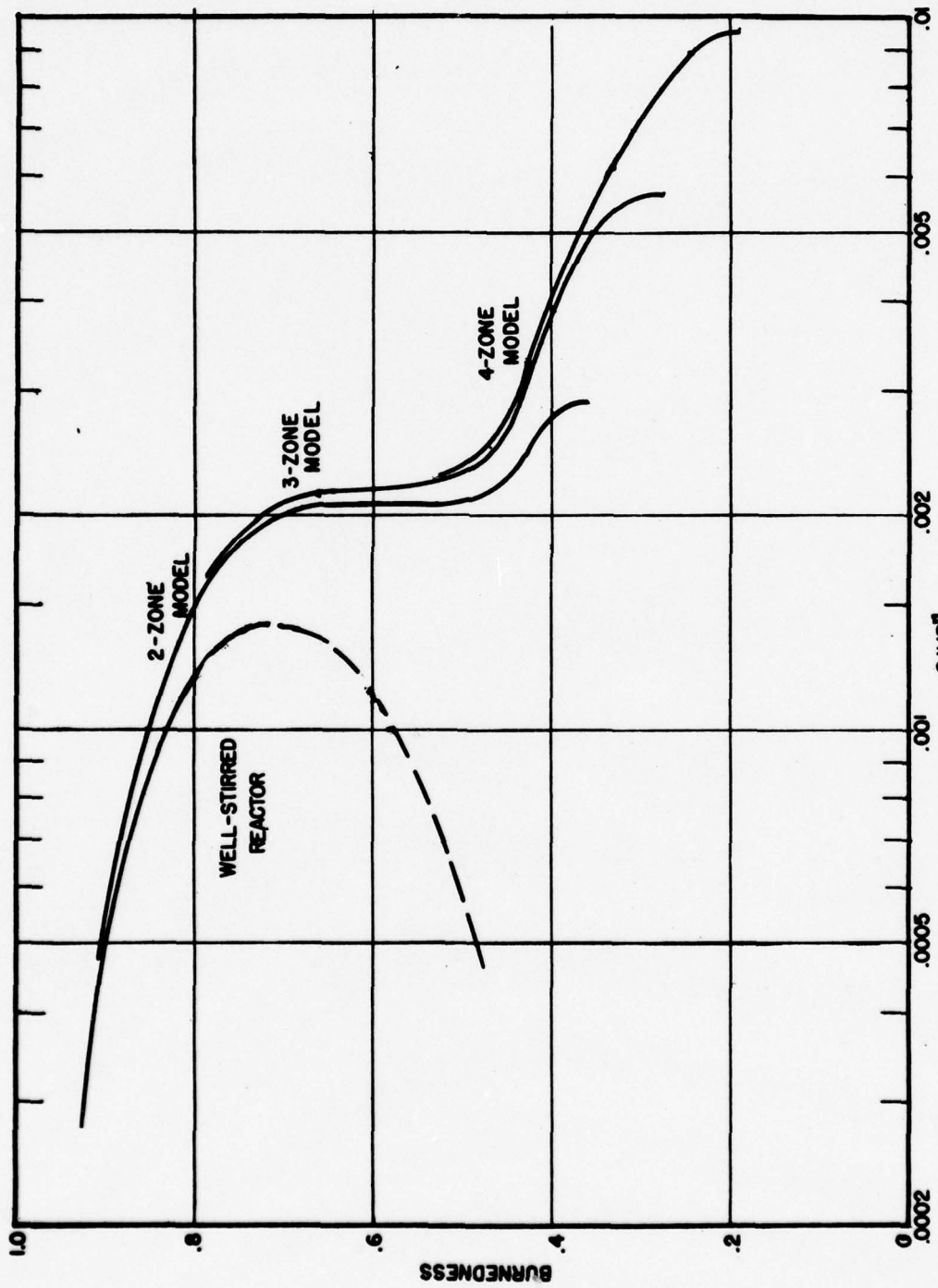


FIGURE II-9: EXTENDED RECIRCULATION MODEL, FIRST ZONE VOLUME AS BASIS, $R=1.0$

main combustion zone blows out, leaving the residual flame, but further increases in flow rate will only cause the residual flame to recede gradually from the main combustion zone. No additional partial blowout of zones within the residual flame are to be expected.

The possibility of designing combustors of much improved stability is also suggested. By deliberately allowing for a zone which is sufficiently sheltered and which is deep enough to allow the residual flame to recede into it, a substantial distance, a chamber equivalent to a high-p model is obtained, having a high ratio of ultimate blowout loading to initial blowout loading.

The use of this extended recirculation model will now permit a fitting of the experimental data obtained in the present experiments. There are two variables in the model, namely, the recirculation ratio and the number of recirculation zones. In addition, allowance must be made for "dead" or inactive zones in the chamber and for gross bypassing of the combustion zones.

Only the variables of recirculation ratio and number of zones will affect the shape of the performance curve. Increasing recirculation ratio will cause a change in the sharpness of the first blowout limit without causing much change in the ratio of the two

blowout limits (Figure VI-10). An increase in the number of zones will increase the relative stability of the recirculation zone (Figure VI-9).

A change in gross bypassing of gases around the combustion zones affects both the outlet burnedness (by dilution) and the relative stability with respect to the stirred reactor. It does not, however, affect the shape of the curve at all. The addition of "dead" space to the combustion chamber model permits the apparent volumetric heat liberation rate to be adjusted so that the model prediction is in conformity with the stirred reactor data. The effectiveness of this type of model in correlating the data on chamber efficiency is demonstrated in Figure VI-11, where the experimental data are compared with a model having a recirculation ratio of one, two or three recirculation zones plus bypassing and dead space. By plotting these data on log-log coordinates, movements corresponding to addition of dead space or bypassing correspond to either a simple lateral and/or vertical displacement of the two curves. (The raw data have been shifted by a constant factor of 3×10^{-3} to facilitate plotting on this graph.)

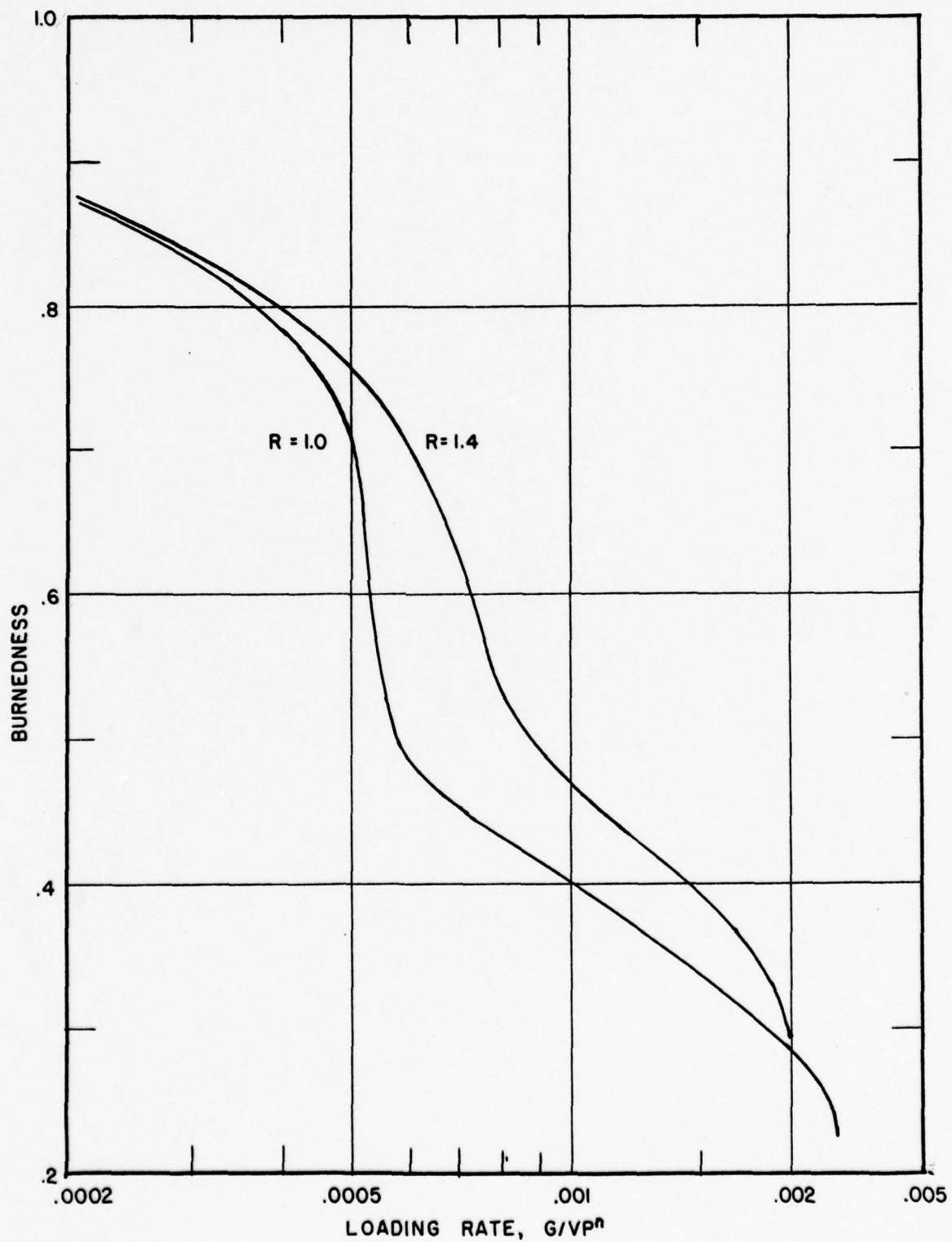


FIGURE VI-10: EFFECT OF RECIRCULATION RATIO IN FOUR-ZONE RECIRCULATION MODEL

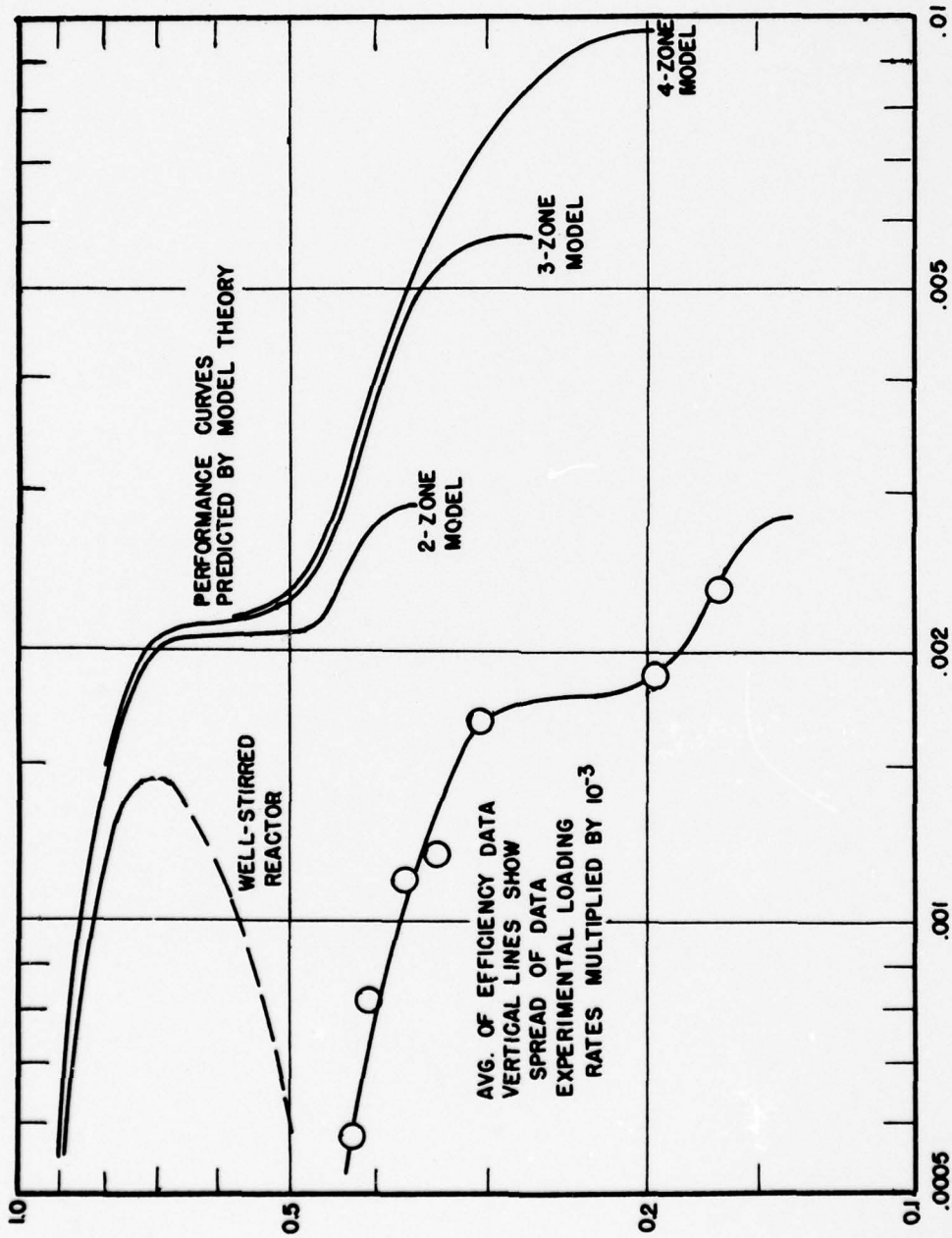


FIGURE XI-II: COMPARISON OF MODEL THEORY WITH EXPERIMENTAL COMBUSTOR PERFORMANCE.

Summary

The demonstration of the ability of simple theoretical combustion chamber models to reproduce the behavior of an experimental chamber in a semi-quantitative manner is of great significance. Previous models of combustion chamber performance have not, as yet, been used in conjunction with an experimental program. In this investigation several theoretical models were considered, and the calculated performance of the models was compared with the experimentally measured performance of a simple chamber which demonstrated characteristics common in many practical chambers.

Ultimately one would hope to use models of this nature to predict the performance of any combustion chamber. Using a relatively small number of variables it has been possible to generate a wide variety of performance curves for various combustor models. Thus, for instance, in moderately well-stirred systems, typical of can-type combustors, the extended recirculation model suggested seems to be applicable to the prediction of residual flame phenomena, and the use of the two-stability-limit model is suggested for the analysis of pressure interaction phenomena. Hopefully extension of these modeling techniques will lead to a general method of combustion chamber analysis, and possibly

permit an a-priori prediction of the combustion chamber performance from fundamental physical data involving only a small number of characteristic zones and their flow interactions.

CHAPTER VII

CONCLUSIONS AND RECOMMENDATIONS

Conclusions

1. The theoretical models of combustion chambers have been investigated. These models have predicted qualitatively phenomena observed in actual combustors.

a) A two-zone model of stirred reactors in parallel was used to predict the effects of pressure interaction between two combustion zones.

b) A two-zone recirculation model in which one zone was fed only partially burned products produced in the first and the first zone received a mixture of fresh gases and burned products from the second zone was used to investigate recirculation phenomena. This model showed the conditions for residual flame, hysteresis, and flickering flame phenomena.

c) An extended recirculation model was investigated which allowed for a more continuous variation in composition in the combustor than could be obtained in a two-zone model. This model showed phenomena similar to those observed in the two-zone model.

2. An experimental combustion chamber, fed by a two-dimensional jet of a pre-mixed fuel/air mixture was built and operated to test the models of combustion chambers quantitatively.

a) All the models predicted that stirred reactor blow-out and combustion chamber loading rates should be displaced from each other by a constant factor. This was not observed. This deviation was postulated to result from the breakdown of certain assumptions and from departure of the reaction kinetics from a mechanism controlled by a single reaction.

b) The two-stability-limit model predicted the displacement of the two stability limits of the experimental reactor to a reasonable approximation.

c) The overall combustion efficiency of the chamber was measured by gas sampling. These data were correlatable by the extended recirculation model.

d) The combustion efficiency of the chamber contents was determined by gas sampling. These data showed a qualitative behavior in agreement with the models. No attempt was made to fit the data quantitatively.

e) The effect of pressure on the blowout loading, $G/VP^{1.8}$ was determined experimentally. An average pressure exponent, "n" of 1.6 was found which compares well with reported literature values of 1.6 to 1.8. A trend of "n" was observed with variation in fuel/air ratio. However, no significance was attached to this trend because of unequal Reynolds numbers between experiments.

Recommendations

(1) The prediction of combustor performance by the use of these models requires experimental data on combustion

efficiency vs loading rate for the well-stirred reactor. There is not yet available an adequate amount of these performance data for the stirred reactor. It is recommended that an experimental program be undertaken to determine these data and to determine whether they are in agreement with the performance predicted from the stirred reactor theory.

(2) Although the experimental program undertaken gives some support to the theories, unexplained phenomena still exist. It is recommended that further experimental work be undertaken to establish methods for fitting the combustion chamber phenomena to the theory. Investigation of certain special phenomena, is also recommended:

a) To fit the present data to existing stirred reactor data it is necessary to postulate substantial bypassing of the combustion zones. An experimental verification of the extent of this bypassing is recommended.

b) The theory has only been fitted at one fuel/air ratio to experimental performance data. It is recommended that other fuel/air ratios be investigated and that particularly, the prediction of the effects of fuel/air ratio changes by the theoretical models be studied.

3. Data on the stirred reactor has indicated some lack of complete mixing. An investigation of the stirred reactor is recommended to determine what the consequences of this lack of mixing are, and to determine which zones in a combustion

- 168 -

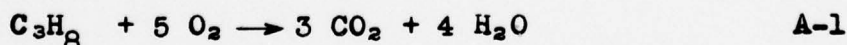
chamber are comparable to a unit volume of both "perfectly" stirred reactor and experimental stirred reactor.

APPENDIX A

DERIVATION OF THE WELL-STIRRED REACTOR EQUATION

The derivation of a generalized well-stirred reactor equation has already been discussed. In the literature several more detailed discussions of the exact algebraic form of the equations have been given for specific postulated stoichiometric schemes (3, 14). Since it was felt that the use of complex stoichiometric schemes did not yield a justifiable increase in accuracy of the model predictions, the derivation of the algebraic relation between burnedness and loading rate used in this thesis was restricted to the simplest possible case in which no intermediate products are postulated.

The stoichiometric equation of the reaction representing the overall combustion reaction was written for propane,



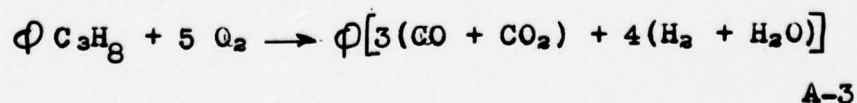
The heat of reaction was assumed to be sufficient to give a 2270°K temperature rise for a stoichiometric mixture, and the heat capacities of the reactants and products were assumed to be equal and independent of temperature so that the fraction of fuel consumed, β , was related to temperature for a stoichiometric mixture by:

$$\beta = \frac{T - T_0}{2270} \quad \text{A-2}$$

In the simplest description of the stirred reactor the identifiable components of the mixture at any stage of completion of combustion are burned products plus fuel and oxygen; therefore only a single variable, β , is necessary to specify the composition of the mixture. If the fraction ϕ of the stoichiometrically required fuel is used, then for each 5 moles of oxygen the moles of each component are given as follows:

C_3H_8	$\phi (1 - \beta)$
O_2	$5(1 - \phi \beta)$
N_2	18.8
H_2O and CO_2	$7 \phi \beta$
<hr/>	
Total mols	$23.8 + \phi (1 + \beta)$

If a rich fuel-air mixture is used, there should be no unburned fuel appearing at completion of combustion (as would be called for by the above stoichiometry for $\phi > 1$). Thus for rich mixtures the stoichiometric equation A-1 is altered to give:



In this equation the summation of oxygen atoms on the right-hand side of the equation must be equal to 10. Longwell and Weiss (24) and Baker (3) have both used this assumption to fit data on the rich side, and in both cases

the authors assumed that the water-gas equilibrium could be used to calculate the composition of the products. The present calculations were simplified by assuming that the heat of reaction contributed by the water-gas reaction was negligible compared to the heat released by the initial combustion step. With this assumption it is not necessary to specify the composition of the mixture to calculate the temperature. The stoichiometry of reaction A-3 yields the following species (basis - 5 moles oxygen):

C_3H_8	$\phi (1 - \beta)$
O_2	5 (1 - β)
N_2	18.8
products	7 ϕ β
total	23.8 + ϕ + (6 ϕ -5) β

For fuel-air mixtures other than stoichiometric the heat balance equation, A-2, relating temperature and burnedness, must be modified. In principle an enthalpy balance should be made to account for dissociation products and water-gas equilibrium, especially for rich mixtures. However, calculations may be greatly speeded by the simplifying assumptions of (1) a constant heat capacity of the gases and (2) ignoring the energy of the water gas reaction and dissociation products. For the present calculations the following temperature-burnedness relations were used:

$$\frac{500,000 \phi}{30 \phi + 190} \quad \beta = T - T_o \quad (\text{lean}) \quad \text{A-4.1}$$

$$\frac{500,000}{30 \phi + 190} \quad \beta = T - T_o \quad (\text{rich}) \quad \text{A-4.2}$$

It should be noted that for a stoichiometric fuel-air mixture both rich and lean schemes are identical.

The composition of the gases in a stirred reactor in which this combustion occurs is a function of the firing rate to the reactor. This function is derived from the reaction rate equation applicable to this reaction. For this case here, only a single equation is required, and this is assumed to be an equation of first order in each of the reactants. The temperature dependence of the rate is indicated by the conventional exponential term:

$$-\frac{dN_F}{Vdt} = \sqrt{T} k' e^{-E/RT} \cdot C_{O_2} \cdot C_F \quad \text{A-5}$$

From the stoichiometry discussed the concentrations of the fuel and oxygen, C_{O_2} and C_F , may be found as the respective mole fraction terms times the molar density of the gas determined from the perfect gas law;

$$\left. \begin{aligned} C_{O_2} &= \frac{5(1 - \phi\beta)}{23.8 + \phi(\beta + 1)} \frac{P}{RT} \\ C_F &= \frac{\phi(1 - \beta)}{23.8 + \phi(\beta + 1)} \frac{P}{RT} \end{aligned} \right\} \text{lean} \quad A-6.1$$

$$\left. \begin{aligned} C_{O_2} &= \frac{5(1 - \beta)}{23.8 + \phi + (6\phi - 5)\beta} \frac{P}{RT} \\ C_F &= \frac{\phi(1 - \beta)}{23.8 + \phi + (6\phi - 5)\beta} \frac{P}{RT} \end{aligned} \right\} \text{rich} \quad A-6.2$$

Since the rate of fuel consumption is given by $G \cdot \beta$;

$$\frac{G}{VP^2} = \frac{k'e^{-E/RT}}{T^{3/2}} \frac{5\phi(1 - \phi\beta)(1 - \beta)}{\beta[23.8 + \phi(1 + \beta)]^2} \quad \text{lean} \quad A-7.1$$

$$\frac{G}{VP^2} = \frac{k'e^{-E/RT}}{T^{3/2}} \frac{5(1 - \beta)^2}{23.8 + \phi + (6\phi - 5)\beta} \quad \text{rich} \quad A-7.2$$

For calculational purposes it is desirable to normalize equations A-7 so that those changes in operating variables which counteract each other will be evident. At the same time it is desirable that each of the groups chosen be independent i.e. so that a change in a factor in one group will not affect the values of the other groups.

In an experiment to determine the reaction rate constants k' and E , the rate constant of the reaction, $k = k'e^{-E/RT}$, will be found at some high temperature, and by varying the temperature k' and E may be found separately. Since this

experiment must be carried out in a temperature region where the reaction proceeds with a reasonable velocity, knowledge of k' at room temperature will be very uncertain. This suggests that an appropriate normalization factor would be the rate constant, k , determined at some high temperature designated as the key temperature, T_K . Temperatures would also be normalized by T_K . This normalization procedure yields the reduced equation;

$$\frac{G}{VP^2} \frac{R^2 T_K^{3/2}}{k' e^{-E/RT_K}} = \frac{e^{-E/RT_K} [(1/T_K) - 1]}{T_r^{3/2}} \frac{5 \phi (1-\beta \phi) (1-\beta)}{[23.8 + (1-\beta)]^2 \beta}$$

A-8

For this investigation a basic stirred reactor curve calculated from A-8 was used to compare the performance curves of the various models. This curve is based on the following constants:

$$\begin{aligned} \phi &= 1.0 \\ T_K &= 2000^\circ\text{K} \\ T_o &= 500^\circ\text{K} \\ T_{af} &= 2772^\circ\text{K} \\ E/RT_K &= 10 \end{aligned}$$

A plot of $(G/VP^2)(R^2 T_K/k' e^{-E/RT_K})$ vs β is shown in Figure A-1 for these constants. This curve (plotted elsewhere in this thesis as G/VP^2 or G/VP^n vs β is used to generate all of the other model performance curves calculated.

In the model investigating the effect of non-uniform fuel-air ratio on combustor performance curves for stirred reactors being fed a rich fuel-air mixture were required. For this purpose Equation A-7.2 was normalized and curves calculated for a ϕ of 1.2 and 1.5 using all other constants shown above the same.

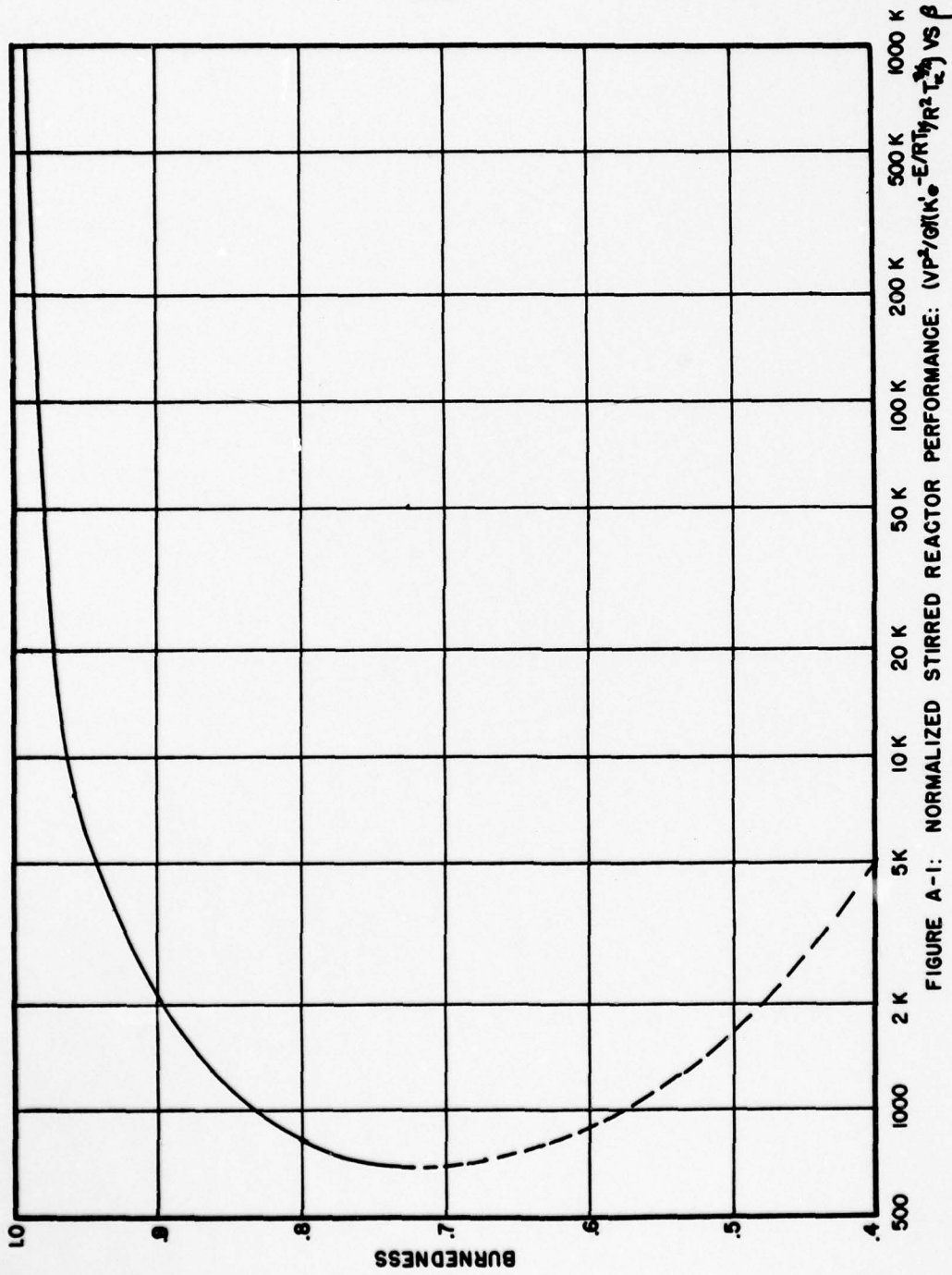


FIGURE A-1: NORMALIZED STIRRED REACTOR PERFORMANCE: $(VP^2/GRK) \cdot (-E/R) \cdot (T_0/T_c)^{1/2}$ VS β

AD-A058 017

PRINCETON UNIV N J JAMES FORRESTAL RESEARCH CENTER
APPLICATION OF WELL-STIRRED REACTOR THEORY TO THE PREDICTION OF--ETC(U)
MAY 58 A H BONNELL
SQUID-MIT-18-T

F/6 21/2

N60RI-105(03)

NL

UNCLASSIFIED

3 OF 3

AD
A058017



END
DATE
FILMED

10-78

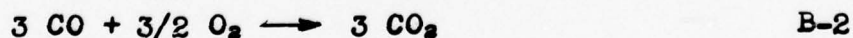
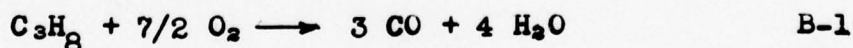
DDC

APPENDIX B

MULTI-STEP KINETIC SCHEMES

Calculational techniques discussed in the main body of this thesis have assumed that the reaction rate of burning gases is limited by a single chemical reaction throughout the composition range of interest. It must be recognized that this is an assumption justified only by the resulting simplifications in the theory and the hope that it will introduce only a small error in the predicted model performance. In fact it is possible to make rigorous allowance for multi-step reaction although for more than two or three steps the calculational work becomes prohibitive.

Calculations of multi-step cases are greatly simplified by the use of graphical techniques to solve the stirred reactor equations. To illustrate the use of such techniques a typical two-step mechanism will be considered. The two steps postulated are:



For this postulated mechanism two variables are required to specify the composition, representing respectively the progress of reactions B-1 and B-2. It is assumed that operation is adiabatic so that the temperature is fixed by the composition and initial temperature of the unreacted

expression.

$$-\frac{dN_{C_3H_8}}{Vdt} = \sqrt{T} k_1' e^{-E_1/RT} C_{C_3H_8} \quad B-3$$

$$\begin{aligned} \frac{dN_{CO}}{Vdt} &= 3 \sqrt{T} k_1' e^{-E_1/RT} C_{C_3H_8} \\ &\quad - \sqrt{T} k_2' e^{-E_2/RT} C_{CO} \cdot C_{O_2} \end{aligned} \quad B-4$$

Substitution for appropriate concentration terms yields:

$$(G/V)d\beta = \sqrt{T} k_1' e^{-E_1/RT} \frac{(1-\beta)}{\xi} \frac{P}{RT} \quad B-5$$

$$\begin{aligned} \frac{3G}{V}d(\beta-\gamma) &= 3 T k_1' e^{-E_1/RT} \frac{1-\beta}{\xi} \frac{P}{RT} \\ &\quad - T k_2' e^{-E_2/RT} \frac{3(5/\phi - 7/2\beta - 3/2\gamma)(\beta-\gamma)}{\xi^2} \frac{P}{RT} \end{aligned} \quad B-6$$

Relative reaction rate constants of reactions B-1 and B-2 as well as a reduced feed rate are now defined:

$$\text{Relative Reaction Rate, } \tilde{r} = \frac{RT_K k_1 e^{-E_1/RT_K}}{p k_2 e^{-E_2/RT_K}}$$

$$\text{and } G_r = \frac{G}{VP^2} \left[\frac{R^2 T_K^{3/2}}{k_2 e^{-E_2/RT_K}} \right]$$

Equation B-5 thus becomes:

$$G_r d\beta = \tilde{r} \frac{e^{-(E_1/RT_K)} (1/T_r - 1)}{T_r^{1/2}} \frac{1-\beta}{\xi} \quad B-7$$

fuel-air mixture. It will be assumed that the oxygen is from air, and consequently specification of composition and temperature requires that allowance be made for the presence of nitrogen. Let the two composition variables, β and γ be defined as:

β = fraction of C_3H_8 consumed by B-1

γ = fraction of CO equivalent to C_3H_8 consumed by B-2.

The composition of the gas corresponding to any pair of β, γ values may now be calculated (let ϕ times the stoichiometrically required fuel be used):

Component	mol pr mo C_3H_8
C_3H_8	$1 - \beta$
O_2	$5 (1/\phi) - 7/2\beta - 3/2\gamma$
N_2	$18.8 (1/\phi)$
H_2O	4β
CO	$3(\beta - \gamma), (\beta < \gamma)$
CO_2	3γ
Total	$\Sigma = 1 + 23.8(1/\phi) + 5/2\beta - 3/2\gamma$
Temperature	$T = T_0 + \frac{\Delta H_1}{C_p} \beta + \frac{\Delta H_2}{C_p} \gamma$

For each reaction postulated there is a corresponding reaction rate expression. For the present case assume that the initial cracking of propane is the rate-limiting step in reaction B-1 and that the combustion of carbon monoxide may be represented by a simple second-order reaction rate

and substituting B-5 into B-6 yields:

$$G_r d\gamma = \frac{e^{-(E_2/RT_K)(1/T_r-1)}}{T_r^{3/2}} \left(\frac{5/\phi - 7/2\beta - 3/2\gamma}{\xi^2} \right) (\beta - \gamma) \quad B-8$$

The calculation of temperature for substitution into B-7 and B-8 is simplified by the relation:

$$T_r = T_r + \Delta_{1r} \beta + \Delta_{2r} \gamma \quad B-9$$

where Δ_{1r} and Δ_{2r} represent the corresponding reduced adiabatic flame temperature rises resulting from complete reaction of reactions B-1 and B-2 at the prevailing fuel-air ratio.

In calculations based on B-7 and B-8, two cases may be distinguished; (1) where it is desired to investigate a single stirred reactor with varying values of ξ , and (2) where it is desired to investigate staged reactors in each member of which the relative reaction rate parameter is the same.

Case I: Single stirred reactor, ξ varying. If a single stirred reactor is considered, then $Gd\beta$ and $Gd\gamma$ may be replaced by $G\beta$ and $G\gamma$ respectively. Corresponding division of each equation by β and γ yields the equations:

$$G_r = \frac{e^{-(E_1/RT_K)(1/T_r-1)}}{T_r^{1/2}} \frac{1-\beta}{\beta} \quad B-10$$

$$G_r = \frac{e^{-E_2/RT_K(1/T_r-1)}}{T_r^{3/2}} \left(\frac{5/\phi - 7/2\beta - 3/2\gamma}{\gamma \xi^2} \right) (\beta - \gamma) \quad B-11$$

Each of these equations may be represented graphically as G_r vs β for constant values of γ (or visa-versa). B-10 is plotted for a ξ value of 1.0. Superposition of the two graphs permits solutions for the values of β and γ corresponding to any given G_r . If these two figures are plotted on a coordinate of $\log G_r$ then changes in ξ are represented by translation of the graphs with respect to each other along the G_r axis, and for any position desired a set of β, γ values may be found. Figures B-1 and B-2 show such a graphical representation of equations B-10 and B-11 for the following constants:

$$\begin{aligned} E_1/RT_K &= 5 \\ E_2/RT_K &= 10 \\ \phi &= 1.0 \\ \Delta_{1r} &= 0.674 \\ \Delta_{2r} &= 0.462 \\ T_{Or} &= 0.25 \\ T_K &= 2000^\circ K \end{aligned}$$

Three typical sets of solutions for ξ of 1.0, 0.3 and 0.1 are given in Figure B-3. Since the absolute magnitudes of the values of G_r in Figure B-3 reflect the normalization procedure they are of no significance in comparing these curves with experimental stirred reactor data. The choice of ξ or relative reaction rate, in this two-step mechanism must be based on the relative performances of the stirred

reactor with respect to some key point (such as the rate at the firing rate giving the key temperature). The correct ξ having been chosen, the absolute values of the reaction rate constants are then found.

Case II: Multi-stage reactors, fixed ξ . In considering a multi-stage reactor system it is necessary to predict the effect of feeding a stirred reactor with a partially burned feed when the burning rate is significantly affected by two (or more) reactions. So long as both reactions are significant in determining combustion rate the relative rates of change of β and γ differ at each point along the single-stage stirred reactor curve. Hence for each postulated degree of combustion of the feed a new stirred reactor curve must be drawn. In the general case, a graphical relation between inlet and outlet composition of a stirred reactor being fed a feed composition β_0, γ_0 is desired.

Since the rate of change of β and γ are specified uniquely by β and γ (i.e. independent of reactor inlet conditions), one may plot lines of constant $d\beta/d\gamma$ on a graph of β vs γ . On such a plot the locus of all possible reactor outlet conditions for any given β, γ combination (or visa-versa) may be represented. For any combination of β, γ represent reactor outlet conditions the $(\beta - \beta_0)/(\gamma - \gamma_0)$ ratio across the reactor must be equal to $d\beta/d\gamma$. From this, loci of reactor outlet conditions from any given β_0, γ_0 combination may be constructed. Similarly loci of plug-flow

reactor conditions may be found.

Given reactor inlet and outlet conditions (found from Figure B-4) the feed/volume ratio is easily found from either Figures B-1 or B-2. Since these figures were plotted as $f_1(\beta, \gamma)/\beta$ and $f_2(\beta, \gamma)/\gamma$, a correction must be made for the ratio $\beta/(\beta - \beta_0)$ or $\gamma/(\gamma - \gamma_0)$.

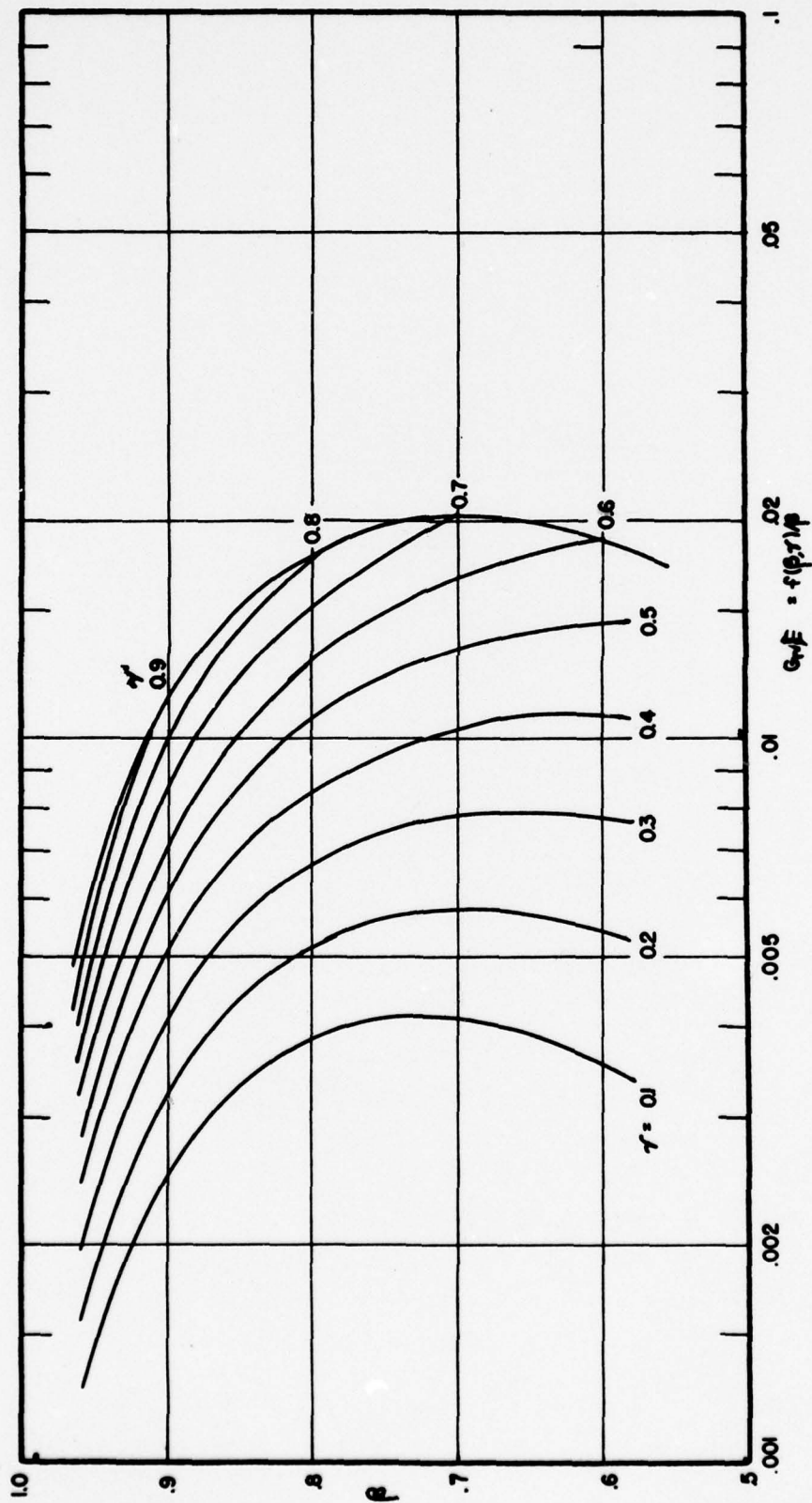


FIGURE B-1: PERFORMANCE OF TWO-STEP REACTION IN A WELL-STIRRED REACTOR: STEP I

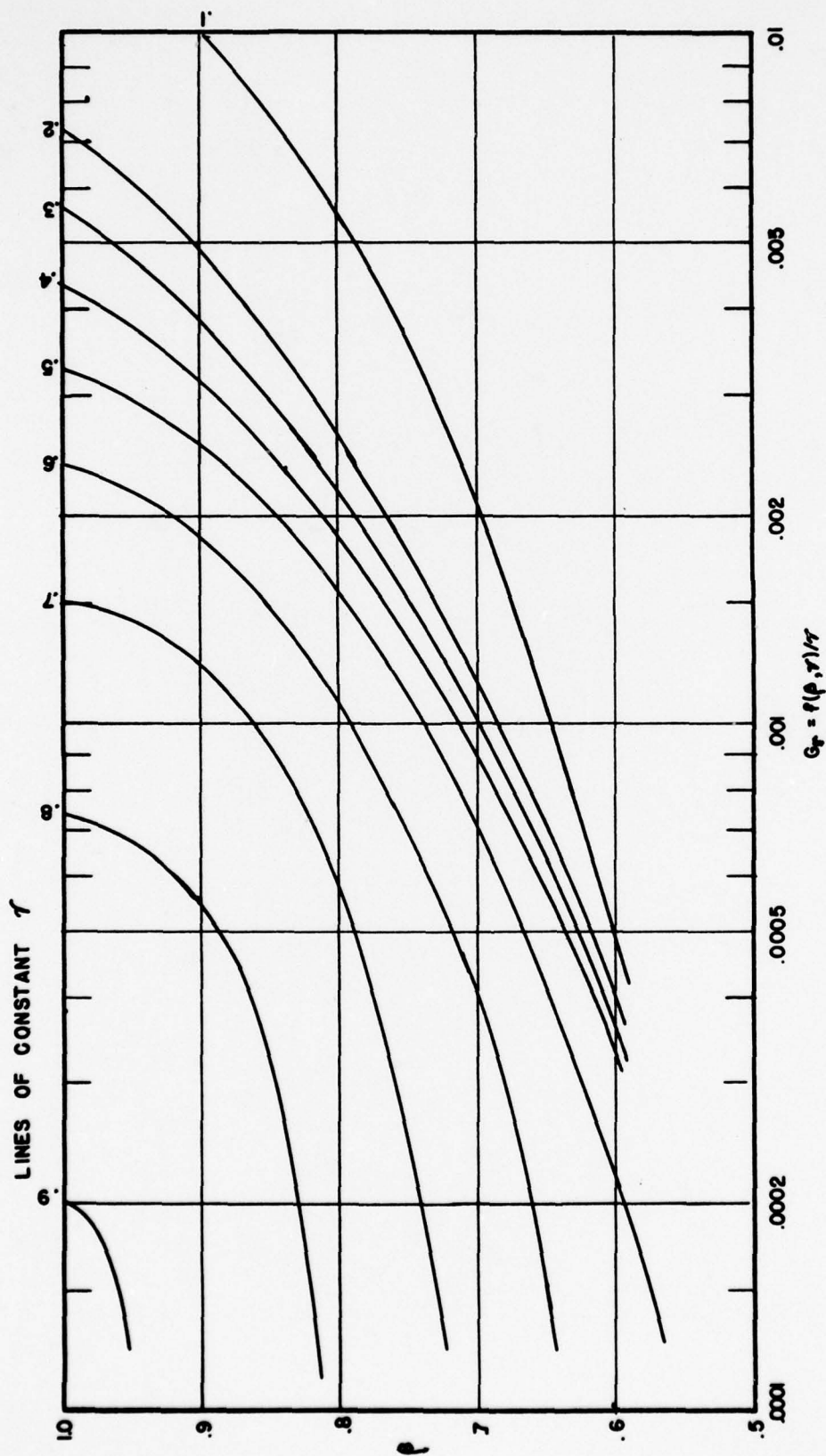


FIGURE B-2: PERFORMANCE OF TWO-STEP REACTION IN A WELL-STIRRED REACTOR: STEP 2

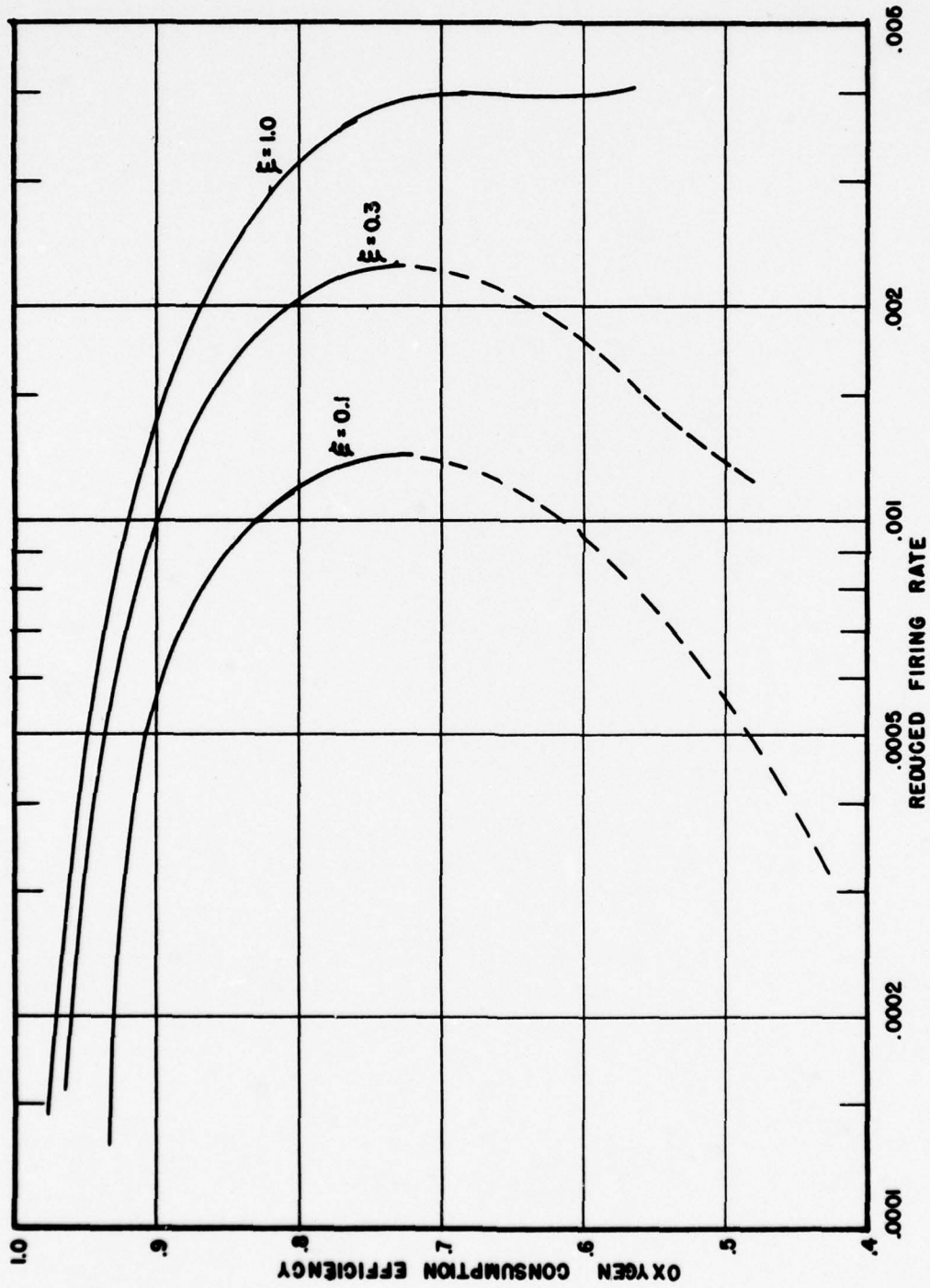


FIGURE B-3: PERFORMANCE OF TWO-STEP REACTION IN A STIRRED REACTOR:
COMBINED RESULTS

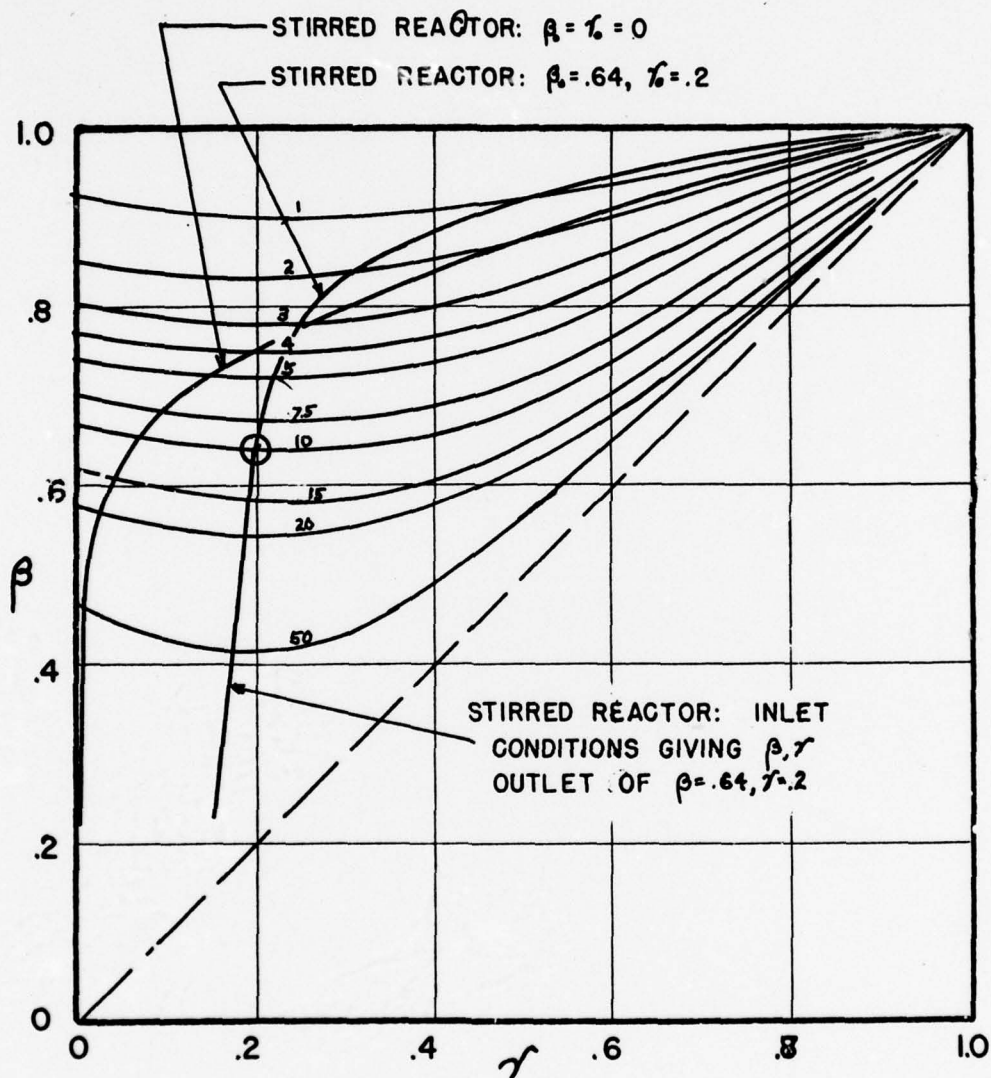


FIGURE B-4: PERFORMANCE OF TWO-STEP REACTION;
LINES OF CONSTANT $d\beta/d\gamma$ ON COMPOSITION
DIAGRAM. $E=1$

APPENDIX C

ESTIMATED HEAT LOSS FROM THREE-JET CHAMBER

Heat losses from the experimental chambers were known to be substantial because of the high surface-volume ratio and because of the opportunity for radiant heat transmission through and from the Vycor windows. Experimental estimation of this heat loss would be very difficult because of the multiple paths (radiation, conduction, convection) by which heat was lost. Heat loss rates were therefore estimated by calculation. The calculations were based on the geometry of the three-jet combustion chamber.

In calculating heat losses from this chamber several parallel mechanism must be considered:

- (1) Convection to the firebrick and Vycor walls followed by:
 - (a) direct or indirect radiation from the firebrick to the ambient gas
 - (b) transfer by convection and radiation from the Vycor walls to the ambient
 - (c) conduction through the firebrick from an inside face to an outside face followed by radiation-conduction transfer to the ambient.
- (2) Gas radiation from the burning gases to the firebrick and Vycor walls followed by a, b, and/or c above.

In addition to these possible multiple-mechanisms, the problem

is complicated by the existence of strong temperature gradients in the firebrick and presumably also in the Vycor, especially when the gases are burning unevenly.

Because the precise accounting for all of these losses is unjustifiably complex, simplifying assumptions to the problem were sought. These are enumerated as follows:

A. Because of the short gas path-lengths and low pressure operation, all heat transfer by gas radiation is neglected.

B. Because of the strong temperature gradients in the firebrick simplifications in the radiation from and convection to the brick are necessary. About 2/3 of each side wall and the entire roof (consisting of flues and spacer bricks) normally glowed visibly -- a bright cherry red. Radiation from the floor and lower portions of the side-walls appeared to be much colder, presumably due to colder gases and/or lower gas velocities in this region. Calculations were simplified by assuming:

- (1) uniform gas temperature,
- (2) side-walls and roof of uniform temperature, receiving heat by convection from the gas and radiating to the floor, Vycor, and ambient,
- (3) the roof has a heat-transfer area equal to an equivalent plane (holes for the flues were ignored),
- (4) radiation from the roof and walls is black,
- (5) the floor receives and loses heat only by radiation and is black,
- (6) heat loss by conduction through the firebrick is

negligible because of the low thermal conductivity of kaolin brick.

C. In the temperature range of interest, Vycor (nearly pure silica) is partly transparent and a partial reflector.

The following assumptions were made:

- (1) Vycor is transparent to radiation of wave-length shorter than 3.7μ and black to radiation of longer wave-length. Hence its absorptivity (or emissivity) is found from the Stefan-Boltzman equation as a function of the temperature of the source (or Vycor). Since all emmitters in the chamber were postulated to be black, complications arising from multiple reflections are avoided.
- (2) Since the reflectivity of Vycor is low (10%) it is neglected.
- (3) Thermal conduction through the Vycor is assumed to be rapid.

D. Heat transfer by convection has been studied in various geometries, but no data specifically adapted to this geometry is reported in the literature. Hence assumed values are necessary. Since most transfer coefficients across gas films are in the range of 1 to 10 Btu/hr ft² °F (17), and are approximately proportional to gas velocity (16), the following relation is assumed for convection from the burning gas to the fire-brick and Vycor;

$$h_g = 10 G/G_{BO} \text{ (Btu/hr ft}^2 \text{ }^\circ\text{F)}$$

where G is the firing rate and G_{BO} is the firing rate at blowout. The transfer coefficient from the Vycor to the ambient air was assumed to be $h_o = 2 \text{ Btu/hr ft}^2 \text{ }^\circ\text{F}$.

E. All back radiation from the surroundings to the chamber is neglected.

With these assumed conditions the heat loss from the burning gas to the ambient air may now be calculated. Radiative heat transfer is calculated by the method of Hottel (16). For any given gas temperature and firing rate all independent parameters are fixed and the heat loss is uniquely determined. However because of the temperature dependence of the Vycor emissivity and absorptivity (assumption C-1 above) it is necessary to evaluate the temperatures of the firebrick, Vycor, and floor. These are found by a heat balance on those respective areas.

A. Heat balance on walls and roof;

$$h_g A_w (T_g - T_w) = A_w F_{wv} \sigma (T_w^4 - \epsilon_v T_v^4) + A_w F_{wf} \sigma (T_w^4 - T_f^4) \quad \text{C-1}$$

B. Heat balance on floor

$$\sigma A_w F_{wf} (T_w^4 - T_f^4) = \sigma A_f F_{fv} (T_f^4 - \epsilon_v T_v^4) \quad \text{C-2}$$

C. Heat balance on Vycor

$$\begin{aligned} h_g A_v (T_g - T_v) + A_f F_{fv} \sigma (\alpha_{vf} T_f^4 - \epsilon_v T_v^4) \\ + A_w F_{wv} \sigma (\alpha_{vw} T_w^4 - \epsilon_v T_v^4) \\ = A \sigma \epsilon_v T_v^4 + h_a A_v (T_v - T_a) \end{aligned} \quad \text{C-3}$$

where:

α_v = absorptivity of Vycor for radiation as a function of source temperature. Subscript vw refers to wall radiation, vf refers to floor radiation.

ϵ_v = emissivity of the vycor, a function of Vycor temperature.

F = direct view factor, fraction of radiation leaving source arriving at sink. First subscript refers to source, (on whose area the view factor is based) and second subscript refers to sink.

h_g = convection heat transfer coefficient from burning gas to walls and Vycor.

h_c = convection heat transfer coefficient from Vycor to ambient air.

Simultaneous solution of equations C-1 to C-3 for each gas temperature and firing rate permits evaluation of T_w and T_v . Heat loss from the chamber is then found by the equation:

$$q = h_g A_w (T_g - T_w) + h_g A_v (T_g - T_v) \quad C-4$$

Figure C-1 gives α_v or ϵ_v of Vycor as a function of Vycor or source temperature based on the assumptions given in C above. This plot must be used in conjunction with a trial and error solution of Equations C-1 to C-3. The heat losses calculated from these equations are shown as functions of gas temperature and firing rate in Figure C-2.

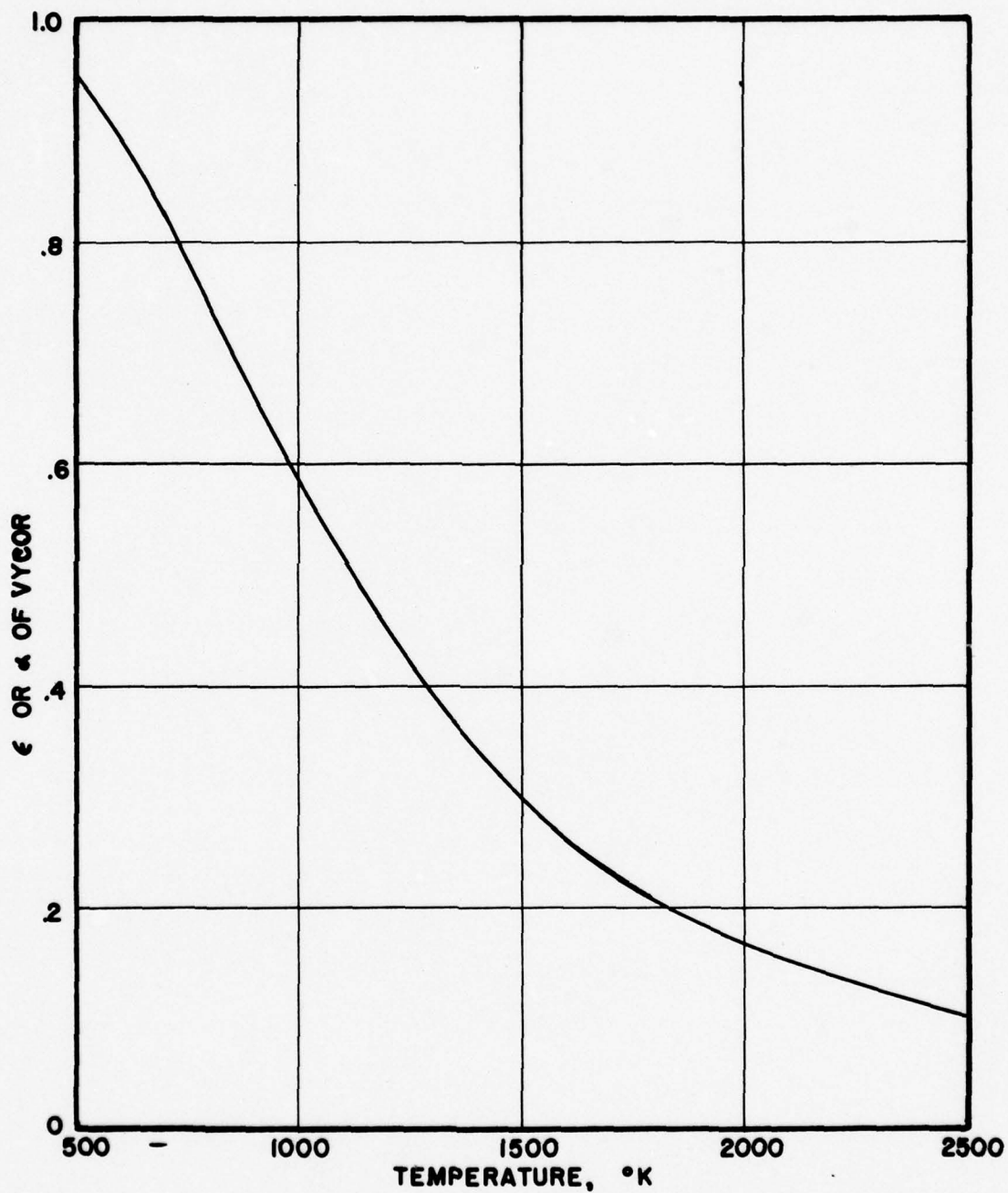


FIGURE C-1: EMISSIVITY OR ABSORPTIVITY OF VYCOR
(% OF RADIANT ENERGY ABOVE $\lambda = 3.7\mu$)

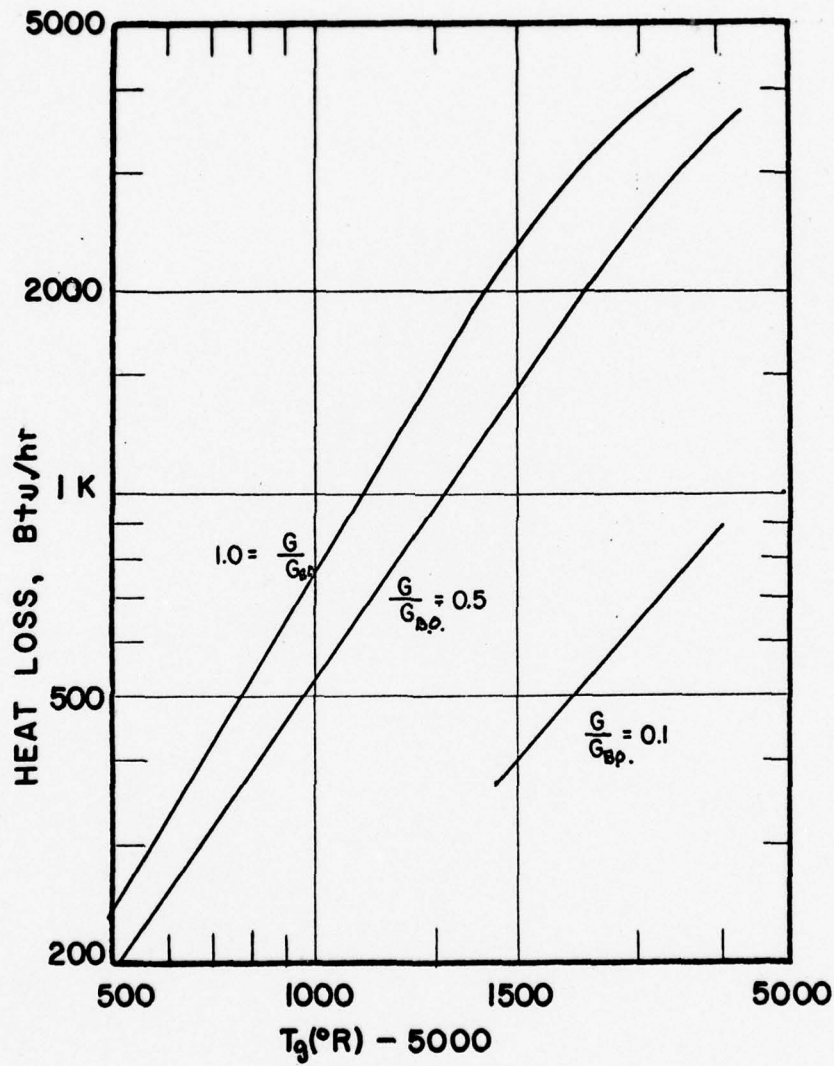


FIGURE C-2: HEAT LOSS OF 3-JET
CHAMBER, $Q = f(T_g, G)$.

APPENDIX D

DETAILS OF EQUIPMENT AND APPARATUS

The combustion chamber used in this work consisted of three parallel two-dimensional jets mounted in a framework holding a firebrick lining. The front and back of the frame were closed with Vycor windows to permit ease of observation. In this chamber recirculation was created by the aspirating effect of the jets. This recirculation could be controlled, if desired, by varying the spacing of the jets; however, in these experiments only one jet spacing was used. Sketches showing the dimensions of the chamber and nozzles are given in Figures D-1 and D-2. (An isometric sketch of the assembly has been given in the main body of this thesis Figure IV-1).

The feed to this chamber was a pre-mixed fuel-air mixture. Fuel and air were metered separately and mixed. This mixture was then manifolded and the manifold mixture to each jet was metered to insure equal distribution of feed. The orifices used in the primary air, fuel and manifold mixture lines were standard square-edge orifices and were calibrated to insure accuracy of metering. Calibration was done with air against a standard orifice set. Corrections were made to the calibration curve for fuel to account for the compressibility and higher molecular weight of propane. A similar correction should have been made to the calibration curves for the manifold

mixture orifices (addition of propane changed the molecular weight but did not affect compressibility); however this correction was small, and since it entered into all three equally, it was not necessary to achieve the desired distribution of feed. A flow diagram showing the orifice designations is given in Figure D-3. Calibration curves for each of the orifices are given in Figures D-4 to D-9. Compressibility factor for propane is given in Figure D-10. (Calculated from data reported by Stearns and George (25)).

A sampling train was constructed to facilitate sampling of the chamber gases. (A flow diagram of this train is given in Figure IV-12). In sampling gases where the gases impinge directly on the probe opening, the velocity of the gases at the probe should be matched to the sampling velocity. To do this it is necessary to meter the sampling rate. This metering was accomplished by means of a capillary flow meter. The metering element was a short piece (about 4") of hypodermic tubing of i.d. 0.049". This was calibrated against a wet-test meter. The calibration curve is given in Figure D-11.

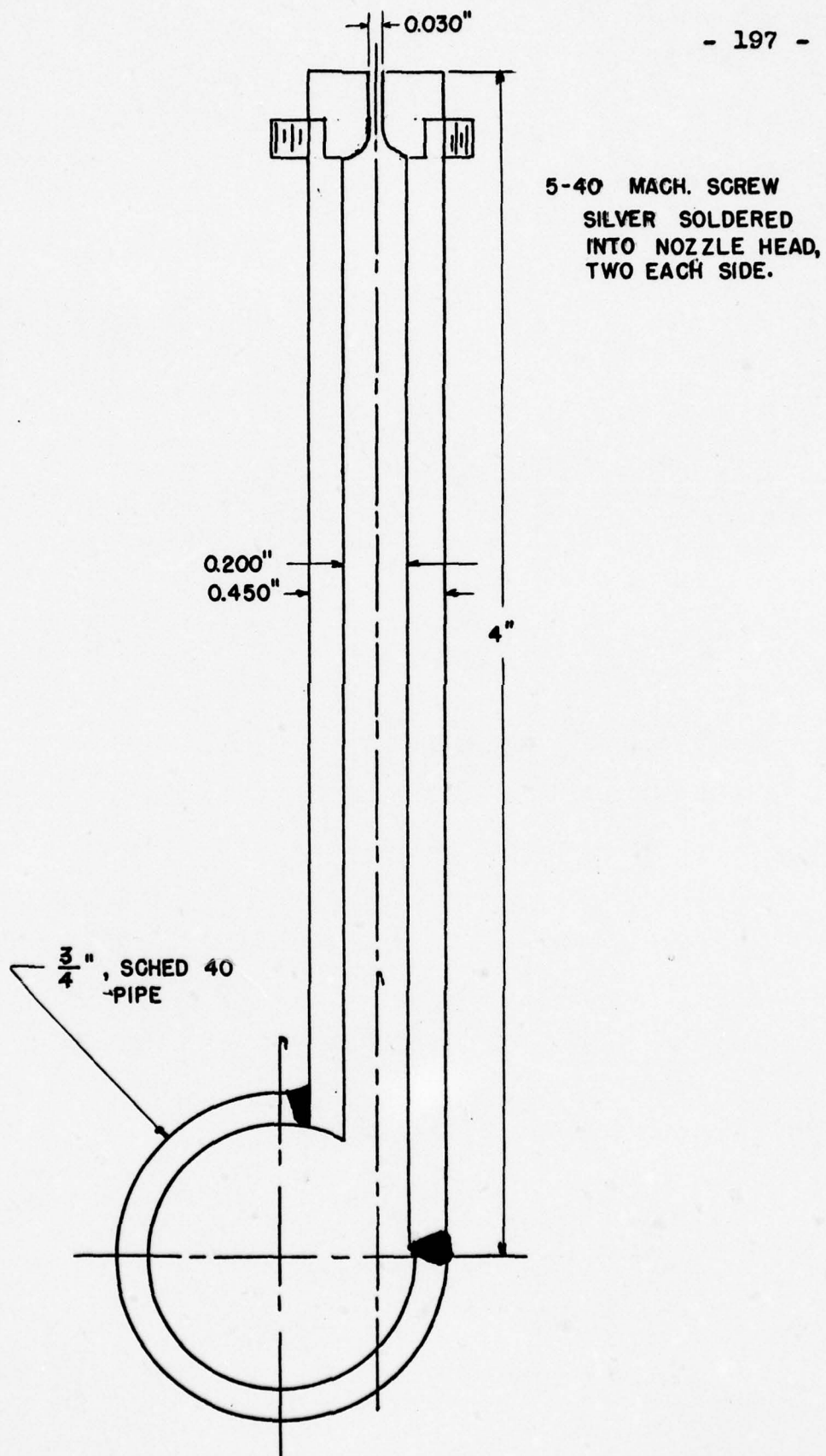


FIGURE D-1: ENLARGED DETAIL OF NOZZLE. SCALE: 2" = 1"

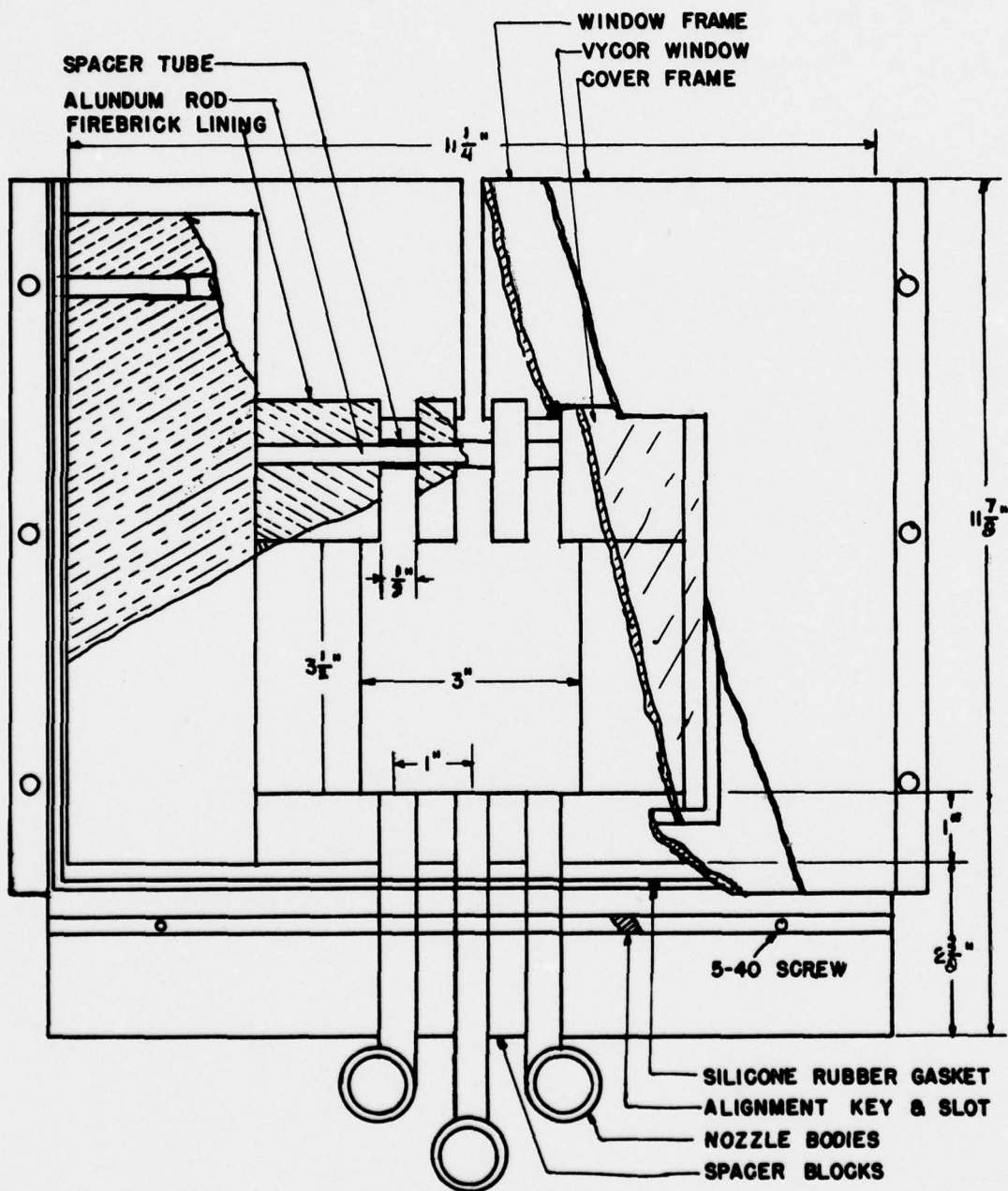


FIGURE D-2: COMBUSTION CHAMBER ASSEMBLY
SCALE: $\frac{1}{8}" = 1"$

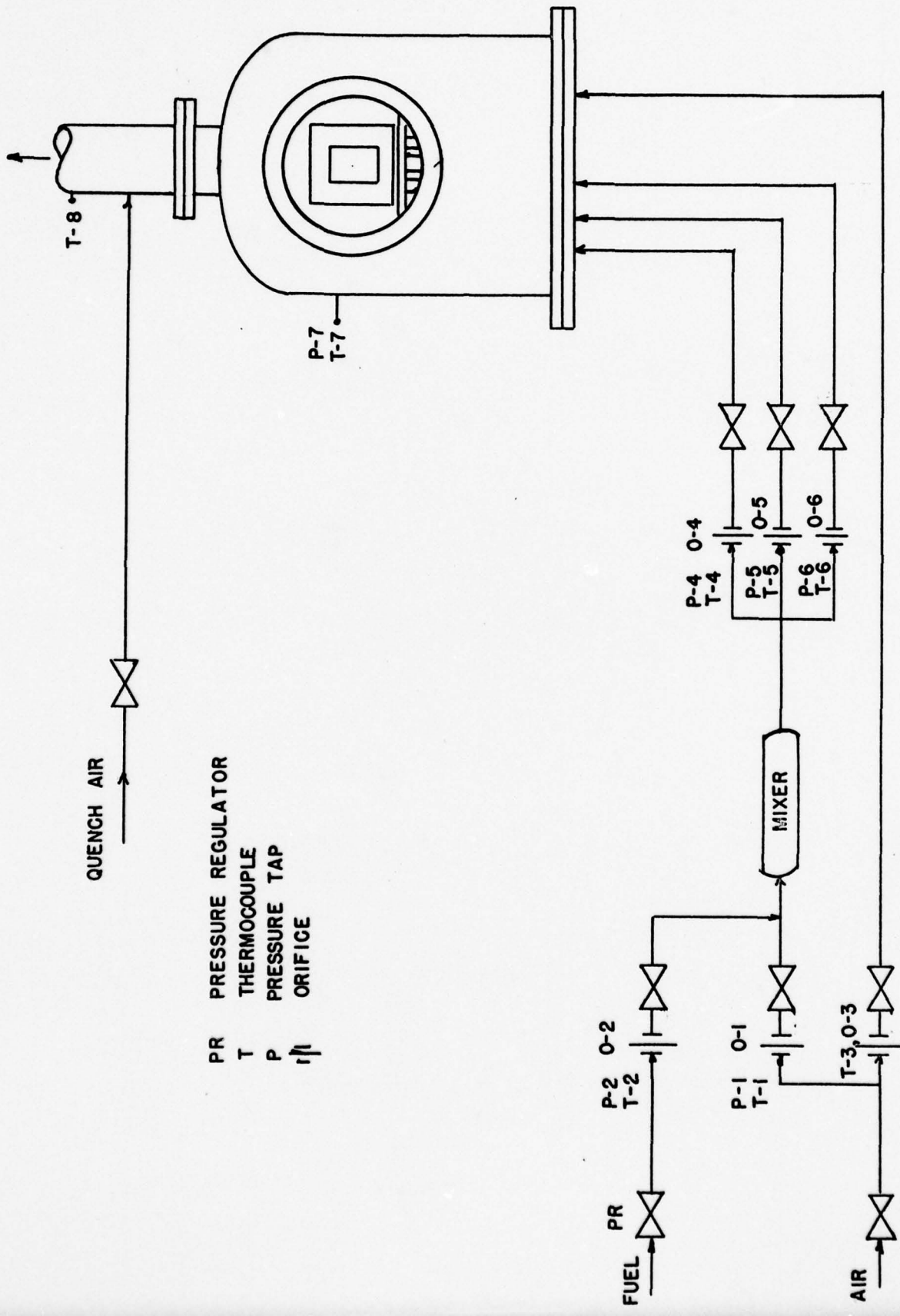


FIGURE D-3: ORIFICE LOCATIONS

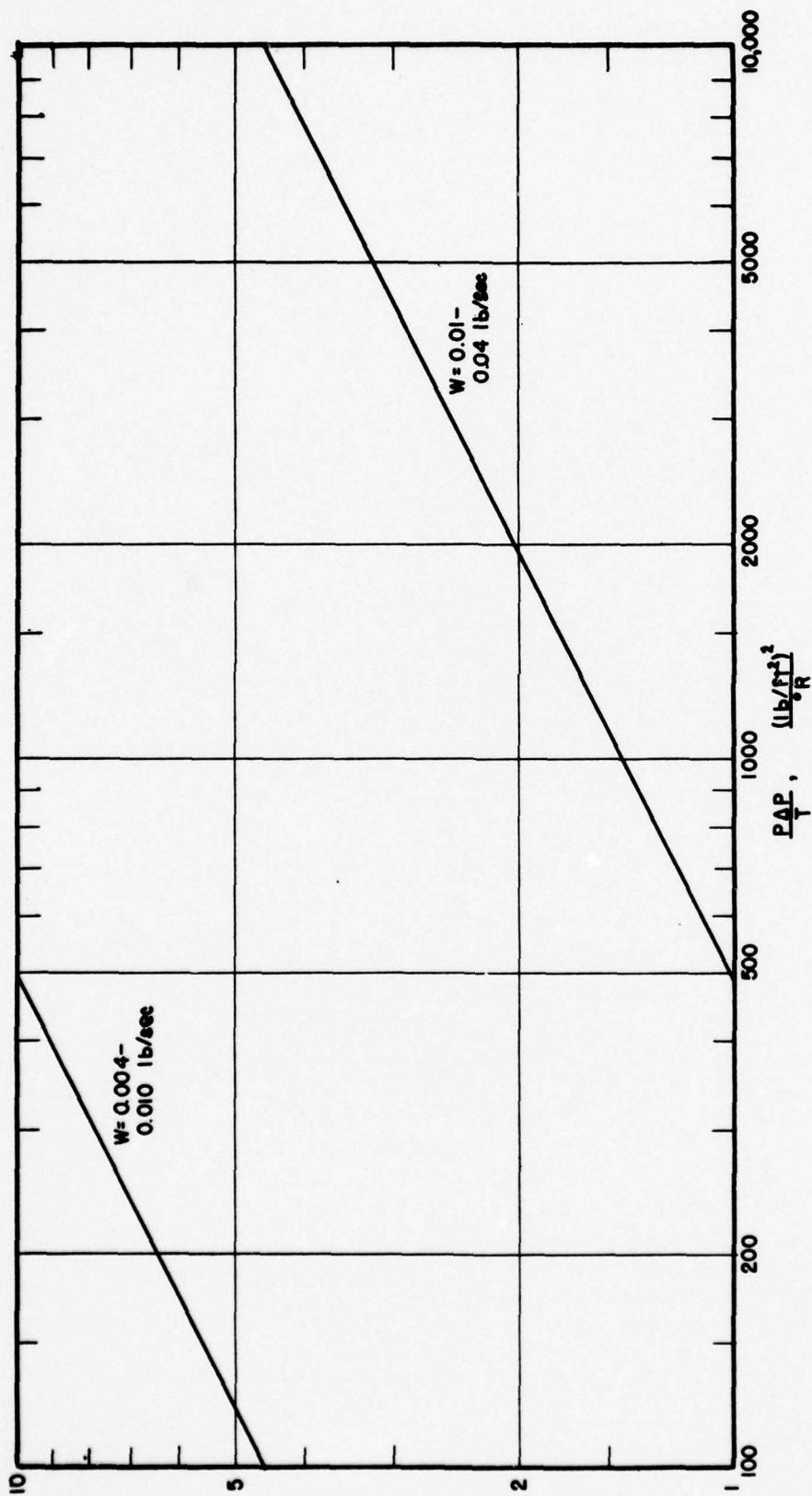


FIGURE D-4: CALIBRATION CURVE, ORIFICE 0-1 LOW RANGE
ORIFICE: 0.348" IN 1 1/2" PIPE
FLUID: AIR

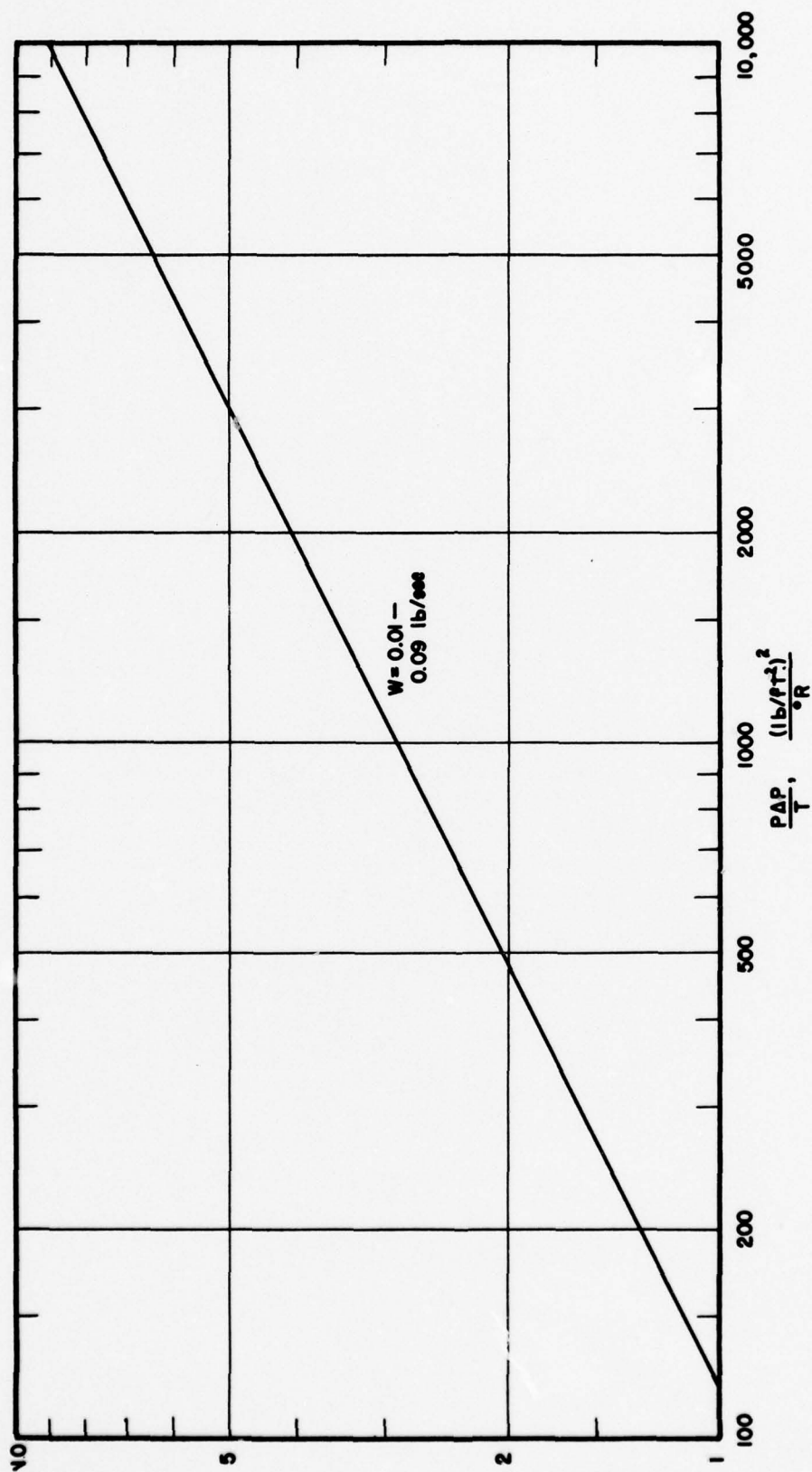


FIGURE D-5: CALIBRATION CURVE, ORIFICE 0-1 MED. RANGE
ORIFICE: 0.500" IN 1½" PIPE
FLUID: AIR

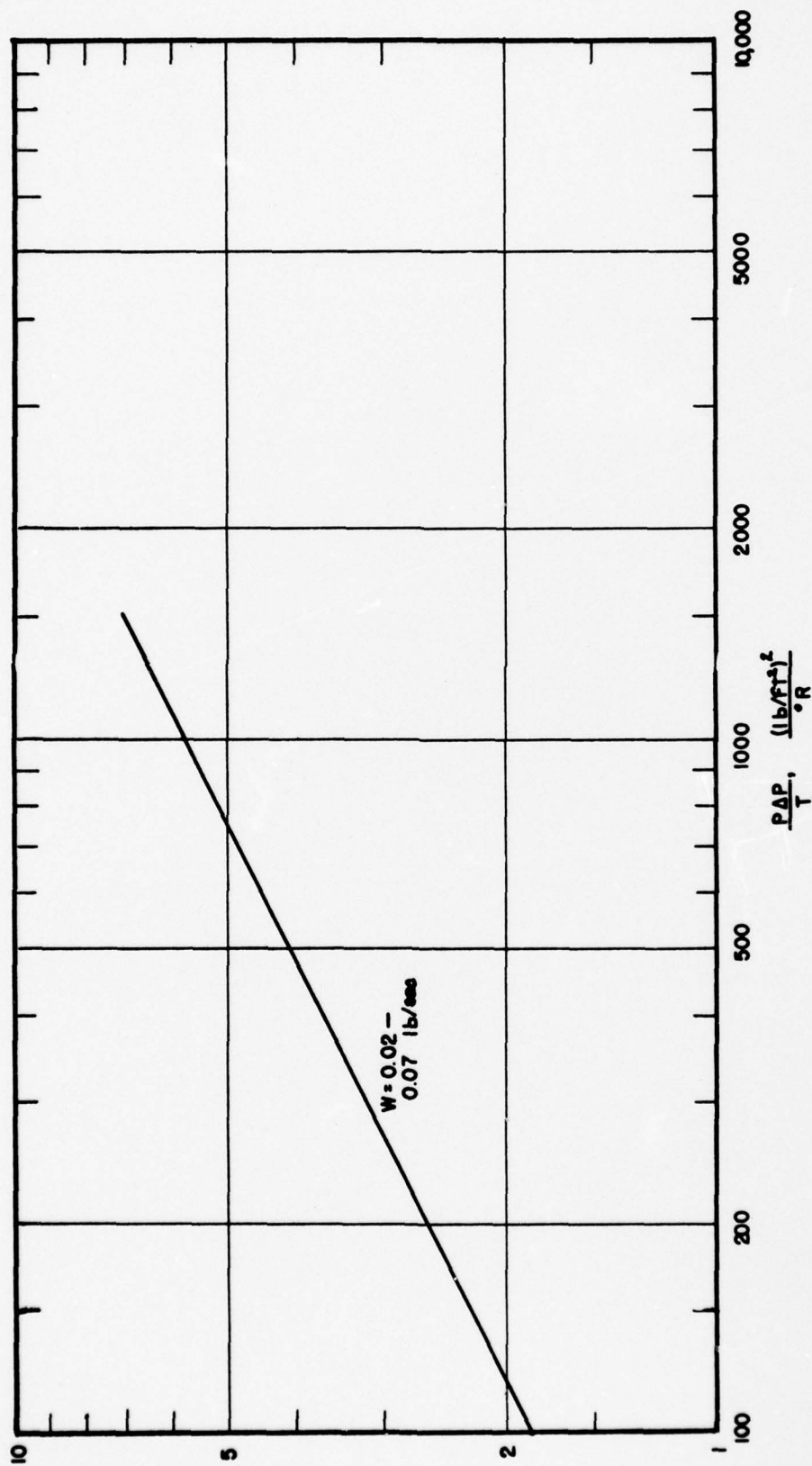


FIGURE D-6: CALIBRATION CURVE, ORIFICE 0-1 HIGH RANGE
ORIFICE: 0.706" IN $1\frac{1}{2}$ " PIPE
FLUID: AIR

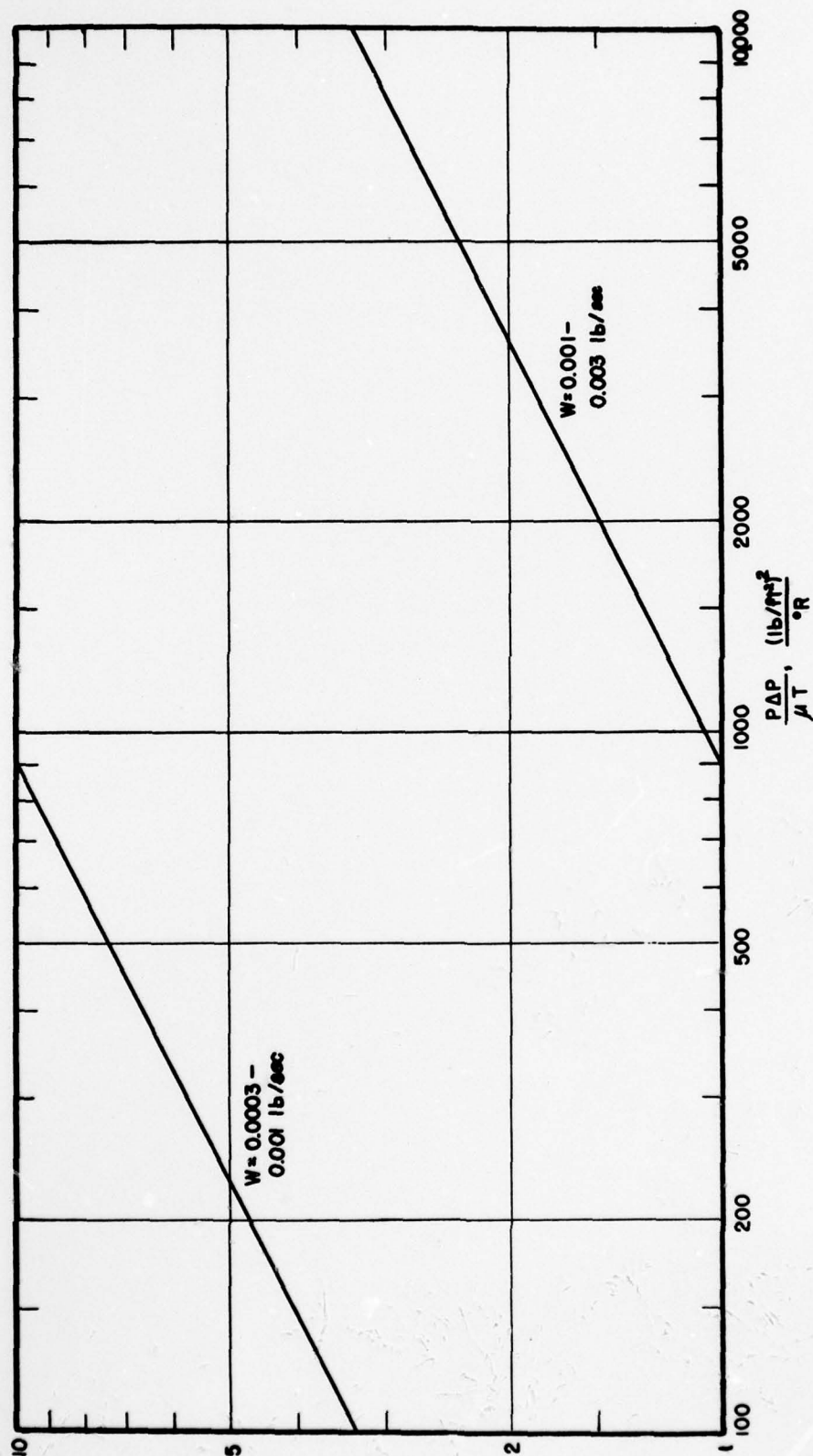


FIGURE D-7: ORIFICE CALIBRATION CURVE, ORIFICE 0-2 LOW RANGE
 ORIFICE: 0.082" IN 2" PIPE
 FLUID: PROPANE

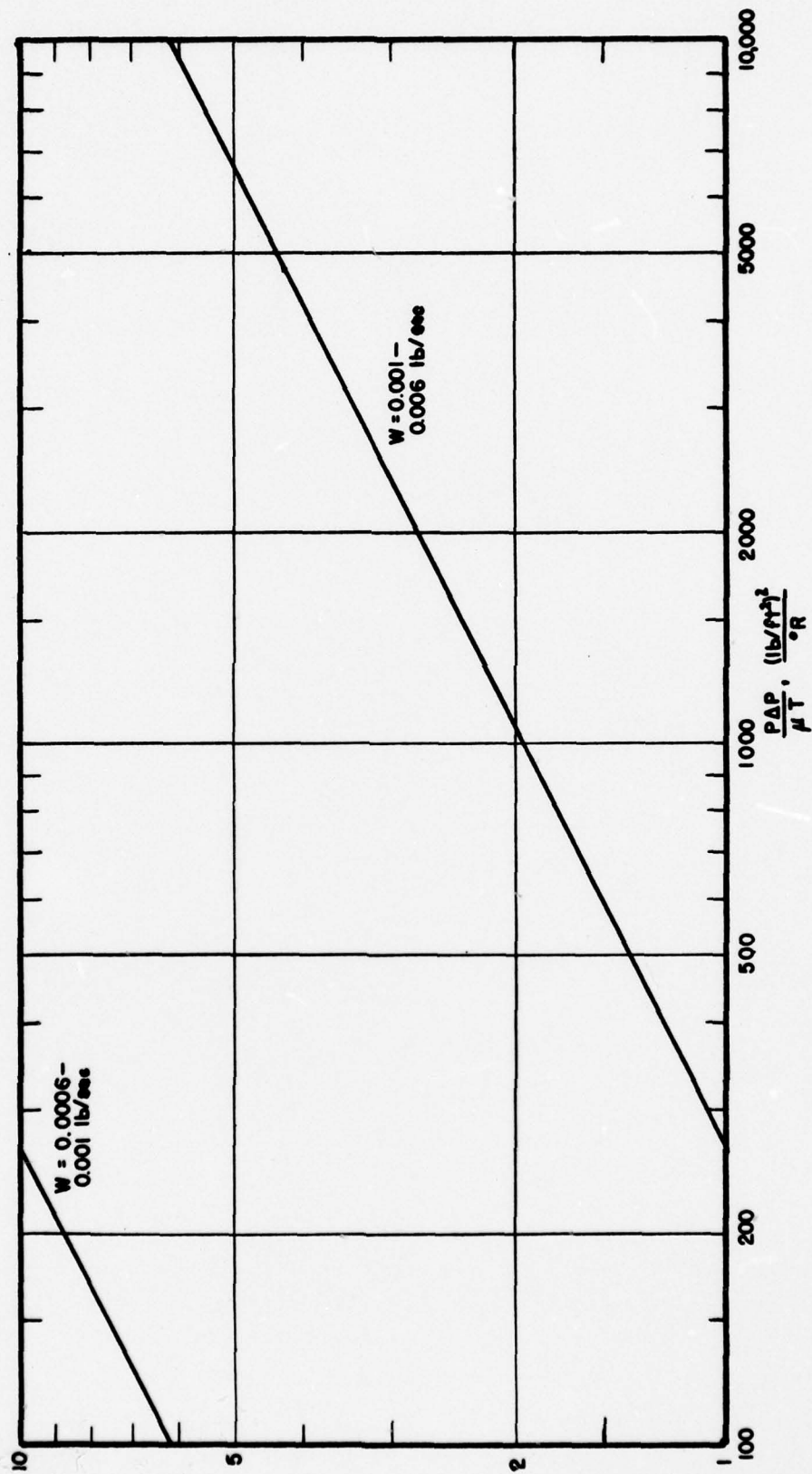


FIGURE D-8: CALIBRATION CURVE, ORIFICE 0-2 HIGH RANGE
ORIFICE: 0.1163" IN 2" PIPE
FLUID: PROPANE

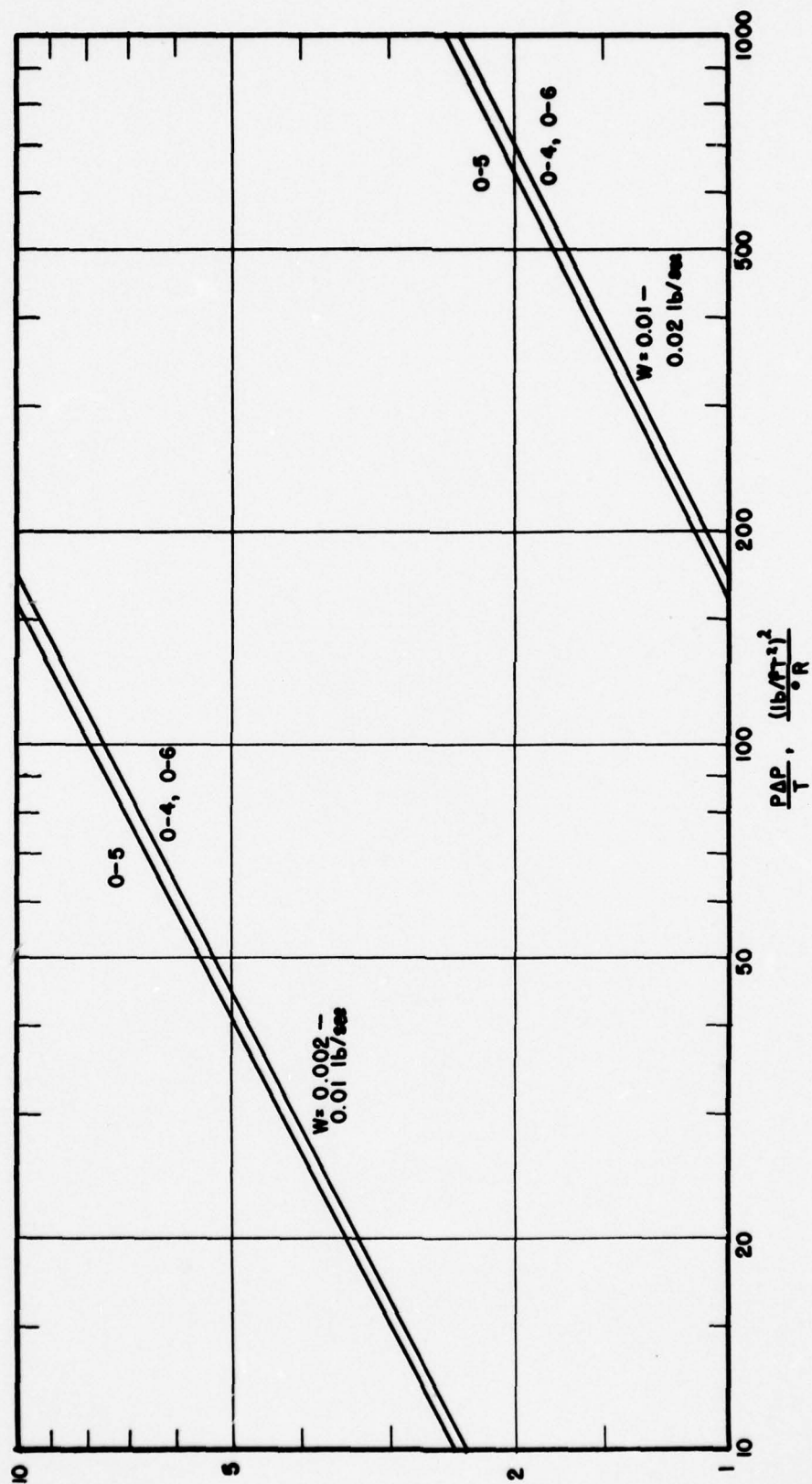


FIGURE D-9: CALIBRATION CURVES: ORIFICES O-4 TO O-6
ORIFICES: 0.4375" IN $\frac{3}{4}$ " PIPE
FLUID AIR

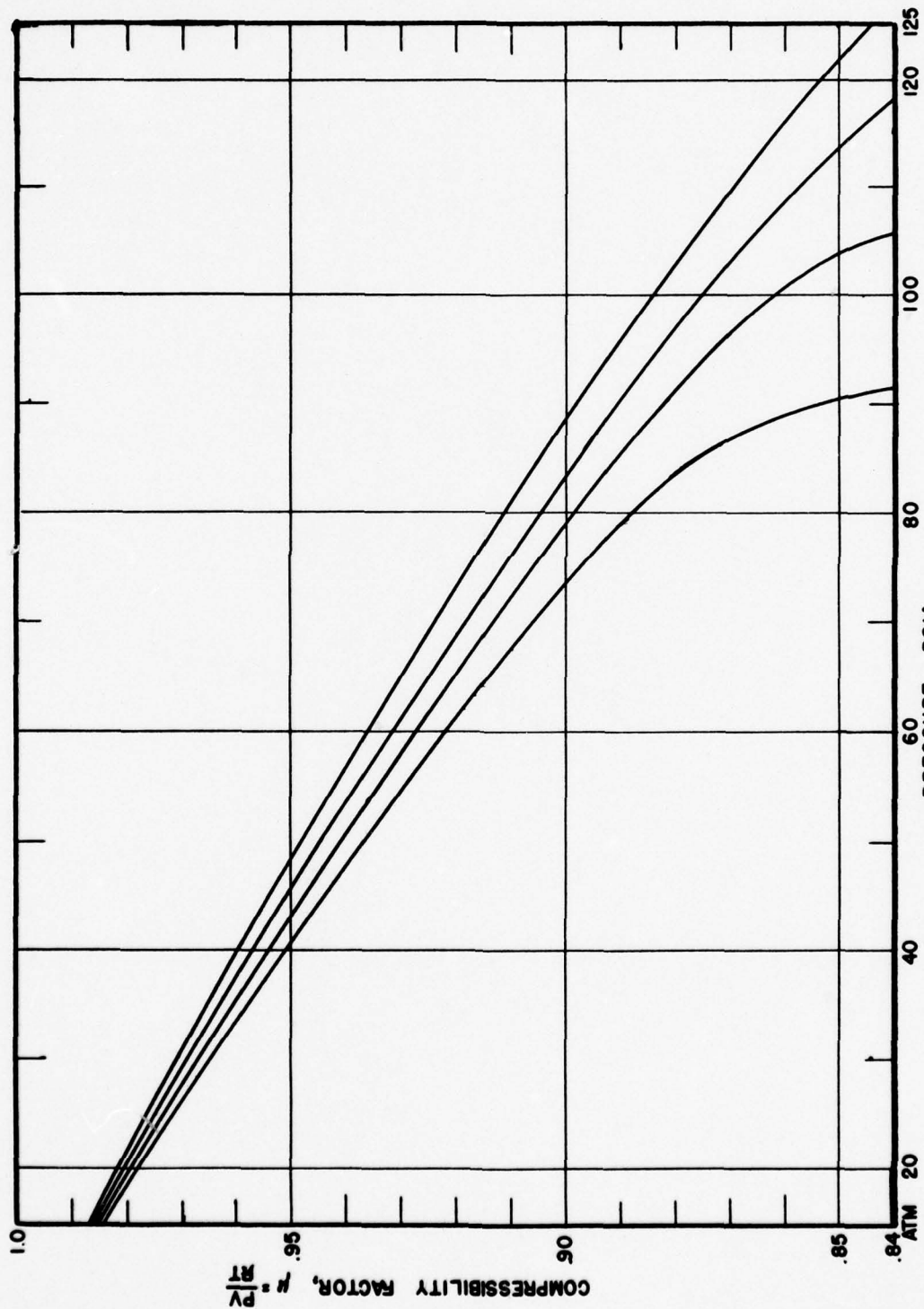


FIGURE D-10: COMPRESSIBILITY OF PROPANE (25)

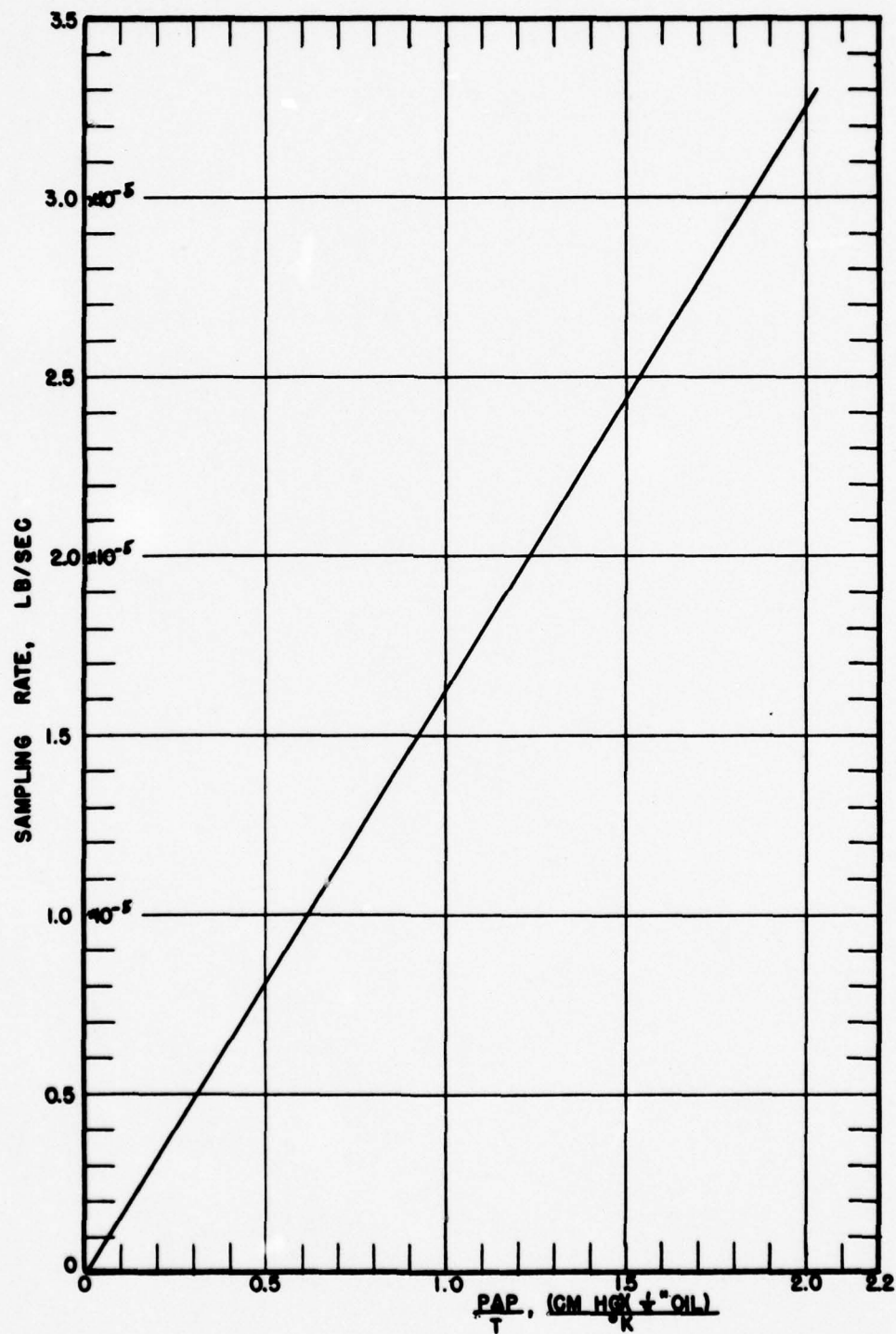


FIGURE D-11: CALIBRATION CURVE FOR CAPILLARY FLOW METER IN SAMPLING TRAIN. FLUID-AIR.

APPENDIX E
SAMPLE CALCULATIONS

A. Calculation of blowout or loading rates (example, Run 4B)

TABLE E-1

DATA OBTAINED IN A TYPICAL RUN

Station	P	ΔP	T
O-1	24.2 psig	9.22" H ₂ O	525°R (0.706" orifice)
O-2	34.8	30.35	513 (0.1163" orifice)
O-4	-4.21"Hg*	17.14	527
O-5	-4.23"*	17.00	527
O-6	-4.26"*	16.15	527
P-7	19.40"*		
atm	30.06"		

* Pressure measured in inches of mercury vacuum.
Negative pressure indicates pressure above atmospheric.

From these data flow rates, w , in lb/sec of gas are calculated. Since the calibration charts for the various orifices are given in $(P\Delta P)/T$ units of $(\text{lb}/\text{ft}^2)^2/\text{OR}$, a conversion factor must be used to account for the units of the measurements. The flow rates calculated from the data of Table E-1 are given in Table E-2. It should be noted from the flow diagram, Figure D-3, that the sum of the flow rates through orifices O-1 and O-2 should equal the flow through orifices O-4 to O-6. Loading rates, fuel-air ratio and other calculated quantities are also indicated in Table E-2.

TABLE E-2

CALCULATED QUANTITIES

	P	ΔP	T	μ	$\frac{PAP}{T}$	conv.	$\frac{PAP \times C}{T}$	w	Figure
0-1	39.0 psia	9.22" H ₂ O	525OR		0.6849	748.8	512.9	0.0429	D-6
0-2	49.6	30.35	513	0.939	3.125	748.8	2340	0.00298	D-8
0-4	33.49" Hg	17.14	527		1.089	367.7	400.5	0.0149	D-9
0-5	33.51"	17.00	527		1.081	367.7	397.5	0.0149	D-9
0-6	33.54"	16.15	527		1.027	367.7	377.6	0.0145	D-9
P-7	10.61"								

- 209 -

$$\text{Fuel-air ratio} = (w_F/w_A)(1/15.68) = 1.096; \quad F = \frac{-\phi}{\phi+1} = .524$$

Loading Rate:

$$\text{Loading} = N_A/VP^{1.8}$$

$$N_A/V = w_A/.3524$$

$$(\text{Volume of chamber} = 0.01215 \text{ ft}^3)$$

$$P^{1.8} = 0.1545 \quad (\text{Figure E-1})$$

$$\text{Loading rate} = 0.761$$

$$\text{Temperature correction} = 1/0.973 \quad (\text{Figure E-2})$$

$$\text{Loading rate corrected to 540OR} = 0.782$$

TABLE E-2

CALCULATED QUANTITIES

P	ΔP	T	μ	$\frac{PAP}{T}$	conv.	$\frac{PAP \times C}{T}$	w	Figure
0-1	39.0 psia	9.22" H ₂ O	5250R	0.6849	748.8	512.9	0.0429	D-6
0-2	49.6	30.35	513	0.939	748.8	2340	0.00298	D-8
0-4	33.49" Hg	17.14	527	1.089	367.7	400.5	0.0149	D-9
0-5	33.51"	17.00	527	1.081	367.7	397.5	0.0149	D-9
0-6	33.54"	16.15	527	1.027	367.7	377.6	0.0145	D-9
P-7	10.61"							

- 209 -

$$\text{Fuel-air ratio} = (w_F/w_A)(1/15.68) = 1.096; \quad F = \frac{-\phi}{\phi+1} = .524$$

Loading Rate:

$$\text{Loading} = N_A/VP1.8$$

$$N_A/V = w_A/.3524$$

$$(\text{Volume of chamber} = 0.01215 \text{ ft}^3)$$

$$P1.8 = 0.1545$$

(Figure E-1)

$$\text{Loading rate} = 0.761$$

$$\text{Temperature correction} = 1/0.973 \quad (\text{Figure E-2})$$

$$\text{Loading rate corrected to 5400R} = 0.782$$

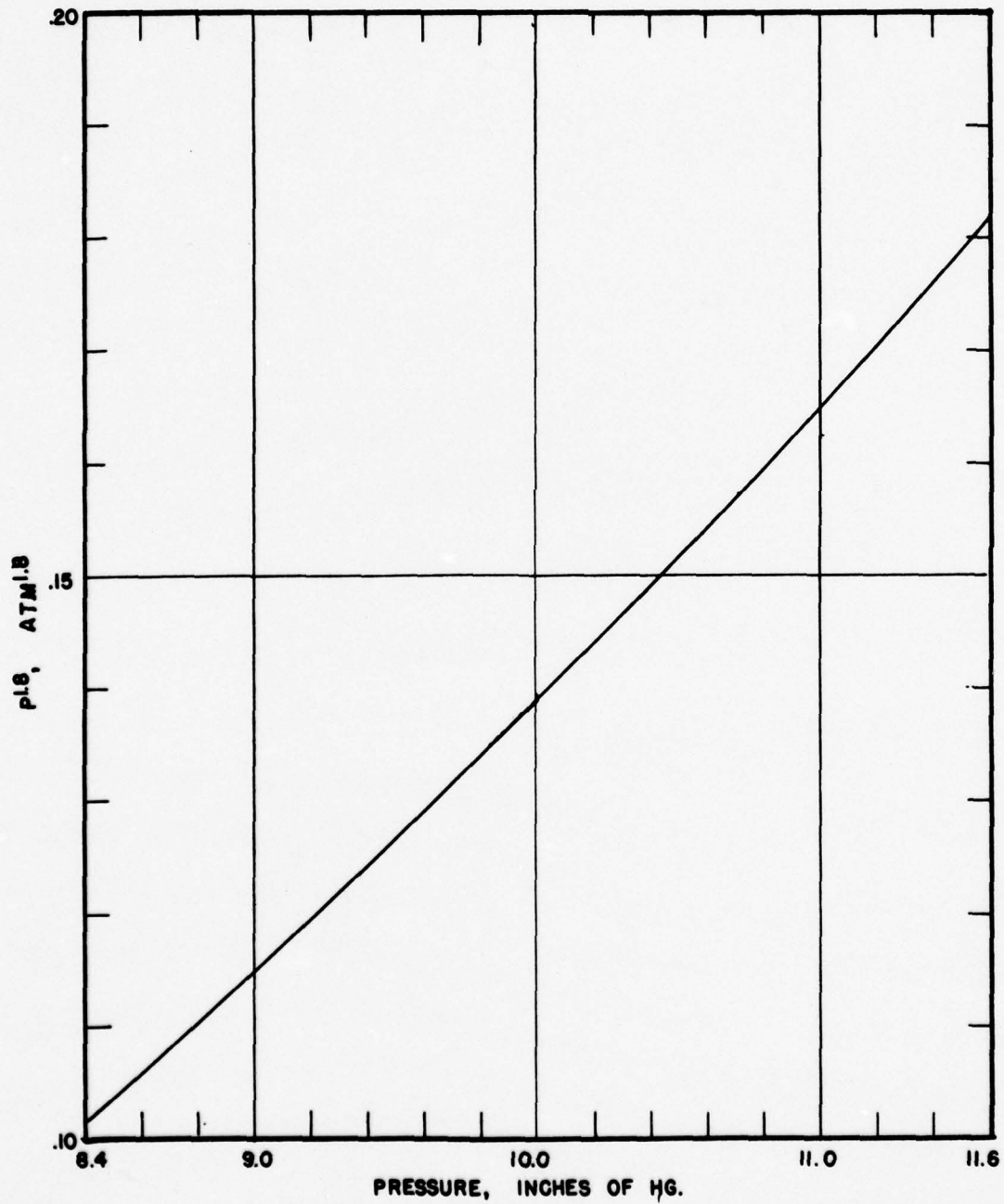


FIGURE E-1: PRESSURE VS pL8

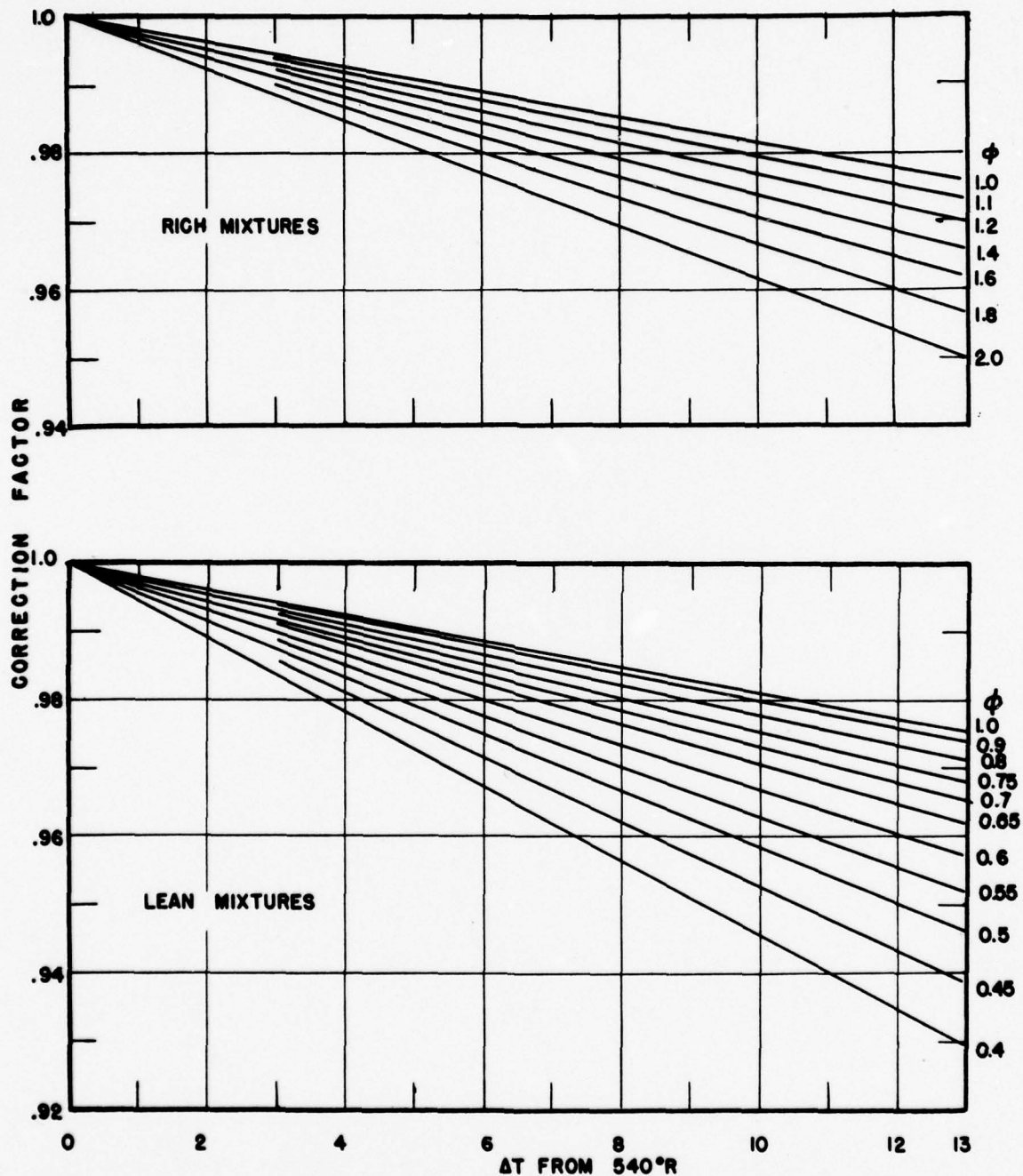


FIGURE E-2: TEMPERATURE CORRECTION FACTORS (14). FOR TEMPERATURE ABOVE 540°R MULTIPLY BY FACTOR. FOR TEMPERATURE BELOW 540°R DIVIDE BY FACTOR.

B. Calculation of combustion efficiency (example Run 86A)

TABLE E-3

DATA OBTAINED IN A TYPICAL RUN

a) Loading rate

	P	ΔP	T	
0-1	56.3 psig	22.26" H ₂ O	537°R	(0.348" orifice)
0-2	29.7 psig	14.22"	531°	(0.1163" orifice)
0-5			537°	
0-7	20.04" Hg vac			
0-9	30.23" Hg			

b) sampling data -- probe position, cold side of flue

	---	rate data	---	
	P	ΔP	T	P _{O₂}
Impact	10.19" Hg	4.9" H ₂ O		
Sample	20.10 mm Hg	33.1 ½" oil	297°K	32.8 mm Hg

From the above data the following quantities are calculated:

a) Loading rate (calculated as in previous example);

$$N_A/VP^{1.8} \bigg|_{540} = 0.620, \quad F = 0.575, \quad A/F = 11.58 \text{ lb/lb}$$

b) Sampling rate;

$$P\Delta P/T = (20.10)(33.1)/(297) = 0.044$$

$$w = 3.67 \times 10^{-5} \text{ lb/sec} \quad (\text{Figure E-3})$$

c) Composition;

$$N_2 \text{ correction}^* = 0.7 \text{ mm} \quad (\text{Figure E-3})$$

$$\frac{\text{Mol dry products}}{\text{Mol wet products}} = 0.856 \quad (\text{Figure E-4})$$

* A correction to magnetic oxygen meters must be made to correct for the magnetic properties of other gases present. It is assumed for this work that the background gas is only N₂. Only a small error is introduced by this assumption.

c) Composition -- continued

Moles O_2 / 100 mols wet products =

$$(33.5)(.856)(100)/(20.10) = 14.26$$

O_2 req'd/100 mol wet prod. = 17.74 (Figure E-5)

$$= 1 - (O_2 \text{ remaining})/(O_2 \text{ req'd}) = 19.7\%$$

d) Estimated gas temperature;

Adiabatic flame temperature = 3755°R (Figure E-6)

$$(T_{af} - 530) + 530 = 1145^{\circ}R$$

e) Sample rate required by impact measurement;

$$P\Delta P/T = (10.19)(4.9)/(1145) = 0.044 \quad (\text{Figure E-7})$$

$$w = 5.79 \times 10^{-5} \quad (\text{Figure E-7})$$

$$w \text{ required} = (.856)(5.79 \times 10^{-5}) = 4.9 \times 10^{-5}$$

(to be compared with 3.67×10^{-5} used)

C. Pressure exponent calculation (example Run 76A)

TABLE E-5

DATA OBTAINED IN A TYPICAL RUN

	P	ΔP	T	
0-1	57.0 psig	2.02" H_2O	544°R	(0.348" orifice)
0-2	43.3 psig	6.20"	536°	(0.1163" orifice)
0-5			540°	
P-7	23.90" Hg vac			
atm	30.08" Hg			

From these data the following quantities are calculated as in example A above:

$$w \text{ of air} = 0.0129 \text{ lb/sec}$$

$$\text{Fuel fraction } F = 0.599$$

C. Pressure exponent calculation -- continued

$$N_A/V = w_A \times 4.26 = 0.0549$$

$$\text{Temp} = 540^\circ\text{R} \quad \text{Temp. Correction} = 1.00$$

$$F = .599 \quad F \text{ correction} = 0.993$$

F correction calculated from relative blowout rates of actual fuel-air mixture and the fuel-air mixture desired. On the rich side this is $F \text{ corr} = e^{7(F-F^*)}$ and on the lean side this is $F \text{ corr} = e^{15(F^*-F)}$.

$$N_A/V)_{540, .600} = 0.0545$$

$$P = 6.18'' \text{ Hg} = 0.207 \text{ atm}$$

A series of these points are taken for a given fuel/air ratio and plotted on log-log paper. The slope of the resulting line is determined.

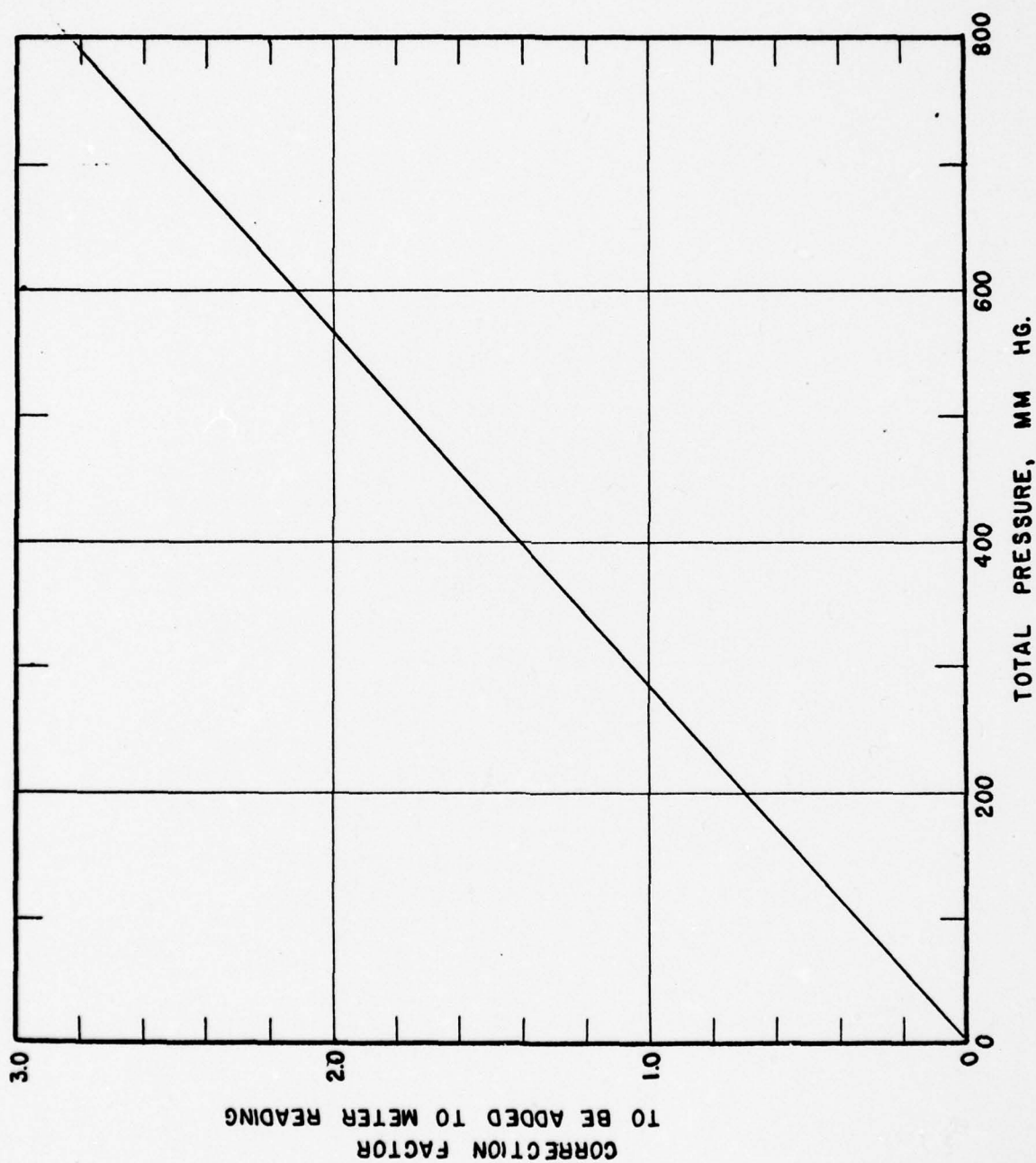


FIGURE E-3: BACKGROUND GAS CORRECTION FACTOR (26)

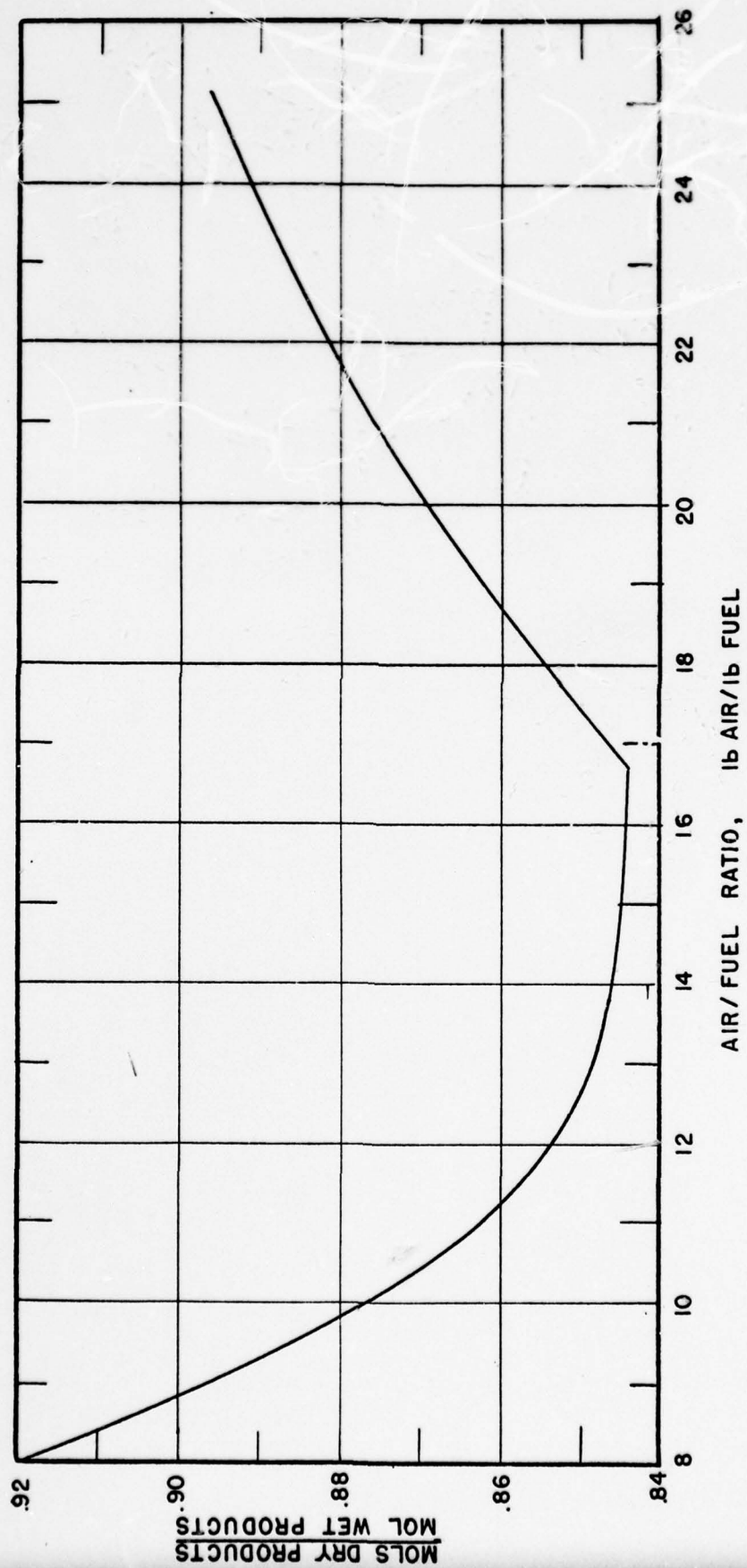


FIGURE E-4: MOLES OF DRY COMBUSTION PRODUCTS PER MOL OF WET PRODUCTS, (25)

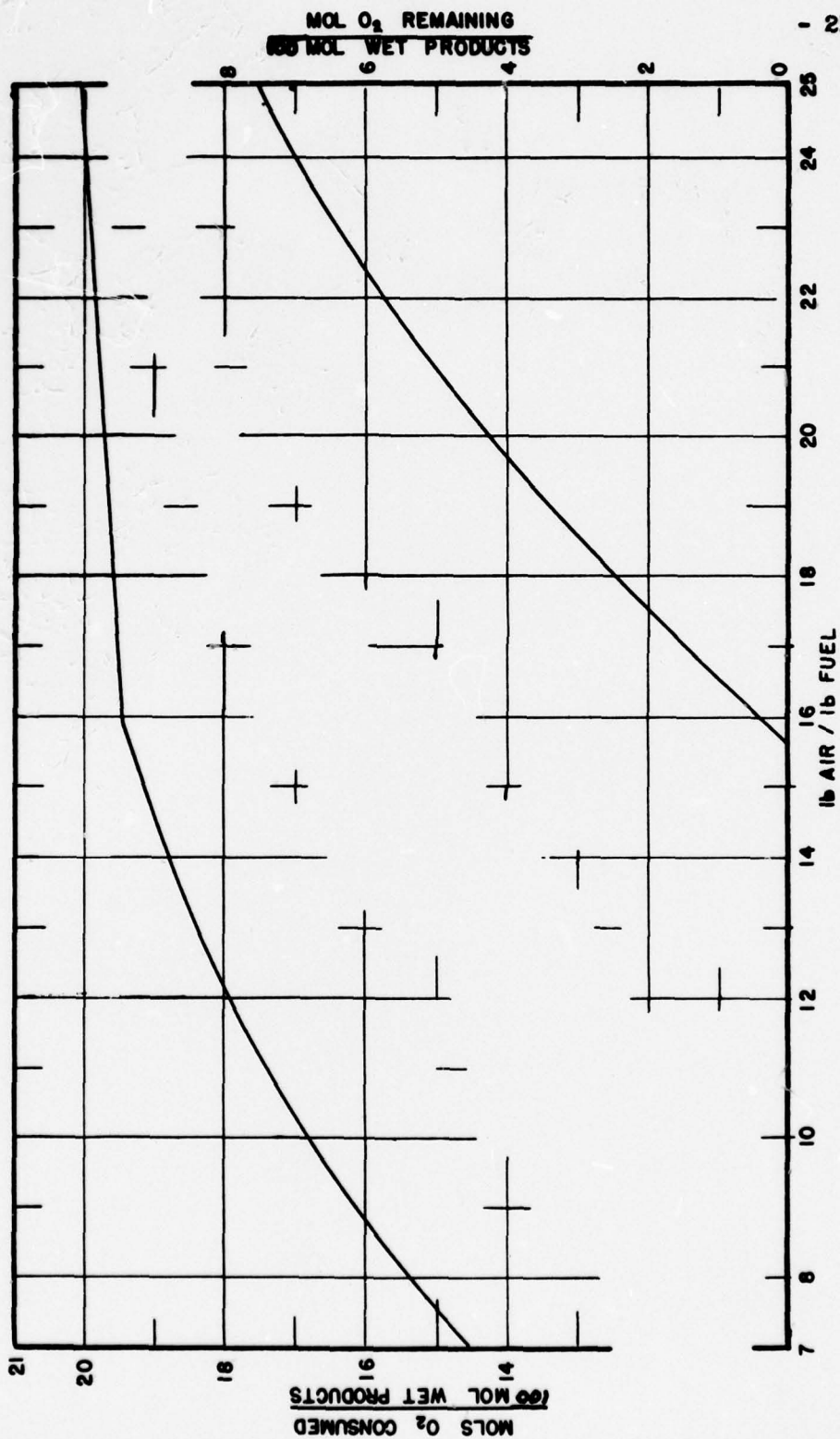


FIGURE E-5: MOLES OF OXYGEN CONSUMED AND REMAINING AT COMPLETE COMBUSTION (25)

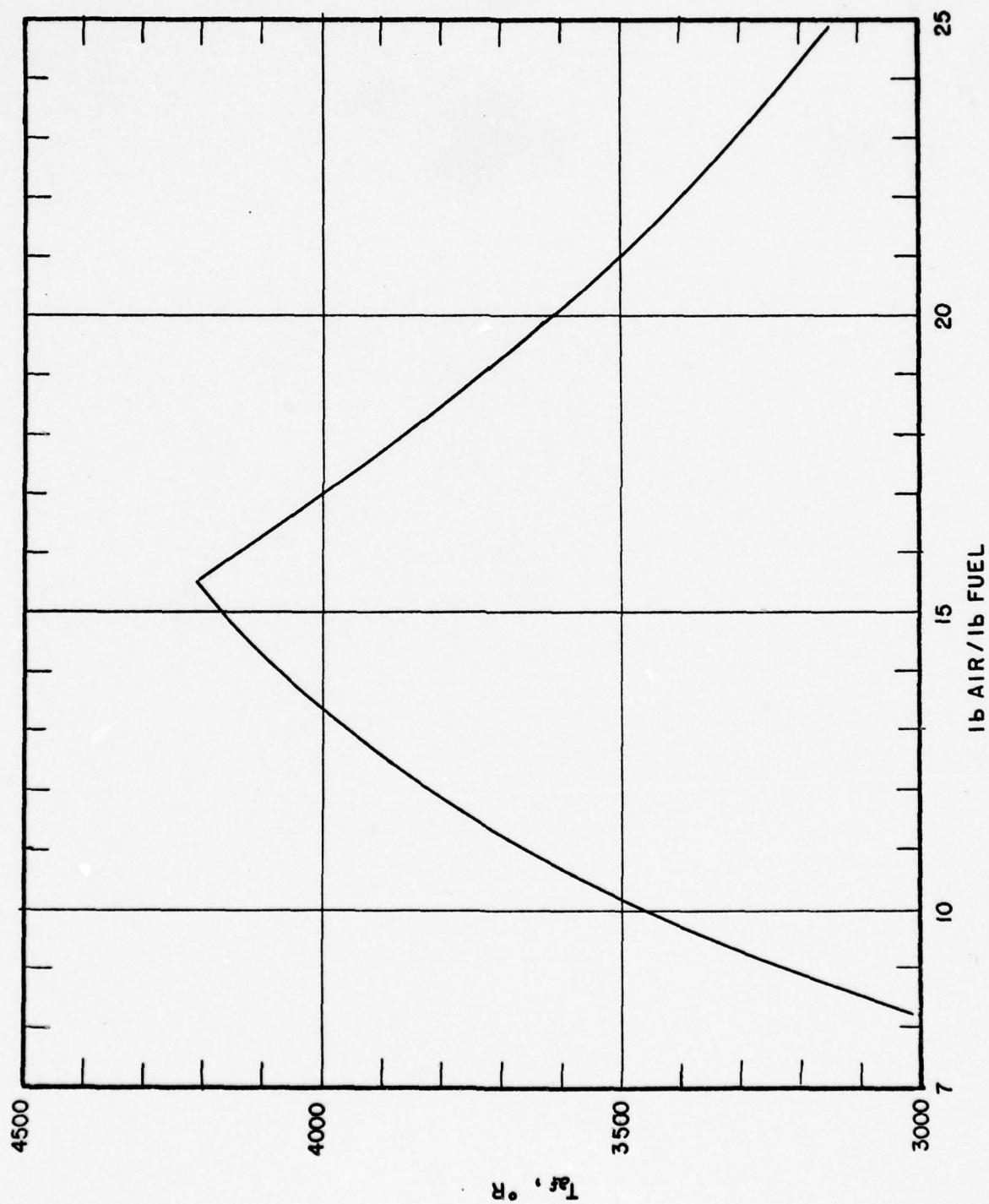


FIGURE E-6: ADIABATIC FLAME TEMPERATURE, $T_o = 70^{\circ}F$ (26)

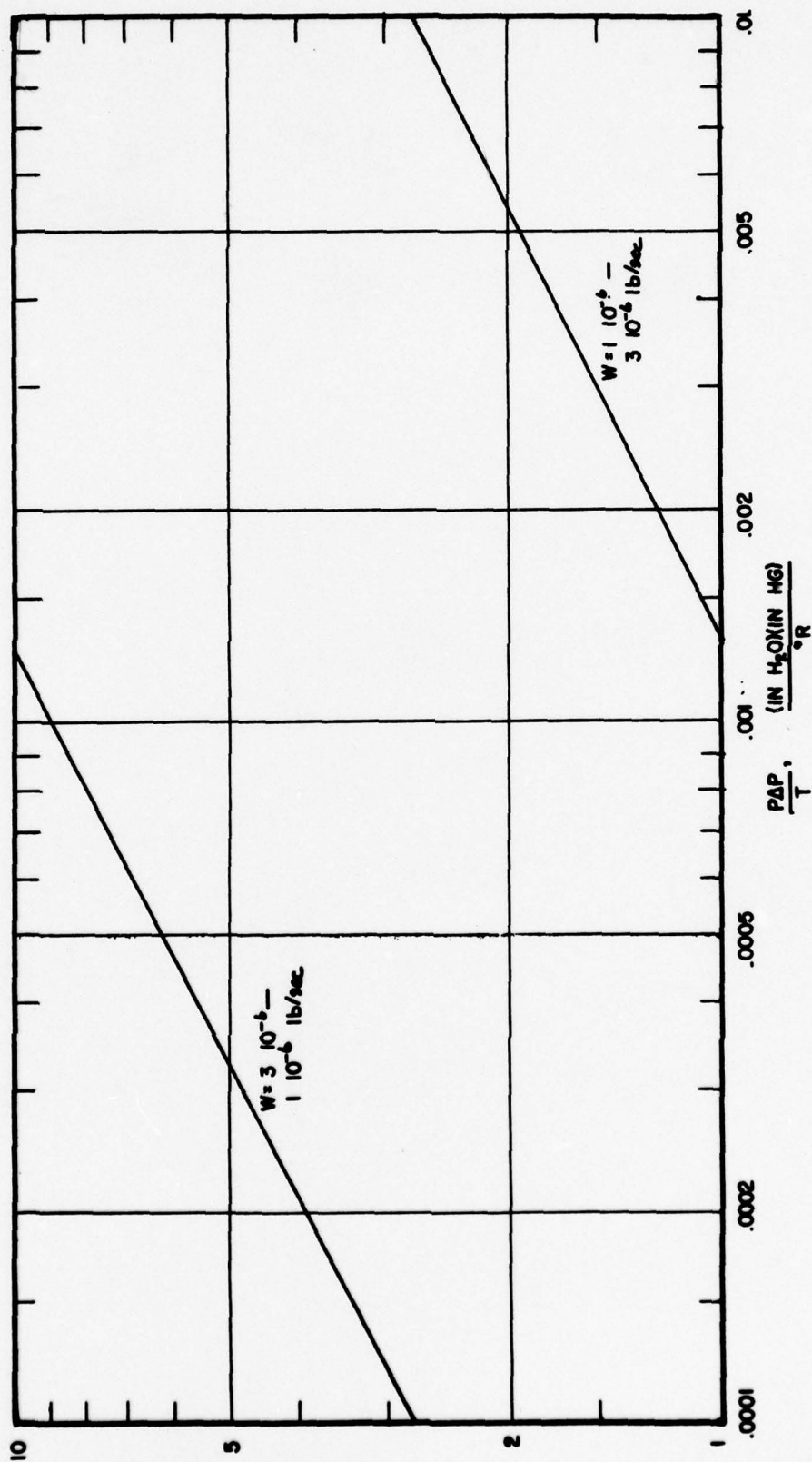


FIGURE E-7: SAMPLING RATE REQUIRED FROM IMPACT PRESSURE MEASURED.
CALCULATED FROM IDEAL PITOT TUBE.

APPENDIX F

SUMMARY OF CALCULATED VALUES

TABLE-F-1

BLOWOUT MEASUREMENTS, THREE-JET CHAMBER

Run	Air rate lb/sec	Pres. in Hg	Temp °R	Loading, $N_A/VP^{1.8}$ lb mol/sec raw	ft^3 atm ^{1.8} corr'd	Gen'l fuel fr'n	Zones blown out
4B	0.0424	10.61	527	0.761	0.782	0.524	1
4C	0.0431	10.62	527	0.722	0.791	0.493	1
4D	0.0445	10.64	527	0.792	0.815	0.445	2
4E	0.0420	10.66	525	0.741	0.765	0.525	1
4F	0.0420	10.66	525	0.741	0.765	0.529	2
4G	0.0420	10.65	522	0.741	0.770	0.469	1
4H	0.0417	10.64	525	0.763	0.790	0.442	2
4I	0.0445	10.71	524	0.803	0.832	0.488	1
4J	0.0473	10.69	524	0.857	0.893	0.470	2
5A	0.0278	10.46	536	0.525	0.530	0.558	1
5B	0.0278	10.48	537	0.524	0.529	0.569	2
6A	0.0264	10.06	538	0.533	0.536	0.554	1
6B	0.0263	9.95	540	0.542	0.542	0.607	2
6C	0.0272	10.14	542	0.541	0.537	0.457	1
6D	0.0272	10.07	542	0.547	0.545	0.428	2
6E	0.0268	10.14	540	0.534	0.534	0.552	1
6F	0.0268	10.11	541	0.534	0.532	0.602	2
6G	0.0270	10.10	542	0.539	0.537	0.460	1
6H	0.0270	10.07	542	0.545	0.542	0.424	2
6I	0.01865	10.28	542	0.361	0.359	0.570	1
6J	0.01865	10.27	542	0.361	0.360	0.619	2
6K	0.01880	10.18	542	0.372	0.370	0.433	1
6L	0.01880	10.18	542	0.372	0.370	0.415	2
6M	0.01900	10.26	542	0.371	0.369	0.506	1
6N	0.01900	10.21	542	0.372	0.370	0.616	2
6O	0.01900	10.23	542	0.372	0.370	0.447	1
6P	0.1900	10.21	542	0.376	0.374	0.413	2
7A	0.0222	10.31	538	0.428	0.430	0.557	1
7B	0.0221	10.29	540	0.428	0.428	0.620	2
7C	0.0220	10.32	540	0.424	0.424	0.485	1

TABLE F-1 continued

Run	Air rate lb/sec	Pres. in Hg	Temp °R	Loading, $N_A/VP^{1.8}$ lb mol/sec raw	$ft^3 atm^{1.8}$ corr'd	Gen'l fuel fr'n	Zones blown out
7D	0.0221	10.29	540	0.428	0.428	0.417	2
7F	0.0219	10.35	541	0.420	0.419	0.560	1
7G	0.0216	10.31	541	0.416	0.415	0.607	2
7H	0.0214	10.36	540	0.411	0.411	0.442	1
7I	0.0215	10.30	540	0.417	0.417	0.411	2
7J	0.0314	10.31	540	0.605	0.605	0.535	1
7K	0.0308	10.19	(540)	0.606	0.606	0.596	2
7L	0.0323	10.33	541	0.623	0.622	0.528	1
7M	0.0323	10.24	543	0.633	0.629	0.590	2
7N	0.0328	10.44	540	0.620	0.620	0.470	1
7O	0.0328	10.36	542	0.629	0.626	0.427	2
7P	0.0329	10.44	538	0.623	0.626	0.471	1
7Q	0.0328	10.42	538	0.623	0.626	0.427	2
*32A	0.0411	10.26	526	0.803	0.828	0.495	1
*32B	0.0450	9.78	523	0.889	0.919	0.456	2
*34A	0.0279	10.56	533	0.511	0.523	0.626	2
*34B	0.0315	10.60	530	0.580	0.600	0.633	2
*34C	0.0276	10.63	533	0.504	0.516	0.648	2
*34D	0.0246	10.69	534	0.445	0.455	0.657	2
*35B	0.0296	10.49	532	0.490	0.502	0.620	1
*35C	0.01735	10.34	532	0.332	0.341	0.655	1
36A	0.0291	10.34	534	0.558	0.568	0.410	1
36B	0.0387	10.36	534	0.738	0.750	0.414	1
36C	0.0487	10.42	531	0.918	0.937	0.431	1
37A	0.0413	9.38	530	0.944	0.965	0.534	2
37B	0.0440	9.37	528	1.009	1.034	0.532	2
37C	0.0418	9.42	530	0.951	0.970	0.531	2
37D	0.0430	9.40	528	0.982	1.000	0.507	2
37E	0.0446	9.48	529	1.001	1.025	0.532	2
37F	0.0424	9.47	529	0.944	0.966	0.533	2
*38	0.0349	9.13	533	0.839	0.854	0.557	2
*39A	0.0403	8.93	534	1.003	1.018	0.561	2
*39B	0.0402	8.95	532	1.001	1.023	0.571	2
*39C	0.0396	8.88	531	1.000	1.023	0.437	2
*39D	0.0395	8.89	531	0.996	1.017	0.694	2
*39E	0.0386	8.96	531	0.956	0.980	0.592	2
*39F	0.0386	9.05	530	0.940	0.967	0.598	2
*39G	0.0385	8.95	530	0.959	0.986	0.434	2
*39I	0.0470	8.96	530	1.177	1.202	0.469	2
*39J	0.0468	8.92	528	1.173	1.222	0.484	2

* These data were disregarded in plotting as they were unreasonable compared to the rest of the data. These values reflect probably the consequences of air leakage and poorly fitting firebricks.

TABLE F-1 continued

Run	Air rate lb/sec	Pres. in Hg	Temp °R	Loading, lb mol/sec raw	$N_A/VP^{1.8}$ ft ³ atm ^{1.8} corr'd	Gen'l fuel fr'n	Zones blown out
40A	0.0367	10.47	533	0.690	0.700	0.609	1
40B	0.0364	10.48	533	0.681	0.690	0.498	1
40C	0.0364	10.34	531	0.688	0.703	0.434	2
40D	0.0309	10.50	531	0.579	0.591	0.605	1
40E	0.0312	10.60	531	0.574	0.585	0.467	1
40F	0.0312	10.50	531	0.578	0.590	0.447	2
41A	0.0330	10.65	533	0.606	0.617	0.561	1
41B	0.0329	10.69	532	0.593	0.603	0.474	1
41C	0.0329	10.61	531	0.429	0.593	0.607	2
41D	0.0335	10.75	531	0.598	0.612	0.559	1
41E	0.0330	10.75	531	0.590	0.601	0.467	1
41F	0.0330	10.70	531	0.592	0.605	0.442	2
41G	0.0270	10.48	530	0.476	0.487	0.582	1
41H	0.0270	10.87	530	0.469	0.485	0.432	2
41I	0.0268	10.80	530	0.474	0.485	0.465	1
41J	0.0268	10.78	530	0.476	0.488	0.428	2
42A	0.0327	9.23	532	0.768	0.780	0.487	1
42B	0.0336	9.23	532	0.787	0.798	0.506	1
42C	0.0336	9.24	534	0.790	0.800	0.598	1
*43A	0.0317	10.13	529	0.631	0.648	0.454	2
*43B	0.0297	9.88	530	0.560	0.579	0.610	2
*43C	0.0463	10.00	530	0.935	0.952	0.469	2
*43D	0.0304	9.88	528	0.632	0.655	0.629	2
44A	0.0377	10.84	525	0.683	0.691	0.590	2
44B	0.0602	10.70	524	1.085	1.120	0.475	2
*45A	0.0385	10.30	524	0.742	0.785	0.629	2
*45B	0.0480	9.45	522	1.090	1.150	0.603	2
*45C	0.0482	9.48	523	1.070	1.125	0.593	2
*45D	0.0438	9.52	523	0.972	1.020	0.612	2
*48A	0.0248	10.17	529	0.498	0.515	0.590	1
*48B	0.0248	10.19	528	0.498	0.517	0.629	2
*48C	0.0417	8.46	525	1.166	1.203	0.540	1
*48D	0.0410	8.46	528	1.100	1.147	0.533	2
49A	0.0255	10.25	540	0.498	0.498	0.561	1
49B	0.0253	10.30	540	0.490	0.490	0.597	2
49C	0.0289	10.27	537	0.560	0.561	0.459	1
49D	0.0302	10.27	536	0.587	0.592	0.448	2
49E	0.0311	10.35	537	0.597	0.603	0.555	1
49F	0.0311	10.27	536	0.605	0.610	0.597	2
49G	0.0332	10.39	538	0.633	0.636	0.462	1

* These data were disregarded in plotting as they were unreasonable compared to the rest of the data. These values reflect probably the consequences of air leakage and poorly fitting firebricks.

TABLE F-1 concluded

Run	Air rate lb/sec	Pres. in Hg	Temp °R	Loading, $N_A/VP^{1.8}$ lb mol/sec raw	$ft^3 atm^{1.8}$ corr'd	Gen'l fuel fr'n	Zones blown out
49H	0.0368	10.34	536	0.704	0.711	0.434	2
49I	0.0347	10.39	535	0.662	0.670	0.540	1
49J	0.0347	10.48	536	0.650	0.657	0.596	2
*51	0.0238	10.18	532	0.468	0.481	0.532	2
52A	0.0317	11.12	535	0.527	0.534	0.634	2
52B	0.0378	11.22	535	0.626	0.635	0.622	2
52C	0.0350	11.20	533	0.580	0.593	0.640	2
52D	0.0367	11.21	533	0.608	0.617	0.535	2
52E	0.0590	11.26	529	0.973	0.995	0.520	2
52F	0.0311	11.22	529	0.515	0.531	0.593	2
*53A							
*53A	0.0340	10.49	531	0.634	0.656	0.636	2
*53B	0.0402	10.61	533	0.737	0.752	0.637	2
*53C	0.0648	10.99	534	1.205	1.22	0.504	2
*53D	0.0402	9.48	535	0.902	0.913	0.604	2
*53E	0.0560	9.52	537	1.245	1.25	0.545	2
*54F	0.0500	9.62	537	1.099	1.095	0.569	2

* These data were disregarded in plotting as they were unreasonable compared to the rest of the data. These values reflect probably the consequences of air leakage and poorly fitting firbricks.

THIS PAGE IS BEST QUALITY PRACTICABLE
FROM COPY FURNISHED TO DDG

TABLE F-2

SUMMARY OF FLAME VOLUME DATA IN THREE-JET CHAMBER

Run	Air rate lb/sec	Pres. in Hg	Temp °R	Loading, $N_A/Vp1.8$ lb mol/sec ft ³ atm ^{1.8} raw	Gen'l fuel fr'n	Vol fr'n of right- hand side	Vol fr'n of left- hand side
18B	0.0233	10.60	531	0.433	0.442	0.308	0.356
18C	0.0368	10.66	530	0.675	0.690	0.335	0.389
19A	0.0291	10.37	530	0.556	0.568	0.294	0.382
19C	0.0332	11.41	532	0.531	0.539	0.336	0.359
19D	0.0331	11.44	531	0.528	0.538	0.321	0.382
19E	0.0359	11.45	531	0.572	0.583	0.362	0.383
19F	0.01925	10.45	535	0.365	0.370		0.476
19G	0.0228	11.46	537	0.364	0.367		0.526
19H	0.0269	10.44	535	0.508	0.525		0.505
19I	0.0302	10.48	535	0.568	0.575		0.455
19J	0.0331	10.52	534	0.616	0.626		0.489
19K	0.0355	10.54	533	0.657	0.669		0.454
19L	0.0383	10.53	533	0.705	0.718		0.475
20A	0.0230	10.88	529	0.392	0.400		0.461
20B	0.0275	10.92	528	0.479	0.492		0.462
20C	0.0309	10.95	528	0.531	0.540		0.540
20D	0.0339	10.98	528	0.583	0.589		0.488
20E	0.0368	11.01	529	0.621	0.636		0.515
20F	0.0391	11.02	528	0.673	0.689		0.502
20G	0.0407	11.05	528	0.696	0.713		0.465
20H	0.0437	11.05	528	0.748	0.765		0.467

TABLE F-3

COMBUSTION EFFICIENCY, THREE-JET CHAMBER

$w = 0.0239 \pm 0.0005$ #/sec, $P = 10.5 \pm 0.4$ "Hg, $T = 531^\circ \pm 2^\circ R$

Loading rate, $N_A/VP^{1.8})_{540} = 0.467$ lb mol/sec ft³ atm^{1.8}

Run	Gen'l fuel fr'n	Left flue	Cntr flue	Right flue
28	0.549	68.7%	62.1%	70.0%
29A	0.566	72.1	64.3	76.8
29B	0.581	69.6	60.8	72.9
29C	0.547	72.6	60.4	76.7
29D	0.534	72.6	62.8	77.8

TABLE F-4

BLOWOUT MEASUREMENTS, ONE-JET CHAMBER

Run	Air rate lb/sec	Pres. in Hg	Temp °R	Loading, $N_A/VP^{1.8}$ lb mol/sec ft ³ atm ^{1.8} raw corr'd		Gen'l fuel fr'n
60A	0.00934	10.18	530	0.276	0.287	0.661
60B	0.00929	10.19	530	0.274	0.285	0.661
60C	0.00923	10.18	530	0.276	0.286	0.651
60D	0.00924	10.17	531	0.274	0.286	0.316
60E	0.00907	10.25	531	0.266	0.277	0.316
60F	0.01180	10.26	531	0.346	0.356	0.630
60G	0.01175	10.20	532	0.347	0.356	0.633
60H	0.01175	10.28	532	0.343	0.353	0.371
60I	0.0118	10.24	532	0.347	0.357	0.359
60J	0.0138	10.25	532	0.405	0.415	0.624
60K	0.0139	10.23	532	0.410	0.420	0.625
60L	0.0138	10.27	532	0.403	0.415	0.359
60M	0.0138	10.39	531	0.395	0.409	0.356
60N	0.01685	10.27	531	0.493	0.507	0.618
60O	0.01680	10.34	532	0.485	0.496	0.608
60P	0.01685	10.27	532	0.493	0.505	0.617
60Q	0.01685	10.30	532	0.491	0.503	0.371
60R	0.01685	10.20	532	0.499	0.531	0.371
61A	0.01505	9.30	535	0.524	0.530	0.625
61B	0.01495	9.19	536	0.533	0.540	0.368
61C	0.01840	9.44	536	0.626	0.633	0.607
61D	0.01840	9.32	538	0.639	0.641	0.590
61E	0.01835	9.33	538	0.637	0.640	0.606
61F	0.01840	9.37	538	0.633	0.636	0.392
61G	0.01840	9.37	538	0.634	0.637	0.383
61H	0.0225	9.18	538	0.805	0.809	0.581
61I	0.0226	9.18	538	0.808	0.809	0.585
61J	0.0226	9.21	538	0.802	0.807	0.410
61K	0.0225	9.26	538	0.794	0.799	0.405

TABLE F-5
COMBUSTION EFFICIENCY, ONE-JET CHAMBER

Run	Air rate lb/sec	Pres. in Hg	Temp °R	Gen'l fuel lb fr'n	Loading, mol/sec raw	$N_A/VP^{1.8}$ ft ³ atm ^{1.8} corr'd*	Oxygen consumption efficiency cm from left-hand wall (hot side)					
							0	1	2	3	4	5
80A	0.00640	10.50	542	0.575	0.180	0.179	81.0	95.9	102.4	100.2	70.4	41.9
80B	0.00760	10.50	542	0.576	0.213	0.215	78.9	92.8	101.9	101.8	74.2	40.5
80C	0.00906	10.62	542	0.576	0.250	0.253	80.2	89.1	102.1	101.7	77.2	38.7
80D	0.01080	10.65	544	0.582	0.296	0.325	39.7	59.3	101.1	97.4	45.4	19.3
81A	0.0128	9.65	543	0.574	0.418	0.408	40.4	46.5	90.8	87.7	31.8	15.9
81B	0.0152	9.76	543	0.577	0.488	0.498	24.2	30.4	72.0	77.8	21.2	12.4
81C	0.0181	9.62	543	0.575	0.565	0.570	17.6	26.1	55.1	67.9	**	**
Overall efficiency												
						LHS	Cntr		RHS	avg		
						(hot)			(cold)			
85A	0.00640	10.13	541	0.575	0.192	0.191	44.9	42.3	41.2	42.8		
85B	0.00905	10.18	541	0.576	0.269	0.272	42.2	42.2	38.6	41.0		
85C	0.01285	10.30	541	0.575	0.373	0.372	38.3	38.3	35.4	37.3		
85D	0.0179	10.11	541	0.577	0.538	0.554	30.4	31.7	30.5	30.9		
85E	0.0259	10.10	541	0.576	0.774	0.782	15.4	18.5	15.8	16.6		
86A	0.0215	10.29	537	0.575	0.625	0.620	19.5	19.9	19.7	19.7		
86B	0.0157	10.29	538	0.567	0.457	0.396	36.8	36.1	31.1	34.7		

* Loading data are corrected for deviations in temperature and fuel-air ratio. The data are corrected to an inlet temperature of 540°R and an inlet F of 0.575

** At this high firing rate the flame is not stable when the probe is inserted across the interior of the chamber this distance.

TABLE F-6

PRESSURE EXPONENT DATA, ONE-JET CHAMBER

Run	Air rate lb/sec	Temp OR	Gen'l fuel fr'n	Loading, N_A/V lb mol/sec ft ³ raw	Corr'd fuel fr'n	Pressure at blowout atmospheres	
72A	0.01685	538	0.596	0.0718	0.600	0.291	
72B	0.00885	538	0.598	0.0377	0.600	0.157	
72D	0.0259	542	0.574	0.110	0.575	0.340	
72E	0.0131	542	0.575	0.0558	0.575	0.184	
72F	0.00882	543	0.600	0.0376	0.600	0.183	
73A	0.00514	543	0.600	0.0224	0.600	0.140	
73B	0.00664	535	0.599	0.0290	0.600	0.146	
73D	0.0191	536	0.573	0.0833	0.575	0.235	0.258
73E	0.0280	538	0.598	0.122	0.600	0.413	0.539
74	0.0168	542	0.596	0.0715	0.600	0.268	0.570
75A	0.00913	(540)	0.452	0.0389	0.450	0.151	0.177
75B	0.00913	541	0.427	0.0389	0.425	0.210	0.235
75C	0.0144	(540)	0.449	0.0613	0.450	0.156	0.188
75D	0.00565	541	0.599	0.0241	0.600	0.119	0.134
75E	0.00618	541	0.577	0.0263	0.575	0.116	0.176
75F	0.00618	541	0.456	0.0263	0.450	0.152	0.171
75G	0.0144	540	0.419	0.0613	0.425	0.234	0.302
75H	0.0251	535	0.597	0.107	0.600	0.330	0.277
76A	0.0129	540	0.599	0.549	0.600	0.207	
76B	0.0183	540	0.590	0.0780	0.600	0.262	
76C	0.0183	540	0.574	0.0780	0.575	0.227	0.241
76D	0.0183	540	0.448	0.0780	0.450	0.203	0.206
76E	0.0183	539	0.423	0.0780	0.425	0.267	0.277
76G	0.0259	538	0.597	0.1103	0.600	0.356	0.360
76H	0.0258	541	0.576	0.1099	0.575	0.290	0.288

* Data corrected to an inlet temperature of 540°R and a fuel fraction indicated.

TABLE F-6 concluded

Run	Air rate lb/sec	Temp °R	Gen'l fuel fr'n	Loading, N_A/V lb mol/sec ft ³ raw	corr'd*	Corr'd fuel fr'n	Pressure at blowout atmospheres
77A	0.00555	537	0.598	0.0236	0.0231	0.600	0.109 0.110
77B	0.00640	538	0.575	0.0272	0.0274	0.575	0.107 0.107
77C	0.00904	538	0.597	0.0385	0.0369	0.600	0.140 0.142
77D	0.00904	540	0.575	0.0385	0.0385	0.575	0.125 0.146
77E	0.0128	540	0.574	0.0545	0.0536	0.0575	0.154 0.152
77F	0.0128	540	0.601	0.0545	0.0554	0.600	0.182 0.182
77G	0.0181	540	0.575	0.0771	0.0771	0.575	0.198 0.210
77H	0.0181	540	0.597	0.0771	0.0736	0.600	0.232 0.257
78A	0.0258	540	0.573	0.1099	0.1066	0.575	0.264 0.267
78B	0.0258	541	0.593	0.1099	0.983	0.600	0.338 0.336
78C	0.0363	541	0.575	0.1546	0.1540	0.575	0.331 0.324
78D	0.0363	547	0.599	0.1546	0.1494	0.600	0.458 0.442
78E	0.0363	542	0.461	0.1546	0.1347	0.450	0.308 0.324
78F	0.0363	541	0.425	0.1546	0.1540	0.425	0.530 0.530
78G	0.0258	541	0.428	0.1099	0.1058	0.425	0.384 0.386
78H	0.0258	540	0.449	0.1099	0.111	0.450	0.295 0.297
79A	0.00636	538	0.424	0.0271	0.0275	0.425	0.161 0.247
79B	0.00637	537	0.451	0.0271	0.0270	0.450	0.150 0.158
79C	0.00904	537	0.425	0.0385	0.0388	0.425	0.235 0.232
79D	0.00904	538	0.451	0.0385	0.0382	0.450	0.180 0.185
79E	0.0128	538	0.426	0.0545	0.0541	0.425	0.285 0.283
79F	0.0128	537	0.452	0.0545	0.0536	0.450	0.203 0.195
79G	0.0181	537	0.424	0.0771	0.0786	0.425	0.324 0.328
79H	0.0181	537	0.450	0.0771	0.0776	0.450	0.232 0.237

* Data corrected to an inlet temperature of 540°R and the fuel fraction indicated.

APPENDIX G

SCHLIEREN PHOTOGRAPHY OF THE THREE-JET CHAMBER

In developing conceptual models of combustion chambers knowledge of the flow pattern as well as of the combustion efficiency pattern is useful in defining regions which may be considered as one zone. Since Schlieren photography permits visualization of density gradients in a gas it was hoped that either still or motion pictures taken via a Schlieren apparatus might help in defining appropriate zones. Still pictures would help show hot and cold regions and motion pictures would help in visualizing flow patterns.

The principles of Schlieren photography have been widely discussed in the literature. A summary has been given by Shipman (20) in discussing the design and operation of a small Schlieren apparatus for the M. I. T. Fuels Research Laboratory. This unit has two 6" diameter, 42" focal-length mirrors as the principal optics. These are mounted on a heavy steel frame to maintain their alignment. The frame was designed to permit assembly around moderate size apparatus. The vacuum tank used in this work was fitted with two opposing windows.

Photographs were taken using a xenon discharge tube supplied through the courtesy of Dr. H. E. Edgerton (7). This tube gave a flash duration of 2 to 3 msec of sufficient intensity to easily expose a panchromatic film with an ASA rating of 100.

The presence of the turbulence found with these short-duration-flash pictures suggested that the regions which were considered as well-stirred zones were in fact somewhat inhomogeneous. The presence of this inhomogeneity also suggested that a single parcel of gas could be identified adequately to permit one to follow its movement over a short timed interval. It was proposed to follow this movement by means of a double-flash picture. This was achieved with a special flash control circuit supplied by Dr. Edgerton. The flash was a spark discharge of about 0.1 sec duration with intervals ranging between flashes of 5 to 100 secs. The intensity of this flash was low enough that special developer was required on high-speed panchromatic film to achieve an effective film speed of 600 to 800 ASA. These pictures did not show the turbulence with sufficient definition to follow a single gas parcel ; however, the shorter flash durations did give substantially clearer resolution of the Schlieren patterns.

Finally high-speed motion pictures (2-3000 frames per sec) were taken of the flame using an Eastman High Speed camera equipped with a synchronizing device to time a strobe-light discharge with each frame exposed, again supplied through the courtesy of Dr. Edgerton. These pictures showed a substantial gas movement; however the movement suggested that it was not gases external to the combustion zone which were being observed rather than flow pattern within the chamber itself. Typical

photographs of the combustion chamber with a Schlieren apparatus are shown in Figure G-1.

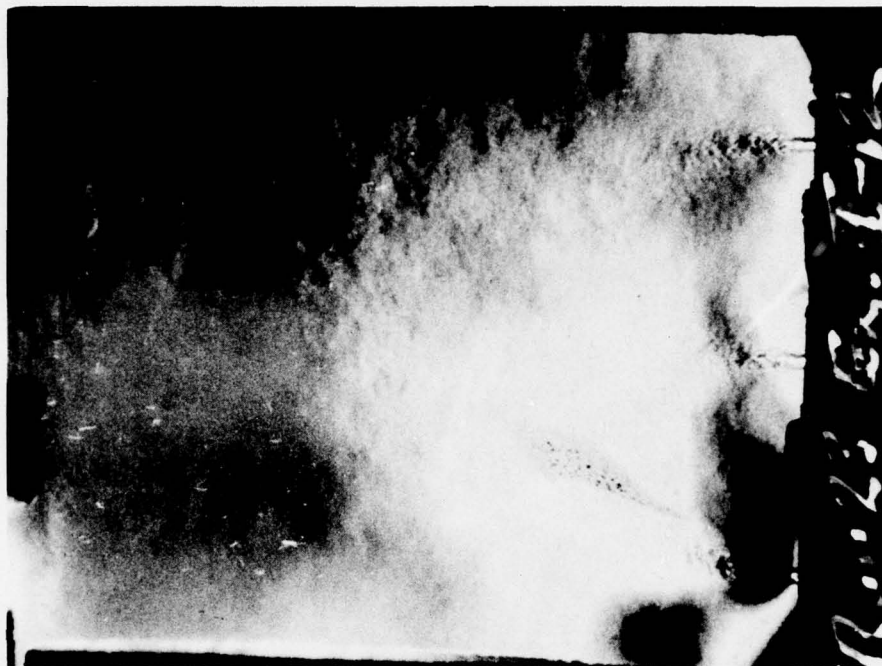


FIGURE G-1: TYPICAL SCHLIEREN PHOTOGRAPHS. LEFT, TWO ZONES ACTIVE; RIGHT, ONE ZONE ACTIVE. FLASH DURATION 0.1 μ SEC.

APPENDIX H

LITERATURE CITATIONS

- (1) A.S.M.E. Research Publication: "Fluid Meters, Their Theory and Applications" 4th edition, (1937).
- (2) Avery, W. H., and Hart, R. W., Ind. Eng. Chem. 45, 1634-7 (1953).
- (3) Baker, M. L., "Combustion in an Intensely Stirred Reactor", Sc. D. Thesis, M. I. T., June (1956).
- (4) Berl, W. G., Rice, J. L., and Rosen, P., Jet Propulsion, 25, 341 (1956).
- (5) Blichner, O., private communication, June (1958).
- (6) DeZubay, E. A., Jet Propulsion 26, 77, February (1956).
- (7) Edgerton, H. A., private communication, November (1956).
- (8) Edgerton, A. C., Saunders, O. A., and Spaulding, L. B., ASME-IME Joint Conference on Combustion, M. I. T., June (1955).
- (9) Hottel, H. C., and Person, R. A., Fourth Symposium on Combustion (International), p. 781, Williams and Wilkins Co., Baltimore (1953).
- (10) Jensen, W. P., private communication, March (1958).
- (11) Koucky, R. W., "Mixing of Enclosed Liquid Jets", Sc.D. Thesis, M. I. T., June (1956).
- (12) Landis, F., "Turbulent Mixing of Coaxial Jets", Sc. D. Thesis, M. I. T. (1950).
- (13) Longwell, J. P., Frost, E. E., and Weiss, M. A., Ind. Eng. Chem., 45, 1629 (1953).
- (14) Longwell, J. P., and Weiss, M. A., Ind. Eng. Chem., 47, 1634 (1955).
- (15) McAdams, W. H., "Heat Transmission", 3rd Edition, Chapter IV, McGraw-Hill Book Co., New York (1954).

- (16) McAdams, W. H., "Heat Transmission" 3rd edition, Chapter IX, McGraw-Hill Book Co., New York (1954).
- (17) Perry, J. H. (editor), "Handbook for Chemical Engineers", 3rd Edition p 467-75, McGraw-Hill Book Co., New York (1950).
- (18) Rosen, P., and Hart, R. W., J1. of Aeronautical Science, 20, 549 (1953).
- (19) Schmidt, E. H. W., and Schoppe, F., Fifth Symposium on Combustion (International), p 343, Reinhold Publishing Co., New York (1955).
- (20) Shipman, C. W., "Flame Stabilization", Sc. D. Thesis, Appendix 5, M. I. T., (1952).
- (21) Shuler, K. E., Fifth Symposium on Combustion (International), p 56, Reinhold Publishing Co., New York, (1955).
- (22) Simon, D. M., and Wagner, P., Ind. Eng. Chem., 48, p 129 (1956).
- (23) Spaulding, D. B., "An Analogue for High-Intensity, Steady-Flow Combustion Phenomenon", I.M.E. Preprint, January (1957).
- (24) Spaulding, D. B., "Theoretical Relationships Between Combustion Intensity and Pressure Drop for One Stream Combustion Chambers", Report 10,181, C.F. 393, Aeronautical Research Council, Great Britain (1957).
- (25) Stearns, W. V., and George, E. J., Ind. Eng. Chem., 35, p 602 (1943).
- (26) Tobey, A. C., Personal communication, April (1958).
- (27) Ubbelohde, A. R., Fifth Symposium on Combustion (International), p 74, Reinhold Publishing Co., New York (1955).
- (28) vonElbe, G., Fifth Symposium on Combustion (International) p 79, Reinhold Publishing Co., New York (1955).
- (29) Weynand, E.E., "Investigation of Mixing of Confined Streams" Sc. D. Thesis, M. I. T., (1953).
- (30) Woo, P. T., "Boundary Layer Effects on Bluff Body Stabilizer", Sc. D. Thesis, M. I. T. (1955).

APPENDIX I

TABLE OF NOMENCLATURE

a	Proportionality constant, Equation III-8.
C	Concentration, moles per unit volume. C_F , fuel concentration C_{O_2} , oxygen concentration.
E	Effective activation energy of overall reaction, stirred reactor equations, Ch. II and III.
F	Generalized fuel fraction, $F = \phi / (1 + \phi)$. Appendix C; F is direct view factor in radiation calculations.
G	Firing rate to stirred reactor or combustion chamber, moles of fuel per unit time.
h	Heat transfer coefficient, Appendix D; h_g , gas film coefficient from burning gas to Vycor and walls; h_c convection coefficient from Vycor walls to ambient air.
J	Fractional contribution of a reactor unit in combustor model to overall combustion rate.
k	Proportionality constants, k_1 and k_2 in equations III-1 and 2 respectively.
k'	Pseudo collision factor in overall reaction. Well-stirred reactor equations, Ch. II and III.
L	Length of combustor, Equation III-4, ff.
\dot{m}	Momentum flux, Equation III-11, ff.
n	Overall order of reaction, well-stirred reactor relations.
N_A	Air firing rate to well-stirred reactor and experimental chamber, lb moles/sec.
p	Number of zones in extended recirculation model.
P	Pressure, atmospheres.
\bar{R}	Gas constant. Recirculation ratio in recirculation models.
T	Temperature, degrees rankine. T_{af} , temperature of an adiabatic flame at complete combustion, T_N ,

nozzle temperature, T_o , inlet temperature of fuel/air mixture, T_K , key temperature in normalization of well-stirred reactor equation, Appendix A.

- U Velocity, Chapter III, U_i inward velocity (toward jet axis), U_o outward velocity (away from jet axis), U_N , nozzle velocity of jet. Chapter VI; overall heat transfer coefficient, defined by Equation VI-1.
- V Volume, cubic feet.
- x Distance coordinate parallel to jet axis.
- y Distance coordinate perpendicular to jet axis.
- Y Fraction of fresh fuel/air mixture reaching a combustion zone.
- Z Fraction of fuel fed to recirculation zone in split-fuel feed model.
- α Reaction order exponent on fuel, well-stirred reactor equations.
- β Burnedness, fractional fuel consumption.
- γ Variables describing the composition of a burning mixture.
- δ Variables describing the composition of a burning mixture.
- ϵ Emissivity in radiation calculations, Appendix D.
- η Oxygen consumption efficiency.
- \bar{F} Relative reaction rates, defined by equation D- , App. D.
- ρ Density.
- σ Stefan-Boltzman Constant, 0.171×10^{-8} .
- Σ Summation of moles present per mole of fuel.
- ϕ Fuel/air ratio; fraction of stoichiometric fuel.

APPENDIX J

BIOGRAPHICAL NOTE

The author was born in Elizabeth, New Jersey and received his elementary and high school education in the public school system of Westfield, New Jersey.

He attended Albion College in Albion, Michigan from 1949 to 1951, and then the University of Michigan in Ann Arbor from 1951 to 1953. He was awarded a B. S. E. in chemical engineering from the University in August 1953.

He entered the Graduate School of M. I. T. in September 1953. While he was at M. I. T. he served as a Research Assistant, Teaching Assistant and Instructor in the Department of Chemical Engineering. He also held a General Motors Fellowship from February 1955 to February 1956, and received several grants from the Teagle Foundation.

The author now holds the position of Assistant Professor of Chemical Engineering at M. I. T. and is director of the Parlin Field Station of the School of Chemical Engineering Practice.